

**Faculty of Science and Engineering
Department of Civil Engineering**

**Measuring the Mechanical Response of
Sand-Rubber Composites as a Geotechnical Material**

Saeid Amiralian

**This thesis is presented for the Degree of
Doctor of Philosophy
of
Curtin University**

December 2017

DECLARATION

To the best of my knowledge and belief this thesis contains no material previously published by any other person except where due acknowledgment has been made.

This thesis contains no material which has been accepted for the award of any other degree or diploma in any university.

Signature:

Date:

ABSTRACT

Considering the amount of scrap tires that is rapidly increasing around the world, finding environmental solutions have been alarmed. The Australian government reported that about 52.5 million EPU (Equivalent Passenger Unit) scrap tires were generated in 2007-2008. However, the specific characteristics of rubber tire including; resilient, lightweight and skin-resistive suggest using the tire in engineering constructions. In this thesis 18 sand composites generated by varying dosages of rubber buffing and cementitious material were comprehensively examined to determine an optimum combination of the stabiliser and rubber, scale effect study, propose a numerical model for predicting the shear strength of composite and interpret the deformation mechanism of composites. The results indicated that the structure of composite is significantly related to the percentage of rubber in the composite. Subsequently, the soil matrix revealed the floating and non-floating cases are associating with composites structure including dense, medium and loose. Based on the maximum dry density results the proposed simple linear regression suggests that the optimum mixing ratio was related to the shape, size, amount and type of additives.

Moreover, scale effect study shows the improvement in the elastic phase of the shear stress behaviour of sand was attributed to the ductile behaviour of rubber. Moreover, a quasi-elastic behaviour was observed in composites containing both rubber and stabilisers. The shear strength parameters of composites containing shear resistance, strain capacity, elastic modulus, apparent cohesion, internal friction angles and dilation angle are affected by the rubber ratio of the composites.

Therefore, a reasonable correlation proposed between the MDD and the shear strength parameters of the sand composites. The result suggested the existence of the optimum content of the stabiliser required for generating the maximum friction angle. The stress-dilation law was proposed to deduce the constant volume friction angle of composites by plotting ϕ_p versus ψ_{max} , obtained from laboratory tests. The compression behaviour of the

composite was also significantly affected by rubber content. The most significant effect of rubber application was observed by investigating the bonding degradation region of composites. The bonding control in all three composites was the same.

However, the ratio of vertical deformation was remarkably affected by the rubber fraction, increasing by using more dosage of the compressible material. The normalized strain has been suggested that the mixtures during the bonding control region the composite was gradually loosed its contact level force and finally were behaved the same as uncemented specimens. Three failure patterns were observed in triaxial specimens accompanying with the composite ingredient. Sand specimens containing only cement have failed with the localised shear band caused to progress the softening behaviour of mixtures after peak strength. A localised bulging failure was observed in sand-rubber mixtures.

Eventually, a failure mode with a combination of crushing at the lower part and localised bulging was observed in cemented sand-rubber mixtures, suggested a hardening in the composite. Increasing the confining pressure caused to reduce the sand-to-sand particle and increase the rubber-to-rubber particle. Two regression models were established based on the degree of availability of shear strength parameters of the studied sand composites.

An overall accuracy of the proposed model is eventually compared by the laboratory data of small direct shear tests. Further investigation was conducted by a microstructural study on cemented sand rubber composite. Results suggest that composites can be contained three phases; (a) the hardened cement paste, (b) the pore structure, and (c) interfacial transition zone (ITZ). The addition of rubber and slag in the composite cause to increase the homogeneity of the composite by modifying the particle shape size, mineral composition, surface roughness and moisture content, the porosity of aggregates and the water-cement ratio. The shear strength characteristic of

the cemented sand-rubber composite is also increased by establishing the chemical components, leads to increasing.

Moreover, in the presence of rubber particles, the amount of alkali-silica reaction (ASR) distress is reduced. Eventually, the elasto-brittle body and elasto-plastic body described the mechanism of deformation of composite simulated. The direct interconnection between sand particles eventually established the force chains in the composite, resulting in an initial phase of deformation. Consequently, a denser structure has been established as a result of particle repositioning and filling the pores of the composite by sand and finer components.

ACKNOWLEDGMENTS

I wish to express my sincere appreciation to those who have contributed to this PhD thesis and supported during this amazing journey.

I would like to express my deepest appreciation to my supervisor, Prof. Hamid Nikraz, for his support, guidance and encouragement.

I would like to express my gratitude to Dr An Deng and Dr Abbas Taheri for their valuable discussions, support and cooperation during this research study.

A tremendous and deep thanks to my lovely family. Words cannot express how grateful I am to Reza, Saeideh, Nastaran, Nasim, Houman, Mehdi and Hasti for all of the kindness, sacrifices, constant help and unconditional support that you've made.

A special thanks to my friends, for listening, offering me advice, and supporting me through this entire study.

Last, but not least, I would like to thank my beloved Dorsa for her encouragement, support and love.

DEDICATION

To

My parents.

Reza and Saeideh.

The angles of my life.

The reason for my existence.

To their endless love, sacrifices, and support.

To

My Dears,

The shining stars of my life,

Nastaran, Nasim, Houman, Mehdi, Hasti

To

My Love,

My Dorsa.

LIST OF CONTENTS

DECLARATION.....	II
ABSTRACT	IV
ACKNOWLEDGMENTS	IV
DEDICATION.....	V
LIST OF FIGURES.....	14
LIST OF TABLES.....	24
LIST OF ABBREVIATIONS	26
CHAPTER1	29
1.1 Introduction	30
1.2 Research Significance	31
1.3 Scope of Work.....	32
1.4 Thesis Outline	34
CHAPTER 2	36
2.1 Introduction	37
2.2 Background Study	38
2.3 A SUMMARY OF LITERATURE	54
CHAPTER 3	55
3.1 Material Selection	56
3.1.1 Sand	56

3.1.2	Rubber.....	57
3.1.3	Portland Cement	58
3.1.4	Slag	59
3.2	Composite Preparation.....	59
3.3	Method and Techniques	63
3.3.1	Experimental Program	63
3-3.2	Microanalytical/ Elemental Observation	67
	SEM (Scanning Electron Microscopy):.....	67
	EDS (Energy-dispersive X-ray spectroscopy):	68
3-3.3	A Summary of Experimental Plan.....	68
CHAPTER 4	71
4.1	Introduction	73
4.2.	Materials and Methods.....	75
4.3	Result and Discussion	77
4-3-1:	Minimum Void Ratio (e_{min})	77
4-3-2:	Small Scale Direct Shear Tests	79
4-3-2-1:	Shear stress-shear strain	80
	I- ST.....	83
	II- STvsR.....	83
	III- STR10	85
	IV- STR20	86
	V- Overall view of mixture shear-strain behaviour	87
4-3-2-2:	Strain capacity behaviour	89
	I- Tangent shear modulus	89
	II- Secant shear modulus.....	92
	III- Volumetric behaviour	97
4-4:	Analysis of Results	107
4-4-1:	Effect of Normal Stress on Peak Shear Strength	107
4-5:	Conclusion.....	114

CHAPTER5	116
5-1: Introduction	119
5-2: Material and Methodology	122
5-3: Results and Discussions	123
5-3-1: Compaction Test	123
5-3-1-1: Maximum Dry Density and Optimum Moisture Content	124
5-3-1-2: Floating and non-floating cases	128
Brief summary... ..	132
5-3-2: Large Direct Shear Test Results.....	133
Brief summary... ..	138
5-4: Large Direct Shear Versus Small Direct Shear	138
5.4.1 Shear Stress–Shear Strain.....	139
Brief summary... ..	141
5.4.2 Shear Modulus	142
Brief summary... ..	143
5.4.3 Maximum Friction Angle	143
5.4.3.1 Scale effect on the maximum friction angle	144
Brief summary... ..	146
5.4.3.2 Peak friction angle and maximum dry density	147
Brief summary... ..	151
5.4.4 Constant Volume State Friction Angle	152
5.4.4.1 Scale effect on the constant volume state friction angle	152
Brief Summary... ..	154
5.4.4.2 Constant volume friction angle and maximum dry density.....	155
Brief Summary... ..	157
5.4.5 Volumetric Strain.....	158
Brief Summary... ..	160
5.4.6 Angle of Dilation	161
Brief Summary... ..	163
5.4.7 Effect of Rubber Particles on Dilation Behaviour	164

5.4.8 Analysing Dilation Ratio	166
Brief Summary... ..	170
5-5 Maximum Dilation Angle.....	170
5-5-1 Maximum dilation angle and peak friction angle.....	170
Brief Summary... ..	175
5-5-2 Empirical Equation for Maximum Dilation Angle.....	175
Brief Summary... ..	179
5.5.3 Constant Volume Friction Angle	179
Brief Summary... ..	183
5.5.4 Stress–Dilation Law	183
Brief Summary... ..	186
5.6 Cohesion.....	187
5.6.1 Comparison of Apparent Cohesion in Large and Small Scales.....	187
5.6.2 Relationship Between Apparent Cohesion and Maximum Dry Density	188
Brief Summary... ..	190
5.6.3 Shear Strength Improvement Index (C_i).....	192
Brief Summary... ..	194
CHAPTER6	196
6-1: Introduction	199
Shear Behaviour	201
Strain Behaviour	202
Compressibility Behaviour.....	202
6-2: Material and Experimental Methodology.....	204
6-3: Result and Discussion	206
6-3-1: One-Dimensional Consolidation Test	206
6-3-1-1 Compression and recompression indices.....	206
6-3-1-2 One-dimensional elastic modulus	212
6-3-1-3 Classification the compression evolution of composites.....	217
6-3-2: Consolidated-Undrained Triaxial Test	222

6-3-3-1 Effect of the ratio of additives on the deviatoric behaviour	223
6-3-3-2 Effect of the confining pressure	228
6-3-3-3 Maximum principle stress ratio	232
6-3-3-4 Analysing the shear strength characteristic	234
6-3-3-4 Young's modulus	235
6-4: Compression and Analysis the Results of Triaxial Tests and Direct Shear Tests	237
6-4-1: Assessing the Intrinsic Constants for Shear Strength.....	237
6-4-2: Experimental Data of Sand Composites	237
6-4-3: Regression Model.....	238
6-5: Microstructural Analysis of the Cemented Sand-Rubber Composite ..	245
6-5-1: Material Characteristics and Phases of the Composite.....	245
6-5-2: Microstructure of Composite	246
6-5-2-1: Cementitious binders.....	247
6-5-2-3: effect of rubber particles on cementitious binders	250
6-5-2-3: Pore structure	252
6-5-2-4: Interfacial Transition Zone (ITZ).....	254
6-5-3: Potential of rubber and slag to create a high-performance composite .	256
6-5-3-1: Characterisation of composites components	256
6-5-3-2: Slag.....	257
6-5-3-3: Effect of slag on cemented sand composite.....	260
6-5-3-4: Effect of rubber on alkali-silica reaction in cemented sand composite	262
.....	
To sum up briefly.....	266
6-5-4: A Physical Model of Failure in Composite	268
6-5-4-1: Mechanism of deformation and binary medium theory	268
CHAPTER7	273
7.1 Summary of Conducted Research.....	274
7.1.1 An Overview of Soil Reinforcement and Conducted Methodology	275
7.1.2 A Summary of Fundamental Experiment Results	276

7.1.3	A Summary of Small Direct Shear Test Results	277
7.1.4	A Summary of Large Direct Shear Test Results	278
7.1.5	A Summary of Compressibility Test Results.....	281
7.1.6	A Summary of Triaxial Test Results	283
7.1.7	A Summary of Microstructural Study	284
7.2	Recommendation and Future Study	286
7.2.1	Recommendation	286
7.2.2	Further Performed Research.....	287
References:		288
Appendix		296
	Compaction test results	297
	Small direct shear results	303
	Large direct shear results	311
	One-dimensional consolidation test results.....	317
	Triaxial test results.....	318

LIST OF FIGURES

Figure 3- 1.Selected material for this research study.	56
Figure 3- 2. Particle size distribution results of selected sand.....	57
Figure 3- 3. Selected rubber buffing	58
Figure 3- 4. Particle size distribution results of selected rubber.....	58
Figure 3- 5. Small direct shear device.....	63
Figure 3- 6. Large direct shear device.....	65
Figure 3- 7. One-dimensional consolidation device.....	66
Figure 3- 8. Automatic triaxial tests system.	67
Figure 3- 9. Evo 40XVP scanning electron microscope.	68
Figure 3- 10. Summary of the performed standards in experimental program.....	69
Figure4- 1. Maximum density of pure sand, sand-additives and pure rubber	78
Figure4- 2. Minimum void ratio of pure sand, sand-additives and pure rubber	79
Figure4- 3. Typical shear stress plot of 18 sand composites at normal stress 500kPa.	81
Figure4- 4. The shear stress plot of sand and stabilised sand with cement, slag and cement-slag.....	83
Figure4- 5. The shear stress plot of sand and stabilised sand with stabilisers and rubber only.....	84

Figure4- 6. The shear stress plot of sand and mixing with 10% rubber.....	86
Figure4- 7. The shear stress plot of sand and mixing with 20% rubber.....	87
Figure4- 8. Summary of peak shear strength value of sand mixtures at a normal stress of 500kPa.....	87
Figure4- 9. Summary of shear resistance behaviour of sand mixtures at a normal stress of 500 kPa.....	88
Figure4- 10. Variation of shear modulus of treated and untreated composites.	90
Figure4- 11. Variation of obtained yielding strain and additives content.	91
Figure4- 12. Initial tangent shear modulus showing the effect of additive on sand stiffness.....	92
Figure4- 13. Variation of shear modulus at the failure point under six normal stresses.....	93
Figure4- 14. Shear strain of composites at their failure point.	94
Figure4- 15. Shear modulus at constant volume.....	95
Figure4- 16. The difference between the shear stress at the failure and shear stress at the constant volume state.....	96
Figure4- 17. The variation of volumetric strain with shear strain for pure sand and treated sand at a normal stress of 500 KPa.	98
Figure4- 18. The variation of dilation ratio of treated and untreated composites..	99

Figure4- 19. A typical plot for the failed envelope of sand composites with the variation of additives.	108
Figure4- 20. A schematic drawing of failure envelope for soil. The slop of dot line shows friction angle at the critical state.....	110
Figure4- 21. The variation of cohesion for sand and treated sands obtained from failure envelope graph	110
Figure4- 22. The friction angle of sand and sand treaded composites	111
Figure4- 23. Variation of the critical state friction angle of sand and treated sand composites.	112
Figure4- 24. Variation of dilation angle of 18 samples.....	113
Figure5- 1. Compaction results of pure sand and of sand reinforced with cement and slag.....	124
Figure5- 2. Compaction results of the pure sand and of sand with 10% rubber and different proportions of cement and slag.....	125
Figure5- 3. Compaction results of pure sand and of sand with 20% rubber and different proportions of cement and slag.....	126
Figure5- 4. Results of standard compaction tests conducted on pure sand and a variety of sand mixtures.	127
Figure5- 5. Schematic representation of soil with a floating case (a) and a non-floating case (b), adapted from (Fragaszy et al., 1990).....	128
Figure5- 6. Generation of the non-floating case upon the addition of 10% rubber to sand (a) and 20% rubber to sand (b).....	129

Figure5- 7. Schematic representation of the void ratio arrangement of the binary packing of materials which was used for calculating the void ratio in the compaction test in the floating and the non-floating states (Fragaszy et al., 1990, Lade et al., 1998).....	131
Figure5- 8. Shear stress–horizontal displacement of the sand with and without the rubber addition at 50-kPa and 250-kPa normal stress.	133
Figure5- 9. Shear stress–horizontal displacement of the sand with and without the stabiliser addition at 50-kPa and 250-kPa normal stress.	134
Figure5- 10. Shear stress–horizontal displacement of the different mixtures of STR10 and STR20 at 250-kPa normal stress.....	135
Figure5- 11. Shear envelopes for a large direct shear test of treated and untreated sand composites.	137
Figure5- 12. Shear stress against the shear strain of sand mixtures, obtained from the small and large direct shear tests at 500-kPa normal stress.	140
Figure5- 13. Secant shear modulus at the failure points of sand composites versus shear strain.	142
Figure5- 14. Friction angle of sand and the treated samples for the peak shear stress in the large direct shear test, compared with the results of the small direct shear test.	145
Figure5- 15. Internal friction angle of sand and treated sand composites at the failure point versus the maximum dry density, where ST, STR10 and STR20 are representative of all the composites of their classes.	150

Figure5- 16. Friction angle of sand and the treated samples in the constant volume state in the large direct shear test, compared with the results of the small direct shear test.	153
Figure5- 17. Internal friction angle of sand and the treated sand composites at a constant volume versus the maximum dry density, where ST, STR10 and STR20 are representative of all the composites of their classes.....	156
Figure5- 18. Volumetric strain in the large-scale (LDS) and small-scale (SDS) cases versus the shear strain for pure sand and the treated sand for a normal stress of 500 kPa until the failure point.	159
Figure5- 19. Angle of dilation of sand and the treated samples for the constant volume state in the large direct shear test, compared with the results of the small direct shear test.....	162
Figure5- 20. The experimental observation from the direct shear test using a composite with 20% rubber. The arrow shows the lower box movement.	164
Figure5- 21. Schematic representation of particle movements in the direct shear test(Bareither et al., 2008).	165
Figure5- 22. Illustrative directions of the state of stresses and the zero extension lines (Roscoe, 1970a, Veiskarami et al., 2011).....	166
Figure5- 23. Dilation ratio versus the horizontal strain of small direct shear tests for the pure sand and the reinforced sand specimens.	168
Figure5- 24. Dilation ratio versus the horizontal strain in the large direct shear tests for the pure sand and the reinforced sand specimens.....	169

Figure5- 25. Results of the maximum dilation angle and the peak friction angle of sand composites obtained on the basis of the composite categories under various normal stress values: (a1) and (a2) ST class; pure sand and a mixture of sand and stabilisers; (b1) and (b2) STR10; sand with 10% rubber and a combination of 10% rubber and stabiliser; (c1) and (c2) STR20; sand with 20% rubber and a combination of 20% rubber and stabiliser. 174

Figure5- 26. Variation of peak friction angle to determine the constant volume friction angle for untreated and treated sand matrices. 178

Figure5- 27. Results of the constant volume friction angle versus the normal stress of sand composites based on the composite categories: (a) ST class; pure sand and mixture of sand and stabilisers; (b) STR10; sand with 10% rubber and a combination of 10% rubber and stabilisers; (c) STR20; sand with 20% rubber and a combination of 00% rubber and stabilisers. 181

Figure5- 28. Stress–dilation law explaining the correlation between $\varphi'_{\text{peak,ds}}$ – $\varphi'_{\text{cv,ds}}$ and ψ_{max} for (a)sand plus stabilisers;(b)sand plus 10% rubber and stabilisers;(c sand plus 20% rubber and stabilisers. 185

Figure5- 29. Cohesion of pure sand and treated sand samples in the large direct shear test, compared with the results of the small direct shear test..... 187

Figure5- 30. Cohesion of pure sand and treated sand composites versus the maximum dry density, where ST, STR10 and STR20 are representative of all the composites of their classes..... 189

Figure5- 31. Cohesion values of the treated and the untreated composites at the peak and at the constant volume state and their difference. 190

Figure6- 1. Vertical effective stress against void ratio for loading and unloading stages for pure sand and stabilised sand composites.....	207
Figure6- 2. Compression index versus maximum dry density of sand mixtures.	209
Figure6- 3. Swell index versus amount of untreated and treated sand composites.	211
Figure6- 4. Coefficient of volume compressibility of sand composites for loading phase of consolidation test.....	213
Figure6- 5. One-dimensional elastic modulus of treated and untreated sand composites.	214
Figure6- 6. One-dimensional elastic modulus correlation ,deduced for sand composites with different RF.....	216
Figure6- 7. Compression curves of the lightly cemented sand composite with the 0%RF, 10% RF and 20% RF.	219
Figure6- 8. Normalised strain of the composites with the 0%RF, 10% RF and 20% RF.	221
Figure6- 9. Relationship between residual strain and rubber fraction of the cemented and uncemented sand composites.	222
Figure6- 10. Effect of the rubber and cement on the deviatoric stress results of sand composites at the confining pressure 50kPa.	224
Figure6- 11. Failure patterns of sand composites; (a) shear banding, (b) and(c) bulging failure.....	225

Figure6- 12. Effect of the rubber and cement addition on the peak deviator stress of sand mixtures.	226
Figure6- 13. Effect of rubber content on the cemented and uncemented sand mixtures strain failure.....	228
Figure6- 14. Effect of confining pressure on the deviator stress of cemented sand with 10% and 20% rubber.	229
Figure6- 15. Peak deviator stress versus confining pressure of sand composites.	230
Figure6- 16. Effect of confining pressure on the axial strain at failure of sand composites.	231
Figure6- 17. Maximum stress ratio results of sand composites at different confining pressures.	232
Figure6- 18. Summary of shear failure envelopes result of sand composites.....	235
Figure6- 19. Young's modulus results of sand composites obtained from triaxial and consolidation tests.	236
Figure6- 20. Comparison of predicted intrinsic constants and examined data of small direct shear test: a) τ_p , b) τ_{cv}	240
Figure6- 21. Comparison of predicted intrinsic constants and examined data of large direct shear test: a) τ_p , b) τ_{cv}	242
Figure6- 22. Comparison of predicted intrinsic constants and examined data of triaxial test: a) τ_p , b) τ_{cv}	244
Figure6- 23. EDS line spectrum results for cement (a) and sand (b).	248

Figure6- 24. Schematic illustration of the interaction among a cement particle surrounded by air bubbles((Du and Folliard, 2005).	250
Figure6- 25. Schematic representation of rubber application in cemented composite; (a) cemented particles, (b) cemented-rubber particles (Du and Folliard, 2005, Hilal, 2016).	251
Figure6- 26. Typical dimensional range of possible pores in a composite (Monteiro, 2006).	253
Figure6- 27. Secondary electron image of slag.....	254
Figure6- 28. Schematic illustration of the interfacial transition zone in a composite (Monteiro, 2006, Hilal, 2016).	255
Figure6- 29. Scanning electron micrograph of; (a) sand, (b) rubber.	257
Figure6- 30. EDS line spectrum results for slag.	260
Figure6- 31. SEM micrograph results for cemented sand composite.	261
Figure6- 32. SEM micrograph results for effect of slag addition on cemented sand composite.	262
Figure6- 33. SEM micrograph results for cemented sand-rubber composite.	264
Figure6- 34. SEM micrograph results for effect of slag addition on cemented sand-rubber composite.	266
Figure6- 35. Micro-fabric of the cemented sand-rubber composite: a) without slag; b) with slag.....	267

Figure6- 36. Schematic diagram of mechanical response: (a) mechanical elements,
(b) binary-medium hybrid unit (Shen, 2006)..... 269

Figure6- 37. SEM micrograph results of cemented sand-rubber composite. 270

Figure6- 38. Schematic presentation of deformation mechanism of cemented sand-
rubber mixture (Zhang et al., 2016) 272

LIST OF TABLES

Table2- 1. Laboratory tests results of sand-rubber mixtures.	41
Table3- 1. Chemical composition of Portland cement.	59
Table3- 2. Chemical composition of slag.	59
Table3- 3. Specific gravity results of soil composites.	62
Table3- 4. Summary of the thesis program.	70
Table4- 1. Properties of materials. Cu: Coefficient of Uniformity, Gs: Specific gravity.	76
Table4- 2. The results of small direct shear test.	101
Table5- 1. Properties of materials. Cu: Coefficient of Uniformity, Gs: Specific gravity.	123
Table5- 2. Results of the standard compaction tests of the treated and the untreated sand composites.	132
Table5- 3. Definition of the three categories of composites divided by their maximum dry density.	148
Table5- 4. Summary of the correlation between the friction angle and the maximum dry density for three categories of composites: Loose, Medium and Dense.	157
Table5- 5. Summary of the obtained equation for three categories of composites: loose, medium and dense.	186

Table5- 6. Summary of the obtained equation for the cohesion of three categories of composites: loose, medium and dense. Cohesion of the treated and the untreated sand composites.	191
Table5- 7. Summary of shear strength improvement index (Ci) for the peak shear stress of reinforced sand composites, obtained from the large and small direct shear tests.	195
Table6- 1. Material properties. Cu: Coefficient of Uniformity, Gs: Specific gravity, ρ_{min} : minimum density, ρ_{max} : maximum density.....	206
Table6- 2. Definition of the three categories of composites divided by their maximum dry density.	208
Table6- 3. Summary of consolidation tests results, performed on the untreated and treated sand composites.	212
Table6- 4. Summary of coefficient of volume compressibility and the one-dimensional elastic modulus of composite obtained from the consolidation tests.	215
Table6- 5. Modulus of elasticity for granular soils(Das, 2013).	217
Table6- 6. Results of optimum moisture content of the treated and the untreated sand composites	249

LIST OF ABBREVIATIONS

ψ	angle of dilation
φ_{cv}	angle of friction at constant volume state
β'	apparent cohesion of the soil at the constant volume
$\varphi'_{peak, ds}$	maximum dilation angle at failure
G_o	bulk specific gravity of the oversized particles
N	coefficient of the dilation angle
C_u	coefficient of uniformity
m_v	coefficient of volume compressibility
C_{cm}	cohesion of cementation
C	cohesion of soil
C_t	Cohesion of tension
C_r	cohesion of the reinforced sand
Cc	compression index
φ'_{cv}	constant volume friction angle
ρ_m	density of the matrix soil
ρ_t	density of the total material
σ_d	deviator stress
q	deviatoric stress
φ'_{ds}	direct shear friction angle
ρ_o	dry density of the oversized particles
EDS	Energy-dispersive X-ray
β	friction angle of the composite at zero dilatancy
φ_r	friction angle of the reinforced sand
h	horizontal displacement
Δl	horizontal displacement
γ	horizontal shear strain
S_c	initial settlement
G_i	Initial tangent shear modulus
ITZ	interfacial transition zone
C_0	intermolecular force
LDS	large direct shear
ρ_w	mass density of water
P	mass of the oversized particles
M_m	matrix mass
V_m	matrix volume
φ_p	maximum angle of friction
ρ_{max}	maximum density
ψ_{max}	maximum dilation angle at the failure
MDD	maximum dry density

γ_d	maximum dry density
σ_1	maximum principle stress
G_{\max}	maximum stiffness modulus
$\left(\frac{dv}{dh}\right)_{\max}$	maximum value of the dilation ratio
p	mean effective pressure
ρ_{\min}	minimum density
P_c	minimum fraction
σ_3	minimum principle stress
e_{\min}	minimum void ratio
$\sigma'v$	Normal effective stress
σ	normal stress
E'_{oed}	one-dimensional elastic modulus
OMC	optimum moisture content
M_o	oversized particles mass
V_{so}	oversized particles volume
D_{10}	particle size (diameter) for which 10% of the particles are smaller
D_{60}	particle size (diameter) for which 60% of the particles are smaller
τ_p	peak value of the shear strength
$\varphi'_{cv,ps}$	plane strain constant volume friction angle
φ'_{ps}	plane strain friction angle
ε_r	residual deformation
RF	rubber fractions
SEM	scanning electron microscope
G	shear modulus
C_i	shear strength improvement index
τ	shear stress
SLR	simple linear regression
SDS	small direct shear
G_s	specific gravity
G	stiffness modulus
C_s	swell index
G_{\tan}	tangent elastic modulus
G_{cv}	tangent shear modulus at the constant volume
G_f	tangent shear modulus at the failure point
dh	the variation of the horizontal displacements
dv	the variation of the vertical displacements
M_t	total mass
V_t	total volume
v	vertical displacement
ε	vertical strain
e	void ratio

ϵ_v	volumetric strain
E	Young's modulus

CHAPTER1
INTRODUCTION

1.1 INTRODUCTION

Around 29 million waste tires or 230,000 tonnes of materials per year are generated in Australia (Australian Tyre Recyclers Association 2006). However, the specific characteristics of rubber tire including; resilient, lightweight and skin-resistive led to use the tire to find a possible sustainable environmentally solution. Rubbers can be used as one of the most reusable waste materials in earth backfills (Edinçliler et al., 2010). The backfill is generated by solidifying soil mass by addition of the percentage of cementitious materials, like cement, fly ash or lime, which are mostly reinforced with geofabrics to improve the stability of infrastructure buildings for which kinds of rubber tires are expected to substitute (Ahmed and Lovell, 1993, Edil and Bosscher, 1994, Zornberg et al., 2004, Tsoi and Lee, 2011, Guleria and Dutta, 2011). In general, tire shreds, tire crumb and tire chips in primary and secondary shredding process, and tire buffings as the by-product are processed. However, regarding the small diameter and the fiber shape of buffings, it is identified as a perfect additive for stabilising the composite material with soil. The integrity, strength, ductility and damping ratio of the backfill can be improved by the solidified cement matrix and altered fabric structure (Lee and Lui, 2000, Shahin et al., 2011, Tsoi and Lee, 2011, Anastasiadis et al., 2012). However, before the technology can be deployed, more research is urgently needed. The mechanical response of rubber soil can be understood if the effects of both structural and friction characteristics are taken into account, which acts a role as important as that of initial void ratio and stress history for a naturally deposited soil. Therefore, the aim of this research is to measure and model the mechanical response of lightly cemented rubber buffing sand and expand the state of knowledge on the behaviour of the material, through a series of laboratory tests, observations and numerical simulation conducted on a series of samples at macro and meso scales and based on the knowledge of damage mechanics.

The term 'meso-scale' in this project refers to a scale larger than the grain scale (particle scale) but smaller than the sample scale (macro-scale), i.e., 1-10.0 mm, which is consistent with the terminology defined by Zaitsev and Wittmann (1981).

1.2 RESEARCH SIGNIFICANCE

This PhD study is designed to be performed in four experimental, numerical and microstructural sections. Four tasks were largely divided into three research streams in terms of investigating the effects of the addition of rubber and/or a stabilizer for sand reinforcement so as to determine an optimum combination of the stabilizer and rubber. Tasks 1-2, the observational scale used in the research, i.e. scale effect study for Tasks 2-3 and to verify the obtained data to propose a regression model based on the availability of input data Tasks 4. By performing Tasks 1-4, a numerical simulation was carried out for predicting the shear strength with different confining pressures. Specifically, an empirical equation, which is capable of predicting the shear intrinsic constants of sand-rubber composites is expected to be developed. The proposed equation accounted for the mechanical responses taken place in the matrix of rubber soil along with the progressive failure of the material and was validated from laboratory experiments based on macro- to mesoscale observations. The microstructural observation eventually explained deformation mechanism of composites. The specific aims include:

1. TO DEFINE A COMPREHENSIVE METHOD FOR GENERATING THE SAND RUBBER COMPOSITES.

The laboratory program was guided the selection of materials, proportions of mixture, technical requirements of both cemented and un-cemented sand-rubber, and thus lead to sustainable design of rubber soil in engineering practice.

2. TO DEFINE THE GEOTECHNICAL CHARACTERISATION OF RUBBER SOIL COMPOSITES.

The research was analysed the mechanical response of rubber soil, and to relate the lightly cemented structure of rubber soil to deformation, strength and progressive failure.

3. TO DEFINE A NUMERICAL MODEL FOR RUBBER SOIL COMPOSITES.

The model approximated the observed mechanical response of rubber soil and therefore the shear strength behaviour of composites has been predicted by a model.

4. TO DEFINE A MICROSTRUCTURAL ANALYSIS OF THE CEMENTED COMPOSITE.

To verify the capacity of proposed mixtures for generating a high performance composite the microstructural properties of both cemented and un-cemented sand-rubber specimens were precisely investigated by a series of micro-analytical investigations.

1.3 SCOPE OF WORK

The carried out research will benefit the geotechnical community by proving the suitability and sustainability of infrastructure systems that use rubber soil, as an element of backfill. By proving that the backfill composite possesses the appropriate mechanical response to make it a material superior to plain earthen backfill, the proposed project will prompt not only more use of waste rubber but further reduce the cost used to construct infrastructure systems and strengthen the sustainability of the systems. The implementation of this research will lead to an in-depth understanding of the mechanical response of rubber soil and a new modeling framework. Eighteen series of samples (18 mixtures of different proportions) were prepared by ascending degree of cementation, i.e., cement addition of 0%, 5% and 10% by weight, slag addition of 0%, 5% and 10% and the addition of rubber buffings of 0%, 10% and 20% by weight. Considering the carried out researches, the proportion of additives has been defined based on the applicability and feasibility of conducted research in industrial projects and type of selected rubber for this research.

The contributions are presented in more detail below:

Task 1: A series of geotechnical tests were performed to investigate the mechanical properties of sand-rubber composites by focusing on the following objectives:

- ✓ To study the effect of the normal stress, 108 small direct shear tests were undertaken with a variety of vertical loads.
- ✓ The importance of the void ratio (e) in composites behaviour was considered by applying the obtained minimum void ratio (e_{\min}).
- ✓ The soil composites were organised based on their specific criteria containing the type and dosage of additives.
- ✓ The composites were studied in terms of shear strength, shear strain and elastic behaviour parameters.

Task 2: The carried out study in Task 1 was evaluated by focusing on the following aims:

- ✓ The effects of the addition of rubber and/or a stabiliser for sand reinforcement will be rigorously investigated to determine an optimum mix of the stabiliser and rubber.
- ✓ The obtained results will then be compared with those of the small-scale tests to determine the scale effect on the composite behaviour.

Task 3: A series of triaxial tests were performed:

- ✓ To a comprehensive study, the results of small direct shear, large direct shear are compared with the triaxial test.
- ✓ To explore the key factors and material parameters that control the critical material behaviour of the rubber soil, such as deformation and failure criteria.

-
- ✓ The typical failure modes – rupture, bulging or shear band – will also be analysed, in order to approximate the progressive failure of the material.
 - ✓ The experimental data of small direct shear, large direct shear and triaxial are conducted to develop an empirical equation which is capable of predicting the shear intrinsic constants of sand composites.

Task 4: A series of microstructural investigation tests were performed:

- ✓ To investigate the microstructural properties of the composite, considering the similarity of the composite component with the high performance concrete.
- ✓ To evaluate the effect of slag and rubber as superplasticizers to improve the performance of the cemented composite.
- ✓ To evaluate the deformation mechanism accompanying with the binary medium model definition.

1.4 THESIS OUTLINE

This thesis is presented in seven chapters with the structure of the thesis illustrated in Figure 1.1. Results and discussion sections are separated into three chapters to precisely discuss the obtained result from a different point of view. To provide a comprehensive presentation, chapters 4, 5 and 6 are individually contained in the background study, as well as the methodology. Thus, chapter one to seven are correspondingly presented as follows:

Chapter 1 contains the introduction of this research, research objective and significance, the scope of work and thesis outline.

Chapter 2 contains a review of the literature relating to this research and a summary of the main conducted researches.

Chapter 3 explains the materials, the composite definition and the conducted techniques for experimental investigation on sand composites. The experimental plan which was performed to study the mechanical response of composite is also described in this chapter.

Chapter 4 contains a series of small direct shear tests conducted on eighteen mixtures including sand, sand rubber, sand stabilisers and sand-rubber-stabilisers composites that were investigated the rubber efficiency for sand reinforcement.

Chapter 5 contains a scale effect study by a series of large direct shear tests on fifteen mixtures to provide a more clear understanding of the small scale results, considering a comparison between cement and slag.

Chapter 6 contains a series of triaxial compression tests, which were performed on nine mixtures to verify the results of direct shear tests, proposing a numerical model for predicting the shear strength properties of the composite. Furthermore, a microstructural observation was evaluated the deformation mechanism of cemented composites.

Chapter 7 contains a summary of the conducted researches in addition to conclusions and recommendations.

CHAPTER 2
LITERATURE REVIEW

2.1 INTRODUCTION

Nowadays, growing population and industrial development are creating several major problems, one of which is environmental pollution (Edinçliler et al., 2010). In this field, rubber tires are known as one of the most problematic sources of waste material (Edinçliler et al., 2010). Regarding the enormous amount of generation and disposal process, a critical issue in all around the world is the requirement of space for storing and transporting scrap tires, and the resulting costs (Edinçliler et al., 2010). Providing an opportunity to waste material offers several advantages, which include: a) reduction in the damage of the natural resources, b) reduction of the disposal methods costs and c) minimising environmental issues (Cabalar, 2011, Ghazavi, 2004, Edinçliler et al., 2010, Yang et al., 2002, Anbazhagan et al., 2016, Zornberg et al., 2004, Hazarika and Yasuhara, 2007). Tires are not preferred for landfilling because of their large volume and resiliency 75% of a tire has void space; tires are not “flat-packed”, which rapidly fills a huge use up landfill area (Cabalar, 2011, Ghazavi, 2004, Edinçliler et al., 2010). These characteristics make waste tires such a huge problem while being landfilled. While, as the rubber is resilient, lightweight and skin-resistive they could be mostly used in earth backfill. There are about 28 million tires stockpiled in Canada, for an instant, of which about 30% are accumulated in landfills (Yoon et al., 2006, Dickson et al., 2001, Edinçliler et al., 2010). Moreover, in Europe, an estimated 3 million tons of tire waste are disposed of annually (Edinçliler et al., 2010). Disposing of this amounts of the waste tire in landfills cannot be a reasonable solution. However, a large amount of waste tire can be potentially used in the geotechnical projects (Cabalar, 2011, Ghazavi, 2004, Edinçliler et al., 2010, Yang et al., 2002, Anbazhagan et al., 2016, Zornberg et al., 2004, Hazarika and Yasuhara, 2007). Therefore, as the rubber is resilient, lightweight and skin-resistive, they could be mostly used in earth backfill (Edinçliler et al., 2010). Thus, the first aim of this chapter is to evaluate the mechanical characteristics of a variety of types of rubber products. Secondly, a summary of results from the conducted research are presented in Table2- 1.

2.2 BACKGROUND STUDY

To evaluate the application of rubber in soil stabilisation projects, the effectiveness of rubber addition on the strength characteristics of soil has been investigated by many studies (Yoon et al., 2006, Cabalar, 2011, Anvari et al., 2017, Anbazhagan et al., 2016, Christ and Park, 2010, Edil and Bosscher, 1992, Zornberg et al., 2004, Tsang et al., 2012, Hidalgo Signes et al., 2015, Attom, 2006, Bosscher et al., 1992, Humphrey et al., 1998, Dickson et al., 2001, Moo-Young et al., 2003, Yang et al., 2002, Ghazavi, 2004).

Earth backfill is a fundamental geomaterial that applied a diversity of infrastructure like embankments, retaining walls and bridge abutments. Moreover, the utilisation of rubber to soil reinforcement can be improved the stability of geotechnical infrastructures. Rubber soil is showing great promise in several aspects, such as decreased unit weight, improved integrity & strength and therefore stability, and facilitated production and placement of backfill. Studies are shown that tire shred inclusion of 10% by weight leads to the reduction of rubber soil unit weight by 10% (Deng and Feng, 2009), as well as reduction in self-weight of backfills. The reason is the ability of rubber soil in flow-able conditions through enabling to move into any irregular or inaccessible space without any remarkable compaction force (ACI Committee 229, 1999). The advantages of rubber soil in engineering applications that soil backfills rarely demonstrated are favourably promoting the sustainability of constructions. Generally, in primary and secondary shredding process used tires are processed to create tire shreds, tire crumb, and tire chips, and in contrast with those, the tire buffings are generated as the by-product of tire re-tread industry. The tire buffings production requires minimal energy, which is produced during the stripping process. The fiber-shaped tire is generated because of contact the surface of worn tires that are stripped of and resurfaced by rubber. Thus, the main purpose of application of tire buffing is utilising as an additive to improvement the soil geotechnical characteristics. A few researches have been carried out for comparing the shear strength parameters of tire buffing by performing the large direct shear tests (Edinçliler 2007, Edinçliler et al., 2004). The test results revealed that due to elongation of the tire buffing

the addition of 10% of tire enhanced the mechanical properties of the material, by increased the cohesion, internal friction angle, and improvement in the compactibility of the soil-tire interface.

However, It can be found a few studies on utilisation of rubber buffing in soil application. Instead of that, research mostly carried out on other types of rubber in geo-base materials. Scholars reports are unanimously shown that inclusion of the even small amount of rubber tire improved both the shear strength and ductility of soils over that measured for the same soil with an identical rubber tire. Nevertheless, they just studied from a laboratory experimental aspects(Masad et al., 1996, Lee et al., 1999, Youwai and Bergado, 2003, Ngo and Valdes, 2007, Özkul and Baykal, 2007, Valdes and Evans, 2008, Kim and Santamarina 2008, Deng and Feng, 2009 and 2011, Lee et al., 2010, Shahin et al., 2011 , Tsoi and Lee, 2011). And also there are a few investigations were conducted on other geotechnical field including; highway embankment, retaining wall and numerical analysis of sand-rubber mixtures (Shalaby and Ahmed Khan, 2002, Humphrey 2007, T Tanchaisawat et al., 2008, Tweedie et al.1998, Garga and O'shaughnessy, 2000, Humphrey 2007, Valdes and Evans, 2008, Huggins and Ravichandran, 2011).

Furthermore, rubber soil usually substantially improved through the addition of a few dosages of cement. It can improve the unconfined compressive strength of soil from about 100 kPa to 400-700 kPa by addition of 5-8% cement (Tsoi and Lee, 2011). The cementation may also lead a cemented blend to a significant enhancement of extensile strength, like 100 kPa on average through the addition of 10 percent of cement addition of 10% (Airey, 1993). Moreover, rubber soil may undergo a unique failure model, as it illustrates in Fig. 1, the deformation continues towards the failure state, the cemented particles break apart around contacts, thereby the shear resistance finally come into effect through the friction resistance generated at particle contacts. In general, the structural uniqueness of rubber soil may lead to outstanding mechanical characteristics at the experimental tests.

There were very limited researches (Tsoi and Lee, 2011) performed to study to develop a constitutive model through laboratory results of rubber cemented soil- tire shred. Of the prior investigation (Tsoi and Lee, 2011) addressing modeling behaviour of rubber soil, the mechanical response of the materials has not been approximated precisely. Aside from the complexity and variability of mixture property, one of the important reasons of unsatisfactory modelling is the negligence of the structural characteristics of rubber soil, which are rarely accounted for in the current widely used models, such as the hyperbolic model (Duncan and Chang, 1970) and the Cam-clay model (Schofield and Wroth, 1968). This means that the elastoplastic hypothesis, which is assumed for a soil mass, is not firmly applicable to depict the mechanical response of rubber soil. The inconsistency in assumption may be ascribed to the inherent uniqueness of the material.

It may be quite straightforward for one to simply introduce a modeling approach addressing continuum solids, e.g., soft or hard rock, concrete or even steel, to describe the behaviour of rubber soil. The lightly cemented structure of rubber soil, however, unlike the heavily bonded and brittle structure of rocks, concrete and metals, rarely works in serious extension or bending states (Hill, 1963), but involves a gradual degradation of bond or loss of structure and an escalating activation of friction with a further strain, which behaves similar to the means of structural soil (Leroueil and Vaughan, 2009, Tsoi and Lee, 2011). Therefore, the rubber soil is not an ideal stiff solid medium and cannot be modeled under the framework suitable for rock or concrete and also difficult to be modeled by the current theories that have been based on the concept of a discrete, homogeneous and elastoplastic medium of small-strain. Table2- 1 presents a summary of laboratory research conducted on sand-rubbr mixtures.

Table2- 1. Laboratory tests results of sand-rubber mixtures.

Reference	Objective and methodology	Test Result
Yoon et al., (2006)	<p>Estimating the application of tire shred-sand mixtures (i.e. 50/50 mixture, by volume) as a fill material in embankment projects.</p> <p>To investigate the settlement behaviour, environmental effects on groundwater quality and a temperature deviation inside the embankment.</p>	<p>Research results revealed that the advantages of sand-tire shreds mixture such budget-friendliness, compactness, free-draining, relatively incompressible and environmental aspects in embankment projects.</p>
Yoon and Abu-Farsakh, (2009)	<p>A series of unconfined compression tests conducted on the sand specimens combined with 8%, 10%, and 12% were cured for seven days. The research was performed to evaluate the effects of moisture content, dry density, the water-cement ratio, and cement content on the strength of cement-sand.</p>	<p>The results indicated that the dry density, moisture content, water-cement ratio, initial void ratio, and cement content are the key parameters to define the strength behaviour of cemented sand mixtures.</p>
Fragaszy et al., (1990)	<p>To evaluate the effect of oversize particles on the compaction, strength and deformation characteristics of the soil, and define its identical model.</p>	<p>The results reveal that oversize particles increase the void ratio of the soil matrix and consequently reduce the relative density of the soil. The laboratory results also suggest that the relative density of the soil matrix is related to the density of the soil around the oversize particles.</p>
Lade et al., (1998)	<p>A series of experimental tests are conducted to evaluate the minimum and maximum void ratios of the variation of sands with different particle size distributions.</p>	<p>The results show that the fine content serves a key role to estimate the sand structure and its related maximum and minimum void ratio. The results also indicate the effectiveness of fine material on the static</p>

		liquefaction potential and compressibility behaviour of the sand.
Cabalar, (2011)	Direct shear tests were conducted to evaluate the effect of rubber particles on the shear strength of sand combined with four different dosages of shredded rubber content (i.e., 5, 10, 20 and 50% by dry weight).	The results show that internal angle of friction and shear strength of sands mixtures are reduced by increasing the dosage of rubber particles.
(Ghazavi and Sakhi, 2005)	The effect of shreds tire shape on the shear resistance of sand-shred specimens has been studied by conducting large direct shear tests. Sand-rubber composites were prepared with two different compaction levels and various percentages of rubber (i.e., 0% 15% 30% and 50%). Tire shreds were made in three widths of 2, 3, and 4 cm and different lengths for each shred width to evaluate the effect of aspect ratio on the shear characteristic of samples.	The results suggest that the shear strength properties of the specimens can be affected by the shred contents, its width, aspect ratio for a given width, compaction, and normal stress. The friction angles of mixtures relatively increase by increasing the rubber content ratio and composite compaction.
Edinçliler et al., (2010)	Large direct shear tests are conducted to estimate the shear strength of various dosages of tire crumb-sand composites. Tire crumb with various dimensions (i.e., between 1 and 3 mm) was mixed with sand to create composites contain 0%, 50%, 10%, 20% and 30% rubber.	The results indicate that shear strength properties of sand increases by adding a tire to the sand. The result also suggested that shear strength properties of sand-tire mixtures are remarkably related to the three parameters including normal stress, processing methods, and tire content.
Anvari et al., (2017)	60 direct shear tests were performed on sand granulated rubber specimens having different rubber content (i.e.,	The results reveal that shear strength of sand specimens at medium density are increased by adding rubber particles at the

	0%, 5%, 10%, 20% and 30%). Sand mixtures were studied by various relative densities (50, 70 and 90%) at different normal stresses of (34.5, 54.5, 74.5 and 104.5 kPa).	lower normal stress. Moreover, this improvement is associated with rubber content, the density of sample and normal stress. The results also suggested that the ductility and flexibility of mixture increased by increasing rubber content.
Anbazhagan et al., (2016)	<p>The effect of granulated rubber sizes and tire chips on the shear strength properties of the sand-rubber mixture has been studied by performing large direct shear tests on two different gradations of sands.</p> <p>Also, the effect of granulated rubber on shear strength behaviour of dry sand has been evaluated by investigating peak shear strength, cohesion, friction angle, secant modulus and volumetric strain.</p>	<p>The result suggested that granulated rubber and tire chips sizes, rubber content and normal stress are the main effective factors on the shear strength properties of the composite.</p> <p>The results also revealed that the peak shear strength of sand remarkably increased by using an optimum size and dosage of rubber particles. Thus, the most strengthened composite has been generated by using 30% of granulated rubber size VI with sand.</p>
Christ and Park, (2010)	To investigate the strength characteristics of frozen rubber-sand composites, a series of uniaxial compressive strength, direct tensile strength, and direct shear strength tests have been performed on sand-rubber mixtures with various dosages of rubber (i.e., 0%, 10%, 15%, 20% and 30%) at low temperatures.	The results indicated that the strength properties of sand-rubber mixtures were affected by rubber content and temperature. Reducing temperature caused to increase the strength properties of sand and sand-rubber specimens, accompanied by a reduction in the subfreezing temperature. However, increasing the rubber content in the sand decreases the strength of the mixture. The results of compaction tests and minimum void ratio suggested that 15% rubber was the optimum dosage to create the sand-rubber mixture. Subsequently, the composite

		with the highest strength capacity was obtained by a lower dosage of rubber and subfreezing temperature.
Zornberg et al., (2004)	To evaluate the optimum content and aspect ratio of tire shreds a series of experimental tests have been performed by large triaxial device. The testing program also studied the effect of confining pressure and relative density on the shear strength of sand-rubber mixtures.	The results revealed that shear strength behaviour of the mixture was affected by tire shred aspect ratio and tire content. In addition, an increase in the axial strain at failure was obtained by increasing the dosage of rubber in the mixture. Increasing the shred aspect ratio leads to the improvement in shear strength, where the optimum tire-sand ratio was found about 35% in the mixture. The confining pressure was found to influence the shear strength behaviour of the composite which is reduced by an increase in the confining pressure.
Hidalgo Signes et al., (2015)	A series of experimental and field tests were conducted to study the properties of a combination of rubber particles and coarse aggregates to use in a sub-ballast layer in the railway lines.	The results indicate that the resistance of coarse aggregates improved by the addition of rubber particles up to 10% by weight. However, the optimum rubber content was found 5% for improving the bearing capacity of the mixture.
Ghazavi, (2004)	The shear strength properties of sand mixed with a various dosage of granular rubber (i.e., 0%, 10%, 15%, 20%, 50%, 70% and 100% by weight) are evaluated by performing direct shear tests. To evaluate the effect of compaction states on the shear strength behaviour,	The results reveal that the shear strength behaviour of the sand-rubber mixture was influenced by normal stress, mixture unit weight, and rubber content. The result also suggested that neither the rubber content nor the compaction states altered the initial friction angle of the mixture. However, the results

	the specimens were compacted in a loose and slight state.	indicate the presence of apparent cohesion in the composite.
Yang et al., (2002)	<p>The mechanical properties of tire chips, ranging from 20 mm to 10 mm were studied by performing confined compression, direct shear, and triaxial tests.</p> <p>The obtained results were synthesised with the data from carried out researches to establish a method to quantify the shear strength and stress-strain response of the tire materials.</p>	The results show that the shear strength behaviour of the shredded tire cannot be affected by tire size. The shear strength envelopes behaved as a power function for applied the normal stress. However the lateral strain ratio is not influenced by the confining pressure. The initial tangent modulus and confining pressure revealed a quadratic equation relationship.
Moo-Young et al., (2003)	A series of large direct shear and large compression tests have been performed to evaluate the mechanical characteristics of tire shreds for use in geotechnical projects.	The results revealed that specific gravity was constant by increasing the size of tire shreds. However the hydraulic conductivity improved from 0.2 to 0.85 cm/s. The results also suggested that the final compaction density was slightly affected by compaction energy. Moreover, increasing the tire shreds size from 50 to 300mm improved the shear strength and compressibility properties of scrap tire.
Attom, (2006)	Direct shear tests were conducted to evaluate the effect of shredded tires on the mechanical properties of three diverse types of sand. Sand specimens were mixed with a variation dosage of rubber 10%, 20%, 30% and 40% by dry weight.	The results show that the angle of internal friction and shear strength of sand mixture improved by adding shredded tire. Moreover, the shear strength characteristics of sand mixtures are improved by increasing the initial dry density of the mixture.

A. Bernal et al., (1997)	A series of experimental tests including direct shear tests, interface direct shear tests, and Geo-synthetic pull-out tests in large scale were performed to evaluate the interaction characteristics of tire shreds and rubber-sand mixed with three types of flexible geogrids and a woven geotextile.	The results revealed that the coefficient of interaction values for tire shreds and rubber-sand mixtures are lower than that of the coefficient of interaction value for sand. Moreover, the results revealed the importance of coefficient of interaction values for designing the geosynthetic-reinforced earth structure containing a dosage of rubber. Increase in shear strength and a decrease in unit weight of sand was obtained by adding tire to the sand mixtures.
Simoni and Houlsby, (2006)	87 large direct shear tests have been conducted to study the strength and dilatancy behaviour of sand-gravel specimens. Research conducted to find a relationship between grain size properties of soil and shear strength resistance.	The results indicated that the shear strength behaviour of a specimen could be defined based on its relative density. Increasing the relative density of mixture causes an increase in the peak friction angle, constant volume friction angle, and dilatancy behaviour.
Hataf and Rahimi, (2006)	The bearing capacity of soil reinforced with shredded waste tire has been studied by conducting a series of experimental test. Five shred contents of 10%, 20%, 30%, 40% and 50% by volume with rectangular shape and aspect ratios of 2, 3, 4 and five were mixed by sand to prepare specimens.	The results show that bearing capacity ratio of sand was increased from 1.17 to 3.9 corresponding with dosage and aspect ratio of the shredded tire, where the maximum BCR is achieved by using 40% of rubber with dimensions of 3 x 12 cm. however, the results indicated an optimum dosage of shredded tire for increasing the BCR of sand.
Zhang et al., (2016)	This research presents the compression behaviour and stiffness characteristic of lightly cemented and	The test results indicated that sand fraction serves a key role in the mass density (ρ), stress-strain characteristics and

	<p>uncemented sand-rubber specimens. Sand specimens were mixed with a various dosage of rubber were simultaneously subjected to a diverse level of normal stress and shear wave velocity. The experimental program was conducted to study the effect of fraction and applied vertical loads on the stress-strain properties contain V_s and small strain modulus of sand-rubber mixtures.</p>	<p>stiffness characteristics of cemented and uncemented sand-rubber specimens.</p> <p>The vertical strain behaved as a function of stress in semi-log scale for lightly cemented sand-rubber specimens. The residual strain of the samples was reduced with an increase in the sand fraction, and its value additionally reduced with the addition of cement into the specimens. Moreover, V_s and G_0 significantly increased by increasing the sand fraction and applied stress.</p>
<p>Amini et al., (2014)</p>	<p>Large direct shear tests were conducted to study the shear strength and dilation properties of cemented sand mixed by 30% uni-sized gravel particles. The seven days cured specimens were tested by a 300 x 300 x 170 mm direct shear device. Specimens made with a diverse range of cement content (i.e.0%, 1% and 2%) and relative density (i.e. 30%, 50%, 70% and 90%) were tested under two vertical loads of 77 and 150 kPa. The experimental program determined the friction angles at peak and constant volume in addition to maximum dilation angle of specimens.</p>	<p>The results suggested that maximum friction angle and dilation angle was increased by increasing the dosage of cement and relative density. However, increase in the vertical load reduced the dilation angle of the specimen. Furthermore, several empirical relationships were proposed to develop shear strength-dilation and estimate the strength properties of cemented specimens based on the characteristics of uncemented specimens.</p>
<p>Cerato and Lutenegger, (2006)</p>	<p>Three square shear boxes with different dimensions 60 mm, 101.6 mm, and 304.8mm were studied to analyse the properties of five types of</p>	<p>The results of direct shear tests indicated that the friction angle might be dependent on the specimen size which is accosting with the sand type and relative density. The results</p>

	sands with different characteristics.	showed that the friction angle of well-graded sand was reduced by increasing the box size.
Edinçliler and Ayhan, (2010)	Two different laboratory plans were conducted to study on the reinforced sand with tire waste content. Firstly, the optimum dosage of tire crumb for justifying the shear strength characteristics of sand-rubber specimens has been estimated by the direct shear test. Secondly, the large-scale direct shear tests were conducted to evaluate the shear strength enhancement combined by rubber addition. Tire crumb and tire buffings were used for this study.	The results indicated the effectiveness of normal stress, tire waste type, aspect ratio and tire content on shear strength behaviour of the mixture. Moreover, the shear strength of specimens was improved by increasing the aspect ratio of the fibers.
Xiao et al., (2015)	This study presented a testing program of large direct shear tests on tire-derived aggregate ranging between 25mm to 75mm combining with sand, concrete, and geo-synthetics. The large direct shear test was conducted by performing 24, 48, and 96 kPa of normal stresses.	The results indicated the dissimilar failure mechanism of tire-derived aggregate and sand. The shear resistance of tire-derived aggregate has continually increased by increasing the shear displacement. The changing behaviour of tire-derived aggregate additionally suggested an increase in shear strength parameters observed by shear deformation. The friction angles of specimens containing tire-derived aggregate showed a similar range of 35-39 degrees.
Bareither et al., (2008)	30 sand backfill specimens containing a diverse range of gravel (i.e.0% to 30%) have been studied by conducting small and large direct shear tests. The research compared the effect of the size of the	The results show that friction angles obtained from small and large direct shear differed between 2 and 4 degrees. Repeatability tests result also statically indicated that the comparable failure envelopes

	<p>direct shear box on shear strength behaviour of sand backfill materials. Eventually, triaxial compression tests were performed on four of the specimens to evaluate the results of large and small direct shear tests.</p>	<p>deduced by both small and large scales of direct shear tests. Moreover, no significant difference has been observed by comparing the failure envelopes results of direct shear tests with the triaxial test.</p>
<p>Afzali-Nejad et al., (2017)</p>	<p>A series of experimental tests were conducted, to study the effect of particle shapes on the engineering response of sand-woven geotextile interfaces with different sand densities and vertical stress. In this research, the granular material was selected from uniformly graded angular fine sand and a blend of rounded glass beads with a specific size distribution.</p>	<p>The results indicated that particle shape affected the peak and residual friction angles, and also the maximum dilation angle of interfaces between soil and woven geotextile. The result showed a similar residual friction angles in soils with and without geotextile. The peak friction angle and maximum dilation angle of angular sand was slightly reduced by the inclusion of a woven geotextile. The experimental results also suggested that increasing normal stress reduced the peak friction angle and maximum dilatation angle of glass beads-woven geotextile interfaces. Eventually, the results integrated a stress-dilation law for utilised specimens.</p>
<p>Wang et al., (2008)</p>	<p>The shear characteristic of geo-cell reinforced soils was evaluated by conducting large direct shear tests on three types of samples including silty gravel soil, geo-cell reinforced silty gravel soil, and geo-cell reinforced silty gravel soil with cement addition. To evaluate the effect of testing technique results of the direct shear test</p>	<p>Test results indicate that the shear stress-strain behaviour of unreinforced soil and geo-cell reinforced soil is non-linear. The shear stress-strain behaviour of the geo-cell reinforced specimen was transformed from non-linear to quasi-elastic behaviour by adding cement to specimens. Improvement in the cohesion of silty gravel soil was observed in geo-cell reinforced soil, which</p>

	were compared with a triaxial compression test.	was additionally increased by adding cement into the reinforced soil. However, using geo-cell and cement did not affect the friction angle of soil.
Edinçliler et al., (2004)	Large direct shear tests and dynamic triaxial tests were conducted to evaluate the potential application of the waste material in highway embankment project. Tire buffing used in the research had diameters ranging between 1 and 4mm and lengths ranging from 2 to 40 mm. The result also compared to the obtained result from a mixture of medium dense sand and fly ash.	The results show that sand-rubber mixtures have a softening behaviour at a large strain. The shear modulus and damping value of rubber increased by mixing with the sand particle. Moreover, the results of sand-fly ash mixture show similar damping values with tire buffing-sand mixture. However, the internal friction angle and shear modulus behaviour of sand-fly ash specimens and were respectively higher and lower than a sand-rubber mixture.
Edinçliler, (2007)	Large direct shear tests were conducted to determine the shear strength and deformation characteristic of sand-rubber buffing mixture containing 5%, 10%, 20% and 30% rubber by weight.	The experimental results indicate that adding 10% rubber to sand changes the deformation behaviour of the specimen to the rigidity of the composite at low strains and softening at large strains.
Mashiri et al., (2015)	In this research, shear strength and dilatancy behaviour of sand-tire chips mixtures have been studied by a series of moto-conic triaxial tests, which were performed on sand combined with different dosages of tire chips.	The result shows that shear strength and dilatancy properties of sand-tire chips mixtures are remarkably affected by tire chips content. The results also revealed the influence of confining pressure and relative density on strength characteristics of mixtures containing shear strength, dilatancy and initial tangent modulus of sand-tire chips mixture.

Youwai and Bergado, (2003)	This research presents a series of triaxial test on compacted sand specimens containing variety dosages of shredded rubber tire.	The results show that reducing the sand ratio in mixture leads to reducing the density, unit weight and shear strength of mixture, alternatively increasing the compressibility properties. The dilatancy behaviour of the sand-shredded mixture was observed similar to a non-cohesive material which can be described within a critical state framework.
Rao and Dutta, (2006)	A series of triaxial and compressibility tests were performed on the sand with different dosage of tire chips and content.	The results indicate that adding 20% tire chips into sand provided a mixture capable of making and structure in highway and embankment project up to around 10 m height.
Neaz Sheikh et al., (2013)	This research evaluated the shear and compressibility characteristics of sand-tire crumb mixture in civil engineering constructions. The sand-tire crumb specimens were prepared for a various dosage of tire crumbs by volume (i.e., 0%, 10%, 20%, 30% and 40%).	The results indicated that increasing the dosage of tire crumbs in the specimens reduced the shear strength of sand-tire crumb mixtures. However, remarkable improve in axial strain associating with peak deviatoric stress has been revealed. Brittleness test results justified the ductility properties of a mixture observed by adding tire crumb in the mixture. The results also suggested that a great ratio of plastic strain progresses by finishing the first cycle of unloading. Therefore, the settlement accompanying the performance of the mixture can be remarkably decreased by preloading.
Lee et al., (2010)	This study presents an investigation on the	Cemented mixture displayed a bilinear behaviour in the semi-

	<p>cementation and bond degradation effects on the mechanical properties of soils. Lightly cemented and uncemented sand samples were mixed with different dosage of rubber particles. Specimens were subjected to vertical loading by oedometer device and simultaneously elastic wave signals containing P- and S- waves were measured by piezo materials.</p>	<p>log plot, which is measured by several mechanisms of deformation. The elastic wave velocities significantly improved because of cementation hardening under a constant vertical load. The elastic wave velocities were reduced by applying an additional vertical load. Moreover, the shear wave velocity suggests three behaviour area corresponding to the sand fraction for both cemented and uncemented mixtures.</p>
<p>Yadav and Tiwari, (2017)</p>	<p>This research presents the geotechnical priorities of cemented clay-crumb rubber specimens by the experimental program including compaction, UCS, STS, CBR, one-dimensional consolidation and swelling pressure tests. The specimens were provided by mixing clay with different dosages of cement (i.e. 0%, 3% and 6%) and crumb rubber ranging between 0.8–2 mm with various content of 0%, 2.5%, 5%, 7.5% and 10%.</p>	<p>The results indicated that inclusion of crumb rubber in cemented clay reduced the UCS and STS in addition to an increase in the flexibility of cemented clay, in tension and compression. The CBR result suggested that specimens containing 6% cement were recognised, which were suitable for the roads with light traffic application. Moreover, the swelling pressure and compression of specimens were reduced by addition of crumb rubber into the mixtures.</p>
<p>Kim and Santamarina, (2008)</p>	<p>This research evaluates the small-strain and zero-lateral strain response of small sand particle and large rubber particles by performing the oedometer test.</p>	<p>The results indicated that the rubber skeleton controlled the specimen's behaviour when the volume fraction of rubber was greater than 0.6. The dimension and incompressibility of rubber particles increased the stiffness of mixtures. Moreover, performing the constrained modulus and shear wave velocity suggested that the</p>

		relative size between the rubber chips and sand particles and their volume fractions are the mainly effective parameters for improving the internal fabric and related macroscale response of sand–rubber composites.
Anastasiadis et al., (2012)	The small strain dynamic characteristics of samples combination of sandy and gravelly soil and granulated tire rubber were investigated by shear modulus and damping ratio during the shear process. Specimens were mixed with various rubber particles ranging from 5:1 to 1:10 and dosage from 0 to 35% by mixture weight.	The results show that the rubber content and the relative size of rubber to soil particles were remarkably affected by the behaviour of specimens. Increasing rubber content in the mixture cause to transform the sand to rubber contacts to rubber to rubber contacts. Moreover, soil-rubber samples indicate higher small-strain damping ratio by increasing the dosage of rubber in the mixture.
Afshinnia and Poursae, (2015)	This paper presents an experimental study on the influence of crumb rubber on reducing the swelling caused by Alkali-Silica Reaction in samples with highly reactive aggregate. Mortar bar specimens were generated by replacing fine aggregates with 0%, 16% and 24% crumb rubber by volume for this study.	The results revealed that utilising 16% and 24% crumbed rubber into mortar bars combinations reduced the Alkali-Silica Reaction expansion around 40%. However, the inclusion of this amount caused to reduce the compressive strength of mortar cubes around 20%. Further investigation by conducting Thermo-Gravimetric Analysis and Scanning Electron Microscopy analysis verified the effect of rubber to reduce the Alkali-Silica Reaction in mortar mixtures.
Gupta et al., (2016)	A series of experimental tests were conducted to study the effect of partial replacement of fine material with rubber tires on compressive strength,	The results showed that using more dosage rubber reduced the compressive strength, static and dynamic modulus of elasticity specimens. Moreover,

	density, water permeability, static modulus of elasticity, dynamic modulus of elasticity and chloride diffusion. Various dosages of rubber (i.e. 0%, 5%, 10%, 15%, 20% and 25%) have been utilised with various water-cement ratios (0.35, 0.45 and 0.55) in this research. Moreover, the cement content has been replaced with two different dosages of silica fume (5% and 10%).	microstructure analysis suggested that the presence of a gap between the rubber and cement particles caused a decrease in the shear strength of specimens.
--	--	--

2.3 A SUMMARY OF LITERATURE

From the literature study, it has been revealed that the by-products of rubber can be used for sand reinforcement, however, studies have been suggested that an experimental program required to define the optimum mixing ratio of composites. Furthermore, some parameters such as rubber content, aspect ratio, compaction force, and normal stress are recognised as the influencing factors on the shear strength of the mixtures. Thus, generating a composite with the maximum capacity significantly depending on the abovementioned parameters which were investigated through a detailed laboratory study.

Therefore, the first objective of this research study is to evaluate the effect of rubber buffing on the mechanical properties of cemented and uncemented sand. As a second objective, a scale effect study was performed by a large-scale direct shear testing device which was conducted to create a more accurate study on shear strength behaviour of composites. In the final part, the triaxial test were conducted to assess the direct shear results, and eventually, the micro-structural of composites were micromechanically analysed.

CHAPTER 3
THE MATERIAL AND TECHNIQUE

This chapter correspondingly presents an introduction of selected material, combination of created composite and performed methodology for this research study.

3.1 MATERIAL SELECTION

The materials used in this study were selected with considering two factors; the economic aspect and the frequency of materials used in geotechnical projects in Western of Australia. The selected materials were available in Perth, and were supplied from industries area contains sand, rubber buffing, cement and slag Figure 3- 1.



Figure 3- 1. Selected material for this research study.

3.1.1 SAND

The sand samples utilised in this study were supplied by university supplier (Holcim, Australia Pty Ltd) Figure 3- 1. Holcim Silica Sand is widely used as a fine aggregate in concrete and mortar.

Particle size distribution has been conducted according to (ASTMD6913, 2017). The final analysis indicated that sand is classified as poorly graded sand (SP), Figure 3- 2.

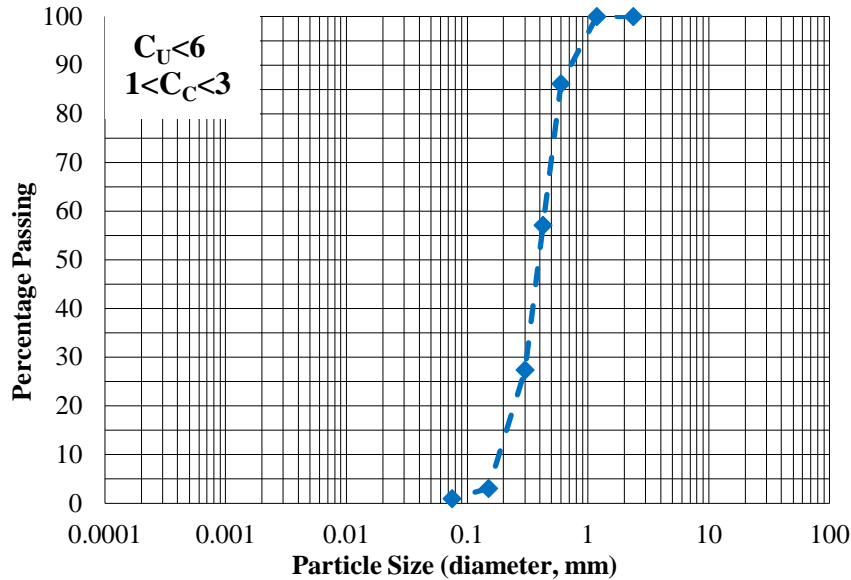


Figure 3- 2. Particle size distribution results of selected sand.

3.1.2 RUBBER

Rubber buffing used in this study were supplied from Tyre Recyclers Pty Ltd Figure 3- 1. Figure 3- 3 shows an image of rubber buffing, along with a sample of crumb rubber and rubber powder. It can be observed that the particle shape of rubber is angular and irregular. To achieve a uniform size of rubber particle, the rubber buffings were sieved. Particle size distribution has been conducted according to AS1289 C 6.1 ST. The final analysis of rubber particle size distribution is presented in Figure 3- 4.



Figure 3- 3. Selected rubber buffing

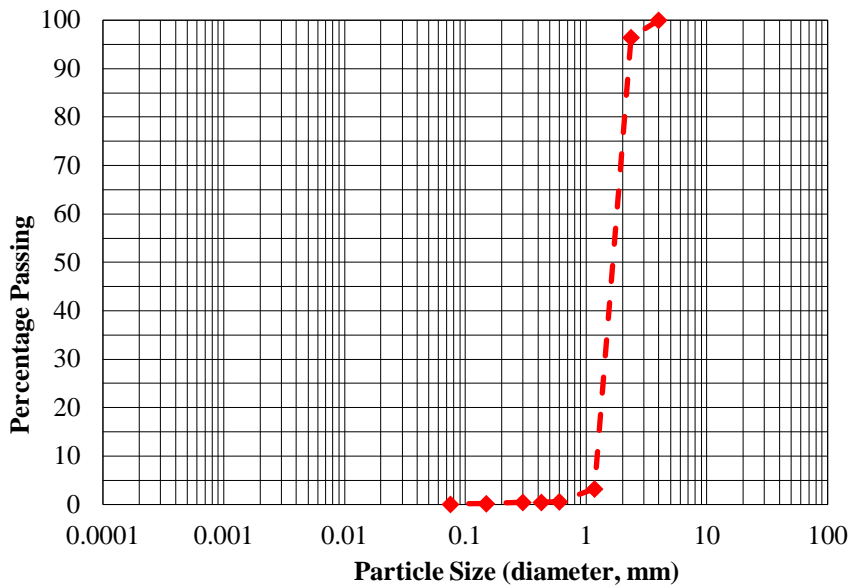


Figure 3- 4. Particle size distribution results of selected rubber.

3.1.3 PORTLAND CEMENT

The Portland cement was used as the cementation agent supplied from Cockburn Cement. Figure 3- 1. Table 3- 1 present the chemical ingredients of the Portland cement, as gained by conducting the X-ray fluorescence studies.

Table3- 1. The chemical composition of Portland cement.

Parameter	Content (%)
CaO	64
SiO ₂	20.1
Al ₂ O ₃	5.4
Fe ₂ O ₃	2.9
MgO	1.3
SO ₃	2.4
Na ₂ O equivalent	0.5
Chloride	0.015
Loss of ignition	2.4

3.1.4 SLAG

Slag is a by-product from the blast furnaces used to make iron, which is highly accessible in Western Australia used in this research study Table3- 1. The chemical composition of Portland cement. Table3- 2 present the chemical ingredients of Ground granulated blast furnace slag (GGBFS) as gained by conducting the X-ray fluorescence studies.

Table3- 2. The chemical composition of slag.

Parameter	Content (%)
CaO	56.3
SiO ₂	24.4
Al ₂ O ₃	7.6
Fe ₂ O ₃	2.3
MgO	2.8
SO ₃	2.5
Na ₂ O equivalent	0.6
Chloride	0.01
Loss of ignition	2.1

3.2 COMPOSITE PREPARATION

Eighteen mixtures including sand, sand rubber, sand stabilisers and sand-rubber-stabilisers composites were separated into three main groups. Specimens have been

prepared based on their identical moisture content on their maximum dry density, which were initially defined by standard compaction tests. The soil composites have been organised into nine categories.

The categories have been selected for obtaining the following aims:

-In a comparable study on the cement, slag, and cement-slag effect on the sand behaviour.

-To an estimate of the rubber application for sand stabilizing.

- To find the optimum combination of additives.

The percentage of cement and slag utilised in the present study was 5% and 10%, and rubber was 10% and 20% of the total mass of composites. The notation of C for cement, S for slag and R for rubber were applied to describe the mixture of composites. The alphabet and number represent the type and dosage of additive, respectively. Thus, the designation of ST, SR and STR represent a group of mixtures containing stabilisers only, rubber only and both stabilisers and rubber respectively.

The first group of specimens was prepared by mixing a various dosage of rubber with sand particles. Three defined mixtures were considered as three individual base components, contain different characteristics as follow:

- Category I (1): Pure sand.
Sand(S) #1
- Category II (2,3): Composed of sand and rubber particles (R)
10 % rubber + sand (SR10) # 2
20 % rubber + sand (SR20) # 3

The second group is generated by combination of cementitious material with sand. Pure sand were mixed with a different dosage of cement, slag and a combination of both cement and slag. Thus, composite define as follow:

- Category III (4,5): Composed of sand and soil stabilisers (ST)
 - 4-1: 5 % cement + sand (SC5) # 4
 - 4-2: 5 % slag + sand (SS5) # 44
 - 5-1: 10 % cement + sand (SC10) # 5
 - 5-2: 10 % slag + sand (SS10) # 55
 - 5-3: 5 % cement + 5 % slag + sand (SC5S5) # 555

Eventually the third and fourth groups were defined the composite contain a variation dosage of rubber and stabilisers agent with sand:

- Category IV(6,7): Composed of sand , 10 percent of rubber and soil stabilisers
 - Category 6:ST5R10
 - 6-1: 5 % cement + 10% rubber + sand (SC5R10) #6
 - 6-2: 5 % slag + 10% rubber + sand (SS5R10) #66
 - Catagory7:ST10R10
 - 7-1: 10 % cement + 10% rubber + sand (SC10R10) #7
 - 7-2: 10 % slag + 10% rubber + sand (SS10R10) #77
 - 7-3: 5 % cement + 5 % slag +10% rubber + sand (SC5S5R10) #777
- Category V(8,9): Composed of sand , 20 percent of rubber and soil stabilisers
 - Category 8:ST5R20
 - 8-1: 5 % cement + 20% rubber + sand (SC5R20) #8
 - 8-2: 5 % slag + 20% rubber + sand (SS5R20) #88
 - Catagory9:ST10R20
 - 9-1: 10 % cement + 20% rubber + sand (SC10R20) #9
 - 9-2: 10 % slag + 20% rubber + sand (SS10R20) #99
 - 9-3: 5 % cement + 5 % slag +20% rubber + sand (SC5S5R20) #999

Therefore, composite reveal an identical specific gravity relating to their material properties. Table3- 3 presents the specific gravity (ASTMD854, 2014) of selected

composite. The results of grain size distribution tests for main sand mixture also present in Table3- 3.

Table3- 3. Specific gravity results of soil composites.

Soil	D ₆₀ (mm)	D ₁₀ (mm)	Cu	Gs
Sand	0.18	0.45	2.5	2.653
Rubber	2.0	1.5	1.3	1.011
SC0R10	0.3	0.4	0.6	2.174
SC0R20	0.3	0.4	0.6	1.996
4-SC5R0	-	-	-	2.717
5-SC10R0	-	-	-	2.725
6-SC5R10	-	-	-	2.299
7-SC10R10	-	-	-	2.037
8-SC5R20	-	-	-	2.331
9-SC10R20	-	-	-	2.088
44-SS5R0	-	-	-	2.660
55-SS10R0	-	-	-	2.681
555-SC5S5R0	-	-	-	2.667
66-SS5R10	-	-	-	2.304
77-SS10R10	-	-	-	2.336
777-SC5S5R10	-	-	-	2.375
88-SS5R20	-	-	-	2.062
99-SS10R20	-	-	-	2.096
999-SC5S5R20	-	-	-	2.092

3.3 METHOD AND TECHNIQUES

3.3.1 EXPERIMENTAL PROGRAM

A series of laboratory experiments indicated for a comprehensive investigation into the selected composites. Laboratory tests were selected to evaluate the geotechnical characteristics of sand composite- on saturated condition based on the identical moisture and density- ranging from fundamental properties to specific parameters including porosity, compactibility, compressibility, and strength. The testing program was precisely designed and result discussed in three main chapters to collect accurate results, required for numerical modeling by following steps:

- ❖ **Chapter 4: Experimental investigation on the potential application of rubber in sand reinforcement.**

This chapter presents results of maximum and minimum density of mixtures, by focusing on its minimum void ratio parameters. Shear strength properties of specimens were studied by performing small direct shear tests with dimension of 63.5mm x 63.5mm (ASTMD3080, 2011), conducted a wide range of normal stresses Figure 3- 5.



Figure 3- 5. Small direct shear device.

Eighteen mixtures including sand, sand rubber, sand stabilisers and sand-rubber-stabilisers composites were separated into three main groups. The soil composites have

been organised into nine categories. The categories have been selected for obtaining the following aims:

-In a comparable study on the cement, slag, and cement-slag effect on the sand behaviour.

-To an estimate of the rubber application for sand stabilizing.

- To find the optimum combination of additives.

The percentage of cement and slag utilised in the present study was 5% and 10%, and rubber was 10% and 20% of the total mass of composites. The notation of C for cement, S for slag and R for rubber were applied to describe the mixture of composites. The alphabet and number represent the type and dosage of additive, respectively. Thus, the designation of ST, SR and STR represent a group of mixtures containing stabilisers only, rubber only and both stabilisers and rubber respectively.

❖ Chapter 5: A comparison study on the shear strength of sand-rubber composites investigated by the small-scale and large-scale direct shear tests.

A series of standard compaction tests were performed using the various mixtures to define the optimum moisture content (OMC) and the maximum dry density (MDD) in accordance with (ASTMD698, 2015), The results of the compaction tests were used for evaluating the MDD of a composite used as a backfill material and the stability of a field problem such as embankments.

Moreover, large direct shear test (ASTMD3080, 2011), performed in this chapter to compare and verify the rubber buffing efficiency for sand treatment Figure 3- 6.



Figure 3- 6. Large direct shear device.

In this chapter, experimental program was conducted to gain a better understanding of the obtained results, considering a comparison between cement and slag. In this experimental program, 15 mixtures, including pure sand, sand–rubber, sand–stabiliser and sand–rubber–stabiliser composites, were divided into three main groups. The percentage of cement and slag used in these experiments was 5% and 10%, respectively, and that of rubber was 10% and 20% of the total mass of the composites. Eventually, the obtained results proposed a relationship to find the optimum dosage of composite ingredient to increase the shear strength properties of sand.

❖ Chapter 6: Shear and Compressibility Behaviour of Sand- rubber composites

The one-dimensional consolidation test (ASTM D2435, 2011), was applied to determine the compressibility characteristics of fifteen mixtures including sand, sand rubber, sand stabilisers and sand-rubber-stabilisers composites were separated into three main groups Figure 3- 7.



Figure 3- 7. One-dimensional consolidation device.

To prepare the sand-rubber composites, the oven dried sand with the different ratio of well-dried rubber was mixed. The gravimetric basis used for the rubber fractions (RF), were performed as 0%, 10%, and 20% (rubber) for the mixtures with and without the cementitious materials. The percentage of cement and slag utilised in the experiment study was 5% and 10%.

Moreover, triaxial compression tests were performed on the pure sand, sand-rubber and sand-rubber cement treated composites. Material was mixed manually, making a homogeneous combination. The shear strength and compression characteristics of composites were examined by LoadTrac II triaxial compression test apparatus. The consolidated-undrained triaxial (CU) test method according to (ASTMD4767, 2011) with confining pressures of 50, 100, 250 and 500 KPa, were conducted on the sand mixtures with the 63 mm diameter and 130 mm height Figure 3- 8.

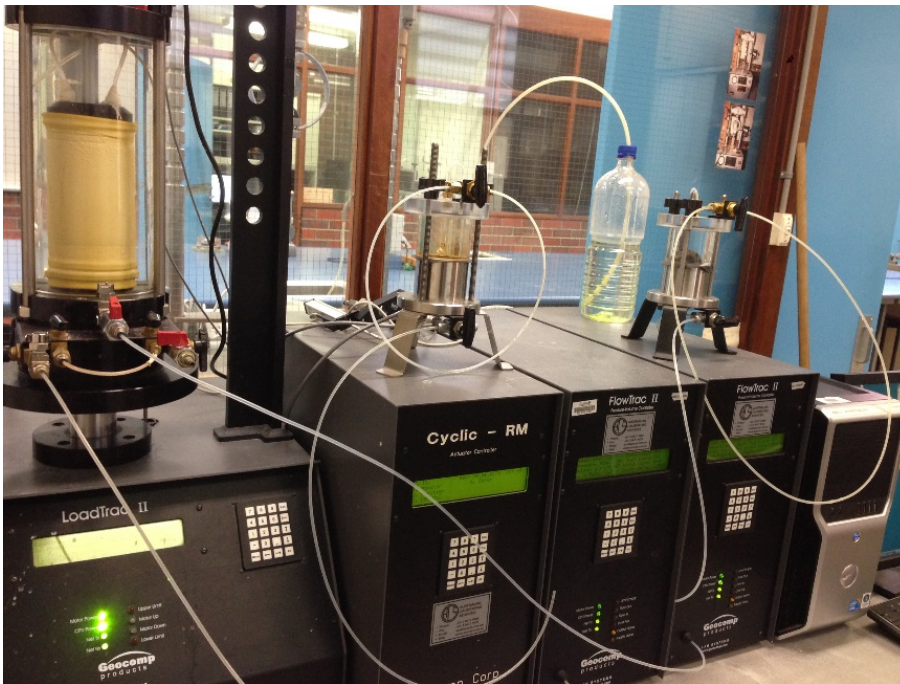


Figure 3- 8. Automatic triaxial tests system.

Thus, the experimental data of small direct shear, large direct shear and triaxial are conducted to develop an empirical equation which is capable of predicting the shear intrinsic constants of sand composites.

3-3.2 MICROANALYTICAL/ ELEMENTAL OBSERVATION

Eventually, deformation mechanism of composite has been studied by conducting the microanalytical/ elemental characterisation observation contain:

SEM (SCANNING ELECTRON MICROSCOPY):

Analysing the microstructure and morphology of the platinum coated specimens, which was conducted via Zeiss Evo 40XVP scanning electron microscope (SEM) at the different accelerating voltages of 15kV and 20kV. The specimens were scanned using a secondary electron detector and a backscattered electron detector Figure 3- 9.



Figure 3- 9. Evo 40XVP scanning electron microscope.

EDS (ENERGY-DISPERSIVE X-RAY SPECTROSCOPY):

The elemental and chemical compositions of specimens were monitored by an energy-dispersive X-ray (EDS) detector Figure 3- 9. The SiLi X-ray detector with an ultrathin window and Oxford Inca software illustrated the X-ray spectra, qualitative and quantitative numeric data.

3-3.3 A SUMMARY OF EXPERIMENTAL PLAN

A summary of the standards of selected experiments was schematically present in Figure 3- 10. In order to provide a comprehensive investigation, a narrow down approach, including a series of fundamental and specific tests, was defined to obtain the research objectives. Each stage of this research contains a specific approach and objectives which were separately investigated in three chapters, explained in Table3- 4.

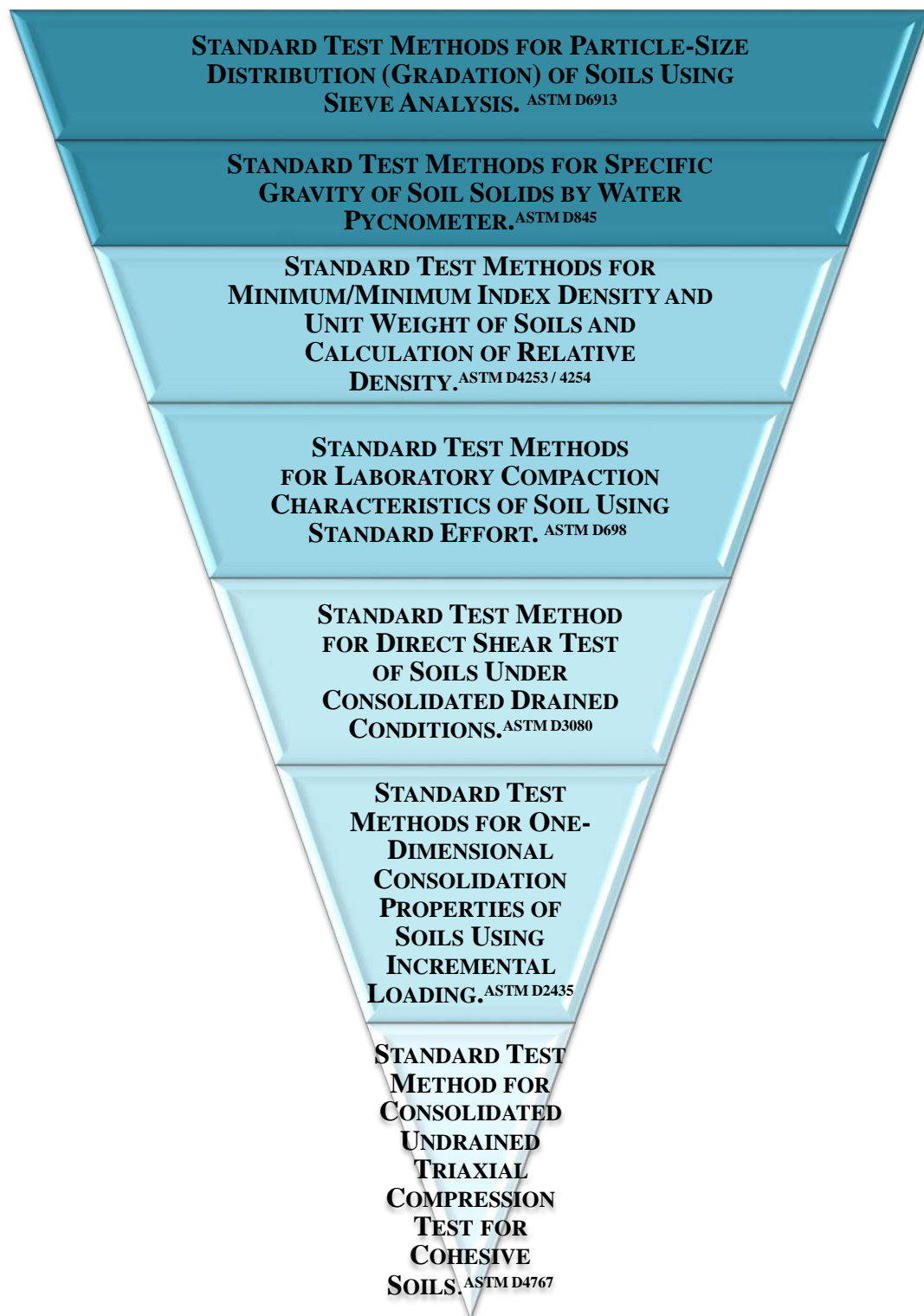


Figure 3- 10. Summary of the performed standards in the experimental program.

Table3- 4. Summary of the thesis program.

Chapter	Technique	Objectives
Chapter 4: Experimental investigation on the potential application of rubber in sand reinforcement.	<ul style="list-style-type: none"> • <i>Minimum Void ratio</i> • <i>Small direct shear</i> 	<ul style="list-style-type: none"> • <i>Minimum Void ratio and composite behaviour</i> • <i>Rubber and shear strength</i> • <i>Rubber and elastic modules</i> • <i>Normal stress and shear strength</i>
Chapter 5: A comparison study on the shear strength of sand-rubber composites investigated by the small-scale and large-scale direct shear tests.	<ul style="list-style-type: none"> • <i>Maximum dry density</i> • <i>Large direct shear</i> 	<ul style="list-style-type: none"> • <i>Floating and non-floating cases</i> • <i>Maximum dry density and composite categorisation</i> • <i>Cement vs. Slag</i> • <i>Scale effect study</i> • <i>Stress-dilation law</i> • <i>Shear strength parameters and maximum dry density</i> • <i>Shear strength improvement index</i>
Chapter 6: Shear and Compressibility Behaviour of Sand-rubber composites.	<ul style="list-style-type: none"> • <i>Compressibility</i> • <i>Triaxial test</i> • <i>Microstructural analysis</i> 	<ul style="list-style-type: none"> • <i>Results verification</i> • <i>Elastic behaviour</i> • <i>Numerical modelling</i> • <i>Deformation mechanism</i>

CHAPTER 4

**EXPERIMENTAL INVESTIGATION ON
THE POTENTIAL APPLICATION OF
RUBBER IN SAND REINFORCEMENT**

This chapter presents the following section:

4.1 Introduction	73
4.2. Materials and Methods	75
4.3 Result and Discussion	77
4-3-1: Minimum Void Ratio (e_{min})	77
4-3-2: Small Scale Direct Shear Tests	79
4-3-2-1: Shear stress-shear strain	80
I- ST.....	83
II- STvsR.....	83
III- STR10	85
IV- STR20.....	86
V- Overall view of mixture shear-strain behaviour	87
4-3-2-2: Strain capacity behaviour	89
I- Tangent shear modulus	89
II- Secant shear modulus.....	92
III-Volumetric behaviour	97
4-4: Analysis of Results	107
4-4-1: Effect of Normal Stress on Peak Shear Strength	107
4-5: Conclusion	114

4.1 INTRODUCTION

The application of rubber for soil reinforcement, specifically on the strength characteristics of soil has been investigated by many studies (Yoon et al., 2006, Cabalar, 2011, Anvari et al., 2017, Anbazhagan et al., 2016, Christ and Park, 2010, Edil and Bosscher, 1992, Zornberg et al., 2004, Tsang et al., 2012, Hidalgo Signes et al., 2015, Attom, 2006, Bosscher et al., 1992, Humphrey et al., 1998, Dickson et al., 2001, Moo-Young et al., 2003, Yang et al., 2002, Ghazavi, 2004). The light unit weight and high strength characteristics have been recognised as the main parameters of waste tire material, which are utilised as a lightweight material for civil constructions (Yoon et al., 2006, Cabalar, 2011, Anvari et al., 2017, Anbazhagan et al., 2016). Owing to the ductility characteristics of rubber, it is suitable for adding to the compressible soil in the embankment, retaining wall and bridge abutment applications (Yoon et al., 2006, Cabalar, 2011, Anvari et al., 2017, Anbazhagan et al., 2016, Hidalgo Signes et al., 2015, Humphrey, 2007, A. Bernal et al., 1997). Previous research has reported that, by applying approximately 30% of tire chips into the sand, its friction angle increases to almost 66 degrees (Anbazhagan et al., 2016). The sand has obtained a higher strength, which corresponds to approximately 35 degrees of internal friction angle (Cabalar, 2011, Ghazavi, 2004, Edinçliler et al., 2010, Yang et al., 2002, Anbazhagan et al., 2016, Zornberg et al., 2004, Hazarika and Yasuhara, 2007). Several studies have evaluated the possibility of tire application to soil stabilisation from the different engineering viewpoints. Shear strength characteristics have been investigated by analysing unit weight, rubber content, applied normal load and the rubber's dimension effect (Anvari et al., 2017, Yoon et al., 2008, Ghazavi, 2004, Moo-Young et al., 2003, Humphrey and Blumenthal, 2010, Attom, 2006, Picornell, 2007). The results have claimed that the rubber content and its unit weight were the most effective parameters on soil strength behaviour. The results also reported the importance of vertical loads, in which samples demonstrated a remarkable compression under low pressures. Bosscher et al., (1992) has proven the field results with the finite element model and

demonstrated an improvement in the compressibility and strength characteristics of soil compared to using either sand or tires only (Cabalar, 2011, Anbazhagan et al., 2016, Hidalgo Signes et al., 2015). Application of a sand-rubber mixture results in a reduction of the volume of material required, which consequently creates steeper slopes due to the generation of a stronger soil with a lower unit weight (Edil and Bosscher, 1992, Lee et al., 1999, Tweedie et al., 1998, Zornberg et al., 2004, Yoon, 2007, Hidalgo Signes et al., 2015). The high capability of rubber application in highway construction has been reported by (Rao and Dutta, 2006), where up to 20% of rubber was applied to make an embankment building 10-meters high (Anvari et al., 2017). The authors suggested that a laboratory experiment was required to determine the optimum size of the rubber and its ratio to obtain the maximum potential for rubber application. In 1992, (Edil and Bosscher, 1992) reported that they obtained a strengthened sand by merely adding 10% of rubber into the dense sand (Anvari et al., 2017, Anbazhagan et al., 2016). The random rubber addition revealed the importance of direction and position of rubber in the sand to obtain a higher strength of sand.

Previous studies have shown that rubber size and content, composites' unit weight and the applied stress on the samples are the main parameters affecting the shear strength properties. However, the majority of previous studies were conducted by researching rubber shreds or rubber chips. Taking into consideration the limitations of these studies on the granulated rubber effect on sand behaviour in detail and number, this chapter is presented as a series of geotechnical tests to investigate the mechanical properties of sand-rubber composites by focusing on the following objectives and methodologies:

-To study the effect of the normal stress, 108 small direct shear (SDS) tests were undertaken with a variety of vertical loads.

-The importance of the void ratio (e) in composites behaviour was considered by applying the obtained minimum void ratio (e_{min}).

-The soil composites were organised based on their criteria as discussed in the methodology chapter.

-The composites were studied in terms of shear strength, shear strain and elastic behaviour parameters.

4.2. MATERIALS AND METHODS

Eighteen mixtures including sand, sand rubber, sand stabilisers and sand-rubber-stabilisers composites were separated into three main groups. The soil composites have been organised into nine categories. The categories have been selected for obtaining the following aims:

-In a comparable study on the cement, slag, and cement-slag effect on the sand behaviour.

-To an estimate of the rubber application for sand stabilizing.

- To find the optimum combination of additives.

The percentage of cement and slag utilised in the present study was 5% and 10%, and rubber was 10% and 20% of the total mass of composites. The notation of C for cement, S for slag and R for rubber were applied to describe the mixture of composites. The alphabet and number represent the type and dosage of additive, respectively. Thus, the designation of ST, SR and STR represent a group of mixtures containing stabilisers only, rubber only and both stabilisers and rubber respectively.

The main properties of all the sand and sand-rubber mixture are summarised in and show the specific gravity for each composite and the sieve analysis of the sand, rubber and sand-rubber particles Table4- 1.

Table4- 1. Properties of materials. Cu: Coefficient of Uniformity, Gs: Specific gravity

Soil	D ₆₀ (mm)	D ₁₀ (mm)	C _u	G _s
Sand	0.18	0.45	2.5	2.65
Rubber	2.0	1.5	1.3	1.01
SC0R10	0.3	0.4	0.6	2.17
SC0R20	0.3	0.4	0.6	2.00

The minimum void ratio of each composite was considered via the standard compaction test measurement, which was performed at the first step of the experimental research. The optimum moisture content (OMC) and maximum dry density (MDD) were considered to sample preparation. The results are comprehensively explained in the next chapter to show the importance of unit weight in soil behaviour.

Direct shear tests were performed based on the (ASTMD3080, 2011) method to determine the shear strength strain behaviour that all nine subgroups of samples were under during the six different normal loads.

The normal stress was divided into two main groups, i.e., low (50, 100 and 250 kPa) and high (500, 750 and 1000 kPa) loads. These ranges were applied to comprehensively evaluate the different additives proportions on the composites' behaviour. The shear test was performed with a 63.5 mm × 63.5 mm (inside diameter) shear box with a horizontal displacement rate of 0.5 mm/min. The height of the specimen was 40 mm, and it was compacted in three layers to achieve the desired parameters of compaction test inside the shear box.

It should be mention that, specimens were prepared based on MDD and OMC which obtained by standard compaction tests.

4.3 RESULT AND DISCUSSION

To determine the importance of the void ratio in defining the optimum sand-rubber mixing ratio, the limit state of compactness (e_{min}) was measured. As it mentioned earlier, the composite has been made with their specific density and water content according to the results of standard compaction test. However, the following section is trying to evaluate the importance of composite material and its effectiveness on the porosity of composite from a different view point.

4-3-1: MINIMUM VOID RATIO (e_{min})

The e_{min} is the minimum compactness amount of soil that can be obtained with the different experimental techniques such as relative density (ASTMD4253, 2016) and (ASTMD4254, 2016). The minimum void ratio can also be obtained when the maximum unit weight is achieved, which is explained in the next chapter. A comparison with a previous study illustrated that using the different methods for defining e_{min} has obtained the results with less than 2% difference (Tavenas and Rochelle, 1972, Simoni and Houlsby, 2006). According to (ASTMD4253, 2016), the maximum index density and unit weight of each sample is determined with the use of a vibratory table. Figure4- 1 illustrates the maximum density of pure sand, sand-additives, and pure rubber obtained from the relative density test. The sand content of material varied based on the proportions of sand and additives (by dry weight) from 0% (subcategories #1, #4 and #5) to 100% (subcategories #2 and #3). Initially, the addition of stabiliser and rubber appeared to have a different effect on the maximum density of sand. The highest amount was achieved by mixing 5% of both cement and slag with sand. Because of the different shape of the cement and slag, the void areas with the sand particles are properly filled. During compression between two types of stabiliser materials, slag has made a denser composite. Conversely, the minimum density is associated with a mixture of sand with 20% of rubber only, which is a closer amount of the pure rubber density. As Figure4- 1 reveals the maximum density of the

composite is associated with the type and quantity of additives and their physical structure. The results are roughly separated into three groups that are closely related to the proportion of rubber in each mixture.

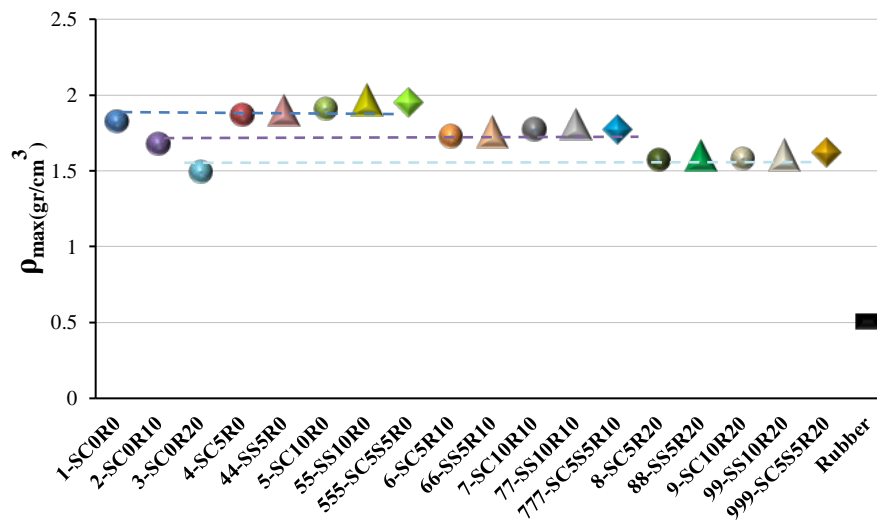


Figure4- 1. Maximum density of pure sand, sand-additives and pure rubber

The minimum void ratio was then calculated, using the maximum density as a function of the additives of samples (Figure4- 2). The sample made with only sand and only rubber were assigned with the minimum void ratio of 0.555 and 1.013, respectively. The result shows that the minimum void ratio of sand has been reduced by adding the stabiliser and continues to decrease by increasing their quantity. Conversely, by adding the rubber, the void has been increased among the sand particles, meaning that the sample containing 20% of rubber only has the highest minimum void ratio. Although it appears that by increasing the dosage of fine material in the matrix with rubber, this trend continues; however, a more in-depth examination reveals there is a specific criterion and point to achieve the smallest minimum void ratio. This behaviour is more accurately discussed once the results of the standard compaction test are obtained, which considers the floating and non-floating state.

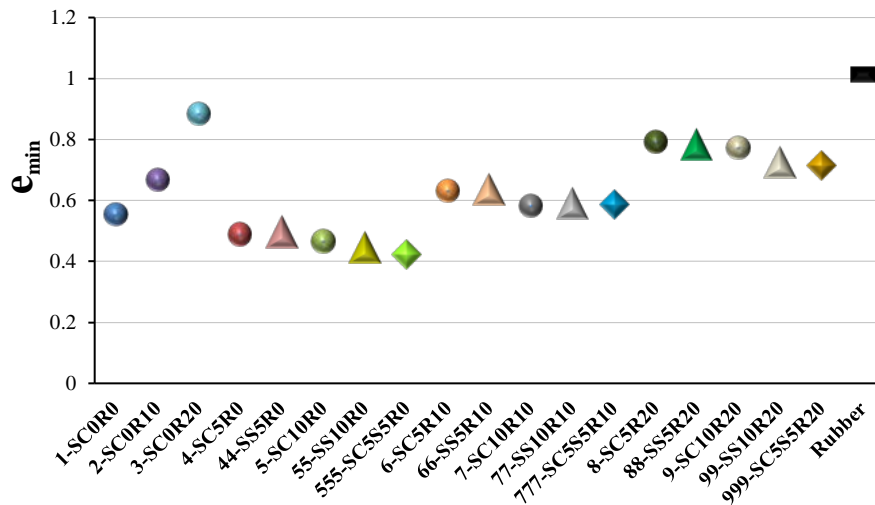


Figure4- 2. Minimum void ratio of pure sand, sand-additives and pure rubber

The relative density results demonstrated that the optimum mixing ratio was related to the shape, size, amount and type of additives. The smallest and biggest minimum void ratio among the sand-stabiliser-rubber composites were associated with SS10R10 and SC5R20, respectively. The results also indicate that the application of rubber as a lightweight material in the sand composites can be effectively utilised to manufacture the geotechnical construction such as retaining walls, backfill and embankments.

4-3-2: SMALL SCALE DIRECT SHEAR TESTS

The influence of rubber and two types of stabiliser on the shear strength behaviour of sand were examined by performing 108 small scale direct shear tests. Two groups of pressure (low and high) were utilised to investigate the nine categories of sand mixtures. The obtained data was then analysed in terms of shear stress-shear strain, volumetric behaviour, elastic parameters and shear strength parameters.

4-3-2-1: SHEAR STRESS-SHEAR STRAIN

The 500 kPa pressure was selected to present the results as this pressure was the boundary of normal stress between low and high-pressure loads. The typical shear-strain plot of SDS tests for all composites are presented in Figure4- 3(a) and Figure4- 3(b). The peak shear strength value is presented as the shear strength behaviour of each sample. The different effects of additives on the sand behaviour are initially recognised. It can be observed that the application of stabiliser by increasing the peak value of samples created a strengthened mixture. The maximum amount of shear stress is associated with the sand mixture containing 5% of both cement and slag. Conversely, the application of 20% rubber created a material with the lowest peak shear strength. Moreover, a similar behaviour of the mixtures with the same dosage of rubber is seen, which verifies the important role of rubber in the characteristics of the specimen. These results may be improved by the relationship between the minimum void ratio and shear strength behaviour, as discussed earlier. For a better analysis, the results of Figure4- 3 are categorised based on the specimen's category in Figure4- 4, Figure4- 5, Figure4- 6, and Figure4- 7.

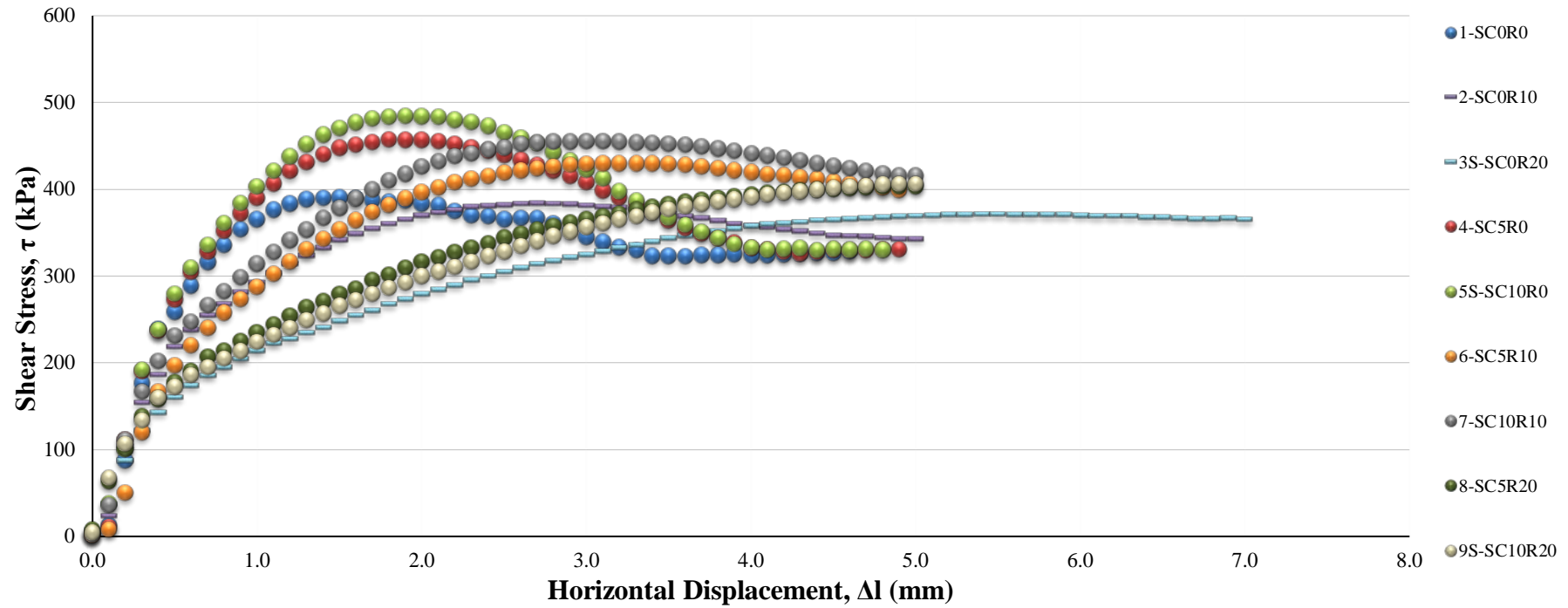


Figure4- 3(a). Typical shear stress plot of 9 sand-cement composites at normal stress 500kPa.

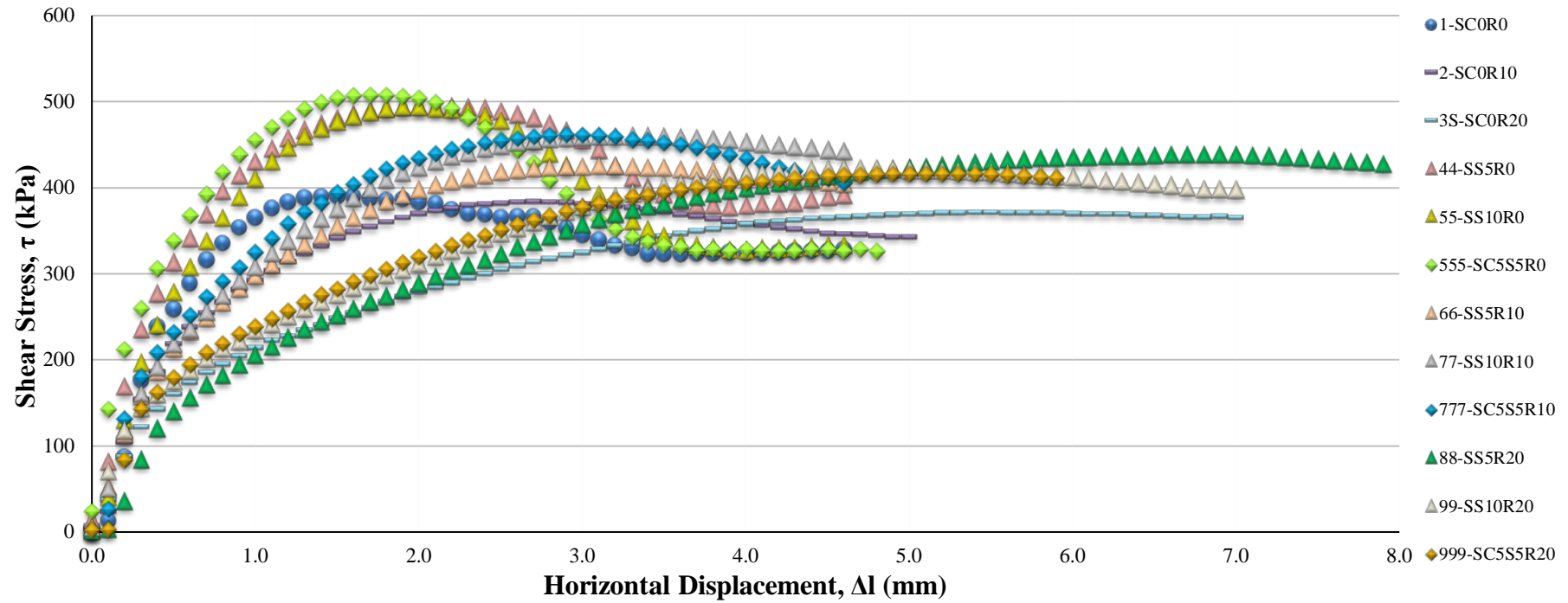


Figure4- 3(b). Typical shear stress plot of 9 sand-slag composites at normal stress 500kPa.

I- ST

A comparative analysis to determine the efficiency of different stabilisers for sand reinforcement was performed. Figure4- 4 illustrates the improvement of the shear strength behaviour of sand after adding stabilisers. The results reveal a very similar tendency for all samples, which is that the stabiliser creates a more uniform and dense composite. The shear value rapidly increased up to the failure point and then tends to a residual state until the end of the test. The application of both cement and slag creates a strengthened mixture, which fails after passing more displacement with a greater stress. It can be concluded that by adding the stabiliser the shear response of sand became a denser composite, which has obvious strain hardening behaviour.

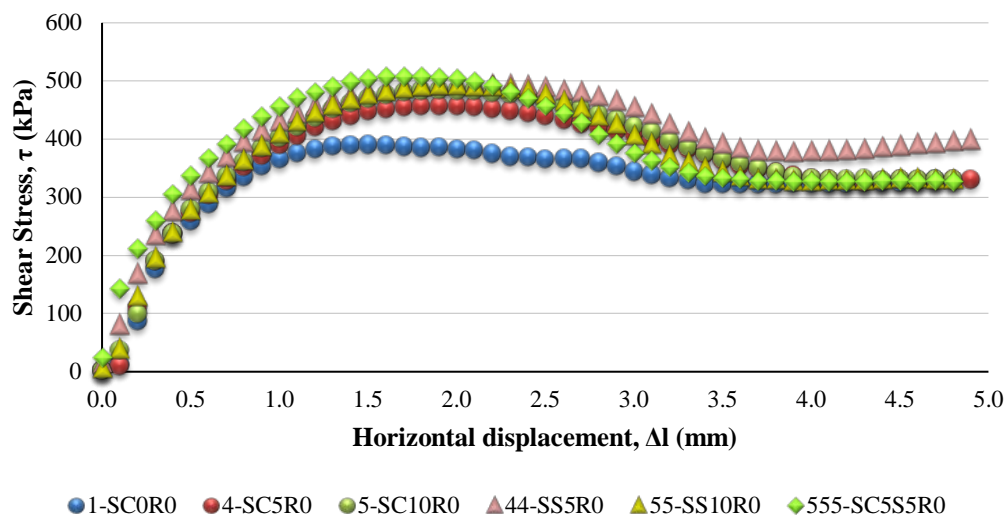


Figure4- 4. The shear stress plot of sand and stabilised sand with cement, slag, and cement-slag.

II- STvsR

Despite the creation of a mixture with a remarkable shear resistance after using rubber, it cannot increase the shear stress value of sand. The shear strain behaviour of composites containing the rubber illustrate a shear stain behaviour with no sudden drop in strength value similar to a typical loose sand Figure4- 5. The slope of the shear strain curve of sand became slower, and failure occurred two and three times faster than the

sand failure point by the addition of 10 and 20% rubber, respectively. This behaviour may occur because of densification of the sand-rubber mixture during the shear movement due to the reduction of the composite's porosity existing because of rubber particles. In fact, samples behave like a medium sand with the advantage of rubber inclusion that interlocks the rubber and sand particles, which generates a strengthened sample of compression to just a loose sand.

Regarding the above finding on evaluating the effects of the stabilisers and rubber on sand behaviour, a composite with the combination of those characteristics must be created.

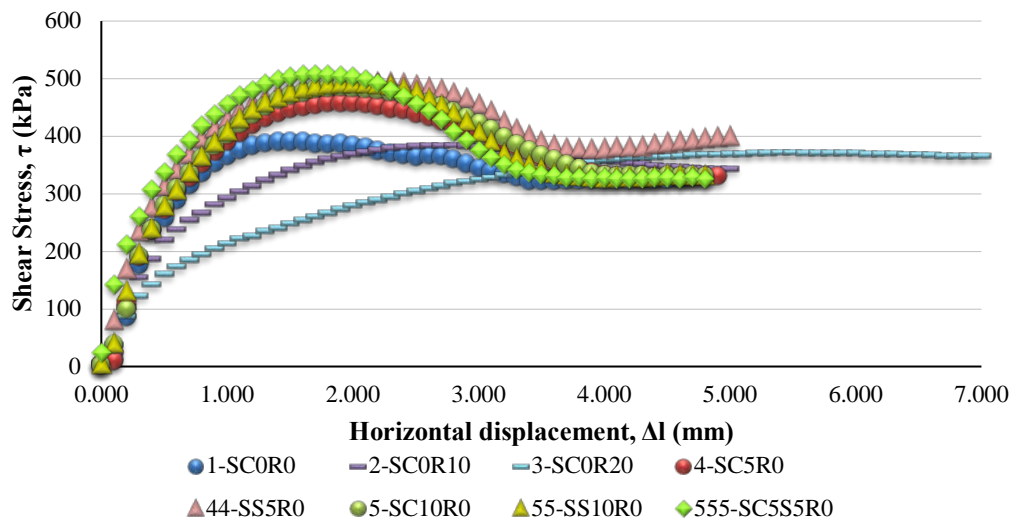


Figure4- 5. The shear stress plot of sand and stabilised sand with stabilisers and rubber only.

The obtained results to this point have expanded the assumption regarding the use of the minimum void ratio for the shear strength behaviour of sampled as well. The results indicate a division of the specimen's behaviour based on the proportion of rubber. Therefore, the results of the samples have been separated into two groups (10% and 20%) of rubber mixing with stabilisers.

III- STR10

As an overall view, Figure4- 6 illustrates the transformation of the steep slope of the sand only sample to the gentle slope of the treated sand. In addition, application of both stabilisers and rubber creates strengthened samples. The addition of stabiliser to the rubber improved the shear strength of samples along with shear resistance. In 5% and 10% of stabiliser mixture with rubber, cement and slag have a similar effect in both categories. Specifically, the combination of 5% of both cement and slag established the maximum amount. The sand's post-failure behaviour has remarkably modified by adding rubber to the mixture. The other important modification was obtained for sand and sand-rubber behaviour after their failure. Although the rubberised sand does not suddenly decrease after the peak value, its shear strength at the residual state is very close to the sand only composite. The sand's particle breakage may be minimised with the application of rubber. This characteristic is remarkably improved when the rubber is mixed with stabiliser, which may generate more bonding and interlocking among the particles. The importance of shear strength is discussed in the following section in greater detail.

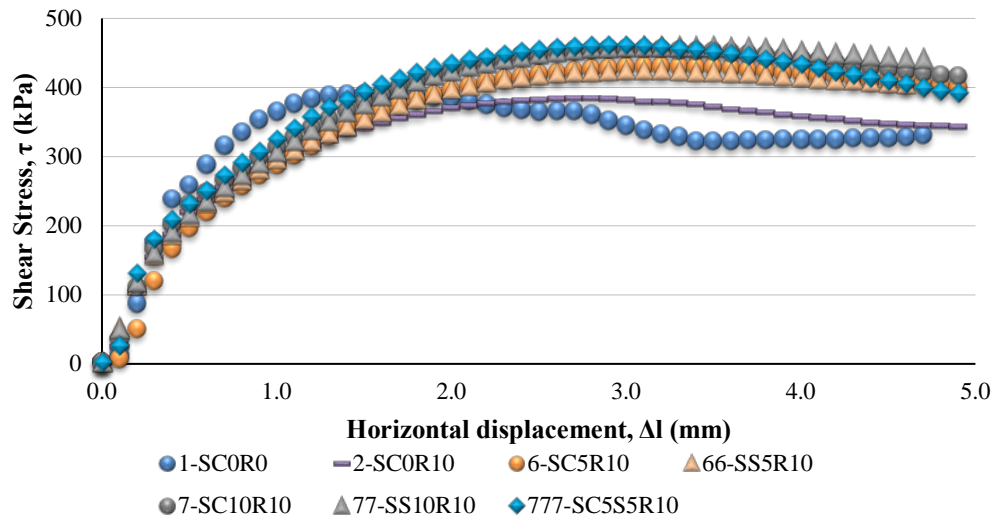


Figure4- 6.The shear stress plot of sand and mixing with 10% rubber.

IV- STR20

To finalise the earlier assumptions, the effect of 20% rubber with and without stabilisers was analysed. Initially, all six treated samples appeared to have a very gentle slope, indicating the importance of the rubber portion of the sample rather than the amount of stabiliser. Figure4- 7 illustrates that the slopes tend to become flat and show a similar linear shear stress behaviour after failure. Then, similar to the STR10 samples, the peak value progressed after the addition of stabilisers to the sand-rubber mixtures. By increasing the rubber content subsequently the shear failure needs to be the higher shear displacement to reach the failure point. This can be explained by the generation of maximum porosity in the STR20 samples and the tendency of the rubber to roll and slide over the finer particles. Increasing the shear resistant ability can move the shear failure point as close as possible to a constant volume state. However, the highest peak value amount was achieved by application of 5% slag.

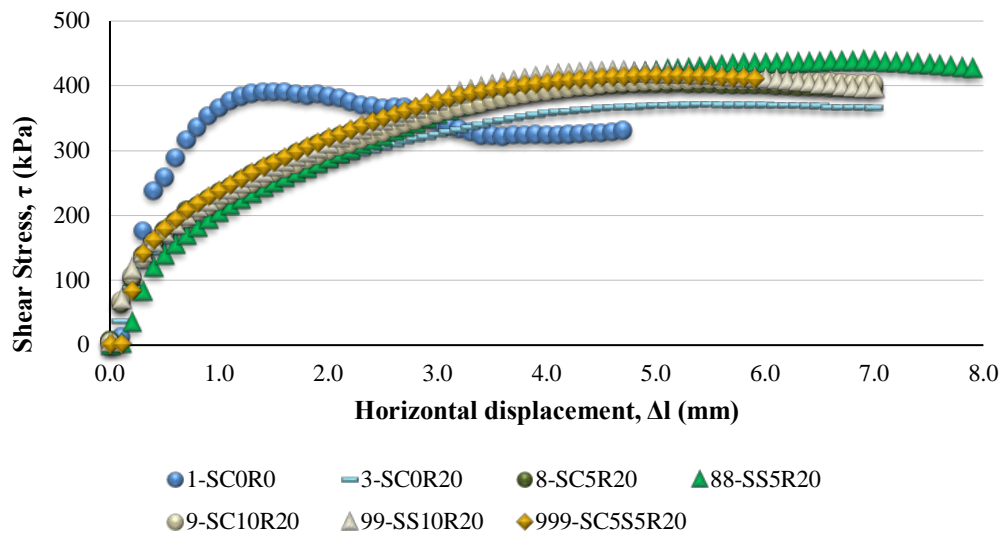


Figure4- 7. The shear stress plot of sand and mixing with 20% rubber.

V- OVERALL VIEW OF MIXTURE SHEAR-STRAIN BEHAVIOUR

The following results are summarised the shear-strain behaviour of all samples after applying a normal stress of 500 kPa.

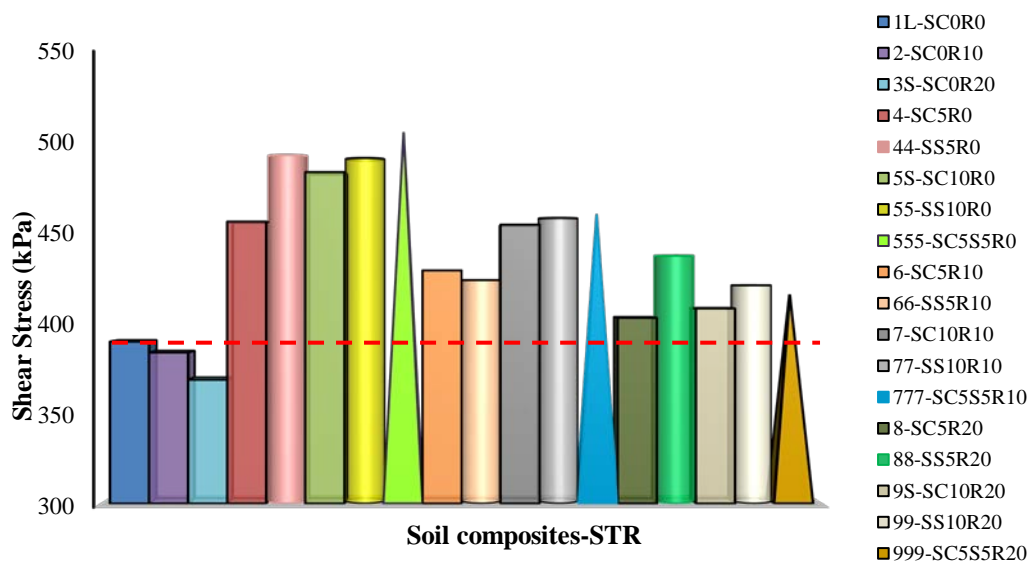


Figure4- 8. Summary of peak shear strength value of sand mixtures at a normal stress of 500kPa.

The maximum peak shear strength value was achieved by a combination of 5% of both slag and cement in sand mixtures, Figure4- 8. The peak shear strength value of SC5S5R0 samples increased to almost 508 kPa from approximately 117 kPa in the sand only peak shear strength value.

The application of rubber only created a sand behaviour similar to a loose sand with a lower shear strength, which was reversely associated with the quantity of rubber. The peak value of sand improved between 13 KPa and 69 kPa, depending on the dosage of both rubber and stabilisers in the STR mixtures.

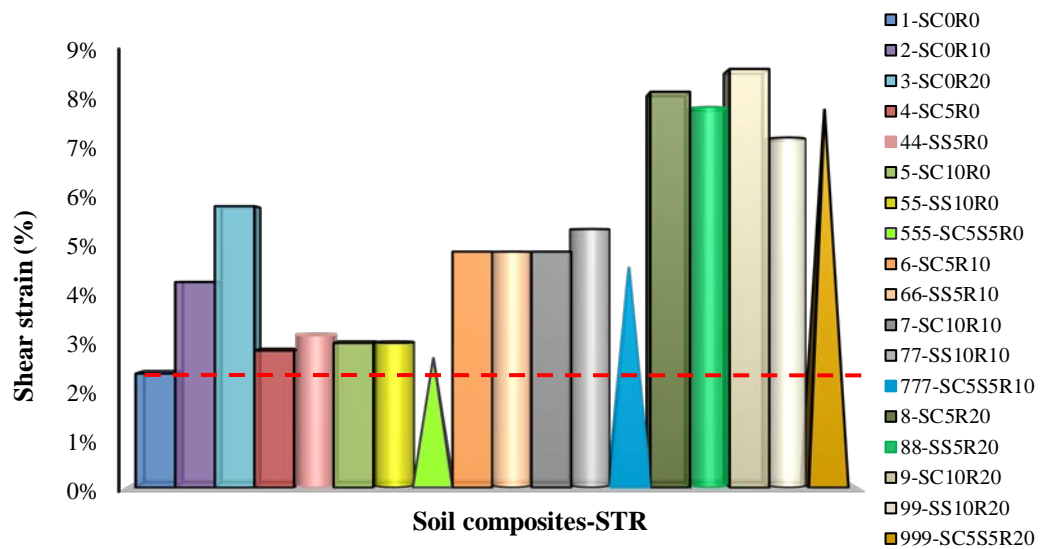


Figure4- 9. Summary of shear resistance behaviour of sand mixtures at a normal stress of 500 kPa.

The application of stabilisers in the sand mixture had only a minor improvement in the shear resistance behaviour of sand, which can happen because of the increment of the fine particles to create a dense and more uniform composite, Figure4- 9.

Whereas, the shear resistance of sand increased two and three times by the addition of 10 and 20% rubber, respectively. Whereas, a one and half times increase were achieved by the addition of stabilisers to the same dosage of rubber.

The SDS result verifies the assumed relationship between the minimum void ratio and soil shear strength properties.

4-3-2-2: STRAIN CAPACITY BEHAVIOUR

Considering the importance of the rubber content as the main factor influencing the soil shear resistance of the composites, the necessity for further investigation was realised. To create a comprehensive investigation of the composites' behaviour, the shear-strain result was specifically analysed for the elastic modulus and volumetric strain parameters.

I- TANGENT SHEAR MODULUS

The typical responses of the elastoplastic material are reversible and non-reversible, which are defined as the elastic and plastic state. Therefore, the initial tangent elastic modulus and shear modulus parameters were analysed.

To study the rubber content and its effect on the strain capacity, the strain capacity of five composites were compared with untreated sand. With the knowledge of the pivotal role of rubber inclusion, the mixture was selected to illustrate the effect of rubber, stabiliser and rubber-stabiliser.

The critical factor for analysis of soil behaviour is the permanent deformation that occurs under plastic strain. The elastic strain is a prior condition for analysing the permanent deformation and needs to be defined first. The plastic behaviour is initialised by the yield stress, which is defined by the boundary of the linear and non-linear strain behaviours. Figure4- 10 illustrates the tangent stiffness response of samples over the shear strain, which becomes zero at the failure point. The point that the slope of the tangent elastic modulus suddenly reduces is recognised as a yielding strain point. The tangent elastic modulus is calculated by:

$$G_{\tan} = \frac{\Delta\tau}{\Delta\gamma} \tag{4.1}$$

where, G_{\tan} , τ , γ are defined as the tangent elastic modulus, shear stress, and horizontal shear strain, respectively. The slope of SC0R20 and SC5S5R20 that contain the highest dosage of rubber was very slow, which is confirmed by the rubber content effect on soil behaviour. Conversely, the sharpest slope was obtained by applying stabilisers only, which indicates the creation of denser and stronger composites.

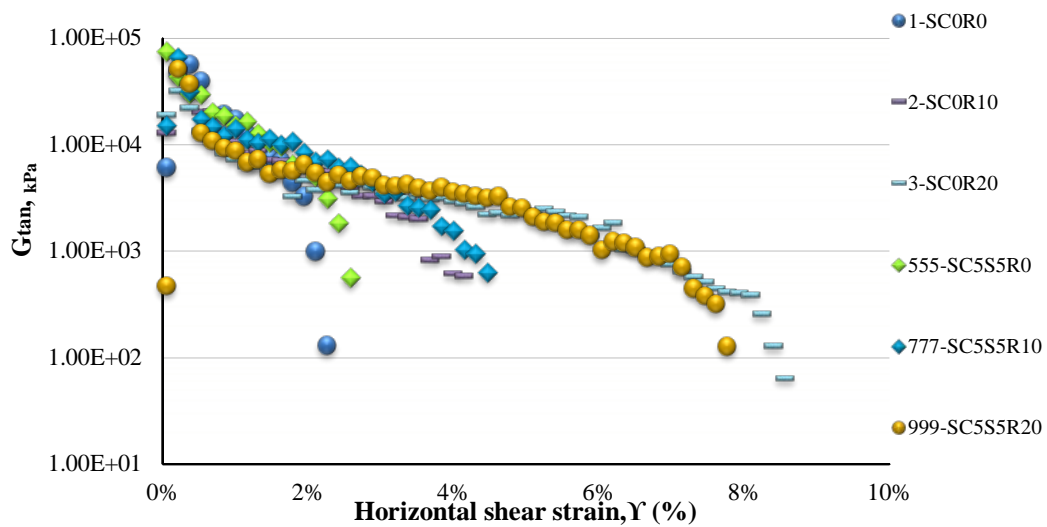


Figure4- 10. Variation of shear modulus of treated and untreated composites.

As shown in Figure4- 11, improvement of the yielding strain point of the sand has a direct relationship with the rubber inclusion, which can be created because of rolling of the rubber particles on each other. Moreover, the ductility of rubber particles can be progressed by the addition of stabiliser to create composites with a large number of connections among the particles. Consequently, the highest strain levels are associated with categories of ST5R20 and ST10R20. In contrast, the minimum modification was obtained after adding stabilisers only.

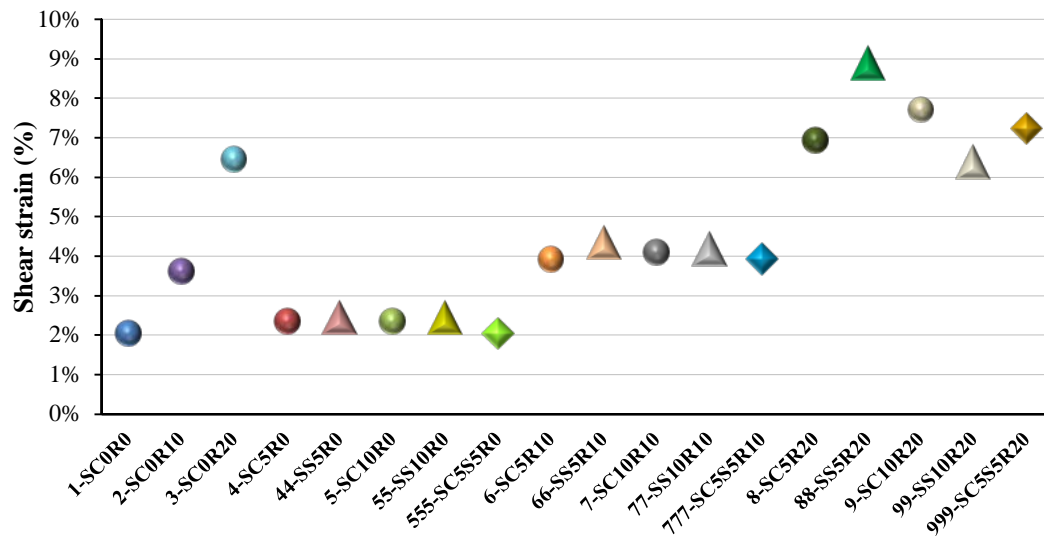


Figure4- 11. Variation of obtained yielding strain and additives content.

The tangent stiffness of the composites was then analysed to determine the possible correlation between yielding strain and yielding stress, Figure4- 12. It was expected that the addition of stabiliser only and rubber only would respectively lead to increase and reduce the stiffness of sand, respectively. The nonlinear deformation begins at the point where associated with the composite material properties. Therefore, plastic deformation will be triggered on at yielding point, where, $3.25E^{+05}$ kPa pressure had to be applied to reach the yielding point of a composite such as SC5S5R0. In addition, the minimum amount of stiffness was established in mixtures containing 20% rubber. Thus, it can be hypothesised that maybe the composites with higher yielding strain have lower shear modulus.

Conversely, there was no correlation between the tangent shear modulus and strength properties, which can be evaluated as the rigidity or flexibility of the material and their resistance to deformation. To demonstrate this assumption, all the mixtures of the STR category have greater shear strength than the pure sand do.

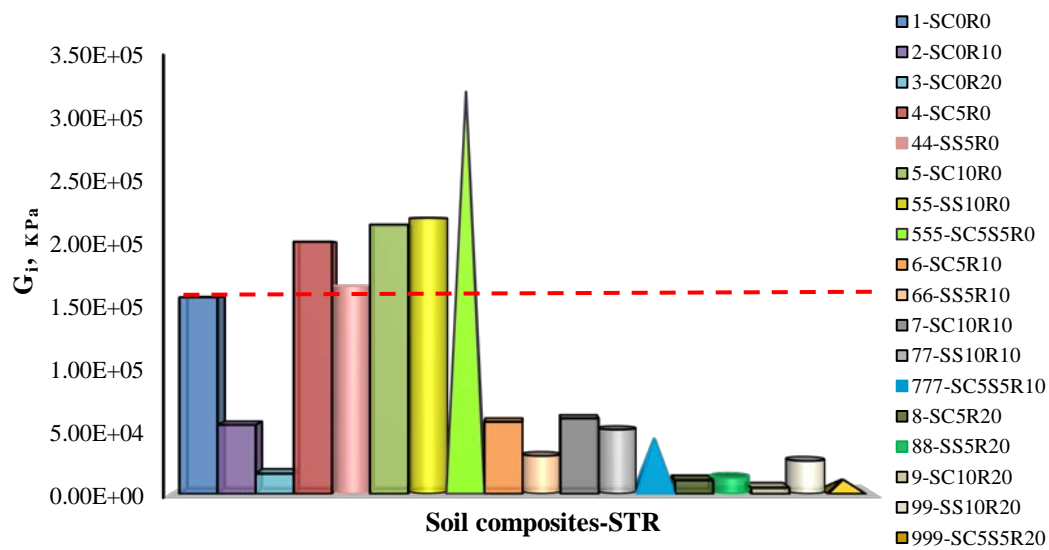


Figure4- 12. Initial tangent shear modulus is showing the effect of the additive on sand stiffness.

II- SECANT SHEAR MODULUS

The secant stiffness of mixtures can be calculated at the failure point and constant volume state. The shear modulus at each desired point was determined by the following equation:

$$G = \frac{\tau}{\gamma} \quad (4.2)$$

where G is the secant shear modulus, τ is the shear stress and γ is assigned with the shear strain. Figure4- 13 demonstrates the variation of shear modulus of sand and other treated sands under six different normal stresses.

The results appear to present three types of behaviour, which are closely related to their rubber content. Such results were expected based on the type of additive applied. The lowest quantity of rubber added increased the rigidity of the composite. Therefore, the mixtures of the ST5R0 and ST10R0 categories had the highest shear modulus, and

the most inflexible composite was established by using the combination of 5% of both slag and cement additions with sand. In contrast, the STR20 mixtures were the most flexible composites in which the minimum shear stiffness for treated sand was with 20% rubber only. The effect of normal stress on the shear modulus behaviour is shown in Figure4- 13. Increasing the normal stress leads to progressing the shear modulus of all the samples. This behaviour illustrates the expected response of the composites depending on their combination of mixtures. Thus, the results of the high-pressure loads clearly show the effectiveness rate of the additives. The difference between highest and lowest shear modulus after applying 1000 kPa normal stress was approximately $1.5E^{+04}$ greater than those difference with 50 kPa of vertical load.

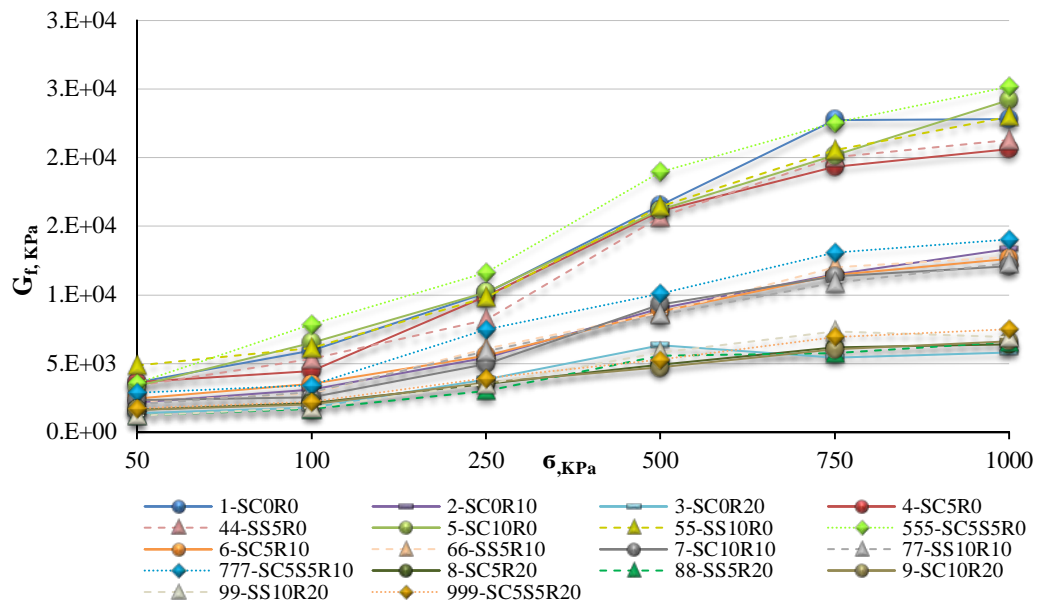


Figure4- 13. Variation of shear modulus at the failure point under six normal stresses.

Depending on the rubber content (0%, 10%, and 20%) the mixtures showed a sharp increase, a gentle progress and a very slight improvement tendency, respectively. Hence, the treatment of sand with the high dosage of rubber (20%) created a composite with the lowest impressionability of vertical load variation. With an insignificant effect of normal stress on STR20 mixtures, they tended to illustrate a linear trend.

Moreover, as discussed earlier, the flexible composite does not have a particularly low shear strength. Therefore, this behaviour may occur owing to the resistance properties of the rubber and its higher dimension to create a more uniform composite with more connections among particles. Figure4- 14 demonstrates the shear resistance of pure sand and stabilised sand under six different normal stresses. The results explain why the composites with higher quantities of rubber tend to have an elastic behaviour. In compared with the other mixtures, the composites containing the 20% rubber have failed at the longer shear displacement. In addition, the composites failure has occurred roughly at the same three ranges of shear strain. The STR20 composites reached failure after passing approximately three-quarters of their total shear displacement, which it was approximately half and less than half for STR10 and ST mixtures, respectively.

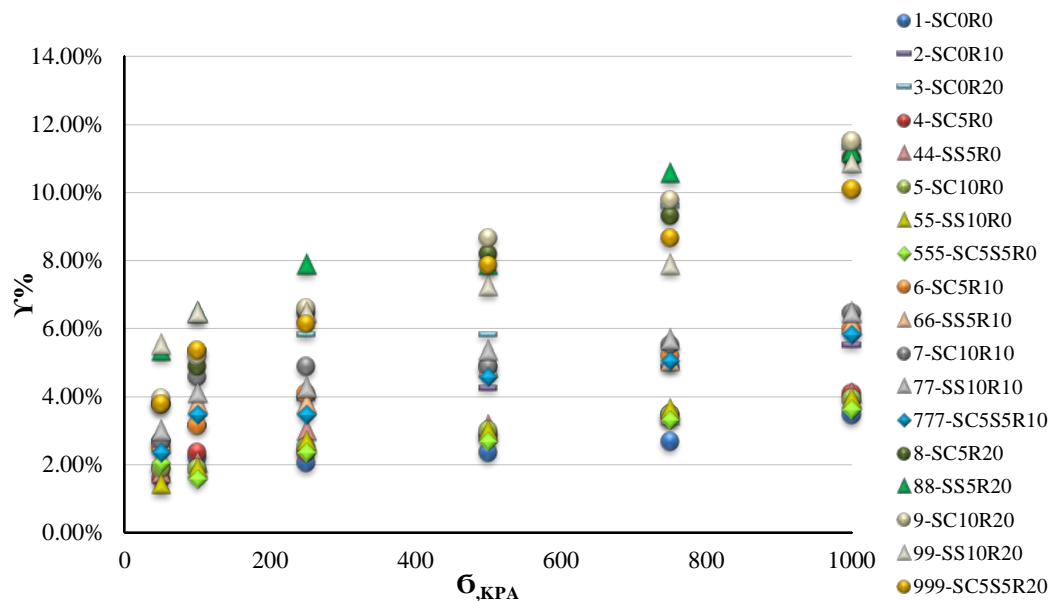


Figure4- 14. Shear strain of composites at their failure point.

The calculation of secant shear stiffness at constant volume area can be hypothesized that the flexible composite can also have great physical strength. A similar trend was obtained after the stability of shear strength and volumetric strain as shown in Figure4- 15. Comparatively, a similar behaviour at constant volume area was

observed that was not a separate tendency at the variation of normal stress. The only division occurred at 750 kPa and 1000 kPa between STR20 and the other composites, which have the higher shear modulus. This could be happened either owing to the dramatic reduction of shear stress of ST mixtures after the failure or a smaller difference between the strain point of failure and the point that needs to start the constant volume state.

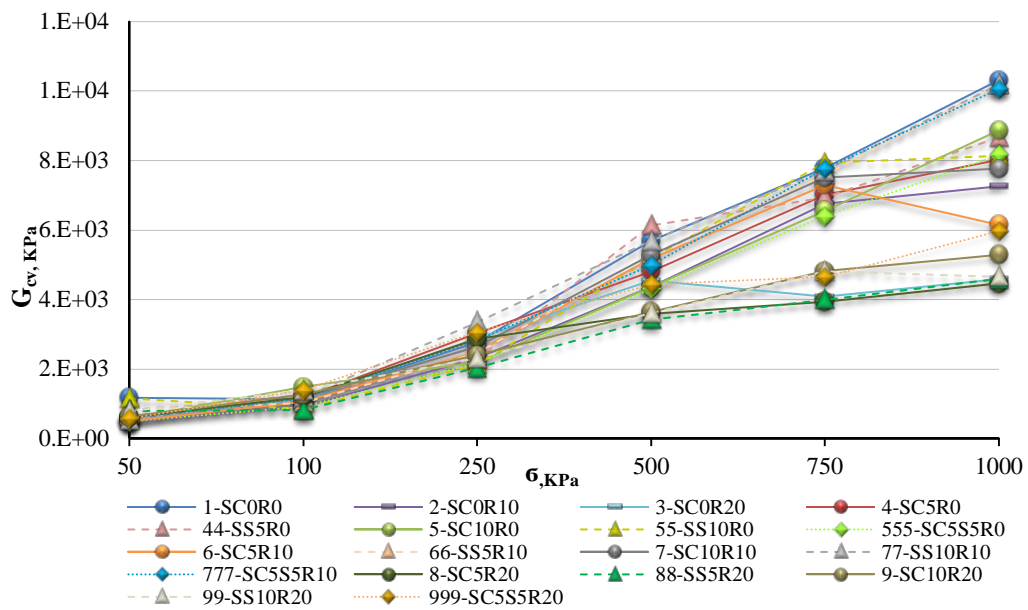


Figure4- 15. Shear modulus at constant volume.

To analysis, the above hypothesis, the difference between peak and constant volume shear stress was calculated. The results revealed an enormous reduction of the shear stress of sand treated with stabilisers after reaching the failure point, Figure4- 16.

The composites of the ST group lost their strength ability up to 181 kPa, which means the creation of rigid composites. This remarkable drop was modified by the addition of 10% of rubber to around 20 kPa. In the same manner, the minimum change was achieved by SC5S5R20, which slightly condensed about 5 kPa. Therefore, it can be expected that the samples with the addition of both rubber and stabilisers have a higher amount of shear stress than other mixtures at the constant volume state. Hence,

by considering the higher strain resistance properties of the composites of group STR10 and STR20, and the minimum reduction of shear stress after failure, the result of Figure4- 16 has been verified.

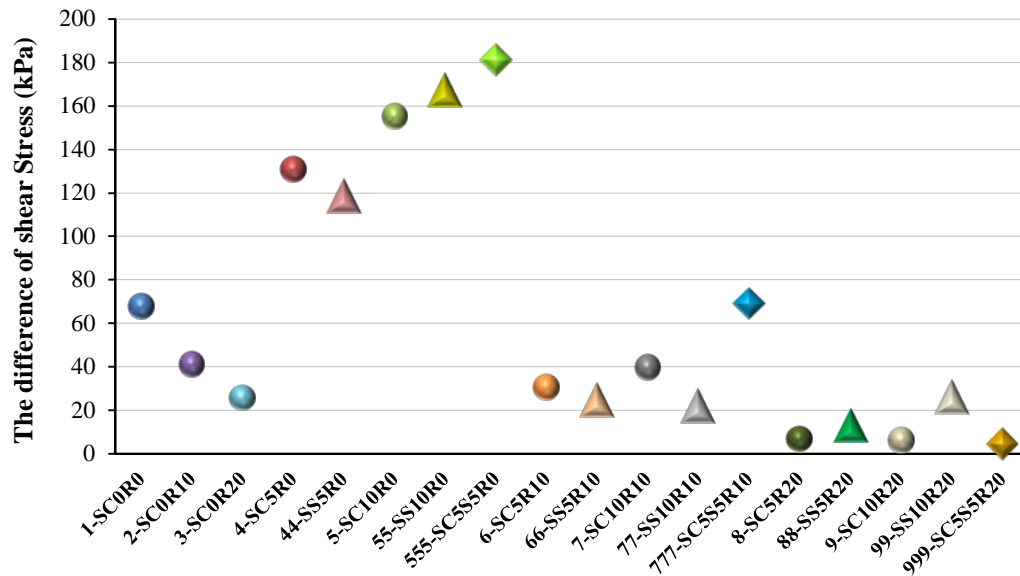


Figure4- 16. The difference between shear stress at the failure and shear stress at the constant volume state.

From all the obtained results to this point, it can be hypothesised that the relationship between the minimum void ratio of composites and its elastic modulus parameters might be corrected. This hypothesis was found to be true because of the creation of a denser composite resulting from the reduction of the matrix void ratio. Also, the decreasing of the matrix void ratio was also observed, when the shear modulus increased with the increment of normal stress. This phenomenon is observed again owing to increasing the inter-particles friction when applying higher vertical loads.

The composites with the addition of both rubber and stabilisers tended to have a stabilised behaviour. This behaviour is obvious in the STR20 groups, which generated

the most flexible composites and the minimum change after the failure, with noticeable strength properties.

To create an accurate study about the constant volume state, the vertical strain of composites needs to be analysed.

III- VOLUMETRIC BEHAVIOUR

The typical plot of the variation of volumetric strain over the shear strain of sand and the other treated sands at a normal stress of 500 kPa is illustrated in Figure4- 17. Based on their vertical movement direction over the horizontal strain (i.e., downward for contraction and upward for dilation) specific behaviour was created. All the samples reveal a behaviour similar to compression at first and the expansion, which is generated by the three kinds of movement. Similar to the earlier data, the dependency of the result of the rubber content was again realised. The pure sand and treated sand with stabilisers similar behaviour showed similar behaviours, which were mostly dilated and their volumetric strain is reduced and then flatted by increasing the shear strain. In between cement and slag, a more expanded behaviour was obtained by slag addition. In contrast, the reduction of dilation has been achieved by the addition of rubber to mixtures.

Consequently, the STR20 samples had a maximum reduction of volumetric strain, in which its contraction became wider. Owing to the ductility characteristics of rubber, applying the vertical stress prevented the finer particles from entering the rubber. This inter-particle movement led to improvement in the compressibility of composites, which is related to the void ratio of composites. Therefore, there is a relationship between the minimum void ratio and the dilatancy behaviour of the composite. Higher porosity can provide greater movement of the fine material to fill the available air and, moreover, penetrate inside the rubber particles. Eventually, the dependency of volumetric strain to the applied vertical load can also be founded.

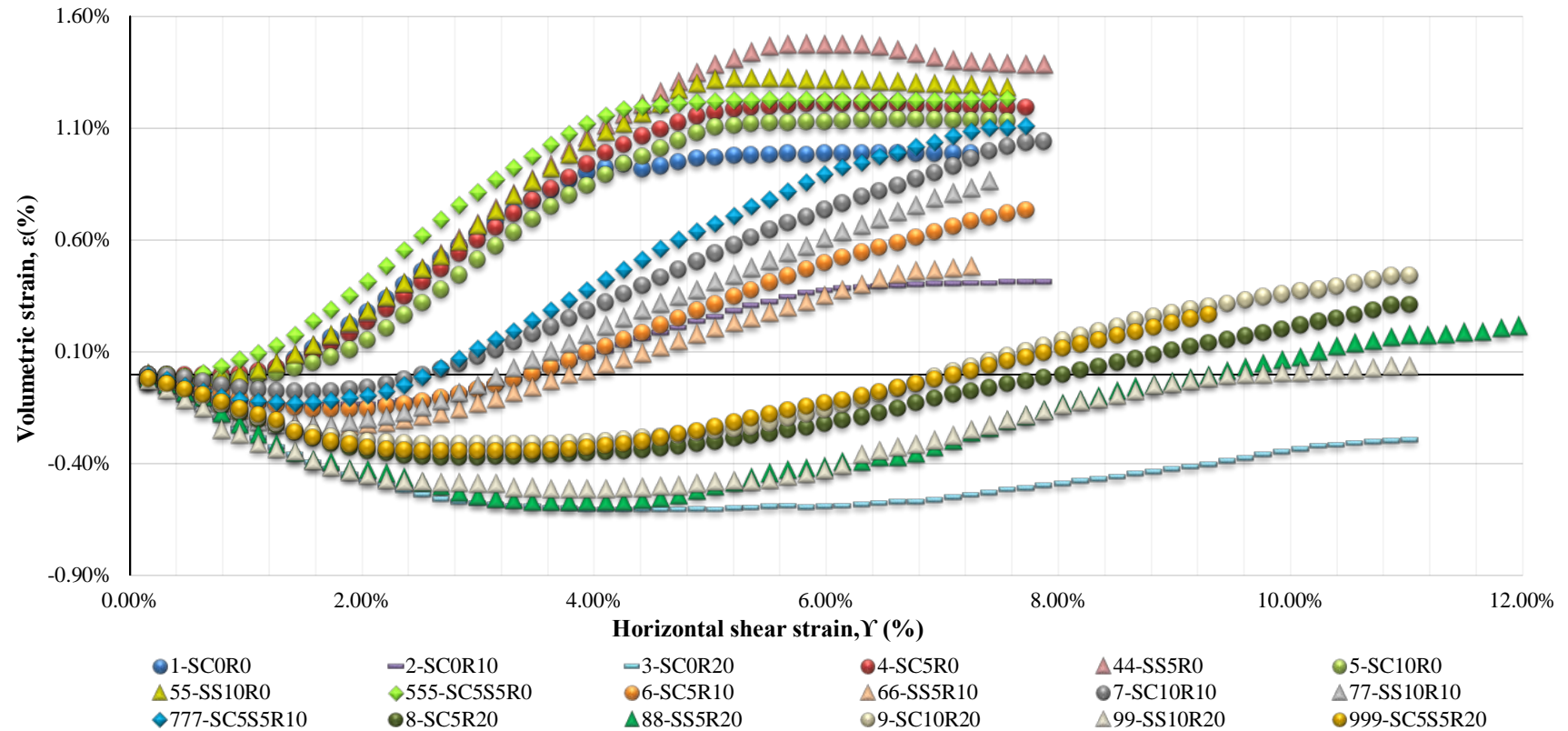


Figure4- 17. The variation of volumetric strain with shear strain for pure sand and treated sand at a normal stress of 500 KPa.

The angle of dilation can be calculated using vertical displacement and horizontal displacement with the following equation:

$$\tan \psi = \frac{dv}{dh} \tag{4.3}$$

where, ψ is the angle of dilation, v is the vertical displacement and h is the horizontal displacement. The maximum $\frac{dv}{dh}$ value is considered to be the angle of dilation at the peak value, which corresponds to the peak value of shear stress.

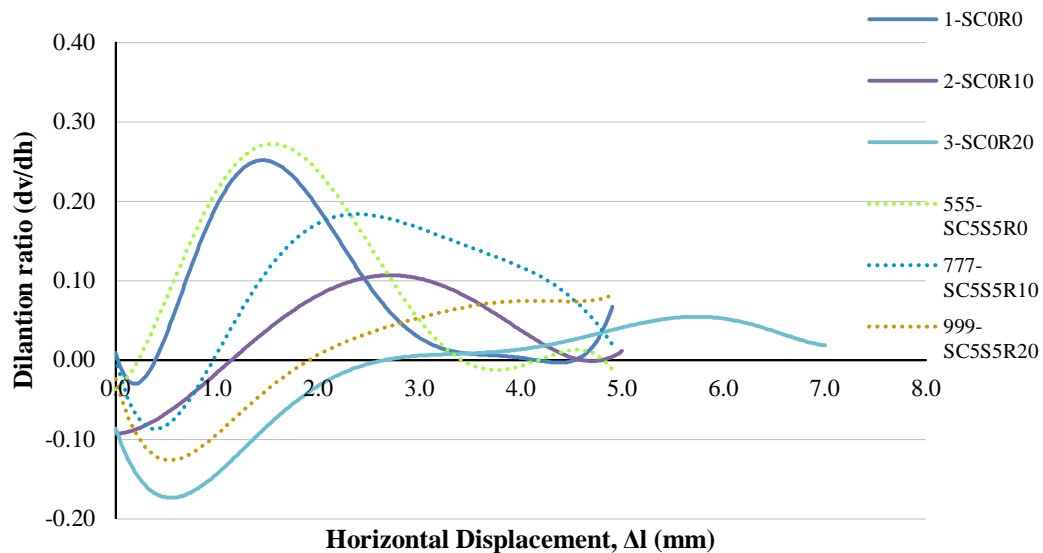


Figure4- 18. The variation of dilation ratio of treated and untreated composites.

Figure4- 18 illustrates the variation of dilation ratio versus the horizontal displacement of pure sand applying a sample in each category. As we observed, with the volumetric behaviour, all the mixtures have the contraction behaviour during the first stage. The highest dilation ratio corresponded to the SC5S5R0 sample, which is a combination of the stabilisers only. On the contrary, the lowest dilation ratio was generated by application of 20% rubber only, which contained the maximum contraction behaviour. The dilation ratio trend was obtained with a contribution of 10% rubber, with and without stabiliser.

Furthermore, the slope of dilation ratio was associated with the type and a number of additives. Comparing the dilation ratio graph to the shear stress-strain behaviour shows a similar behaviour of dilation ratio and shear stress variation, with the horizontal displacement. The dilation tended to be flattened at the constant volume, which suggests the importance of the angle of dilation.

Thus, increasing the contraction, reducing the dilation, generating a flexible mixture, improving the shear resistance and minimising the shear strength reduction after the failure are recognised as several of the advantages of rubber application in sand treatment.

The explained result only presents results from one of the applied loads. To provide a comprehensive and more accurate conclusion, data of all normal stresses are presented in Table4- 2.

Table4- 2. The results of small direct shear test.

COMPOSITE	σ	$\tau_p(\text{kpa})$	$\tau_{Cv}(\text{kpa})$	$G_f(\text{kpa})$	$G_{cv}(\text{kpa})$	$\gamma\%$
1-SC0R0	50	41.19	32.30	3.63E+03	1.18E+03	1.89%
	100	80.17	68.80	5.93E+03	1.13E+03	2.21%
	250	208.00	166.70	1.02E+04	2.79E+03	2.05%
	500	390.90	322.30	1.65E+04	5.69E+03	2.36%
	750	609.00	477.90	2.27E+04	7.78E+03	2.68%
	1000	790.40	633.30	2.28E+04	1.03E+04	3.47%
4-SC5R0	50	57.64	41.85	3.66E+03	5.97E+02	1.58%
	100	105.70	71.18	4.47E+03	1.18E+03	2.36%
	250	234.10	176.80	9.90E+03	3.03E+03	2.36%
	500	457.10	326.00	1.61E+04	4.81E+03	2.84%
	750	670.20	542.00	1.93E+04	7.02E+03	3.47%
	1000	844.80	632.10	2.06E+04	8.02E+03	4.10%
5-SC10R0	50	63.57	35.52	3.36E+03	5.89E+02	1.89%
	100	123.10	78.33	6.51E+03	1.48E+03	1.89%
	250	257.10	166.40	1.02E+04	2.20E+03	2.52%
	500	484.70	329.40	1.62E+04	4.36E+03	2.99%
	750	698.80	495.80	2.02E+04	6.56E+03	3.47%
	1000	954.10	684.30	2.42E+04	8.87E+03	3.94%

2-SC0R10	50	58.09	38.96	2.17E+03	4.90E+02	2.68%
	100	98.24	72.16	3.11E+03	9.16E+02	3.16%
	250	213.50	182.40	5.42E+03	2.32E+03	3.94%
	500	384.20	342.90	9.03E+03	4.35E+03	4.26%
	750	560.60	532.40	1.15E+04	6.76E+03	4.89%
	1000	735.60	686.10	1.33E+04	7.26E+03	5.51%
3-SC0R20	50	52.46	45.85	1.39E+03	5.74E+02	3.78%
	100	95.43	89.80	1.78E+03	1.14E+03	5.35%
	250	224.50	218.00	3.85E+03	2.88E+03	5.83%
	500	369.05	343.20	6.33E+03	4.54E+03	5.83%
	750	523.70	514.20	5.45E+03	4.08E+03	9.61%
	1000	656.70	650.40	5.79E+03	4.59E+03	11.34%
6-SC5R10	50	61.94	41.64	2.46E+03	5.05E+02	2.52%
	100	110.80	83.28	3.51E+03	1.06E+03	3.16%
	250	228.80	193.10	5.58E+03	2.50E+03	4.10%
	500	429.90	399.20	8.80E+03	5.17E+03	4.89%
	750	595.10	574.40	1.14E+04	7.29E+03	5.20%
	1000	755.60	678.20	1.26E+04	6.15E+03	5.98%
8-SC5R20	50	61.94	48.41	1.64E+03	6.14E+02	3.78%
	100	104.60	92.61	2.14E+03	1.20E+03	4.89%

	250	227.90	226.40	3.53E+03	2.87E+03	6.46%
	500	403.50	396.50	4.93E+03	3.60E+03	8.19%
	750	573.90	552.40	6.17E+03	3.94E+03	9.29%
	1000	705.60	689.50	6.40E+03	4.47E+03	11.02%
7-SC10R10	50	62.83	45.30	2.34E+03	5.69E+02	2.68%
	100	115.60	92.61	2.53E+03	1.18E+03	4.57%
	250	243.50	209.20	4.98E+03	2.66E+03	4.89%
	500	455.40	415.40	9.32E+03	5.27E+03	4.89%
	750	626.20	579.10	1.14E+04	7.50E+03	5.51%
	1000	780.60	734.20	1.21E+04	7.77E+03	6.46%
9-SC10R20	50	64.16	51.27	1.63E+03	6.40E+02	3.94%
	100	106.40	99.43	2.05E+03	1.26E+03	5.20%
	250	239.60	227.30	3.62E+03	2.40E+03	6.61%
	500	408.70	402.60	4.72E+03	3.65E+03	8.66%
	750	588.30	584.40	6.02E+03	4.82E+03	9.77%
	1000	761.70	749.90	6.62E+03	5.29E+03	11.50%
44-SS5R0	50	58.94	42.18	3.39E+03	8.19E+02	1.74%
	100	109.10	72.72	5.33E+03	1.25E+03	2.05%
	250	245.70	173.40	8.19E+03	2.29E+03	3.00%
	500	494.30	377.00	1.57E+04	6.14E+03	3.15%

	750	694.10	514.30	2.00E+04	6.94E+03	3.47%
	1000	872.10	668.90	2.13E+04	8.67E+03	4.10%
55-SS10R0	50	68.96	54.83	4.86E+03	1.15E+03	1.42%
	100	116.00	67.57	6.13E+03	8.58E+02	1.89%
	250	263.20	168.50	9.83E+03	2.14E+03	2.68%
	500	492.60	326.90	1.65E+04	5.19E+03	2.99%
	750	744.50	499.50	2.05E+04	7.93E+03	3.63%
	1000	906.10	641.00	2.30E+04	8.14E+03	3.94%
555-SC5S5R0	50	73.36	40.92	3.58E+03	5.01E+02	2.05%
	100	123.60	71.13	7.84E+03	9.21E+02	1.58%
	250	274.70	167.40	1.16E+04	2.17E+03	2.36%
	500	507.80	326.30	1.90E+04	4.32E+03	2.68%
	750	745.80	483.80	2.25E+04	6.40E+03	3.31%
	1000	912.40	642.70	2.52E+04	8.16E+03	3.63%
66-SS5R10	50	59.72	48.08	2.23E+03	8.19E+02	2.68%
	100	107.10	81.50	2.83E+03	1.03E+03	3.78%
	250	229.70	190.60	6.07E+03	2.47E+03	3.78%
	500	424.50	401.30	8.69E+03	5.31E+03	4.89%
	750	605.90	573.60	1.20E+04	7.59E+03	5.04%
	1000	784.00	770.80	1.28E+04	1.02E+04	6.14%

77-SS10R10	50	61.05	38.32	2.04E+03	5.47E+02	3.00%
	100	118.70	91.87	2.90E+03	1.19E+03	4.10%
	250	250.10	232.30	5.88E+03	3.35E+03	4.26%
	500	459.20	438.90	8.58E+03	5.69E+03	5.35%
	750	616.90	595.00	1.09E+04	7.71E+03	5.67%
	1000	795.00	786.00	1.23E+04	1.02E+04	6.46%
777-SC5S5R10	50	67.87	39.59	2.88E+03	5.86E+02	2.36%
	100	118.70	90.09	3.42E+03	1.17E+03	3.47%
	250	259.00	218.30	7.47E+03	2.83E+03	3.47%
	500	461.70	392.40	1.01E+04	4.98E+03	4.57%
	750	659.60	611.70	1.31E+04	7.77E+03	5.04%
	1000	818.10	776.20	1.40E+04	1.01E+04	5.83%
88-SS5R20	50	65.20	62.29	1.22E+03	7.94E+02	5.35%
	100	110.10	90.24	1.70E+03	8.19E+02	6.46%
	250	237.70	224.60	3.02E+03	2.04E+03	7.88%
	500	438.20	426.60	5.56E+03	3.43E+03	7.88%
	750	609.50	573.00	5.77E+03	4.00E+03	10.55%
	1000	735.10	709.80	6.57E+03	4.60E+03	11.18%
99-SS10R20	50	66.09	64.16	1.20E+03	7.88E+02	5.51%
	100	115.40	109.40	1.79E+03	1.39E+03	6.46%

	250	226.30	215.30	3.50E+03	2.32E+03	6.46%
	500	421.60	396.80	5.82E+03	3.60E+03	7.25%
	750	578.20	530.80	7.34E+03	4.82E+03	7.88%
	1000	750.50	720.00	6.91E+03	4.66E+03	10.87%
999-SC5S5R20	50	66.09	46.70	1.75E+03	5.77E+02	3.78%
	100	118.20	107.40	2.21E+03	1.39E+03	5.35%
	250	241.20	237.10	3.93E+03	3.07E+03	6.14%
	500	416.50	411.90	5.29E+03	4.43E+03	7.88%
	750	601.80	571.50	6.95E+03	4.65E+03	8.66%
	1000	756.90	743.00	7.51E+03	5.97E+03	10.09%

4-4: ANALYSIS OF RESULTS

Shear strength characteristics and volumetric behaviour of the mixtures were examined concerning the type, the portion of additives and the different vertical loads. Thus, the influence of rubber and stabiliser on the friction angle and shear strength at the failure point at a constant level has been analysed separately considering the variation of rubber and stabilisers content. Also, the cohesion and angle of dilation of the mixture were analysed.

4-4-1: EFFECT OF NORMAL STRESS ON PEAK SHEAR STRENGTH

The typical plot of small direct shear test for variation of normal stress for pure sand and 17 treated sands with different quantities of additives present are shown in Figure4- 19. The specific response of mixtures considering the portion of additives at the different vertical loads revealed their shear strength characteristics. Plotting the peak shear stress over the normal stress described the failure envelope of each composite, which leads to defining the cohesion and peak friction angle. Thus, there is a higher effectiveness of stabiliser than rubber for improving the shear resistance of sand. Implementation of a number of stabilisers create samples with great strength ability among the composites, with the highest peak achieved by the 10% stabiliser and the lowest belonging to the 20% rubber only.

Through the investigation into the effect of normal stress on the composites behaviour, two main findings were reported. First, the shear strength progress was directly related to the increment of normal stress. This can occur by the reduction in the void ratio of mixtures, which is caused by overburden pressure affecting the improvement of the interlocking capacity of materials. Also, under the higher amount of vertical load, the difference of peak shear stress also increased. This trend is observed after applying the high-level loads including 500 kPa, 750 kPa, and 1000 kPa.

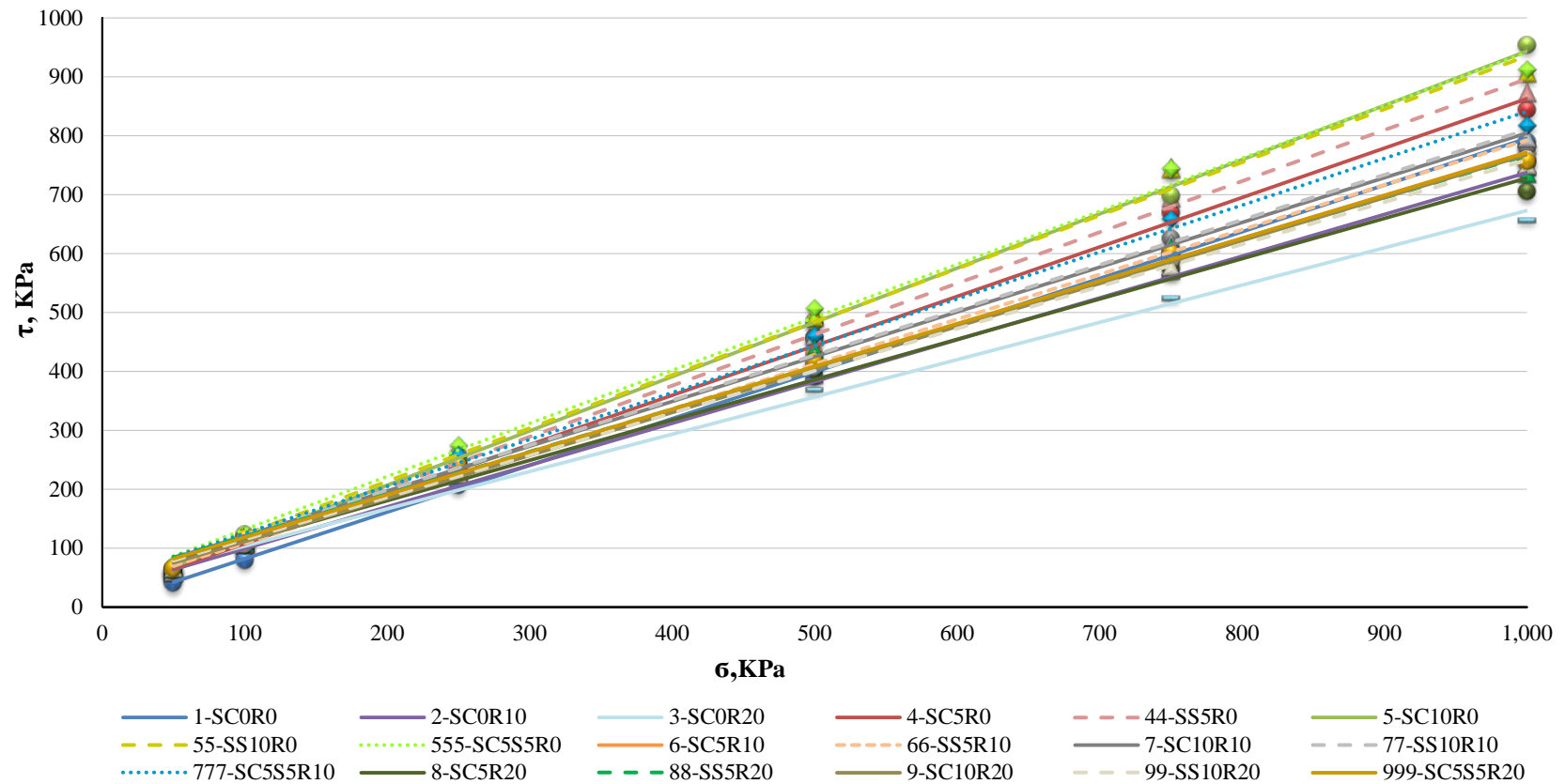


Figure4- 19. A typical plot for the failed envelope of sand composites with the variation of additives.

Second, the rubber only application revealed two different behaviours influenced by two different pressure groups. The sand-rubber mixtures behaved similarly with the reinforced composite when applying the first three vertical loads; however, this behaviour was reversed during the second category of normal stress. Thereby, the STR10 and STR20 samples have a lower shear stress than pure sand does. This can be explained that, under applying a high level of pressure, the composite has lost a greater amount of its void ratio. The lower porosity means a lower space for moving the rubber particles over and beside each other for creating more connections among the particles. The rearrangement of the composite particles was limited to fill the voids among the particles and inside of the rubber with the finer units, rather than the larger particles. This trend is more justifiable when the second lowest peak shear corresponds to the composites of the ST5R20 category. Thus, the result has revealed a dominant role of rubber on the sample in combination with the stabiliser and rubber.

The cohesion of soil (C) is the obvious shear strength at the zero normal stress to monitor the effects of intermolecular force (C_0), which can normally be ignored, cementation (C_{cm}) and soil tension (C_i) on the shear strength of soil (Figure4- 20). It should be noted that soil tension caused by the surface tension of water particles in unsaturated soils disappears after full saturation. Moreover, due to the availability of cementing particles in soil, and creating chemical bonding among the particles is introduced (Budhu, 2008).

Figure4- 20 illustrates the variation of cohesion values of pure sand and treated sand with the variety of additives. It can clearly be seen that the application of both stabilisers and rubber created a mixture with a developed capacity to maintain more integrated particles. It can be assumed that the cohesion value of sand has been improved by the generation of soil tension and cementation, where the maximum value is achieved with the combination of 5% of both cement and slag and 20% rubber. The

increment of rubber content does not necessarily lead to a significant improvement, in which the same behaviour was observed as for the stabiliser addition.

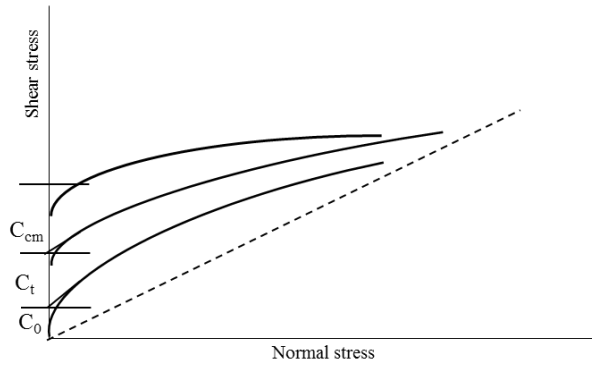


Figure4- 20. A schematic drawing of failure envelope for soil. The slop of dot line shows friction angle at the critical state.

Nevertheless, regarding the importance of internal friction on the soil strength characteristics, it cannot be assumed that the mixture with the maximum cohesion value has the greatest shear resistance.

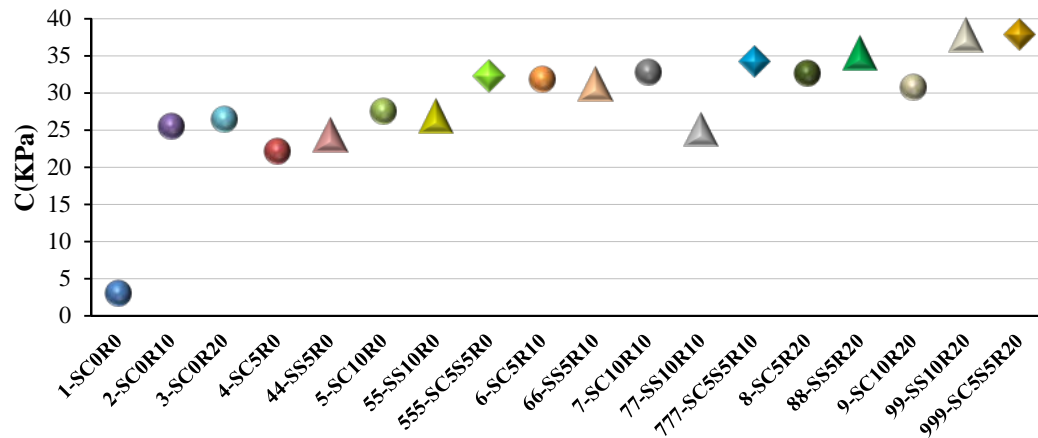


Figure4- 21. The variation of apparent cohesion for sand and treated sands obtained from failure envelope graph

The angle of internal friction was analysed to create an appropriate understanding of the shear strength properties of mixtures. Similar to the cohesion value, the friction angle of sand increased after utilising the additives (Figure4- 21). Thus, the progress of internal friction is directly related to increasing the dosage of additives, whereas the

rubber showed different behaviour. To describe the different behaviour of rubber, a sufficient percentage, angularity shape and ductility characteristics of rubber all contributed to improving the friction angle of the composites. The rubber inclusion led to their participating in the rearrangement and interlocking of the mixture's particles, consequently resisting against the creation of a shearing zone. By utilising the rubber over the mixture capacity, the more area of the mixture was occupied by the rubber particles. Thereby, the interface of rubber particles became more dominate than the sand-rubber boundary inside the mixture. Thus, in addition to the minimum shear resistance ability, SR20 has the lowest angle of friction (i.e., 39°), which was similarly reported by earlier research (Anvari et al., 2017). Whilst, SC5S5R0 with approximately 48° creates the maximum angle of friction, which has the greatest shear strength properties.

Eventually, the friction angle of all the mixtures of ST5R10, ST10R10, ST5R20 and ST10R20 category similarly increased, with an improvement between three and seven degrees of friction angle (Figure4- 22).

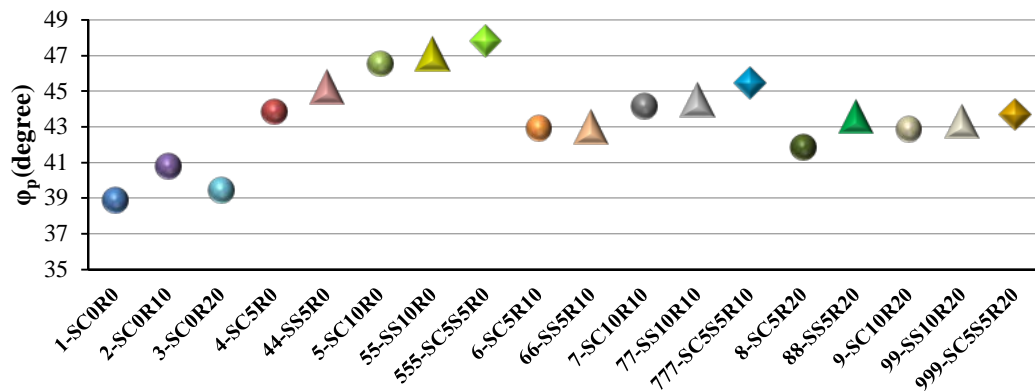


Figure4- 22. The friction angle of sand and sand treaded composites

After passing the failure point, the mixture moves to the steady state, where the shear continues without any variation of void ratio, volume and shear stress. The minimum shear strength that a soil can have at this stage presents by the angle of friction at the critical state, Figure4- 23 illustrates the plots for variation of friction

angle at the constant volume state with the different sand mixtures (Figure4- 23). The friction angle of sand at the critical state is 33° , where the minimum improvement was obtained with SC5S5R0 mixture by just one degree. However, the most effective results were achieved with the ST5R20 and ST10R20 composites, with eight degrees improvement. By increasing the rubber content the critical state friction angle progressed, which showed a different response to internal friction angle. Therefore, by the readjustment of particles due to the failure, and greater possibility of the rubber-sand interface, a denser mixture could be generated.

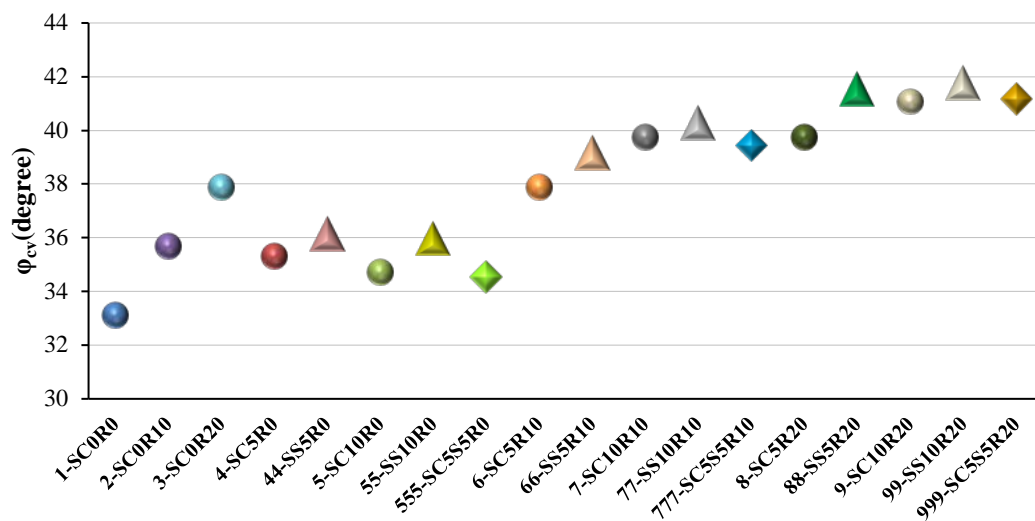


Figure4- 23. Variation of the critical state friction angle of sand and treated sand composites.

Then, the critical role of the angle of dilation to estimate the sand shear strength characteristics was determined by comparing the angle of friction at the failure and constant volume. The variation in the volumetric strain of soil during the shear process was measured by the dilation angle, which can be related to the cementation of soil. The failure envelope trend gradually deviated from being straight as a result of dilation effect to improve the shear resistance of the soil.

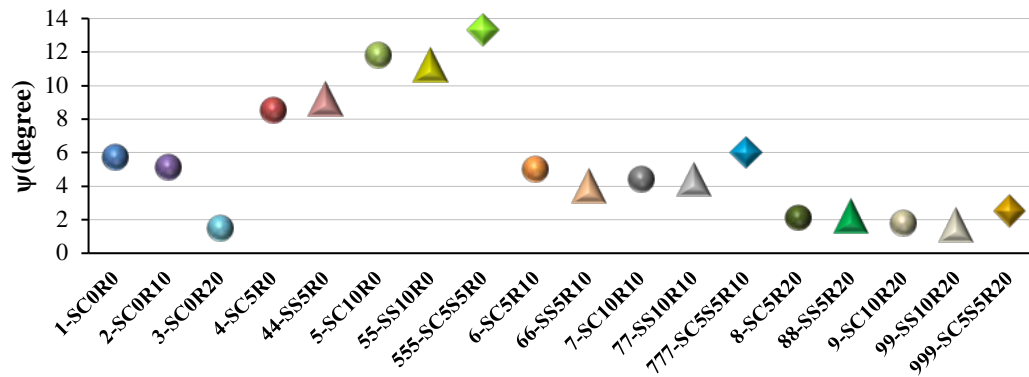


Figure4- 24. Variation of dilation angle of 18 samples

The maximum angle of dilation corresponding to the composite groups treated with stabilisers only (Figure4- 24). The maximum angle of dilation corresponded to SC5S5R0 and the minimum value was assigned to SR20. Nevertheless, it cannot be claimed that the specimen with the minor dilation angle has lower shear strength capacity, where sand has significantly reinforced the mixture of both stabiliser and rubber. Thus, considering the reasonable improvement of shear strength, in addition to minimising the dilation angle, the combination of additives can create composites with a more steady behaviour before and after the failure.

4-5: CONCLUSION

A series of small direct shear tests were conducted on pure sand and treated sand with various quantities of cement, slag and rubber addition. The tests were carried out to analyse the shear strength properties of sand composites with the consideration of:

Applying low and high levels of vertical loads to distinguish the normal stress effect on the shear strength parameters.

A comparable analysis to evaluate the application of stabilisers and rubber both alone and in combination to obtain the optimum achievement.

Hence, 108 small direct shear tests were performed on the 18 different sand mixtures to make the following conclusions:

1. The results for the maximum density of mixtures were separated into three groups influenced by the rubber content. The maximum value obtained by applying the stabilisers only and, then, the material with the contribution of 10% and 20% rubber have low density, respectively. In contrast, the minimum void ratio value revealed the opposite behaviour.
2. The degree of improvement in shear strength was oppositely connected to the quantity of rubber in the composites. The treated sand with rubber only had the minimum shear strength, which behaves similar to the loose sand. The maximum shear strength was achieved by the combination of 5% of both slag and cement on sand mixtures with no participation of rubber.
3. Nevertheless, the strain resistance of sand was directly associated with the rubber proportion in the matrix. The results were categorised into the three groups influenced by their rubber proportions, and the highest strain capacity was for the composites of the ST5R20 and ST10R20 categories.

4. Overall, the composites with higher yielding strain showed lower shear modulus than those with lower yielding strain. The composites with the addition of both rubber and stabilisers tended to have stabilised behaviour. This behaviour is most obviously observed in the STR20 groups, which generated the most flexible composites and the minimum change after the failure with noticeable strength properties.
5. The connections between the minimum void ratio of composites and the elastic modulus parameters were observed. Creating denser composites occurred because of the reduction of the matrix void ratio. Increasing the normal stress also leads to the decreasing of the matrix void ratio due to increasing the inter-particles friction under higher vertical loads.
6. The highest dilation ratio was obtained with applying equally the 5% cement and slag sample. On the contrary, the maximum contraction behaviour was generated by application of 20% rubber only.
7. The cohesion value of sand was improved by introducing the soil tension and cementation, due to the stabiliser and rubber utilisation in the sand treatment.
8. SC5S5R0 with approximately 48° and SR20 with 39° obtained the maximum and minimum improvement of sand's friction angle, respectively.
9. The friction angle of sand was effectively improved in the composites of ST5R20 and ST10R20 group, with an eight-degree improvement, whereas the minimum improvement was assigned to the SC5S5R0 group.
10. In sand, the addition of either 5% or 10% of any of the stabilisers with 20% rubber has the minimum value of dilation angle, which has the most stable behaviour before and after failure.

CHAPTER5

**A COMPARISON STUDY ON THE SHEAR
STRENGTH OF SAND-RUBBER
COMPOSITES INVESTIGATED BY THE
SMALL-SCALE AND LARGE-SCALE
DIRECT SHEAR TESTS**

This chapter presents the following section:

5-1: Introduction	119
5-2: Material and Methodology	122
5-3: Results and Discussions	123
5-3-1: Compaction Test	123
5-3-1-1: Maximum Dry Density and Optimum Moisture Content.....	124
5-3-1-2: Floating and non-floating cases	128
Brief summary.....	132
5-3-2: Large Direct Shear Test Results.....	133
Brief summary.....	138
5-4: Large Direct Shear Versus Small Direct Shear	138
5.4.1 Shear Stress–Shear Strain.....	139
Brief summary.....	141
5.4.2 Shear Modulus	142
Brief summary.....	143
5.4.3 Maximum Friction Angle	143
5.4.3.1 Scale effect on the maximum friction angle	144
Brief summary.....	146
5.4.3.2 Peak friction angle and maximum dry density	147
Brief summary.....	151
5.4.4 Constant Volume State Friction Angle	152
5.4.4.1 Scale effect on the constant volume state friction angle	152
Brief summary.....	154
5.4.4.2 Constant volume friction angle and maximum dry density.....	155
Brief summary.....	157
5.4.5 Volumetric Strain.....	158
Brief summary.....	160
5.4.6 Angle of Dilatation	161
Brief summary.....	163

5.4.7 Effect of Rubber Particles on Dilation Behaviour	164
5.4.8 Analysing Dilation Ratio	166
Brief summary... ..	170
5-5 Maximum Dilation Angle.....	170
5-5-1 Maximum dilation angle and peak friction angle.....	170
Brief summary... ..	175
5-5-2 Empirical Equation for Maximum Dilation Angle.....	175
Brief summary... ..	179
5.5.3 Constant Volume Friction Angle	179
Brief summary... ..	183
5.5.4 Stress–Dilation Law	183
Brief summary... ..	186
5.6 Cohesion.....	187
5.6.1 Comparison of Apparent Cohesion in Large and Small Scales.....	187
5.6.2 Relationship Between Apparent Cohesion and Maximum Dry Density	188
Brief summary... ..	190
5.6.3 Shear Strength Improvement Index (C_i).....	192
Brief summary... ..	194

5-1: INTRODUCTION

Although soil reinforcement with stabilisers such as cement and slag improves soil strength, it might be insufficient for providing a soil with a reasonable tension capacity (Park, 2009). Recently, various types of reinforcement materials have been developed to enhance the engineering properties of soil in terms of both soil strength and soil tension (Cerato and Lutenecker, 2006, Edinçliler and Ayhan, 2010, Yoon and Abu-Farsakh, 2009, Xiao et al., 2015, Bareither et al., 2008, Afzali-Nejad et al., 2017, Wang et al., 2008). Further, a composite containing a soil mass or any other similar reinforcement material with engineering characteristics such as strength and tension is known as reinforced soil. This soil can be systematically or simply reinforced by orienting it in a specific direction or by randomly distributing it with rubber added as a stabiliser, respectively. Several researches, have reported that the use of rubber for sand reinforcement remarkably improves both the strength and the stiffness of sand (McGown et al., 1978, Hoare, 1979, Elgart et al., 1975, Gray and Al-Refeai, 1986, Gray and Maher, 1989, Al-Refeai, 1991, Infante et al., 2016, Hataf and Rahimi, 2006, Simoni and Houlsby, 2006, Zhang et al., 2016, Veiskarami et al., 2011, Amini et al., 2014, Cerato and Lutenecker, 2006, Edinçliler and Ayhan, 2010, Yoon and Abu-Farsakh, 2009, Xiao et al., 2015, Bareither et al., 2008, Afzali-Nejad et al., 2017, Wang et al., 2008). In comparison with plain sand or sand treated only with stabilisers, the sand with added rubber exhibits relatively high extensibility and considerably reduced shear strength after a failure. Furthermore, some researchers have founded several effective parameters on the shear strength properties including particle size, shape and gradation of the composite material. Moreover, the extent of improvement of a mixture's engineering characteristics has been defined as a function of several factors such as the rubber type, length and aspect ratio, and rubber content.

Based on the location and the proportion of rubber in a mixture, the arrangement of rubber particles within the soil is normally two- or three-dimensional. In such a case, the addition of soil in a specific direction (i.e. one dimension) is a difficult application.

In a field application, soil reinforcement with rubber is achieved using a random, homogeneous combination of soil and rubber. The advantage of using randomly distributed rubber on the oriented reinforcement is the decreased possibility of the creation of planes of weakness parallel to the direction of rubber addition. The addition of rubber, up to a specific amount, increases the maximum strength of the soil; in particular, it increases both the cohesion and the angle of friction of the soil. Thus, the addition of rubber to the soil improves the apparent cohesion of the soil.

In embankment construction, a considerable amount of direct shear force with relatively small tyre chips should be applied to the rubber for creating a lightweight mixture with the soft soil (Elgart et al., 1975, Al-Refeai, 1991, Gray and Maher, 1989, Edinçliler and Ayhan, 2010, Zhang et al., 2016, Veiskarami et al., 2011, Xiao et al., 2015, Bareither et al., 2008, Afzali-Nejad et al., 2017, Wang et al., 2008, Tavenas and Rochelle, 1972, Webster and Santoni, 1997). Such an application typically yields a cohesive force of approximately 8 kPa and a friction angle ranging between 19° and 25° (Humphrey and Blumenthal, 2010, Humphrey et al., 1998, Humphrey, 2007, Edinçliler and Ayhan, 2010, Amini et al., 2014). Another study reported an increase in the shear strength of the material irrespective of the rubber content. The abovementioned application of the shear force on the sand and a sandy silt mixture with rubber chips (up to 30% by volume) demonstrated an increase in the soil cohesion and a corresponding increase in the shear resistance. Further, several studies have reported that the friction angle of the sand increased to 65° from 34° after the addition of tyre chips (30% by volume) (Edinçliler and Ayhan, 2010, Edinçliler et al., 2010, Edil and Bosscher, 1992, Edil and Bosscher, 1994, Ahmed and Lovell, 1993). The possibility of using tire shreds for sand reinforcement was investigated by (Foose et al., 1996, Edinçliler and Ayhan, 2010, Infante et al., 2016). This previous study revealed the effects of five factors, namely the vertical load, mixture unit weight, rubber length and content, and the location of the rubber particles in the soil. The results thus obtained emphasised that the mixture unit weight and the rubber content

are the two most important parameters that affect the shear strength of the reinforced soil. Attom (2006), studied the shear strength properties of sand by using direct shear tests (Edinçliler and Ayhan, 2010). The results revealed that the use of rubber could improve both the shear strength and the friction angle of the sand mixture. A variety of sand–tyre shred mixtures having different shred content, shred aspect ratios and thicknesses were prepared to study the effects of the size of the rubber shreds and the unit weight on the shear characteristics of the soil (Ghazavi and Sakhi, 2005, Ghazavi, 2004, Anvari et al., 2017). The results of a large shear box test revealed that the shear content, shear width and its aspect ratio, level of compaction and the vertical load applied for the direct shear test affected the result.

Although many previous studies involved the use of tire shreds and tire chips, the application of rubber buffing to sand is not a common method (Edinçliler and Ayhan, 2010, Edinçliler et al., 2004, Edinçliler, 2007). Edinçliler performed large direct shear (LDS) tests for the application of rubber buffing to sand (Edinçliler and Ayhan, 2010, Edinçliler et al., 2004). They considered a width range of 1 mm to 4 mm, and lengths ranging from 2 mm to 40 mm. The application of 10% tire buffing by weight modified the hardening behaviour of the mixture at a low strain, to a softening response at a large strain (Edinçliler, 2007, Xiao et al., 2015). The initial hardening was attributed to the shape of the fibers used for the rubber buffing, which may be considered an advantage under a low strain loading condition. In contrast, the application of 10% rubber buffing to low-plasticity kaolinite clay did not lead to any change in the shear strength and the compaction behaviour of the mixture (Özkul and Baykal, 2006, Edinçliler and Ayhan, 2010).

Considering the limited existing research on the application of rubber buffing to soil reinforcement, particularly with the addition of a soil stabiliser, the following research were designed and performed. In this section, the effects of the addition of rubber and/or a stabiliser for sand reinforcement will be rigorously investigated to determine an optimum mix of the stabiliser and rubber. The obtained results will then be

compared with those of the small-scale tests to determine the scale effect on the composite behaviour.

5-2: MATERIAL AND METHODOLOGY

The experiments discussed in the earlier chapter were performed to verify the rubber buffing efficiency for sand treatment, and the tests that will be discussed in this chapter were conducted to gain a better understanding of the obtained results, considering a comparison between cement and slag. In this experimental program, 15 mixtures, including pure sand, sand–rubber, sand–stabiliser and sand–rubber–stabiliser composites, were divided into three main groups. The percentage of cement and slag used in these experiments was 5% and 10%, respectively, and that of rubber was 10% and 20% of the total mass of the composites. The letters and numbers used represent the type and the proportion of the additive, respectively. The notations of C for cement, S for slag and R for rubber describe the composite mixtures. Thus, the designations of ST, SR and STR present a group of mixtures containing only stabilisers, only rubber and both stabilisers and rubber, respectively. The details of all the composite combinations are presented in “3.2 Composite Preparation section”. A combination of specimens was selected to compare the effect of each type of additive separately and of a combination of additives to develop a composite with optimum efficiency. A series of standard compaction tests were performed using the various mixtures to define the optimum moisture content (OMC) and the maximum dry density (MDD) in accordance with ASTM D698 (D698, 2015). The results of the compaction tests were useful for evaluating the MDD of a composite used as a backfill material and the stability of a field problem such as embankments.

Then, a series of LDS tests under a normal stress of 50, 100, 250 and 500 kPa were carried out to study the shear stress, volumetric and shear–strain behaviours both at the peak and in the constant volume state. A 500 kPa vertical load was applied to investigate the effect of a relatively high level of normal stress on the strength

properties of the composites and to generate a more comparable scale effect. The shear test was conducted using a 300 mm × 300 mm (inside diameter) shear box with a horizontal displacement rate of 0.5 mm/min. The specimen height was 130 mm, and the specimen was compacted in three layers to achieve the desired parameters for the compaction test inside the shear box.

The main properties of all the sand and sand-rubber mixture are summarised in and show the specific gravity for each composite and the sieve analysis of the sand, rubber and sand-rubber particles Table5- 1.

Table5- 1. Properties of materials. Cu: Coefficient of Uniformity, G_s: Specific gravity

Soil	D₆₀	D₁₀	C_u	G_s
Sand	0.18	0.45	2.5	2.65
Rubber	2.0	1.5	1.3	1.01
SC0R10	0.3	0.4	0.6	2.17
SC0R20	0.3	0.4	0.6	2.00

5-3: RESULTS AND DISCUSSIONS

5-3-1: COMPACTION TEST

Densifying soil by applying stress on the soil released the available air among the particles and replaced it with water to eventually settle the soil. Therefore, the MDD properties of soil were the most important factors affecting the shear strength of the soil. These properties were related to the capacity of a composite to attract water molecules. Thus, soil needed OMC to achieve MDD, considering the material structure and component.

5-3-1-1: MAXIMUM DRY DENSITY AND OPTIMUM MOISTURE CONTENT

The results of the standard compaction tests for a variety of sand mixtures are presented in Figure5- 1, Figure5- 2 and Figure5- 3.

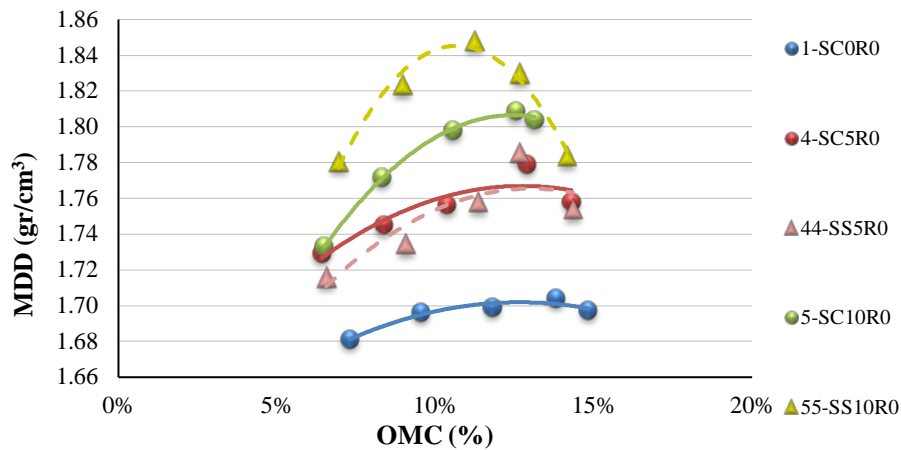


Figure5- 1. Compaction results of pure sand and sand reinforced with cement and slag.

The addition of stabilisers to sand increased the MDD and decreased the OMC of the mixture as illustrated in Figure5- 1. These changes were attributed to the increasing fraction of the finer material as a result of the stabiliser addition to the sand. Filling the pores of the composite by stabiliser particles created a more uniform mixture and consequently, decreased the amount of space that could be filled with water. This behaviour was observed by increasing the proportion of both cement and slag, which had a similar effect on the compaction properties of sand. For a comparison of the effects of the cement and slag application on the dry sand density, we ensured that the sand mixture with slag had high MDD and low OMC. This negligible behaviour suggested either different shapes of the cement and slag particles or a relatively quick reaction between the cement and the sand particles. Because of the higher proportion of calcium in cement, the possibility of flocculation in the sand–cement mixture was greater than in the sand–slag mixture.

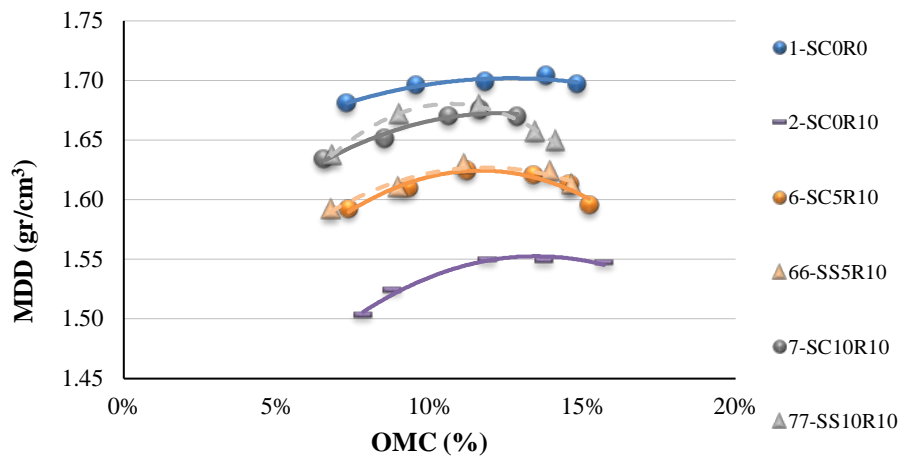


Figure5- 2. Compaction results of the pure sand and sand with 10% rubber and different proportions of cement and slag.

In contrast, the addition of rubber to sand decreased the MDD and OMC of the sand matrix, as illustrated in Figure5- 2 and Figure5- 3, respectively. This tendency was boosted by increasing the proportion of rubber, which reflected the lightweight characteristics of rubber. Filling the available space among the particles of the matrix with an equivalent volume of a ductile material condensed the effect of the applied load on the mixture. Moreover, the low water absorption of rubber reduced the OMC of the mixture. Hence, the MDD of R10 and R20 was 1.55 gr/cm³ and 1.37 gr/cm³, corresponding to almost 12% and 9.5% moisture, respectively. Note that the MDD and OMC of pure sand was 1.704 gr/cm³ and 13.81%, respectively. Thus far, the results revealed two different effects of the additives on the sand compaction properties: the MDD and OMC increased upon the addition of cement and slag and decreased after the addition of rubber for sand reinforcement. Further, the compaction characteristics of composites with both 10% and 20% rubber improved when the stabilisers were added to the mixtures. However, this improvement was not significant, and the MDD and OMC of the mixtures of the STR10 and the STR20 groups were lower than those of pure sand.

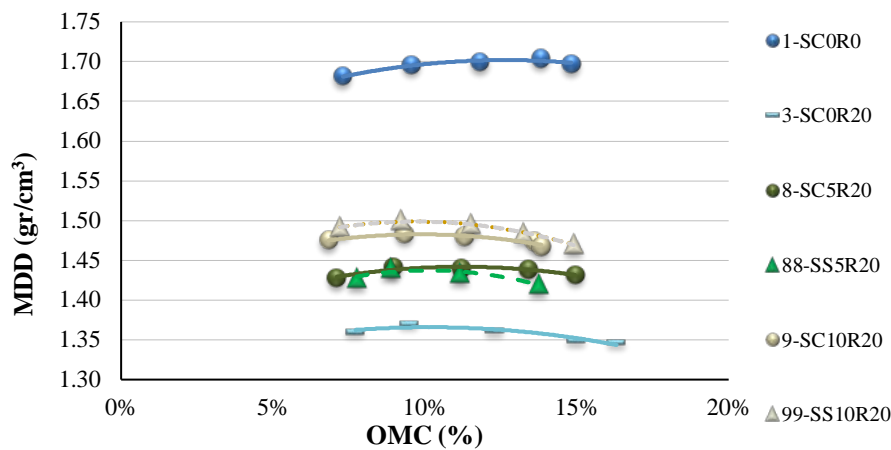


Figure5- 3. Compaction results of pure sand and sand with 20% rubber and different proportions of cement and slag.

Considering a number of independent variables affecting the compaction properties, including the type and proportion of additives, we obtained the following results. Note that to define an accurate single empirical formulation, the best combination of the most effective parameters should be considered. Therefore, a large number of experimental tests are required, which is beyond the scope of this chapter. Thus, the results of MDD were separately predicted by simple linear regression (SLR), as shown in Figure5- 4. The category of results was selected on the basis of the first consideration to create the mixtures; moreover, the results revealed the importance of the rubber content in determining the behaviour of the mixtures. The MDD values of each group of mixtures varied with the proportion of either cement or slag. The accuracy of the SLR empirical formulation was reasonable, and the MDD was determined using a correlation value of $R^2 = 0.9047$, $R^2 = 0.9805$ and $R^2 = 0.9718$ for the reinforcement of pure sand, sand with 10% rubber and sand with 20% rubber, respectively, with a stabiliser.

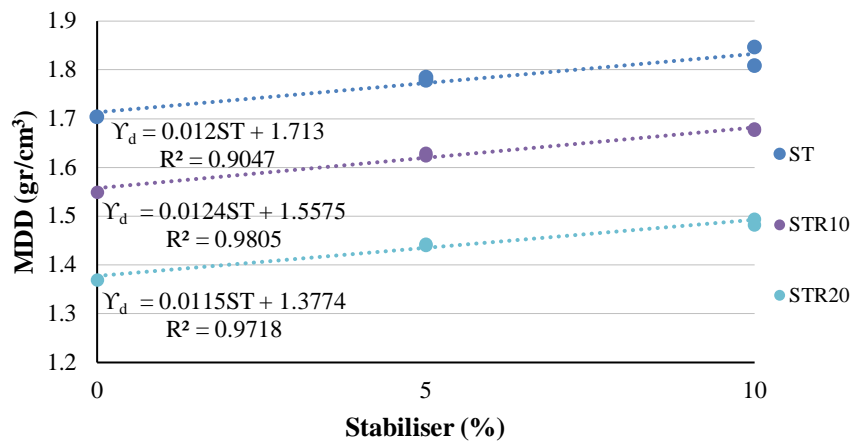


Figure5- 4. Results of standard compaction tests conducted on pure sand and a variety of sand mixtures.

The maximum dry density results demonstrated that the optimum mixing ratio was related to the shape, size, amount and type of additives. The smallest and biggest minimum void ratio among the sand-stabiliser-rubber composites were associated with SS10R10 and SC5R20, respectively. The results also indicate that the application of rubber as a lightweight material in the sand composites can be effectively utilised to manufacture the geotechnical construction such as retaining walls, backfill, and embankments.

Affecting by the rubber content in composites, the addition of the same dosage of stabiliser in sand stabilisation can reveal a different effect on maximum dry density of composite. It can be hypothesised that, increasing the rubber proportion in composites result in minimizing the stabiliser effectiveness for increasing the density of composite.

However, the accuracy of SLR empirical formulation and proposed hypothesis need to be evaluated by increasing the number of experimental, proportion of rubber in composite and dosage and kind of stabiliser, which is beyond the scope of this chapter.

5-3-1-2: FLOATING AND NON-FLOATING CASES

With the definition of oversized particles, the obtained result may be explained by discussing the floating and non-floating cases of soil mixtures with oversized particles (Yoon et al., 2006, Fragaszy et al., 1990, Yoon and Abu-Farsakh, 2009, Lade et al., 1998). An oversized particle is a particle larger than the required size for a specific test apparatus. Although rubber particles cannot be considered oversized particles, with their large dimensions and low unit weight, they behaved like oversized particles in the mixtures. A schematic representation of a soil structure containing oversized particles and the matrix material is presented in Figure5- 5(a) for sand containing rubber particles, and Figure5- 5(a) and (b) shows the representation for soil containing stabilisers as well. A floating state is a condition in which oversized particles are scattered in the composite with a small ratio to the total material, as shown in Figure5- 5(a).

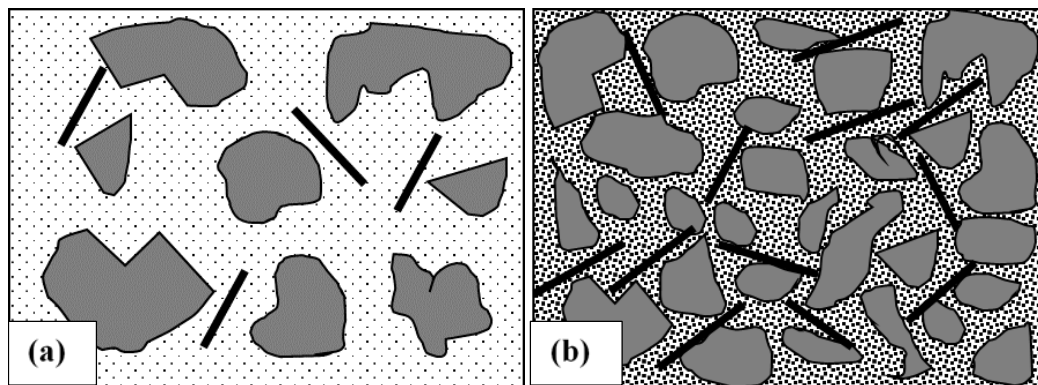


Figure5- 5. Schematic representation of soil with a floating case (a) and a non-floating case (b), adapted from (Fragaszy et al., 1990)

Depending on the distance between the other material and the oversized particles, the matrix soil was divided into two components: a soil grain that had end-to-end oversized particles was called a near-field matrix, and that with the particles further apart was called a far-field matrix. In the case wherein the maximum percentage of rubber was 20% of the weight of the total soil, and considering the shape of the rubber particles, we verified the first assumption that the possibility to connect the rubber particles was low. A laboratory investigation revealed that the non-floating case was

generated as a result of the rubber addition. Figure5- 6(a) and (b) clearly illustrate the creation of the non-floating case of sand treated with a rubber material; the non-floating case became increasingly apparent with an increase in the proportion of rubber.

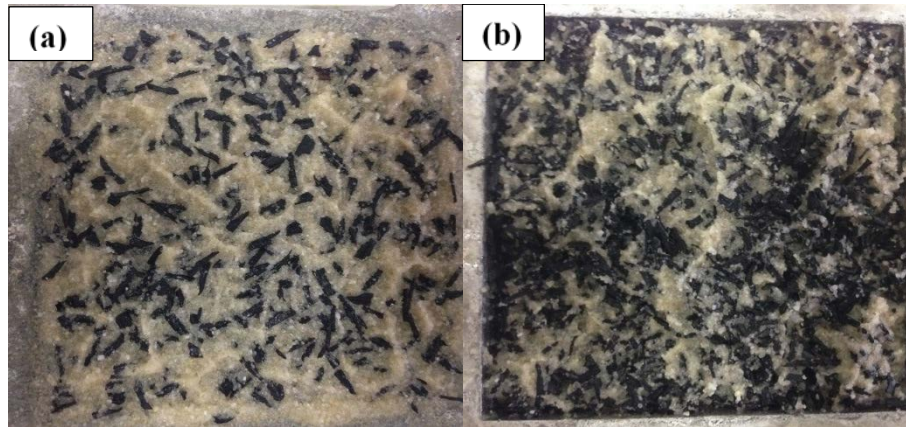


Figure5- 6. Generation of the non-floating case upon the addition of 10% rubber to sand (a) and 20% rubber to sand (b).

In contrast, many studies have reported that the considerably high ratio of the total material could be attributed to the presence of oversized particles. Therefore, in the non-floating case, the matrix material simply filled the space between the oversized particles and thus, did not affect the maximum density of the soil matrix, as shown in Figure5- 6(b). The consideration of ideal packing and real packing was essential for evaluating the effect of oversized particles on the mixture density (Yoon et al., 2006, Fragaszy et al., 1990).

The mass and the volume of the total soil, considering the oversized particles floating in the matrix, can be defined as follows:

$$M_t = M_m + M_o = (1 - P)M_t + PM_t \quad (5.1)$$

$$V_t = V_m + V_{so} \quad (5.2)$$

where M_t , M_m , and M_o denote the mass of the complete structure (total mass), matrix and oversized particles, respectively, and P represents the decimal fraction of the mass of the oversized particles.

Further, V_t , V_m , and V_{so} denote the volume of the complete structure (total volume), matrix and the solid for the oversized particles.

Therefore, the density of the total material (ρ_t) can be defined as follows:

$$\rho_t = 1/[(P/G_o\rho_w) + ((1 - P)/\rho_m)] \quad (5.3)$$

where ρ_m , ρ_w and G_o denote the density of the matrix soil, mass density of water and bulk specific gravity of the oversized particles, respectively.

Further, note that $G_o\rho_w$ is different from ρ_m , which does not contain any void space. The second case is of non-floating oversized particles, wherein the volume of the total mass (V_t) is replaced by the volume of the non-floating particles (Zornberg et al., 2004). The availability of the void space in the non-floating case and the density of the total material would thus be different. To calculate the density of the total mass, the dry density of the oversized particles alone (ρ_o) was calculated by dividing the mass of the oversized particles (p) by the total volume of the soil (ρ_t).

Hence, we determined the minimum percentage of oversized particles required in the mixture to create the non-floating case. Depending on the soil structure and the relative density of the oversized particles, the minimum fraction (p_c) can be expressed by the following equation:

$$P_c = 1/[1 + \rho_m (1/\rho_o - 1/G_o\rho_w)] \quad (5.4)$$

Thus, the oversized particles and the matrix particles affect the dry density of mixtures used in the compaction tests. If the maximum amount of the oversized particles in the mixture is denoted by P , then the real experimental data can be separated into the two main areas, namely, the floating area ($p \leq p_p$) and the non-floating area ($p \geq p_c$).

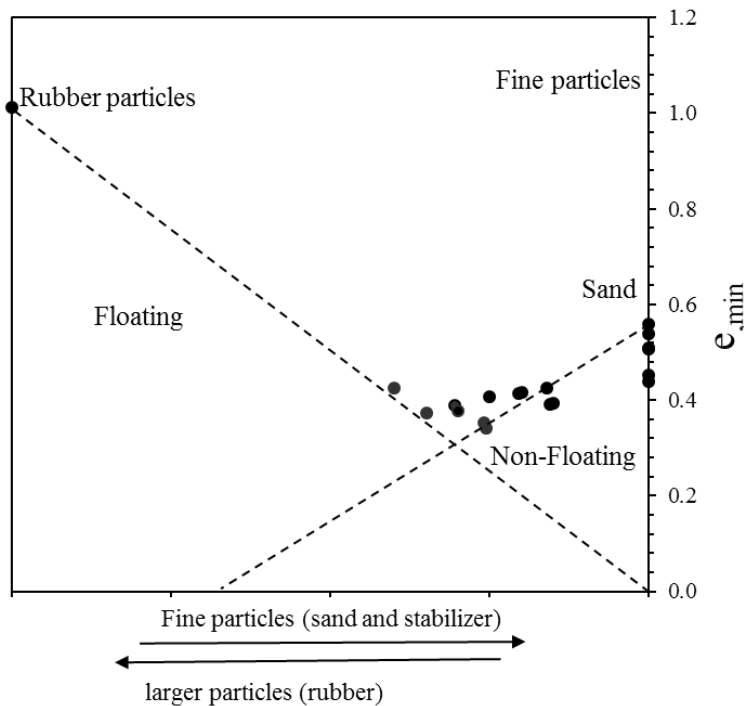


Figure5- 7. Schematic representation of the void ratio arrangement of the binary packing of materials which was used for calculating the void ratio in the compaction test in the floating and the non-floating states (Fragaszy et al., 1990, Lade et al., 1998).

By plotting a graph based on the obtained minimum void ratio, we defined the floating and the non-floating states and consequently, the minimum portion of sand required to generate a non-floating matrix. Figure5- 7 shows the minimum void ratio of the specimens, which was calculated and plotted as a function of the rubber content of the sand mixtures.

The maximum and minimum void ratios were assigned to the rubber particles and the fine particles, respectively. The finer the particles were, the lower was the void ratio in the soil mixture; thus, the highest void ratio was obtained for the soil with only

rubber added. Thus, the addition of sand to a constant amount of rubber, while maintaining a fixed volume, increased the weight of the composites by filling the available voids in the matrix. The total volume of the mixture and its minimum void ratio were increased by filling all the voids among the rubber particles (oversized particles) with the finer components (matrix material). From the obtained results, we inferred that the addition of a stabiliser to the sand–rubber composites changed the floating case of the matrix to a non-floating case, in which a relatively large number of particles affected the soil behaviour.

BRIEF SUMMARY...

A summary of the compaction results is presented in Table5- 2. The addition of stabilisers to sand increased the MDD and decreased the OMC of the mixtures.

Table5- 2. Results of the standard compaction tests of the treated and the untreated sand composites.

SAMPLE	OMC (%)	MDD (gr/cm³)
1-SC0R0	13.81%	1.704
2-SC0R10	14.77%	1.583
3-SC0R20	10.21%	1.400
4-SC5R0	12.90%	1.766
44-SS5R0	12.66%	1.765
5-SC10R0	12.54%	1.807
55-SS10R0	11.30%	1.845
555-SC5S5R0	11.34%	1.855
6-SC5R10	11.66%	1.624
66-SS5R10	12.07%	1.629
7-SC10R10	11.85%	1.673
77-SS10R10	11.10%	1.679
777-SC5S5R10	10.45%	1.666
8-SC5R20	11.12%	1.478
88-SS5R20	14.16%	1.484
9-SC10R20	10.96%	1.546
99-SS10R20	10.38%	1.562
999-SC5S5R20	10.96%	1.546

In contrast, the addition of rubber to sand reduced the MDD and the OMC of the sand matrix. This tendency was boosted by increasing the proportion of rubber added; this boost was attributed to the lightweight characteristics of rubber. Eventually, the addition of a stabiliser to the sand–rubber composites changed the floating case of the matrix to a non-floating case, in which a relatively large number of particles affected the soil behaviour.

5-3-2: LARGE DIRECT SHEAR TEST RESULTS

The shear stress–horizontal displacement behaviour was evaluated using the LDS tests of a variety of sand composites. The tests were performed at vertical loads of 50 kPa, 100 kPa, 250 kPa and 500 kPa for the four categories of materials classified on the basis of their additives, with considerable rubber content and either cement or slag used as a stabiliser. The results for the composites from the SR, ST, STR10 and STR20 groups at the 50kPa and 250kPa normal stress are presented in Figure5- 8, Figure5- 9 and Figure5- 10, respectively. In summary, the strain softening behaviour of pure sand was modified after the rubber inclusion, as shown in Figure5- 8.

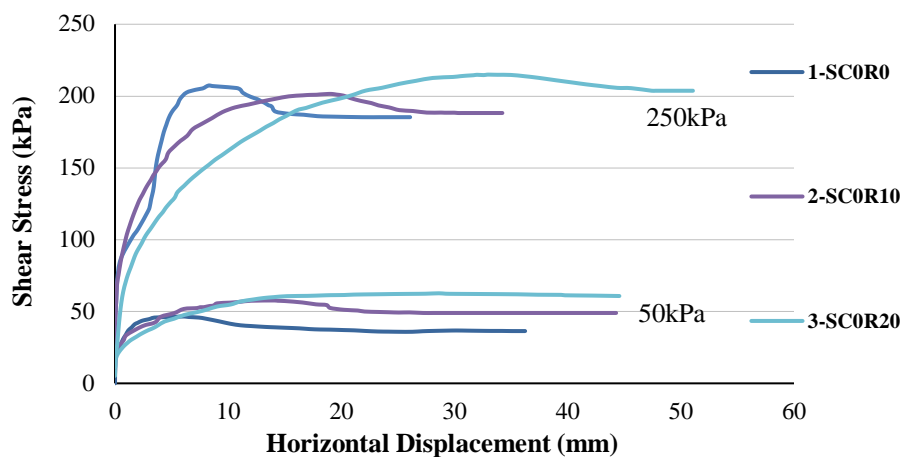


Figure5- 8. Shear stress–horizontal displacement of the sand with and without the rubber addition at 50-kPa and 250-kPa normal stress.

The typical strain softening trend of sand showed a sharp increase at the beginning and a dramatic loss of strength after reaching the peak with an increase in the shear

displacement over time. This behaviour was boosted by increasing the normal stress, as the slope of the sand's shear stress was steeper than that of its behaviour at a lower vertical load. However, the duration of the recoverable behaviour of sand was increased by the addition of rubber to the composites. Consequently, the increasing linear trend of sand shear up to the failure point was modified into a curved line, which was clearly observed in the case of SC0R20.

The improved elastic phase of the shear stress behaviour could be related to the ductile behaviour of rubber. Further, the results indicated the effect of the amount of normal stress on the composite strength. The SC0R20 composite generated the highest shear resistance even after an increase in the vertical load, in contrast to the SC0R10 mixtures, and was thus concluded to have the lowest strength. Although the utilisation of 10% rubber to increase the shear strength of sand was effective at 50 kPa, this increase stopped with an increase in the normal stress. Exerting relatively high normal stress helped us to realise the characteristics of each composite and thus, led to a more reasonable evaluation of the effects of the additives. The composites of the ST group exhibited the softening behaviour with different applied vertical loads, as shown in Figure5- 9.

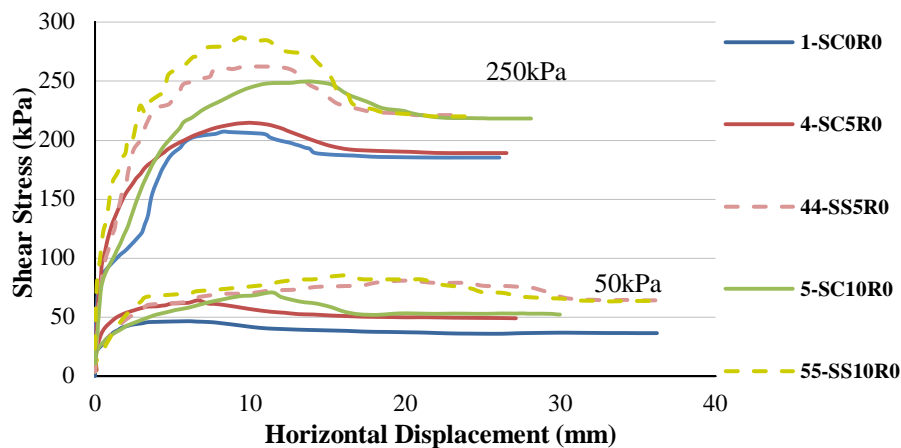


Figure5- 9. Shear stress–horizontal displacement of the sand with and without the stabiliser addition at 50-kPa and 250-kPa normal stress.

Increasing the normal stress yielded the same result as that obtained for the composites of the SR groups. The composites exhibited an increase in the shear stress up to the peak value and then a reduction in their resistance to a constant value with an increase in the horizontal displacement. This trend was considered to be an effect of the stabiliser and created a denser composite because of the addition of finer particles and the subsequent filling of the pores of the sample. Consequently, establishing a remarkable degree of interlocking improved the internal friction on the interface of the composite particles. Therefore, more shear force was required to overcome the interlocking and the internal friction generated in the mixture. A comparison of the cement and the slag application revealed that the addition of slag was more effective than the addition of cement in increasing the peak value of the sand mixture, even in a relatively low proportion. For example, the maximum shear strength at 250 kPa normal stress of SS10R0 and SS5R0 was 287 kPa and 262 kPa, respectively. The results, thus obtained revealed the high strength and the high strain ability of the stabiliser and the rubber. We expected the mixtures containing rubber and stabilisers to generate a composite with a combination of the abovementioned specific characteristics.

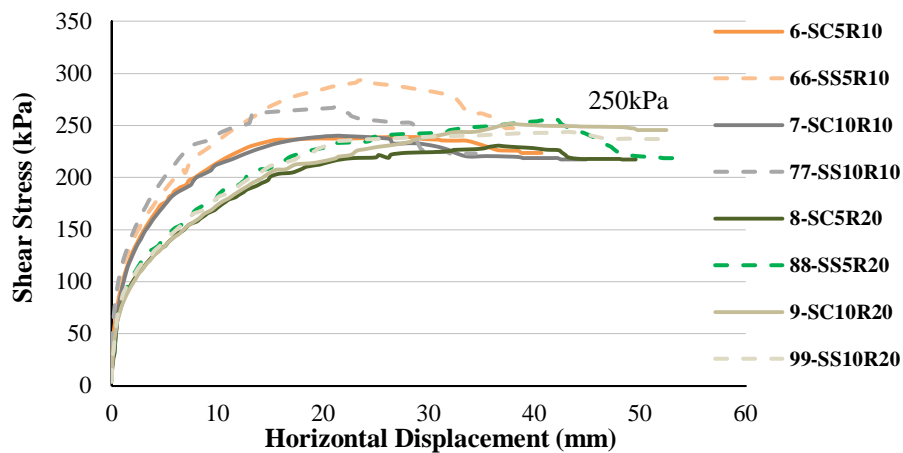


Figure5- 10. Shear stress–horizontal displacement of the different mixtures of STR10 and STR20 at 250-kPa normal stress.

The results of the composites with a mixture of 10% and 20% rubber with 5% and 10% cement and slag at 250 kPa normal stress are presented in Figure5- 10. A quasi-elastic behaviour was observed in all the composites. The addition of a stabiliser to rubberised sand led to the integration of the rigidity and the flexibility characteristics and eventually generated the inelastic response that was almost elastic, with a broad displacement of the high strength properties. Moreover, the composites' behaviour showed their dependence on the rubber content; here, the most pivotal role was played by 20% rubber. Thus, the composites were affected more by the rubber content than by the stabiliser content and thus, exhibited rubber-like characteristics. In contrast, the STR10 mixtures exhibited more strength improvement than the STR20 mixture in the cases of both the stabilisers. The STR10 composites were affected by the power of the stabiliser in the cases of both 5% and 10% content. The addition of 10% slag to an SR10 mixture caused a 100-kPa improvement in the shear resistance; however, this mixture failed at a 6-mm resistance.

Eventually, the maximum shear strength of each composite was plotted against the different applied normal stress values to determine the linear shear envelopes Figure5- 11 shows the shear envelopes with a proper correspondence for all the 15 sand mixtures.

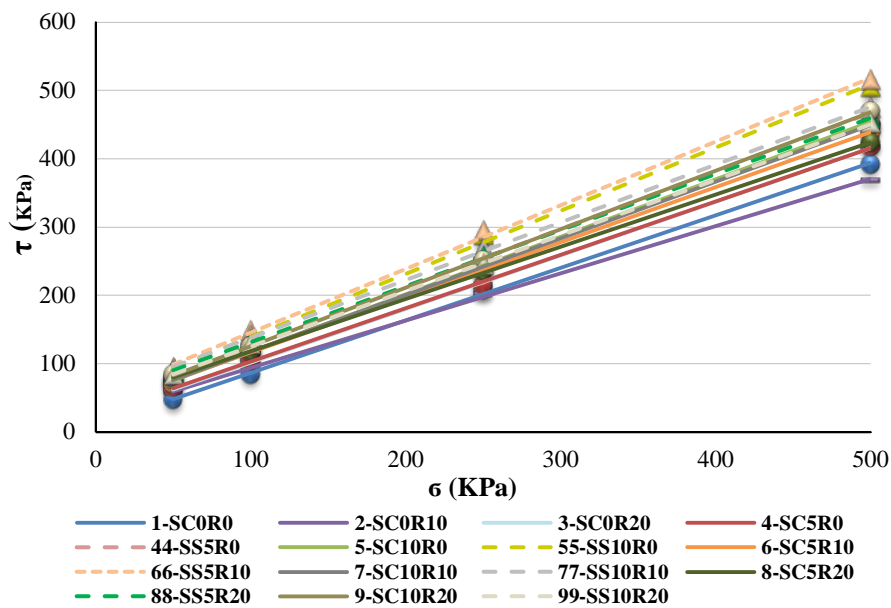


Figure5- 11. Shear envelopes for a large direct shear test of treated and untreated sand composites.

The correlation coefficient of the linear regression of the composites was greater than 0.99 in all the considered cases. Further, the addition of a certain proportion of slag to the mixtures generated a composite with a capacity to withstand greater force. For example, the SR10 mixture became the most reinforced mixture after the addition of 5% slag despite having the lowest shear resistance. Thus, the composite with the slag addition and with or without the rubber inclusion exhibited the highest peak value of shear strength with all the normal stresses when all the considered composites had a similar ratio of cement, as shown in Figure5- 11. Furthermore, different behaviours of mixtures depending on the type and proportion of additives were observed by applying higher pressure. The difference between the lowest and the highest peak values at 50 kPa, 100 kPa, 250 kPa and 500 kPa was calculated to be approximately 46 kPa, 63 kPa, 83 kPa and 148 kPa, respectively.

BRIEF SUMMARY...

The improvement in the elastic phase of the shear stress behaviour of sand was attributed to the ductile behaviour of rubber. The results also indicated the importance of the amount of normal stress applied concerning the strength behaviour of the composites.

Moreover, a denser composite was obtained by the addition of a stabiliser material and by filling the pores of the sample. Sand stabilisation with a cementitious material led to a significant degree of interlocking which improved the internal friction on the interface of the composite particles.

Eventually, a quasi-elastic behaviour was observed in composites containing both rubber and stabilisers. The addition of a stabiliser to a sand–rubber mixture integrated both the rigidity and the flexibility characteristics, and eventually generated an inelastic response that was almost elastic, with a broad displacement of the high strength properties.

5-4: LARGE DIRECT SHEAR VERSUS SMALL DIRECT SHEAR

The scale effect on the soil composite strength was investigated with a comparable series of direct shear tests on two small and large scales. In comparison with the use of the small direct shear test, testing the strength properties of composite materials including the boundary effect and device friction by using the LDS test will be more applicable to soil composites on-site. To investigate the effect of the normal stress on the shear strength, the results of LDS and SDS with the 500kPa normal stress were compared. Based on the SDS test results, the SC0R0, SC0R20, SC10R0 and SC10R20 composites were selected to analyse the scale effect on the shear strain–shear stress, volumetric strain and shear module characteristics.

5.4.1 SHEAR STRESS–SHEAR STRAIN

A typical curve associated with the shear stress–shear strain for SDS and LDS subjected to 500 kPa of normal stress is presented in Figure 5-12. A small-scale direct shear test generated a stress–shear strain behaviour with a sharper initial slope than the large-scale test. Three forms of the shear stress–shear strain curves were observed from the direct shear tests, which were dependent on the material combination of the mixtures. The first shape was assigned to pure sand and sand mixed only with cement; here, the shear stress sharply increased to the peak value and then, gradually decreased to a large strain stress. Typically, failure was defined as the peak value of strain softening. For such composites, the ultimate stress normally occurred upon a small increase in the shear strength after the initial tangent. Accordingly, we found a very small difference between the yielding strain and the failure strain. This strain softening behaviour was more obvious in the SDS result, which revealed less space for particle movement and consequently, less time required to reach the failure point. In both the large and the small boxes, the peak value for sand was approximately 390 kPa, with just 1% difference in the shear strain. Further, the addition of a 10% stabiliser to sand increased the maximum shear strength in both the SDS and the LDS tests.

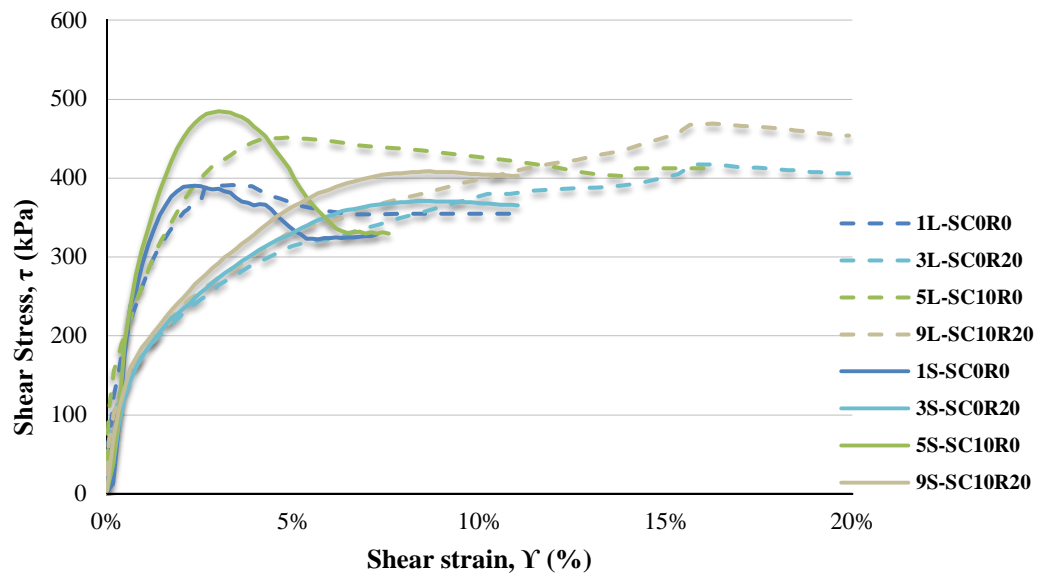


Figure5- 12. Shear stress against the shear strain of sand mixtures, obtained from the small and large direct shear tests at 500-kPa normal stress.

However, this improvement in the small-scale test was twice more than that in the large-scale test. Therefore, the composite strength decreased considerably after a failure.

The second shape was generated by an incremental trend of shear stress until the ultimate stress point was achieved and was relatively stable afterward. This behaviour was only observed when the small direct shear test was performed for composites containing 20% rubber. This evidence has been supported the importance of rubber particle for alternating the composite response form softening to hardening behaviour.

On the other hand, the third shape was obtained when the strength characteristics of the SC0R20 and SC10R20 composites were examined by the LDS device. Not only did the shear stress increases to a failure point with a similar trend in the SDS test, but it also gradually increased at a constant rate at a larger displacement. This behaviour generated a number of interactions among the particles inside the shear box, which increased because of the large size of the shear box. The scale effect was clearly observed on the shear strength behaviour of a composite containing the added rubber,

as hypothesised earlier. Within the larger space, the number of rubber particles could be moved, which then generated the strain hardening. The application of a shear force on composites with a loose structure moved the particles closer and generated a more uniform mixture. Hence, strain hardening was established by the process of plastic deformation. Strain hardening occurred from the yielding point to the failure point. This area is called the strain hardening region, because of the dependence of the curve shape on the strain rate. The movement of particles is called slip, which can be improved by applying a vertical load on the composites. More displacements along with the same slip increased the grain boundaries in a specific area. Furthermore, the higher ratio of the grain boundary could be attributed to the higher portion of finer particles. Eventually, because of the cement addition, more grain boundaries were generated, which strengthened the mixture.

BRIEF SUMMARY...

The generation of a sharper initial slope with a small-scale device than a large-scale device suggested the dependence of the initial shear modulus on the direct shear box size. The dependence of a sand composite mixture on the three types of shear stress–shear strain curves was perceived from the direct shear tests. Firstly, a typical softening behaviour was exhibited by the composites of the ST group. This strain softening behaviour was more noticeable in the SDS result. Next, a unique behaviour was exhibited by a sand composite containing 20% rubber on the SDS test: the shear stress increased to the ultimate stress point and then, remained relatively stable afterwards. The scale effect triggered the third type of behaviour which was clearly observed as the shear strength behaviour of a composite containing both rubber and stabilisers. Increasing the grain boundaries in the same slip led to strain hardening for plastic deformation. The addition of a cementitious material increased the number of connections among the grain boundaries and subsequently, improved the strength characteristic of the mixture.

5.4.2 SHEAR MODULUS

The estimation of the soil stiffness is important for engineering projects (p226).

The stiffness–strain behaviour of soil is defined by the stiffness modulus (i.e., G).

The maximum stiffness modulus G_{max} and the secant modulus at the failure point are two important parameters used for predicting soil plasticity.

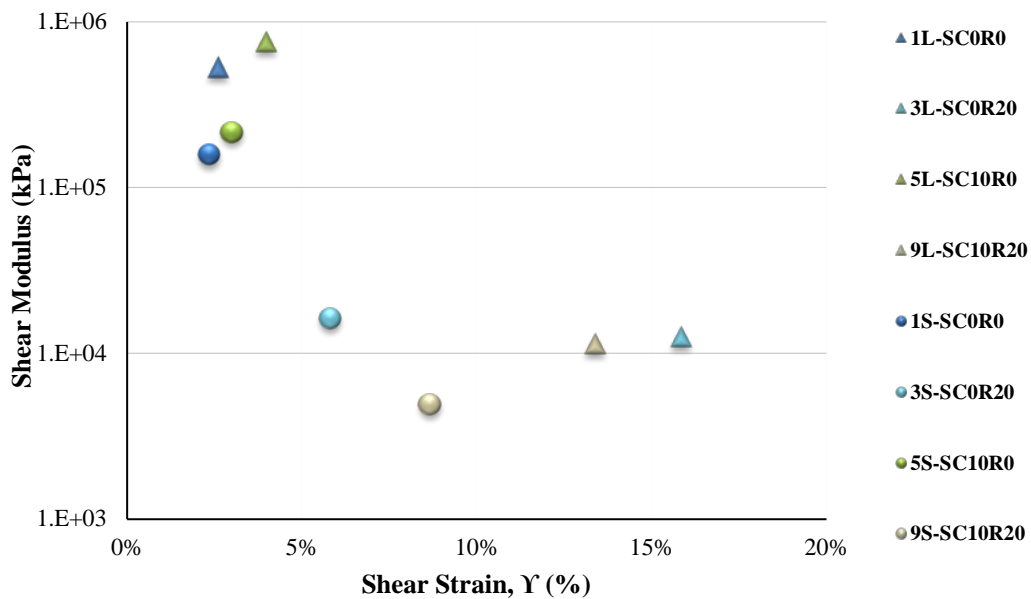


Figure5- 13. Secant shear modulus at the failure points of sand composites versus shear strain.

Figure5- 13 presents the secant shear modulus results of pure sand and the treated sand composites obtained using two large- and small-scale tests. The results revealed that the box demotion was more effective on the strain behaviour of composites than on their strength. A comparison of the SDS and the LDS results indicated similar results for the shear modulus at the failure point. However, to analyse the scale effect on the soil behaviour, the composites required a greater deformation force on the larger scale. Subsequently, the difference was related to the elastic properties of the composites. Thus, we hypothesised that a flexible material has more resistance to deformation, leading to a slower rate of shear force increment.

A study on the strain behaviour also revealed that composites failed to pass a larger displacement on the larger scale. This trend was remarkably observed for composites containing rubber, indicating the shear resistance improvement of the sand mixture. SC0R20 exhibited the highest shear resistance among the composites, which reached the peak value at around 16% shear strain.

Although utilising a combination of cement and rubber with sand resulted in the lowest stiffness in the SDS test, the LDS test output indicated a composite with a reasonable amount of both stiffness and strength. Therefore, we inferred a relationship between shear resistance and soil elasticity, as suggested earlier. Hence, the scant stiffness could be gradually reduced by increasing the shear strain.

BRIEF SUMMARY...

The scale effect on the shear modulus behaviour of a composite was clearly observed, which affected the shear resistance of the composite. This result suggested that the use of rubber led to an improvement of the strain resistance in the sand mixture. Sand reinforcement with the ductile material increased the composite flexibility and subsequently, caused a failure at a large displacement.

5.4.3 MAXIMUM FRICTION ANGLE

To evaluate the scale effect on the shear strength, the friction angles of the composites at the failure point and in the constant volume state were analysed. The data were compared with the results of the SDS tests for each specimen. Next, the friction angle of the composites was defined individually to draw a correlation with the composite's density.

5.4.3.1 SCALE EFFECT ON THE MAXIMUM FRICTION ANGLE

The friction angles of sand composites with and without additives at the failure point are shown in Figure 5-14. The results were divided into three main categories, including five composites per group, containing 0%, 10% and 20% rubber addition (i.e., ST, STR10, and STR20, respectively). Overall, the composite containing rubber exhibited a greater value in the LDS test than in the SDS results, except SC0R10. Further, the addition of only 10% rubber decreased the internal friction of sand by 3°. Although the lowest friction angle was assigned to SC0R10, compared with the small box, most of the composites exhibited higher internal friction at the failure point. This behaviour was quite different from that observed in the SDS test: the decrease in the friction angle of sand resulted in the addition of rubber. Thus, the scale effect revealed the mechanical properties of rubber.

Despite of few differences, which might be observed due to the effect of rubber particles, the scale effect comparison was revealed a fairly similar trend in both scales. For instance, in the LDS test, the maximum friction angle was assigned to the SS5R10 composite, while the addition of only 10% cement generated a composite with the highest internal friction angle in the SDS test. Considering the general similarity of result, therefore, the additional analysis has been conducted in further sections by focusing on the large direct shear box results. The importance of direct shear box dimension to show the influence of rubber particles is also analysed and presented in following sections.

In contrast, as in the SDS test, sand reinforcement with only the cementitious material led to an increase in the internal friction angle of pure sand. A comparison of the stabiliser material revealed the same results as those obtained in the case of the small box. Using the cementitious materials only for sand reinforcement, we found that the same percentage of slag was more effective than cement. The maximum friction angle of pure sand was improved by approximately 0.2° per percentage point

of cement addition. The corresponding improvement for the slag–sand composites was three times higher. Further, considering the importance of the curing time, we found that the addition of slag for sand stabilisation generated a composite with a higher shear strength than sand containing cement within a short period.

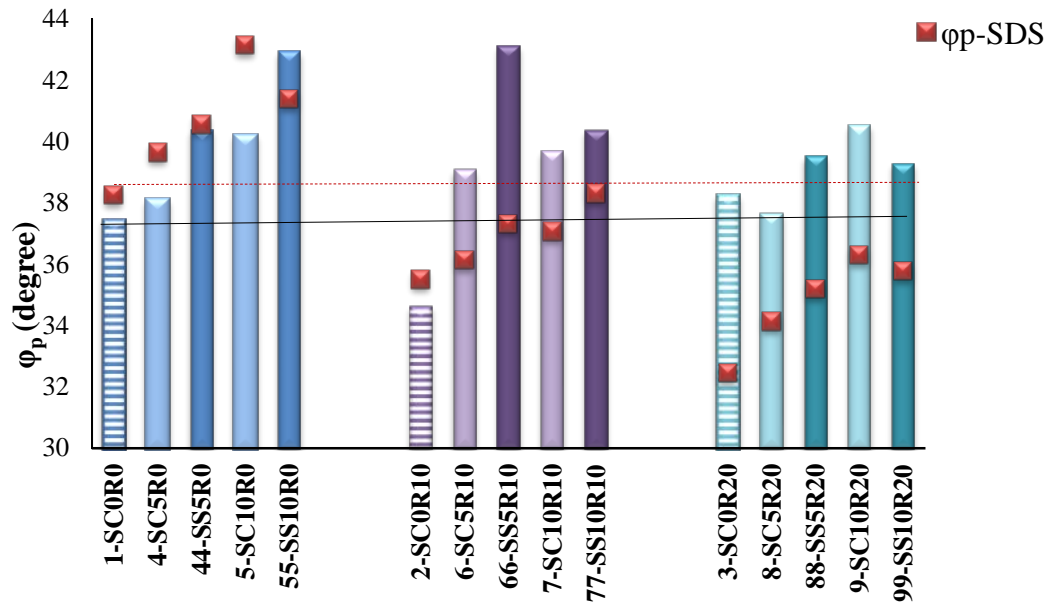


Figure5- 14. Friction angle of sand and the treated samples for the peak shear stress in the large direct shear test, compared with the results of the small direct shear test.

The application of rubber only shows an incremental improvement trend for the friction angle of sand. Dissimilar to the SDS data, the addition of 20% rubber not only did not generate the lowest internal friction in the pure sand but also exhibited a similar result to that of the SC5R0 composite (i.e., more than 38°). The minimum improvement was obtained by the application of 10% rubber only. The friction angle of the SC0R10 samples was approximately 3° lower than that of the pure sand; however, it significantly increased to between 5° and 9° upon the addition of 5% and 10% cementitious material, respectively, for example. Moreover, the combination of slag with 10% rubber almost generated a composite with a higher friction angle than that of cement. The slag suggested the existence of the optimum proportion of additives. Note that in both scales, an upward trend was detected by increasing the

stabiliser content and the samples had a more similar range of the maximum friction angle in the SDS test.

The composites of the STR20 category exhibited a considerably similar friction angle. Regarding the reasonable improvement in the friction angle of SC0R20, a lower difference was observed after the addition of stabilisers. However, the addition of a stabiliser to sand with 20% rubber increased the friction angle by 2°. The results of the large-scale test were similar to those of the small-scale tests. As in the case of the small scale, the addition of 5% slag was found to be more effective than that of 5% cement, with a minor change in friction angle reduced by increasing the proportion of slag. Moreover, the friction angle of SC5R20 improved even after doubling the proportion of cement added to sand with 20% rubber, which generated the highest friction angle among the composites of the SRT20 category. The STR10 and STR20 composites exhibited a similar trend on both the considered scales and in the case of the larger scale, the composites demonstrated the effects of the use of rubber in sand reinforcement.

BRIEF SUMMARY...

The results were divided into three main categories by the proportion of rubber added: 0%, 10% and 20% added rubber (i.e., ST, STR10, and STR20, respectively).

Overall, the composite containing rubber obtained a greater value in the LDS test than in the SDS test, except SC0R10. The application of only 10% rubber reduced the internal friction of sand by 3°.

The use of cementitious materials only for sand reinforcement yielded the same results as the small box. Note that on both scales, an upward trend was detected by increasing the stabiliser content, and the samples had a more similar range of the maximum friction angle in the SDS test. A comparison of the stabiliser material also revealed that the same percentage of slag was more effective than cement. Moreover,

an increase in the proportion of added rubber for stabilising sand showed an incremental improvement trend for the friction angle of sand. The STR10 and STR20 composites exhibited a similar trend on both scales, and on the larger scale, the composites demonstrated the effects of the use of rubber in sand reinforcement. Regarding the reasonable improvement in the friction angle of SCOR20, a lower difference was observed after the addition of stabilisers.

5.4.3.2 PEAK FRICTION ANGLE AND MAXIMUM DRY DENSITY

Considering the different components of the composites, we found a correlation between the internal friction angle and the MDD of the composites. Based on their MDD, the composites were categorised into three main groups with respect to their material properties. The MDD of the composites was strongly related to the proportion of rubber added to generate the composite structure. Subsequently, ST, STR10 and STR20 were considered specimens with a dense, medium and loose structure, respectively. A combination of the maximum rubber ratio and the minimum stabiliser ratio led to the formation of the loosest composite (i.e. SCOR20: 13.998 kN/m³). In contrast, the composite with the maximum density contained the maximum content of stabilisers as the finer material, with 0% rubber inclusion (i.e. 18.453 kN/m³). Therefore, based on the rubber ratio, the material categories were defined as described in Table5- 3. Note that the separation was relatively defined on the basis of the composites investigated in this research. Moreover, different methods were used to interpret the direct shear test results for the analysis of the shear strength properties of soil from different viewpoints (Simoni and Houlsby, 2006) Considering the mobilisation of the friction angle on the central plane as the plane strain friction angle of the soil (φ'_{ps}), we calculated the mobilised friction angle of the plane strain as follows:

$$\varphi'_{ps} = \tan^{-1} \left(\frac{\tau}{\sigma'v} \right) \quad (5.5)$$

where τ and $\sigma'v$ denote the shear stress and the normal stress, respectively.

Table5- 3. Definition of the three categories of composites divided by their maximum dry density.

Soil structure	Category	MDD (kN/m ³)
Loose	STR20	
Material with 20% rubber, and its combination with cement or slag.	SC0R20, SC5R20, SS5R20, SC10R20,	13.98–15.62
Medium	STR10	
Material with 10% rubber, and its combination with cement or slag.	SC0R10, SC5R10, SS5R10, SC10R10,	15.82–16.79
Dense	ST	
Material with 0% rubber, and its combination with cement or slag.	SC0R0, SC5R0, SS5R0, SC10R0,	17.04–18.45

The estimated value is normally slightly lower than the actual value of the friction angle; hence, for a reasonable definition, it is called the direct shear friction angle (φ'_{ds}). The measurement of the vertical and the horizontal movement helps formulate the relationship between the plane strain friction angle and the direct shear friction angle. To find such a correlation, we simultaneously assumed the direction of the principal stress with the incremental trend of the principal plastic strain. Davis, conducted a coaxiality analysis on the basis of Mohr's circle (Simoni and Houlsby, 2006, Davis and Poulos, 1968). In this technique, the direct shear angle of friction is contained within the plane strain friction angle, where φ'_{ds} is smaller than φ'_{ps} and can be calculated as follows:

$$\tan\varphi'_{ds} = \frac{\sin\varphi'_{ps} \cos\psi}{1 - \sin\varphi'_{ps} \sin\psi} \quad (5.6)$$

where φ'_{ds} , φ'_{ps} and ψ denote the direct shear friction angle, plane strain friction angle and the angle of dilation, respectively.

In contrast, on the basis of a flow rule, the plain strain in the constant volume state can be used to find a correlation between the direct shear angle and the plane strain friction angle (Simoni and Houlsby, 2006, Rowe, 1969). Flow rules were introduced by Taylor and Rowe (Taylor, 1948, Rowe and Barden, 1964) for interpreting the results of a direct shear test (Pedley, 1990, Jewell, 1980, Simoni and Houlsby, 2006). Using the flow rules, we connected the plastic deformation of soil to the state of stress, which was related to the shear resistance of soil in the critical state, as follows:

$$\tan\varphi'_{ds} = \tan\varphi'_{ps} \cos\varphi'_{cv,ps} \quad (5.7)$$

where φ'_{ds} , φ'_{ps} and $\cos\varphi'_{cv,ps}$ denote the direct shear friction angle, plane strain friction angle and the plane strain constant volume friction angle, respectively.

From the above observation, we inferred the importance of soil behaviour in the critical state. The friction angle at a constant volume denoted the minimum shear strength capacity of the soil after a failure. The friction angle in the constant volume state was estimated using the parameters measured in the direct shear test, including the peak shear strength and the dilation angle.

Therefore, the friction angles at the peak value and in the critical state were alternatively analysed to obtain a better representation of the behaviour of the composites. With respect to the ductility behaviour of the rubber material, the constant volume state and the dilation angle were studied further as follows.

Based on the above description and the composite categories, the mobilised direct shear friction angle and the MDD of the three classes of composites are shown in Figure5- 15. Internal friction angle of sand and treated sand composites at the failure point versus the maximum dry density, where ST, STR10, and STR20 are representative of all the composites of their classes. Henceforth, considering the

greater value of the mobilised direct shear friction angle and its different definition, we refer to the friction angle of material at its maximum density as the friction angle. In general, each group included some amount of stabilisers, either cement or slag. For a comprehensive investigation, the trend results of cement and slag were considered. The composites with the loose and the medium structures exhibited a non-linear trend, which was attributed to the addition of rubber. Moreover, the correlation between the internal friction and the MDD confirmed the previous assumption on the importance of a composite's density with respect to its strength characteristics. In all classes, the composites with added slag exhibited a higher value than the cement-treated mixtures.

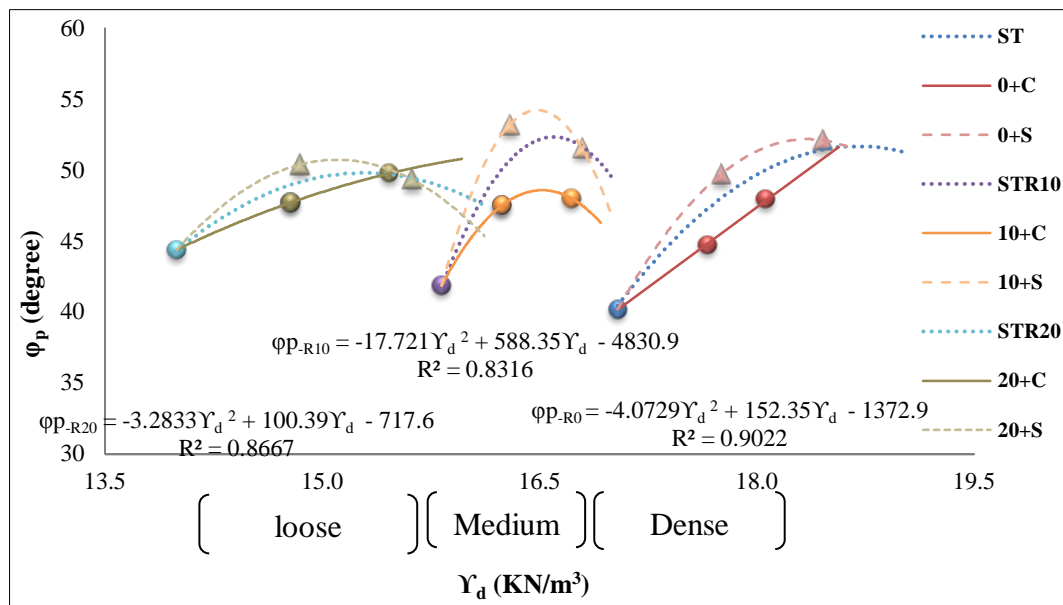


Figure5- 15. Internal friction angle of sand and treated sand composites at the failure point versus the maximum dry density, where ST, STR10, and STR20 are representative of all the composites of their classes.

In the specimens of the ST category with the zero-rubber inclusion, increasing the proportion of cementitious materials led to an increase in both the density and the internal friction angle. Moreover, the application of slag generated a steeper

incremental trend and subsequently, a higher friction angle than the addition of cement. This behaviour was also observed in composites containing 10% rubber. The results revealed the existence of the optimum content of a stabiliser to generate the maximum friction angle. The optimum point was estimated for the MDD of the considered mixtures. We found that the addition of a cementitious material altered the mixture with a low internal friction angle (i.e., SC0R10) into a strong composite with the maximum internal friction angle (i.e., SS5R10). The results again suggested the ability of slag to generate higher internal friction in the treated composites. Further, the importance of estimating the optimum dosage of a stabiliser was recognised in the STR20 class mixtures. In general, the friction angle of a composite gradually increased with an increase in the MDD even upon the addition of 10% stabiliser. However, the addition of 10% slag resulted in a slight reduction of the friction angle. This behaviour was observed in two other groups, suggesting the properties of slag and creating a denser composite. Therefore, the LDS test results showed the necessity of estimating the optimum density of a composite for creating a composite with excellent shear strength characteristics. Considering the composite results of the ST, STR10 and STR20 classes, the maximum value was obtained for the composite with 10% rubber and stabilisers. Further, defining the optimum point of the representative graphs of composites classes revealed that this trend decreased with an increase in the rubber content.

To better evaluate the internal friction, the friction angle of the specimens in the constant volume state will be discussed next.

BRIEF SUMMARY...

The MDD of the composites was strongly related to the proportion of the added rubber with respect to the formation of the composite structure. Subsequently, ST, STR10, and STR20 were called specimens with a dense, medium and loose structure, respectively.

A reasonable correlation between the MDD and the internal friction angle of the sand composites was found. In the specimens of the ST category with the zero-rubber inclusion, increasing the proportion of cementitious materials led to an increase in both the density and the internal friction angle. This behaviour was also observed in composites with 10% rubber. Further, the result suggested the existence of the optimum content of the stabiliser required for generating the maximum friction angle. The optimum point was estimated for the MDD of the mixtures. The importance of estimating the optimum proportion of a stabiliser was illustrated by the STR20 class mixtures. In general, the friction angle of a composite gradually increased with an increase in the MDD even upon the addition of 10% stabiliser.

5.4.4 CONSTANT VOLUME STATE FRICTION ANGLE

As an important factor, the constant volume state was analysed for gaining a better understanding of the effect of the addition of rubber on the strength of the composites. First, the data were compared with the results of the SDS tests for each specimen. Second, the friction angles of the composites at a constant volume were estimated individually to draw a correlation with the density of the composites.

5.4.4.1 SCALE EFFECT ON THE CONSTANT VOLUME STATE FRICTION ANGLE

The friction angles of the treated and untreated sand at a constant volume are shown in Figure 5-16. The reinforced sand composites exhibited a relatively high friction angle in this state, which was similar to the results of the SDS test. The composites with the lowest and the highest friction angle at the failure point had the minimum and maximum degrees in the constant volume state; the friction angles of SC0R10 and SS5R10 were 34.5° and 40.7° , respectively. Hence, in the case of the large-scale test, a greater value for most of the composites was observed; a similar trend was observed in the small-scale test. Again, we observed an increasing trend for the ST category and determined the optimum combination for the STR10 and STR20 groups. Among the

three categories, the combination of only cement or slag exhibited the lowest amount of friction angle at a constant volume. The addition of only 5% cementitious material to sand did not improve the sand's friction angles in the residual state. However, effective results were found by increasing the proportion of stabilisers to 10%. This behaviour could be attributed to the formation of a rigid composite that dramatically collapsed beyond the failure point. Compared with the cemented sand, the composite with slag had a higher friction angle and less deformation. However, this difference was reduced after the addition of 10% stabiliser.

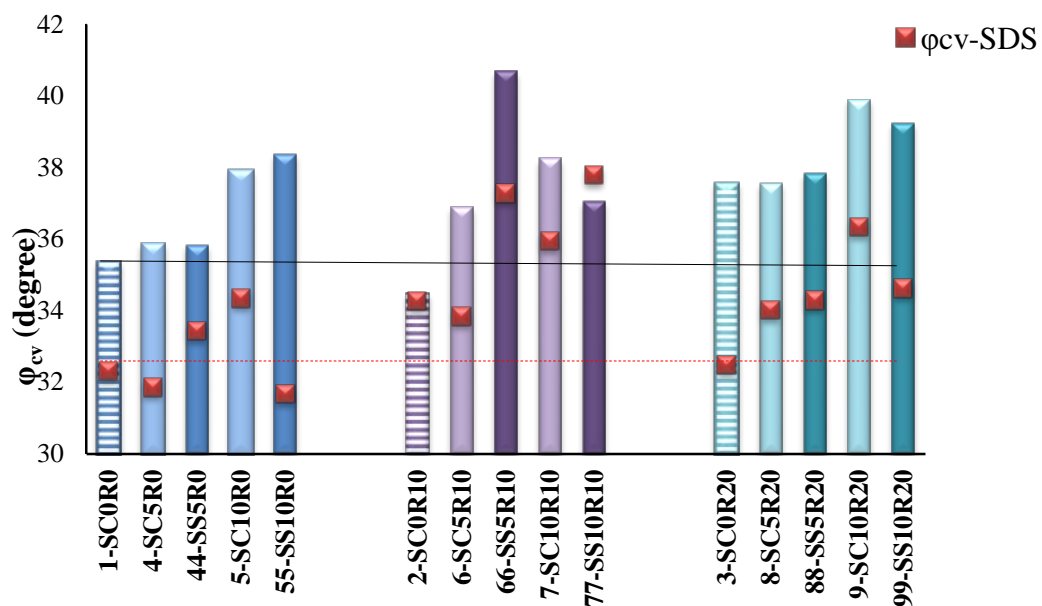


Figure5- 16. Friction angle of sand and the treated samples in the constant volume state in the large direct shear test, compared with the results of the small direct shear test.

The results of SC0R10 and SC0R20 were the same as those observed at the failure point. The use of only 10% rubber decreased the friction angle in the residual state. In contrast, sand containing 20% rubber demonstrated the remarkable effects of the addition of rubber for sand reinforcement. The addition of only 10% rubber led to the same results of approximately 34° on both scales. Despite the different values obtained in the large-scale test, the scale effect comparison for STR10 mixtures showed similar outcomes. Adding the cementitious material to the SC0R10 composite significantly

increased the friction angles in the constant volume state. Slag was found to be more effective upon the addition of 10% rubber, where the maximum angle was exhibited by the SS5R10 composite. The scale effect study similarly illustrated that combining 10% rubber and 5% slag with sand led to the formation of a sand mixture with the greatest strength capacity. The results also suggested that increasing the proportion of slag in the STR10 composites decreased the friction angle of the sand–rubber mixtures, which is dissimilar to the result obtained for the cemented composites. This trend was observed in the case of the small shear box. Further, a reasonable estimation of the type and percentage of the additives for sand treatment minimised the composite’s deformation

In contrast, the addition of 20% rubber even without the stabiliser addition considerably improved the behaviour of pure sand in the residual state. Subsequently, specimens in STR20 class have similarly behaved to each other, where can be suggested the composite behaviour were mostly influenced by the rubber content than dosage and kind of stabilisers. With an incremental trend, the addition of the cementitious material with 20% rubber to sand exhibited a very similar result. The addition of 5% and 10% slag and cement similarly improved the behaviour of the composites. Dissimilar to the results of the SDS, the composites in the large-scale test were affected by the box size and demonstrated that the use of different types of stabilisers did not have the same effect on the composite’s behaviour as the addition of rubber. Thus, the addition of 10% stabiliser to a composite maintained the increasing trend; however, the result suggested the availability of the optimum combination of additives for the formation of a composite with a relatively high friction angle in this category.

BRIEF SUMMARY...

The stabilised sand mixtures exhibited a relatively high friction angle in the constant volume state, which was a roughly similar trend to that of the results of the SDS test.

The mixtures with the minimum and maximum friction angle at the peak value maintained the lowest and the greatest degrees in the constant volume state; the friction angles of SC0R10 and SS5R10 were 34.5° and 40.7° , respectively.

A similar trend was observed in the small-scale test by using LDS along with a higher value for most of the composites. Further, an incremental trend for the ST category and the necessity of determining the most effective ratio for the STR10 and STR20 groups were found.

5.4.4.2 CONSTANT VOLUME FRICTION ANGLE AND MAXIMUM DRY DENSITY

Using the obtained results, we plotted the composite behaviour separately for the three classes versus the maximum dry density, as shown in Figure 5-17. Further, the composites were classified again into the ST, STR10, and STR20 groups on the basis of the rubber content. Each class had three types of composites, including different percentages of the cementitious materials, i.e., 0%, 5% and 10%. Moreover, at constant volume, the composites exhibited a similar trend to their tendency at the peak value. The results demonstrated the importance of determining the optimum point to form a composite with the maximum angle in the residual state. The composite without any cement or slag content exhibited the relationship between the composite density and its friction angle at a constant volume; the proportion of the added rubber was approximately 10%. This trend was different from that observed at the failure point which showed a linearly decreasing trend from the lowest MDD at SC0R20 to the SC0R0 composites. Moreover, considering the maximum value in each illustrative category, the graph showed a different trend from that observed at the failure point. At this time, the maximum point was found for STR20, which was very close to the maximum point of STR10. The highest value of the friction angle at a constant volume sharply dropped until the highest value for ST. The composites of the STR20 class revealed a similar trend; their representative graph indicated a relationship with an

excellent agreement with the results. The results suggested the importance of the rubber content in defining the composite's behaviour at a constant volume with the minimum dependence on the type of stabilisers. Moreover, the dependence of the composites' behaviour on the type of stabiliser was attributed to the decrease in the rubber content in the composites.

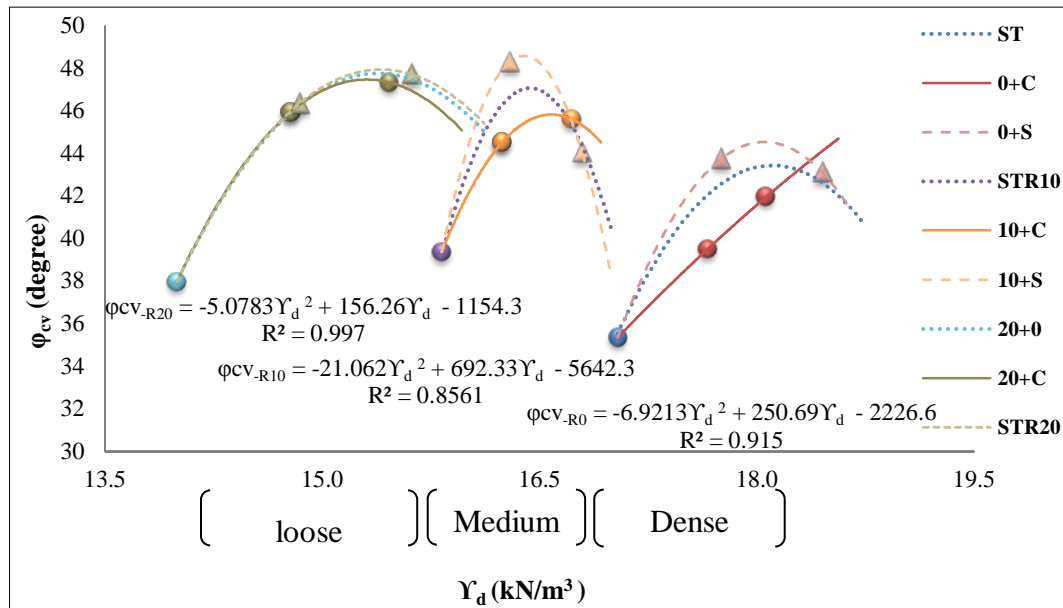


Figure5- 17. Internal friction angle of sand and the treated sand composites at a constant volume versus the maximum dry density, where ST, STR10, and STR20 are representative of all the composites of their classes.

In general, replacing the cement with the mixture of sand and 10% rubber with slag revealed the same tendency. However, the specimens had lower density and consequently, a lower peak in the constant volume state. Regarding the different amounts of mixtures, the obtained correlation to predict the composite behaviour exhibited a reasonable agreement.

In contrast, the results for the composite with no added rubber revealed the minimum friction angle, which confirmed the importance of the addition rubber for maintaining the soil structure past the peak value. An increase in the proportion of the stabiliser increased the MDD and formed a denser composite, which dramatically lost

its strength after a failure. With respect to the effects of the addition of a stabiliser material to improve the MDD and its relationship with the angle of friction of the composite, the results showed a good agreement with the obtained correlation.

Therefore, there is evidence to suggest that the availability of rubber material in composite lead to generate a soil with the higher value of friction angle at constant volume state. It might be suggested that, the consequences of post failure of soil mass can be minimised by utilising a combination of rubber and cementitious materials for soil reinforcement.

BRIEF SUMMARY...

The results suggested a strong relationship between the composite density and its friction angle either at the failure point or in a constant volume area for each series of the sand matrix. All the three categories exhibited a similar trend with the existence of the optimum ratio of the combination of additives. Increasing the ratio of additives in the sand matrix decreased the friction angle. Moreover, the addition of slag and cement to the composites resulted in a similar value, which suggested the effect of composite density on the microstructural shape of sand composites with additives. Table5- 4 presents the obtained equations for the maximum friction angle and the constant volume friction angle.

Table5- 4. Summary of the correlation between the friction angle and the maximum dry density for three categories of composites: Loose, Medium and Dense.

Soil structure	Maximum friction angle	Constant volume friction angle
Loose (STR20)	$\varphi_p = -3.2833\gamma_d^2 + 100.39\gamma_d - 717.6$ $R^2 = 0.8667$	$\varphi_{cv} = -5.0783\gamma_d^2 + 156.26\gamma_d - 1154.3$ $R^2 = 0.997$
Medium (STR10)	$\varphi_p = -17.721\gamma_d^2 + 588.35\gamma_d - 4830.9$ $R^2 = 0.8316$	$\varphi_{cv} = -21.062\gamma_d^2 + 692.33\gamma_d - 5642.3$ $R^2 = 0.8561$

Dense	$\varphi_p = -4.0729\gamma_d^2 + 152.35\gamma_d - 1372.9$ $R^2 = 0.9022$	$\varphi_{cv} = -6.9213\gamma_d^2 + 250.69\gamma_d - 2226.6$ $R^2 = 0.915$
(STR0)		

Note that the difference between the friction angles at the peak value and the constant volume needs to be analysed for a better understanding of the composite behaviour. Hence, the dilation angle will be analysed next.

5.4.5 VOLUMETRIC STRAIN

Figure 5-18 illustrates the vertical displacement of sand composites in two small- and large-scale cases at a vertical load of 500 kPa until the occurrence of a failure. The composites in the larger box demonstrated a broader vertical movement. The larger scale provided more space for particle movement with a lower variation of the vertical movement. This led to a more comprehensive demonstration of the effects of the additives on the composite behaviour. The composites with no added rubber exhibited a very similar volumetric strain, where the failure occurred at around 0.4% and 0.5% for sand and cemented sand, respectively, in both the small- and the large-scale cases.

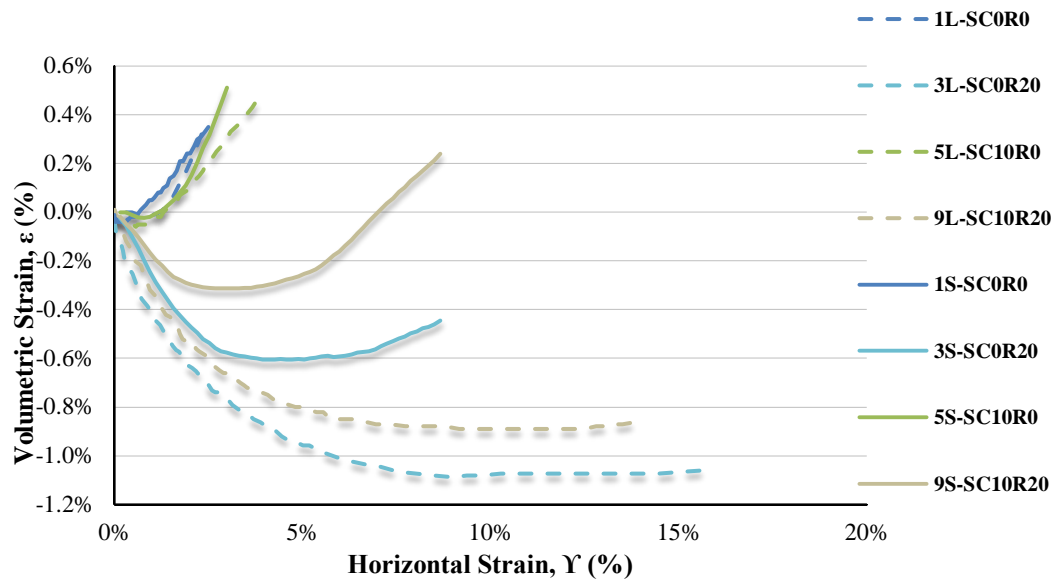


Figure5- 18. Volumetric strain in the large-scale (LDS) and small-scale (SDS) cases versus the shear strain for pure sand and the treated sand for a normal stress of 500 kPa until the failure point.

Thus, smaller particles could be systematically arranged irrespective of the size of the box to obtain a uniform structure. Further, a dilatancy behaviour was clearly observed in the sand mixtures with no added rubber. After a minor reduction in the initial part of the deformation, the volumetric strain increased as the shear strain reached the failure point. Because a greater amount of dilation is observed in the case of a denser composite, the dilation of sand was enhanced with cement addition to obtaining increased volume expansion. Hence, the scale did not affect the behaviour of the composites of the ST class in terms of the volumetric strain.

In contrast, the composite with the addition of only rubber had the minimum density and the level of dilatancy with both box sizes. A relatively loose mixture was compacted under the shear application. Moreover, the contraction behaviour of the sand–rubber mixture was more obvious in the LDS test which revealed the shape and the ductility behaviour of rubber. Upon the application of the LDS, the SC0R20 mixture failed at a strain approximately twice that in the case of the SDS. This remarkable improvement suggested the scale effect for determining the dependence of

a ductile material on a relatively large area for revealing its characteristics. Moreover, at the larger scale, the specimen was dilated at 1.2% strain, which was approximately 0.6% in the small box. The dilation tendency has been remarkably modified to a slighter trend in the LDS test.

For the composite with a combination of cement and rubber, the addition of rubber expanded the period of the initial volumetric reduction in the cement-treated sand. The addition of rubber deteriorated the dilation behaviour of the sand–cement mixture, forming a composite with a medium structure. The composite exhibited a contraction behaviour because of the properties of rubber; however, composite is expanded after escaping the void among the particles. Similar to SC0R20, the SC10R20 mixture exhibited less dilation at the large scale than at the small scale. Further, the volumetric strain and shear strain had a similar relationship in both the LDS and the SDS cases.

BRIEF SUMMARY...

Composites with a larger scale exhibited a wider vertical movement. The relatively large scale provided more space for particle movement to demonstrate the characteristics brought about by the additives. Sand treated with only the stabilisers showed that small particles could be systematically organised irrespective of the size of the box to create an identical structure. Alternatively, the sand–rubber mixtures had the minimum density and the amount of dilation in the large and small boxes. The contraction behaviour of the sand–rubber mixtures was more obvious on the larger scale, which revealed the shape and the ductility of rubber. The specimens containing both cement and rubber expanded during the initial volumetric reduction in the cement-treated sand.

Investigating the volumetric strain behaviour can lead to a better understanding of the composite strength characteristics. The behaviour of the soil before and after a failure is an important parameter for the estimation of the soil properties, defined by the angle of dilation.

5.4.6 ANGLE OF DILATION

To analyse both volumetric strain and shear strain at the same time, the angle of dilation was considered. The angle of dilation is defined as the ratio of the plastic volume change to the shear strain for the analysis of the plastic volumetric strain during the shear process. Figure 5-19 shows the results of a comparison of the LDS and the SDS data for the untreated and treated sand mixtures. The scale effect on the dilation angle was obviously observed, where excluding a few composites, the dilatancy of the mixture was reduced by increasing the box dimensions. The difference may be attributed to the larger space for increased particle movement during the direct shear test. With the larger space, more particles could be rearranged to fill the composite's pores either in the consolidation step or in the shear phase, which directly affected the plastic volume behaviour of the specimens. Thus, overall, the results revealed a minimisation of the expansion behaviour of the specimens with a large scale.

The scale effect was significantly observed for the STR mixtures wherein the lack of added rubber considerably affected the composite deformation. The dilation angle of sand in the LDS test was reduced to one-third of its value in the SDS test where about 6 degrees. SS10R0 exhibited the maximum angle of dilation of 4.56° , while this composite revealed an angle of dilation twice that in the small box. Moreover, once again, the application of slag generated more expandable composites. Thus, cement-treated sand could maintain its dense structure even after a failure. The addition of cement not only led to an increase in the internal friction angle of sand but also retained

the constant dilation of sand. Note that increasing the proportion of either cement or slag did not affect the dilation angle.

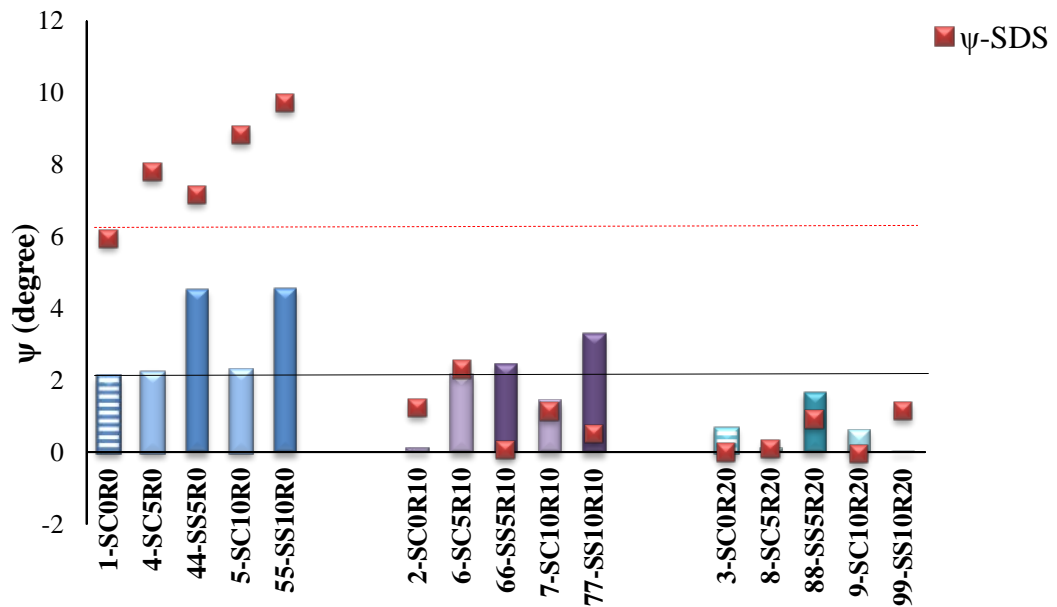


Figure5- 19. The angle of dilation of sand and the treated samples for the constant volume state in the large direct shear test, compared with the results of the small direct shear test.

The results of the mixtures of the STR10 class revealed the effects of the addition of rubber on the reduction of the dilatancy of sand. Although with the larger box, the lower amounts have been revealed, the dilation angle of composites was similar to the obtained results of the small size. The addition of only 10% rubber formed a composite with a zero angle of dilation. However, this impressive behaviour was negatively affected by the addition of cementitious materials. As in the case of the mixtures of the ST group, the addition of cement formed a composite with lower dilatancy than slag. The second lowest dilation angle ($<1.5^\circ$) in this category was obtained by the addition of 10% cement. In contrast, different behaviour from STR10 composites in two scales can be suggested the scale effect on the sand mixtures. In general, when the larger box was used, the slag-treated specimens were affected more than the other samples.

The results of all the five specimens in the STR20 class revealed the lowest difference between the large and the small boxes. Moreover, as in the case of the SDS test, the use of 20% rubber for the sand treatment generated a composite that exhibited contraction behaviour. Excluding the behaviour of SS5R20, we found that the dilation angles of the composites were $<1^\circ$. This behaviour was observed in the SDS test as well. The results suggested that the use of 20% rubber for sand reinforcement increased the shear resistance of the composite, thereby illustrating the ductility of rubber and subsequently, minimising the reduction of the strength of the composite after a failure. In other words, because of the hardening behaviour of the composites belonging to the STR20 class, the friction angles of the sand matrixes in the failure area and the constant volume state were similar. Therefore, these specimens exhibited the lowest dilatancy.

BRIEF SUMMARY...

We concluded from the results that the application of 10% rubber led to the most controversial results with respect to the scale effect on sand mixtures. Increasing the proportion of added rubber deteriorated the dilation characteristics of the sand mixtures. The results of the composites containing 20% rubber in a large box exhibited more similarity with the small box results among the three categories. Moreover, the composites containing the added cement yielded similar results in the cases of both large and small boxes. It can be suggested that the properties of additives, where affected on the identical characteristics of the composite, can be comprehensively analysed by the larger scale. The described results revealed the importance of the mechanical properties of the composite constituents, which were revealed in the large-scale experiment. In particular, the physical shape and the ductility of rubber play an important role in the shear strength and the shear strain behaviour. The composites containing 20% rubber exhibited more strength at a larger displacement; this could be attributed to the generation of more interactions among the composite particles and the shear box.

5.4.7 EFFECT OF RUBBER PARTICLES ON DILATION BEHAVIOUR

In addition to the mentioned behaviour, the direct shear test performed using a composite containing 20% rubber indicated the movement of the top cap of the direct shear box during the test, as shown in Figure5- 20. This occurrence was clearly observed upon the application of a high vertical load (i.e., >500 kPa), which required longer displacement to reach the failure point. The particles seemed to have moved toward the front of the box and eventually generated a relatively high particle-to-particle force in this area.

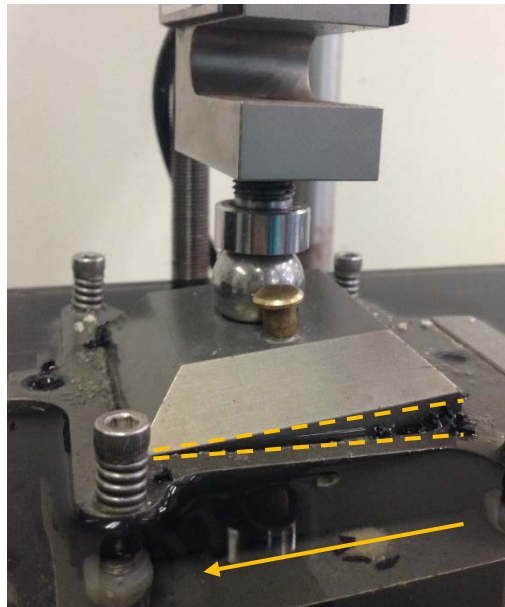


Figure5- 20. The experimental observation of the direct shear test using a composite with 20% rubber. The arrow shows the lower box movement.

Figure5- 21, shows a schematic representation of the particle movement in the direct shear test. This phenomenon led to the movement of rubber particles from the back of the box to the front of the box. The particles interacted with the top side at the front of the box to resist composite failure.

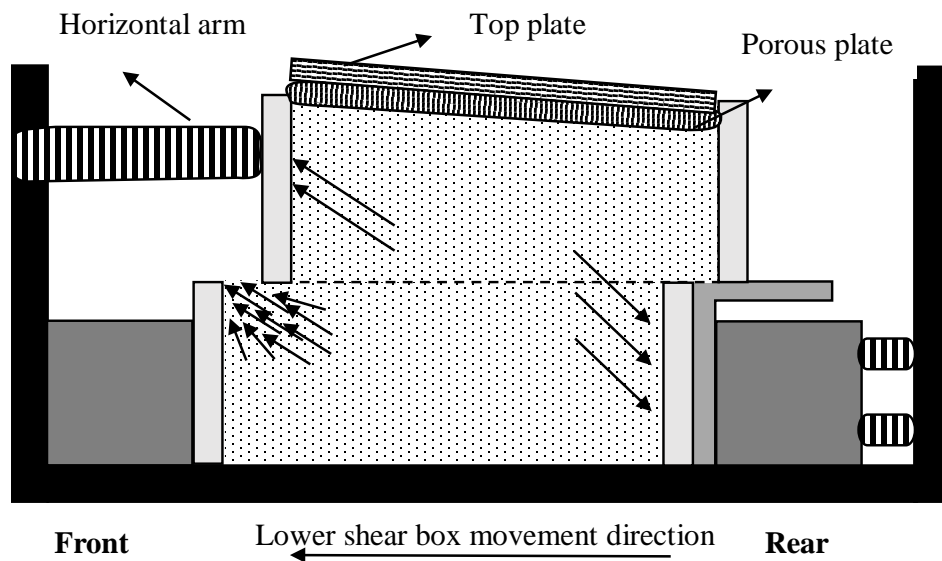


Figure5- 21. Schematic representation of particle movements in the direct shear test (Bareither et al., 2008).

Typically, the particles moved toward the gap at the front of the shear box because of the shear movement and the subsequent particle assembly in this area.

Regarding the physical properties of rubber, this procedure has been occurring very slow and requiring the large displacement. Due to the availability of cement which was played the connection role among the rubber and sand particles, overcoming the particles boundaries needs to the greater shear force. Note that the dilation observed at the front of the box was reported by several studies. District element modeling for particle movement revealed a similar behaviour in the direct shear test (Bareither et al., 2008).

Hence, the particle accumulation at the front of the box could create a new type of inter-force. The addition of the particle box interactions to the force among the particles increased the shear resistance of a mixture.

Therefore, further analysis from a different point of view is required according to the described observations.

5.4.8 ANALYSING DILATION RATIO

Alternatively, the rate of dilation of the specimens was determined by a measurement of the vertical deformation versus the horizontal shear displacement. Considering the horizontal plane of the direct shear box to be a zero extension line, we estimated the angle of dilation on the basis of the results of Mohr’s circle. The zero extension lines theorised by Roscoe in 1970 were used to analyse the stress–strain behaviour of the soil (Roscoe, 1970a, Veiskarami, et al., 2011). Further, two compressive and tension strains were perpendicularly directed to any state of strain, as shown in Figure5- 22.

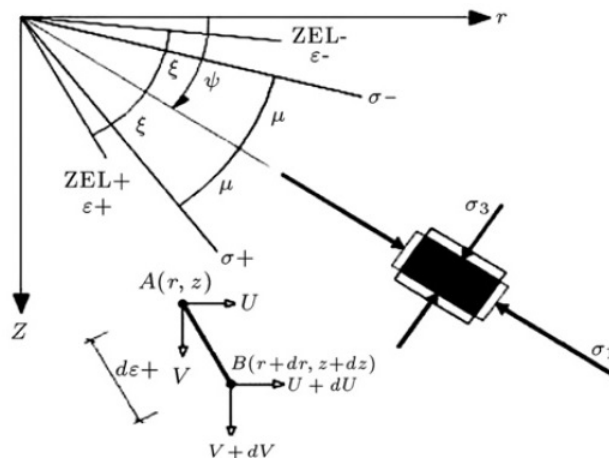


Figure5- 22. Illustrative directions of the state of stresses and the zero extension lines (Roscoe, 1970a, Veiskarami et al., 2011).

Subsequently, two incremental directions of the linear axial strain were observed, defining the zero extension lines (ZEL), particularly the plus (ε⁺) and minus (ε⁻) directions.

The angle introduced as a result of the intersection of these lines with any point can be defined as follows:

$$2\xi = \frac{\pi}{2} - \nu \tag{5.8}$$

where ν denotes the angle of dilation.

Considering the same direction for the major principal stresses and strains (co-axiality), we defined the state of stresses, strains and the zero extension lines as follows:

$$\text{ZEL}^+ \quad \frac{dz}{dr} = \tan(\psi + \xi) \quad (5.9)$$

$$\text{ZEL}^- \quad \frac{dz}{dr} = \tan(\psi - \xi) \quad (5.10)$$

$$\xi = \frac{\pi}{4} - \frac{\nu}{2}$$

where ψ denotes the angle intercepting the major principal stress and the horizontal direction. Therefore, we need to investigate the vertical displacement of a composite to define its dilation behaviour. The results of the small-scale test also emphasised the need to further study the scale effect on the dilation behaviour of composites. Therefore, the dilation ratio of sand composites are presented in Figure5- 23 and Figure5- 24 (i.e. for the small and the large scale, respectively). A comparison of the dilation ratio of the two scales confirmed the earlier results of the dilation angles of the composites.

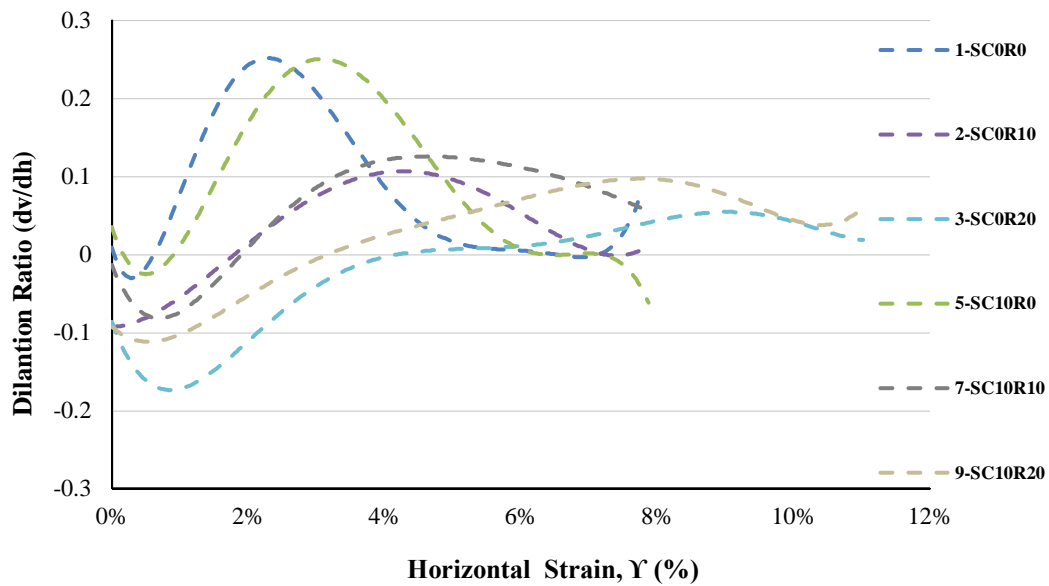


Figure5- 23. Dilation ratio versus the horizontal strain of small direct shear tests for the pure sand and the reinforced sand specimens.

On the whole, the composites revealed similar results to those observed in Figure5-19. Moreover, the composites with the smaller scale had a higher dilation ratio. For example, the direct shear test with the smaller box showed a dilation ratio 2.5 times greater than that in the case of the larger scale. Figure5- 23 shows a similar result for the analysis of the scale effect on the composite performance.

A further investigation on the dilation ratio focused on the large-scale result of establishing a possible relationship with the dilation angle. Figure5- 24 presents the dilation ratio results of sand and reinforced sand for various proportions of additives. The composites exhibited three typical types of dilation ratio behaviour because of their varied components. The vertical displacement of pure sand exhibited a dilation behaviour with no initial contraction; here, the peak value of the dilation ratio was obtained at approximately 2% horizontal displacement.

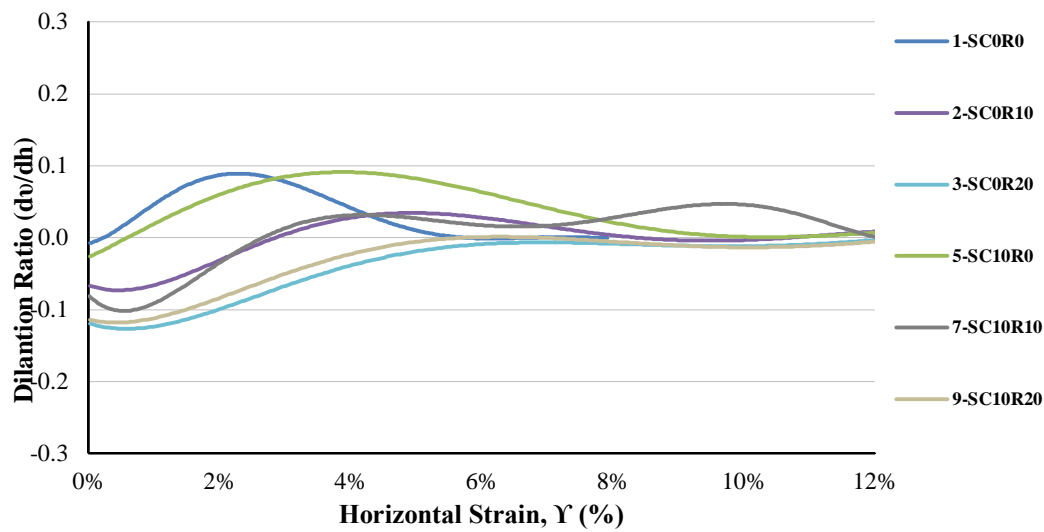


Figure5- 24.Dilation ratio versus the horizontal strain in the large direct shear tests for the pure sand and the reinforced sand specimens

This trend was slightly boosted by the addition of 10% cement, generating a denser composite that expanded during the shear process. The SC10R0 mixtures with a very small contraction movement gradually mobilised to 4% horizontal strain to achieve a dilation ratio greater than that of pure sand. The sand treatment with cement increased the dilation characteristics of pure sand but formed a stronger composite at a constant volume within the larger displacement. Another way to view these results is to observe the effect of the rubber addition to the sand mixtures with and without cement. The addition of rubber to the sand composites significantly reduced the dilation ratio of the composites. Moreover, establishing an initial contraction which can be related to the mechanical properties of rubber. A comparison of the dilation ratios of SC0R10 and SC0R20 showed that increasing the proportion of rubber increased the contraction behaviour and led to a slower tendency of the composite to reach the peak value. The slope of the dilation ratio was reduced, and the composite did not expand at the failure point. In this case, the dilation ratio of 0.097 of sand decreased to 0.036 upon the addition of 10% rubber and finally, became zero when the proportion of the added rubber increased to 20%. Although combining 10% rubber and 10% cement generated a minor difference at first and the end of the shear stage, this trend did not change

considerably upon the addition of cement to the sand specimens containing 20% rubber. The dilation ratio result of SC10R10 revealed that the hardening behaviour of the composite increased after rearranging the particles of the composite.

BRIEF SUMMARY...

The dilation ratio was defined on the basis of the zero extension lines theory, by a calculation of the vertical displacement of the composite against the horizontal displacement. The scale effect revealed that the sand specimens had a relatively high dilation ratio.

The composites exhibited three typical types of dilation ratio behaviour depending on the components of the composites. The vertical displacement of the untreated sand indicated the dilation behaviour with no initial contraction behaviour. Moreover, a relatively strong composite with considerable dilatancy was formed by the addition of the cementitious material. The vertical displacement of the sand became constant with a larger displacement as a result of the stabilisation. In contrast, the addition of rubber to the sand composites significantly reduced the dilation ratio of the composites. The slope of the dilation ratio decreased, and the composite did not expand at the failure point.

5-5 MAXIMUM DILATION ANGLE

5-5-1 MAXIMUM DILATION ANGLE AND PEAK FRICTION ANGLE

As expected, the maximum dilation ratio was associated with the highest value of the shear strength where the sample failed. With respect to this point, the angle of

dilation at the failure point ψ was calculated as follows (Afzali-Nejad et al., 2017, Lings and Dietz, 2005):

$$\psi = \tan^{-1} \left(\frac{dv}{dh} \right) \quad (5.11)$$

where dv and dh denote the variation of the vertical and the horizontal displacements, respectively, generated during the shear phase.

Thus, the variation of the dilation angle with the horizontal strain of each composite was calculated. With this in mind, the direct shear test using various normal stresses generated specific dilation ratio graphs. With respect to this fact, different normal stresses led to a variety of shear strengths for the same composites. Hence, performing a direct shear test with various values of the normal stress introduced the maximum friction angle and the maximum dilation angle at the peak value. The friction angle of each mixture at each point was calculated by dividing the shear strength by the applied normal stress (e.g., Simoni and Houlsby, 2006, Afzali-Nejad et al., 2017, Lings and Dietz, 2005, Zornberg et al., 2004, Dove and Jarrett, 2002, Fioravante, 2002). Subsequently, the peak friction angle was calculated as follows:

$$\varphi_p = \tan^{-1} \left(\frac{\tau_p}{\sigma} \right) \quad (5.12)$$

where τ_p and σ denote the peak value of the shear strength and the applied normal stress, respectively.

Further, according to Equation(5.13), the maximum dilation angle at the failure point was calculated as follows:

$$\psi_{\max} = \tan^{-1} \left(\frac{dv}{dh} \right)_{\max} \quad (5.13)$$

where $\left(\frac{dv}{dh}\right)_{\max}$ denotes the maximum value of the dilation ratio generally observed around the failure point.

Hence, based on the above equations, the peak friction angle and the maximum dilation angle of the three categories (i.e., ST, STR10 and STR20) of the composites are presented in Figure5- 25(a1, a2, b1, b2, c1 and c2). Considering the different behaviour and failure mechanisms of composite affecting by either cement or slag, the main component of the categories was defined as discussed earlier, (i.e., pure sand, a mixture of sand and 10% rubber, and a mixture of sand and 20% rubber). Subsequently, three composites with the different densities affecting by adding the stabilisers were, therefore, proposed to find the correlation between the two explained methods. Eventually, from now on, cement and slag were considered to be similar stabiliser materials. The typical behaviours of the peak friction angle and the maximum dilation angle are plotted against the normal stress for sand and a sand mixture with 5% and 10% stabilisers in Figure5- 25(a1 and a2), respectively. In the case of pure sand and the stabilised sand, ϕ_p and ψ_{\max} decreased with an increase in the normal stress. The maximum values of the friction angle and the dilation were observed for the ST10 class; this indicated that an increase in the stabiliser content formed a composite with a higher friction angle and dilatancy. Moreover, the difference in the composite behaviour was gradually minimised by increasing the normal stress, revealing the effect of the application of a load on the soil behaviour. To look this behaviour another way, based on the initial densities the result can be analysed. Further, the ϕ_p and ψ_{\max} behaviours were mutually related at the initial density of the composites. The soil with a greater density exhibited a greater peak friction angle and maximum dilation angle at an identical vertical load.

A similar comparison was considered for the STR10 class to analyse the effect of the addition of rubber on the soil strength characteristics (Figure5- 25b1 and b2). Overall, the addition of 10% rubber to the composites of the ST group generated a

similar trend. Moreover, the graphs showed a reduction of the dilatancy behaviour of the composites in the STR10 class. However, a comparison of φ_p and ψ_{\max} values of the sand–rubber composite with and without a stabiliser revealed the significant effect of the stabiliser on the composite behaviour. Considering the results of ST category, showing the lower difference, this behaviour was observed. Further, note that the addition of 10% rubber reduced the effect of the stabiliser ratio. Both the ST5R10 and the ST10R10 classes revealed similar results as they had similar initial density. Further, the addition of cementitious materials to the combination of sand with 10% rubber effectively reduced the initial void ratio of the sand mixture. However, this improvement indicated the availability of an optimum ratio of stabiliser where did not observed any significant difference after that point. The importance of composite density with respect to the determination of the optimum proportion of additives was discussed in an earlier section (Table5- 3). Eventually, the variation of the peak friction angle and the maximum dilation angle of a combination of sand and 20% rubber with and without the cementitious materials at different normal stresses are presented in Figure5- 25(c1 and c2). In general, the φ_p and ψ_{\max} values of the STR20 class exhibited trends similar to those observed for the two other categories. Moreover, increasing the rubber content of the STR10 mixtures to 20% led to the formation of composites with similar peak friction angles and maximum dilation angles. As in the case of the STR10 class, the results of the STR20 class revealed the effects of cementitious materials on φ_p and ψ_{\max} ; however, these effects were minimised. Performing the direct shear test with the higher normal stresses this behaviour was significantly observed. Further, the difference in the maximum dilation angle of the STR20 class at 500 kPa was negligible. Therefore, the use of 20% rubber for sand reinforcement formed a composite, which was considerably affected by the properties of the added rubber. Further, the initial density of the sand–rubber mixture did not change remarkably upon the addition of cementitious materials, which in turn led to similar values of φ_p and ψ_{\max} in this group.

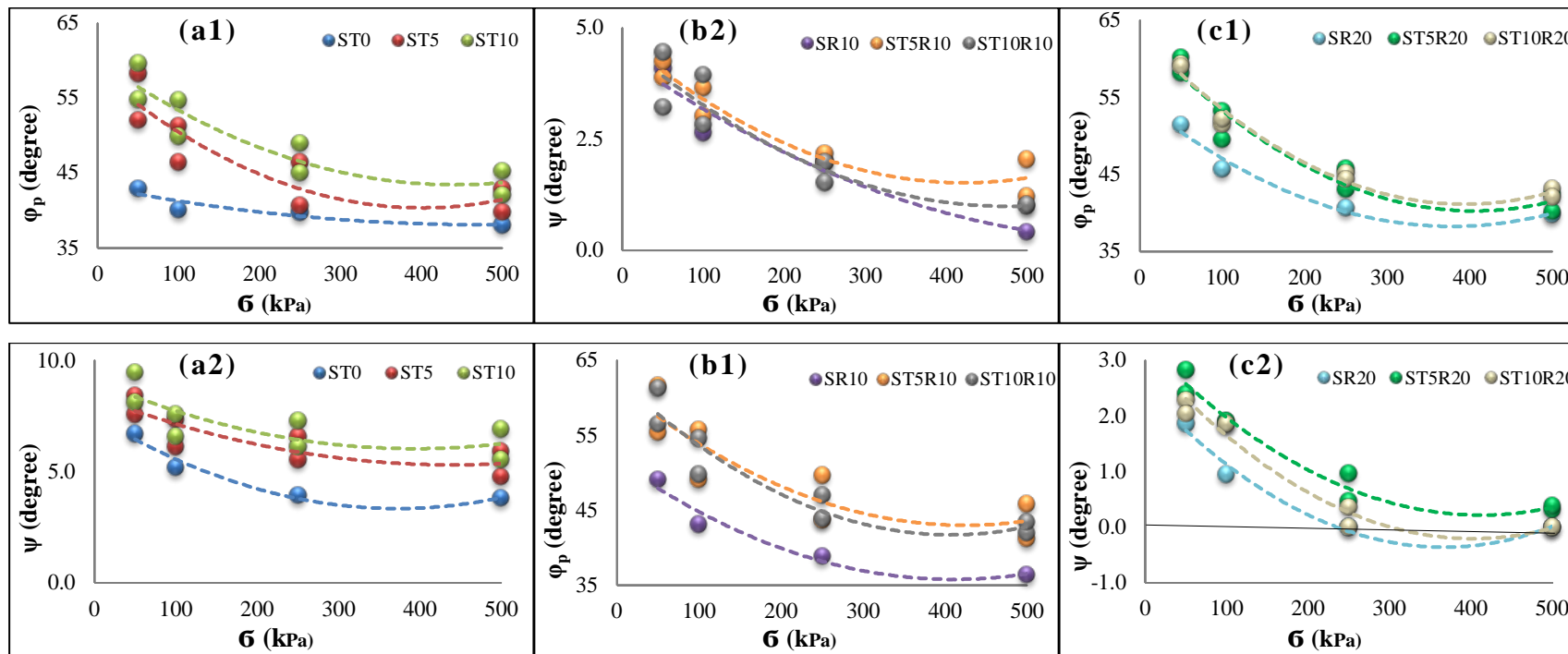


Figure5- 25. Results of the maximum dilation angle and the peak friction angle of sand composites obtained on the basis of the composite categories under various normal stress values: (a1) and (a2) ST class; pure sand and a mixture of sand and stabilisers; (b1) and (b2) STR10; sand with 10% rubber and a combination of 10% rubber and stabiliser; (c1) and (c2) STR20; sand with 20% rubber and a combination of 20% rubber and stabiliser.

BRIEF SUMMARY...

The typical behaviour of the peak friction angle and the maximum dilation angle was plotted against the normal stress for sand and a sand mixture with cementitious materials. The maximum values of the friction angle and the dilation were related in the case of the ST10 class, which implied that increasing the stabiliser content led to the formation of a composite with a relatively high friction angle and dilatancy. The addition of rubber to the composites of the ST group exhibited an almost similar trend. Moreover, the graphs showed the reduction of the dilatancy behaviour of the composites in both the STR10 and the STR20 classes. However, a comparison of the φ_p and ψ_{max} results of the sand–rubber mixture with and without the stabiliser revealed the effect of the stabilisers on the sand and rubber only composite behaviour. In general, the φ_p and ψ_{max} values of the STR20 class implied the generation of composites with similar peak friction angles and maximum dilation angles. Increasing the rubber ratio for sand stabilisation caused to generate a composite which was considerably affected by the rubber properties.

5-5-2 EMPIRICAL EQUATION FOR MAXIMUM DILATION ANGLE

An identical relationship between the variation of the peak friction angle and the maximum dilation angle for each class can be summarised. Therefore, the relation can be approximated on the basis of the following empirical equation:

$$\varphi_p = \alpha\psi + \beta \quad (5.14)$$

where β denotes the friction angle of the composite at zero dilatancy.

The area with no dilatancy can be equalled to the constant volume state. Stopping the deformation after the failure, the state where the normal stress, shear strength, and volumetric behaviour were constant was the constant volume state (Poulos, 1981,

Amini et al., 2014). A number of studies have been carried out on sand specimens to provide an estimation of the critical states (Coop and Atkinson, 1993, Cuccovillo and Coop, 1998, Amini et al., 2014). These studies have reported some difficulties in detecting the area of the critical state, namely the effect of cement addition on the friction angle, particularly in the case of the larger strain. However, the small strain measurement was suggested as a reliable technique to evaluate the constant volume state, where the stress and strain behaved heterogeneously. Several methods have been developed to estimate the constant volume friction angle, which interpreted the direct shear data of either a single or multiple tests Simoni and Houlsby, 2006. One of the simplest methods is the measurement of the mobilised friction angle at a point with zero dilation rate. Further, the energy correction method was defined by Taylor (1948), plotting the $(\tau/\sigma + dv/du)$ against the shear displacement. Subsequently, the point with the constant amount of $(\tau/\sigma + dv/du)$ was considered the constant volume state. Alternatively, using the multiple tests, drawing a line based on the calculated τ/σ and dv/du of the peak point with an interception was defined as the friction angle in the constant volume state in the third method. The last not the least is performing the multiple test, defining the peak friction angle and maximum dilation angle for each individual normal stresses. By plotting ϕ_p versus ψ_{max} , the constant volume friction angle (i.e. ϕ'_{cv}) was obtained from the best fit line. Conducting multiple tests minimises the possible error. Hence, similar with the small strains measurement, this method is known as an accurate technique.

Therefore, according to equation (16), Figure5- 26(a, b and c) show the following results for the stabilised and un-stabilised specimens for each class. The obtained equations showed a good agreement with the laboratory results. Considering the pure sand as an untreated specimen, the effectiveness of rubber with respect to increasing the constant volume friction angle was clearly observed. The use of 10% rubber led to a minor improvement in the ϕ'_{cv} value of sand; this value was significantly increased by the addition of 20% rubber to the pure composite. In both the STR10 and the STR20

categories, a mixture's friction angle at constant volume was boosted by the introduction of a stabiliser. In contrast, the addition of stabilisers only remarkably reduced the φ'_{CV} value of sand. Therefore, we hypothesised that the softening behaviour of sand was boosted by the addition of cementitious materials. That is, a strong composite was generated, which dramatically lost its strength after a failure.

Another way to view these results is to reveal the incremental linear relationship between the peak friction angle and the maximum dilation of the composites, as shown in Figure 5-26(a, b and c). Sand reinforcement with stabilisers only resulted in a sharp increment in dilation trend compared with the other additives. Increasing the value of φ_p not only led to a higher ψ_{max} but also a difference between two angles, which subsequently decreased φ_{CV} . We verified the mentioned hypothesis: the composite strength decreased considerably after a failure.

In contrast, the use of rubber for sand reinforcement minimised the difference between φ_p and ψ_{max} . The introduction of rubber into the sand matrix not only reasonably modified the φ_p and ψ_{max} values of the composite but also improved φ_{CV} with and without a stabiliser addition. This effect was observed by increasing the rubber ratio, was remarkably keeping composite tendencies close to each other, even after conducting the cementitious material in sand-rubber reinforcement.

With respect to the benefits of performing a direct shear test with a large strain, the obtained results of the contact volume revealed further information about soil characteristics, which will be analysed in the following section.

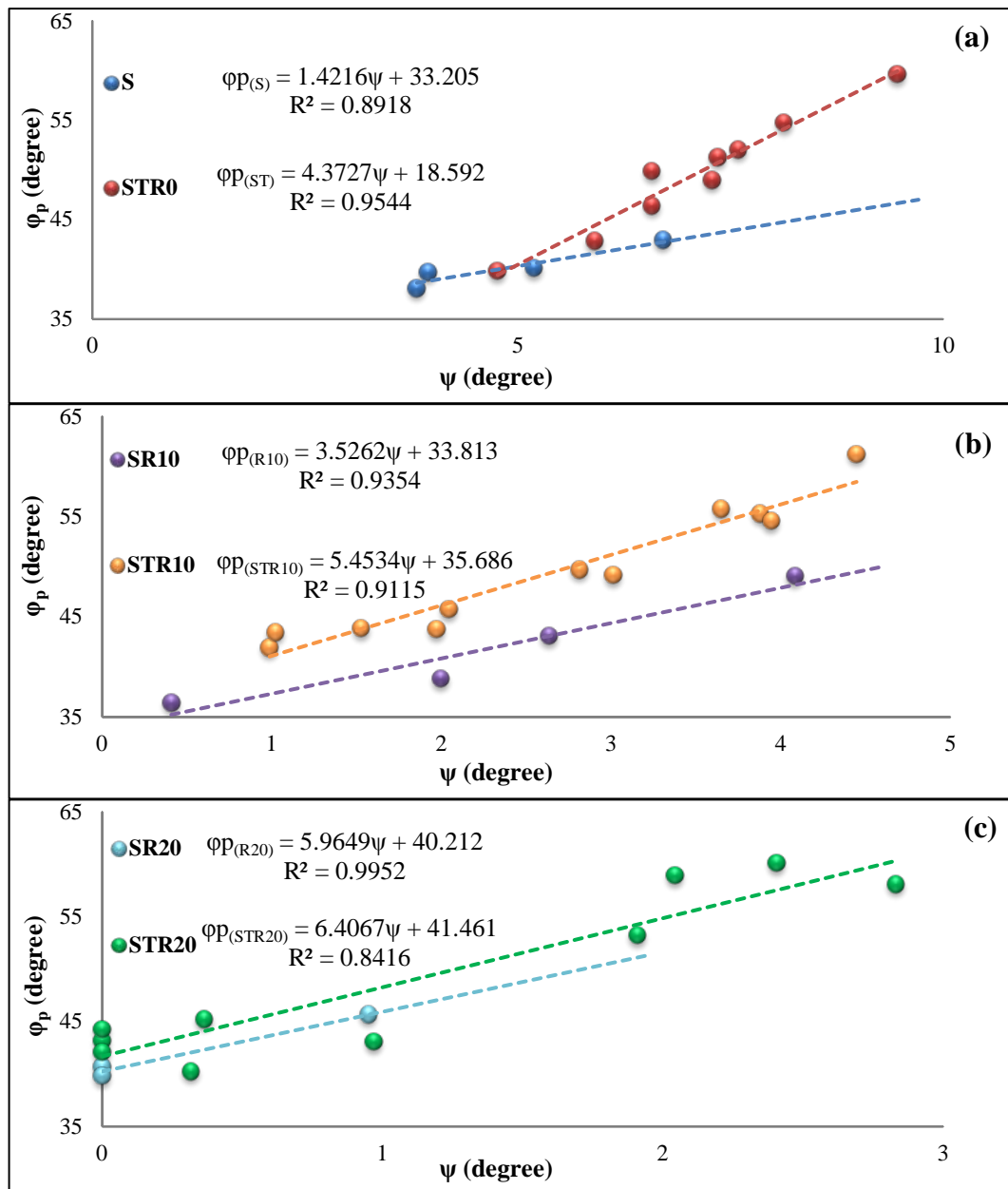


Figure5- 26. Variation of peak friction angle to determine the constant volume friction angle for untreated and treated sand matrices.

BRIEF SUMMARY...

Multiple tests were conducted to determine the peak friction angle and the maximum dilation angle for each considered normal stress. By plotting φ_p versus ψ_{\max} , we obtained the constant volume friction angle from the best fit line. Considering pure sand to be an untreated specimen, we found that the addition of rubber increased the constant volume friction angle. The use of the rubber material led to an improvement in the φ'_{cv} value of sand. In both the STR10 and the STR20 categories, a mixture's friction angle at constant volume was boosted by the introduction of a stabiliser. In contrast, the application of stabilisers only remarkably reduced the φ'_{cv} value of sand. Increasing the value of φ'_p not only led to a higher ψ_{\max} value but also increased the difference between the two angles and subsequently, reduced φ_{cv} .

We concluded that the addition of rubber materials for sand reinforcement with cementitious materials associated had several advantages including an improvement of the strength properties and the shear resistance, retention of the soil strength even after a failure, and a reduction of the dilatancy behaviour of soil.

5.5.3 CONSTANT VOLUME FRICTION ANGLE

The LDS test revealed the possibility of investigating the constant volume state. In this state, the composites exhibited stable behaviour in terms of volumetric behaviour, void ratio, normal stress and shear stress. This state was called steady state by (Dove and Jarrett, 2002, Frost et al., 2002, Afzali-Nejad et al., 2017) and residual state by Koerner, (2012) and Tabucanon et al., (1995). Thus, as discussed earlier, the constant volume state was selected for this study. On the basis of the relationship between the normal stress and the constant volume friction angle, the constant volume was calculated as follows (Tabucanon et al., 1995, Dove and Jarrett, 2002, Fioravante, 2002, Lings and Dietz, 2005, Afzali-Nejad et al., 2017):

$$\varphi_{cv} = \tan^{-1} \left(\frac{\tau_{cv}}{\sigma} \right) \quad (5.15)$$

The same as peak friction angle and maximum dilation angle results, analysing ϕ_{cv} of composite has been depicted in three main groups. Overall, Figure5- 27(a, b and c) have been shown almost similar results with the deduced friction angles of Figure5- 26. The use of cementitious materials in the sand treatment of the ST class had only a minor effect. Contrast with that, the outcomes of sand-rubber mixtures were shown a significant increment in the friction angle of the composite at the constant volume was. Once more time, the result suggested the greatest achievement obtaining by a combination of 10% rubber plus 5% of stabilisers. Moreover, the composites of the STR20 class exhibited the most similar improvement among the mixtures, thereby proving the relationship deduced from Figure5- 26. Therefore, sand reinforcement with 20%rubber exhibited more interlocking among the sand and the rubber particles and formed strong composites, as shown inFigure5- 27(c). This process was additionally boosted by combining this mixture with a certain amount of cementitious materials containing finer particles to increase the connections among the composite's particles. Resulting from this a composite comprising the characteristics of flexibility, asperity, and cohesion. The further analysis will be described that how the combination of rubber and cementitious material could be stocked the composite's structure by increasing the attractive intermolecular force.

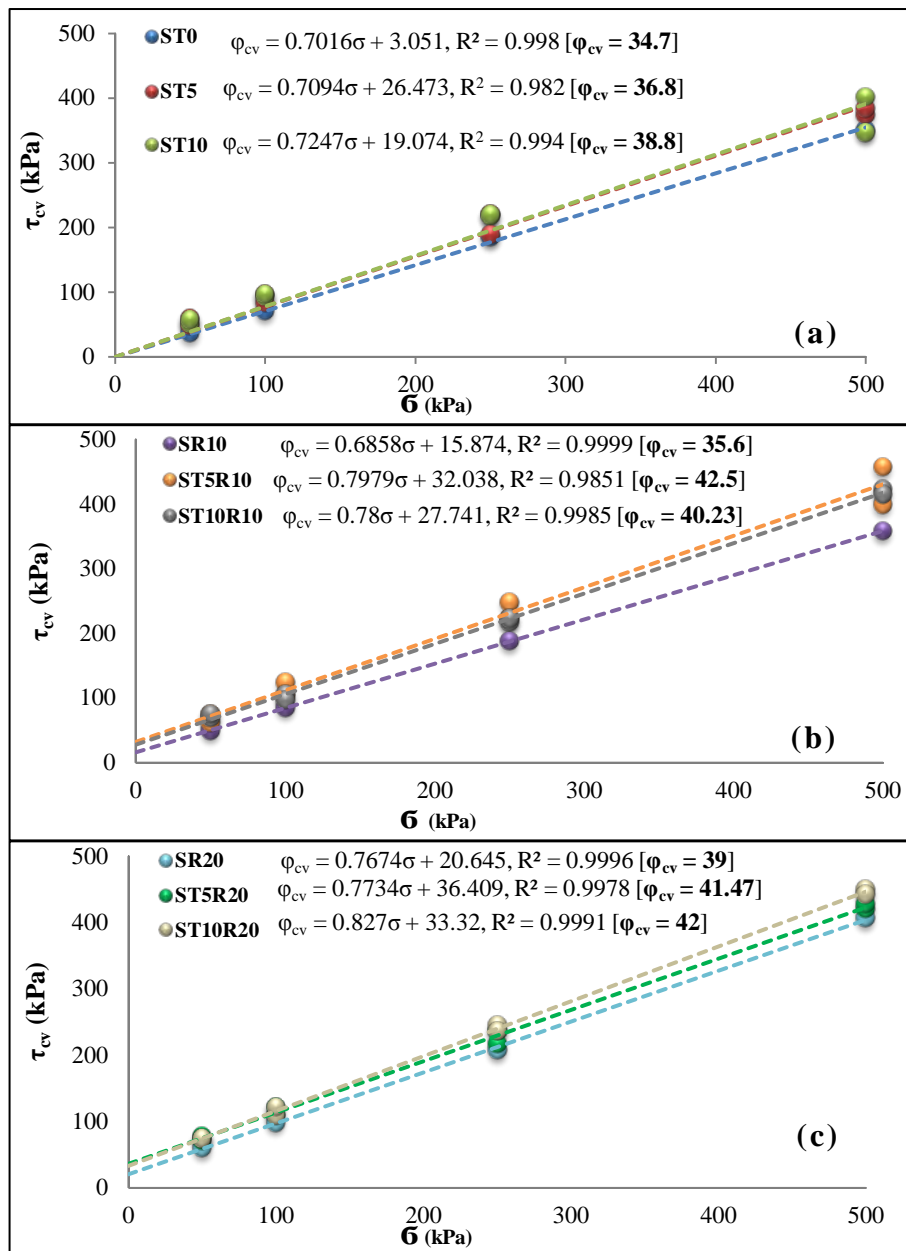


Figure5- 27. Results of the constant volume friction angle versus the normal stress of sand composites based on the composite categories: (a) ST class; pure sand and mixture of sand and stabilisers; (b) STR10; sand with 10% rubber and a combination of 10% rubber and stabilisers; (c) STR20; sand with 20% rubber and a combination of 00% rubber and stabilisers.

With this in mind, on the basis of the linear equation results of the composites, we formulated the following empirical equation:

$$\varphi_{cv} = \alpha' \sigma + \beta' \quad (5.16)$$

where β' denotes the apparent cohesion of the soil at the constant volume state shear stress, considering a zero dilation angle in the constant volume state. Consequently, the results revealed the effectiveness of additives with respect to the generation of the apparent cohesion in the sand even after a failure. However, the importance of creating a composite with the optimum ratio of additives to achieve the maximum improvement was implied by the results of all the categories. Overall, adding 20% rubber with dosages of cementitious materials has been established the composite with the highest intermolecular force. It seems that, the combination of soil tension (Gratchev et al.) and cementation (C_{cm}) were significantly kept the particles connection even after the failure. Nevertheless, it does not mean that performing the greater amount of additives resulted in a greater increments. Subsequently, adding five percentages of stabiliser into the composites of both STR10 and STR20 classes, was found to be more effective than addition of 10% stabiliser. It is worth mentioning that, comparing the results of sand composites, treating with either rubber or stabiliser only indicates two different behaviour. Increasing the proportion of the stabiliser added from 5% to 10% reduced the effectiveness of the stabiliser with respect to improving the cohesion of sand at the constant volume. Thus, an increase in the stabiliser content formed a composite with a relatively rough surface, increasing the vulnerability of the surface area. In contrast, increasing the rubber content improved the cohesion of sand after a failure, and the surface roughness of the composite was reduced by the flexibility of the rubber particles. In other words, after a failure, the material with a capacity to create cohesion tension was more effective than a material with the capacity to create cementation cohesion. Accordingly, in a combination of rubber and a stabiliser, increasing the rubber content not only improved the effectiveness of the stabiliser but also minimised

the loss of the electrostatic force among the composites, because of the increasing stabiliser content.

BRIEF SUMMARY...

A composite's friction angle at a constant volume exhibited an almost similar behaviour to the maximum friction angle. The addition of cementitious materials for the sand stabilisation of the ST class had only a small effect. In contrast, the use of rubber particles for sand reinforcement showed a significant improvement in the friction angle of the composite at the constant volume. Subsequently, the results revealed the effectiveness of additives with respect to the generation of the apparent cohesion in sand even after a failure. In general, the use of 20% rubber with a certain proportion of cementitious materials formed a composite with the highest intermolecular force. Further, a combination of soil tension (Gratchev et al.) and cementation (C_{cm}) kept the particles together even after a failure.

On the whole, particles with the flexibility characteristic could be easily moved on the contact surface. Subsequently, the composite exhibited only a minor change in both the mobilised shear strength and the volumetric strain. Associating the capacity of cementitious material for connecting a greater number of particles, in addition of the elastic capacity of rubber particles, leads to generate the composite with a greater strength capacity and significant elastic tension for reducing the dilatancy behaviour.

5.5.4 STRESS–DILATION LAW

The results revealed a possible relationship between the friction angle and the dilation angle of the composites on the basis of the stress–dilation law. According to previous research, on the basis of the flow rules, the direct shear test results can be predicted (Taylor, 1948, Rowe and Barden, 1964, Simoni and Houlsby, 2006). One of the most comprehensive studies on this subject was conducted by Bolton (1986, 1987)

using the flow rule theory. The empirical relationship was successfully evaluated by using the experimental results of a variety of sand types; it can be expressed as follows:

$$\varphi'_{ps} = \varphi'_{cv,ps} + 0.8\psi \quad (5.17)$$

A good agreement (i.e., $R^2 = 0.9166$) was observed for predicting the results for pure sand in this research. Further, a greater coefficient for the dilation angle was observed:

$$\varphi'_{ps} = \varphi'_{cv,ps} + 0.91\psi \quad (5.18)$$

Given the fact that, Equation (5.17) was predicted the results of sand only, yet the difficulties of adducting the theoretical interoperation, Bolton's empirical is suggested a framework for deriving a possible equation for the examined composites. In contrast, the difference between the values of the dilation angle obtained using different method is neglected in Equation(5.18). It has been observed in the results of direct shear with large and small boxes.

Thus, by combining Equations (5.13) – (5.18) to determine the correlation between the maximum dilation angle of a composite and the difference in the friction angles at the failure point and constant volume, we obtained the following:

$$\varphi'_{peak, ds} - \varphi'_{cv, ds} = N\psi_{max} + M \quad (5.19)$$

where as a function of the friction angles, N denotes the coefficient of the dilation angle, which is affected by the type of soil used. Considering the other parameters such as composite properties and different test methods and scales, the coefficient M was introduced to comprehensively obtain a more accurate correlation. Hence, based on the obtained experimental results presented in Figure5- 28, $\varphi'_{peak, ds} - \varphi'_{cv, ds}$ against ψ_{max} is presented in Figure5- 28(a1,b1 and c1). Here, we observed that the $\varphi'_{peak, ds} - \varphi'_{cv, ds}$ value was linearly related to the ψ_{max} value of the indexical composites.

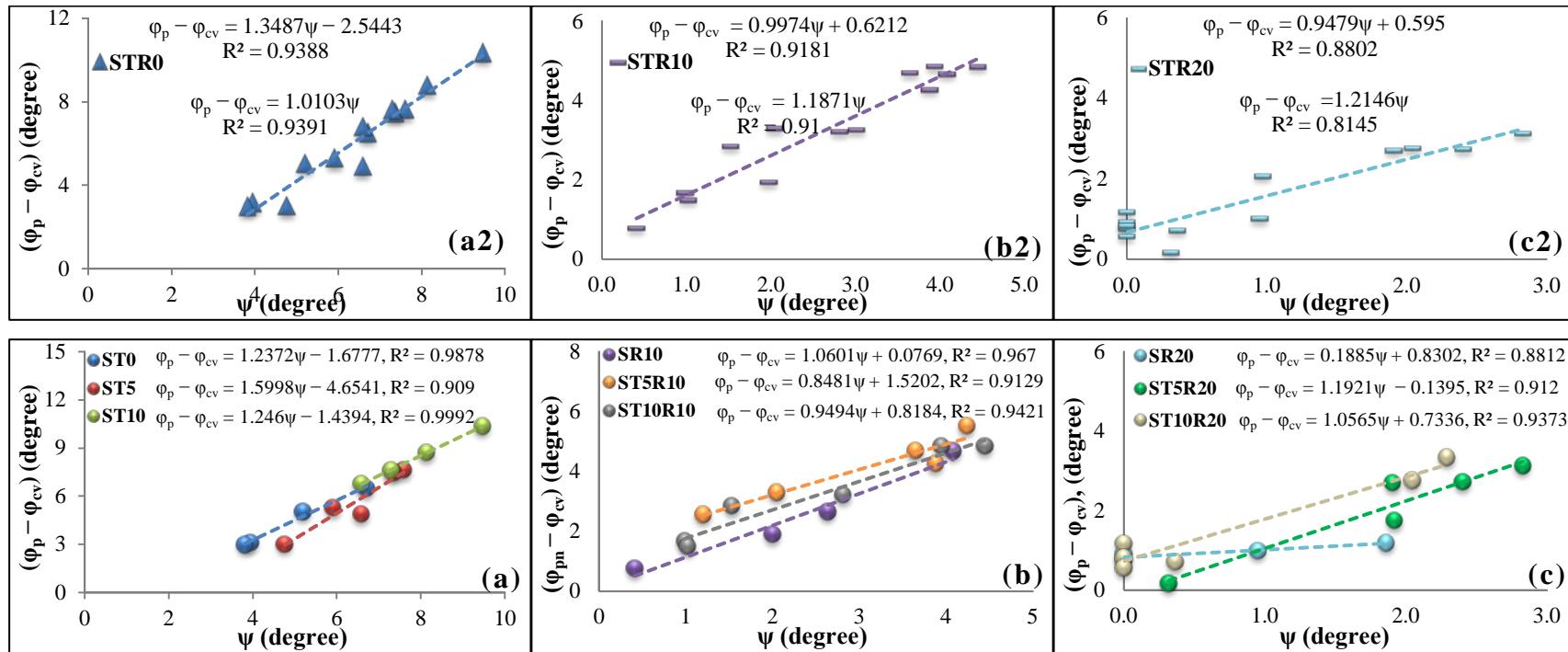


Figure 5- 28. Stress–dilation law explaining the correlation between $\phi'_{peak,ds} - \phi'_{cv,ds}$ and ψ_{max} for (a)sand plus stabilisers;(b)sand plus 10% rubber and stabilisers;(c) sand plus 20% rubber and stabilisers.

A good agreement between the obtained trends and the experimental results was obtained for all the composites. Considering the relationship between the stress–dilation law suggested by Equation(5.19), we have shown the final relationship for each group of sand composites in Figure5- 28(a2, b2, and c2). Composite’s equation was identified based on the dosage of rubber, presenting the composite characteristics. Further, on the basis of Bolton’s equation, a simplified form of the proposed correlation was also derived, which showed a good agreement as well.

BRIEF SUMMARY...

A summary of the proposed equations (i.e., $\varphi'_{peak, ds} - \varphi'_{cv, ds} = N\psi_{max} + M$) and a simplified form (i.e. Bolton’s equation) of these equations is presented in Table5- 5.

Table5- 5.Summary of the obtained equation for three categories of composites: loose, medium and dense.

Soil structure	Linear equation	Simplified equation
Loose (STR20)	$\varphi_p - \varphi_{cv} = 0.9479\psi + 0.595$ $R^2 = 0.88$	$\varphi_p - \varphi_{cv} = 1.2146\psi$ $R^2 = 0.81$
Medium (STR10)	$\varphi_p - \varphi_{cv} = 0.9974\psi + 0.6212$ $R^2 = 0.92$	$\varphi_p - \varphi_{cv} = 1.1871\psi$ $R^2 = 0.91$
Dense (STR0)	$\varphi_p - \varphi_{cv} = 1.3487\psi - 2.5443$ $R^2 = 0.94$	$\varphi_p - \varphi_{cv} = 1.0103\psi$ $R^2 = 0.94$

5.6 COHESION

5.6.1 COMPARISON OF APPARENT COHESION IN LARGE AND SMALL SCALES

Figure5- 29 presents the results of the scale effect on the cohesion values of the treated and the untreated sand composites. In the case of the larger scale, the composites exhibited a greater value of cohesion. Note that the sand's cohesion was significantly increased by the addition of either stabilisers or rubber. To compare the effectiveness of the addition of a stabiliser or rubber only, the apparent cohesion generated by the cementation (i.e., with the stabilisers) caused to established more connection among the sand particles. In contrast, the sand containing only added rubber generated a surface tension force as a water film was formed among the particles.

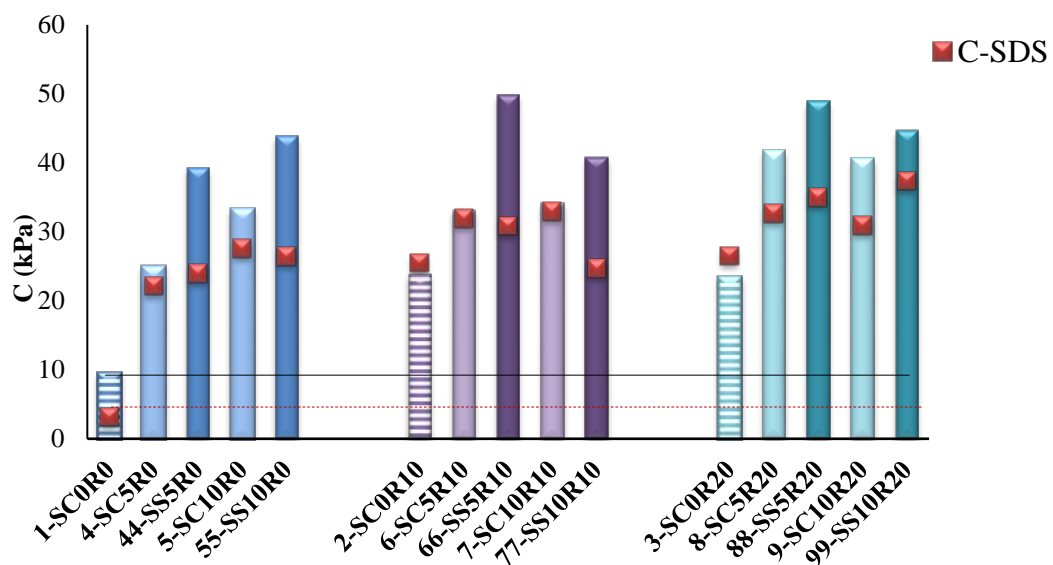


Figure5- 29. The cohesion of pure sand and treated sand samples in the large direct shear test, compared with the results of the small direct shear test.

Thus, the introduction of the rubber particles into the sand mixture led to the formation of a composite with a variety of particle shapes filling the gaps among the sand particles. Subsequently, increasing the surface tension by the water film formation ensured that more sand–rubber particles remained connected.

Therefore, a combination of rubber and a cementitious material for sand stabilisation resulted in a greater cohesion value. The maximum improvement was obtained by combining 5% slag with 10% rubber. Adding 10% rubber to this composite generated a similar value of approximately 49 kPa. Note that the STR20 class achieved the greatest level of cohesion, suggesting the effectiveness of using a combination of rubber and stabilisers for sand reinforcement. This result was observed for the STR10 class as well, leading to cementation and surface tension cohesion by using two different types of additives. Moreover, the results suggested that the particle size and density of a composite play a pivotal role in determining the shear strength behaviour of a soil matrix.

5.6.2 RELATIONSHIP BETWEEN APPARENT COHESION AND MAXIMUM DRY DENSITY

The plot of the cohesion value of the composites versus the MDD verified the abovementioned assumption. The trends of the composites shown in Figure5- 30 indicate that the maximum cohesion was obtained at a specific density.

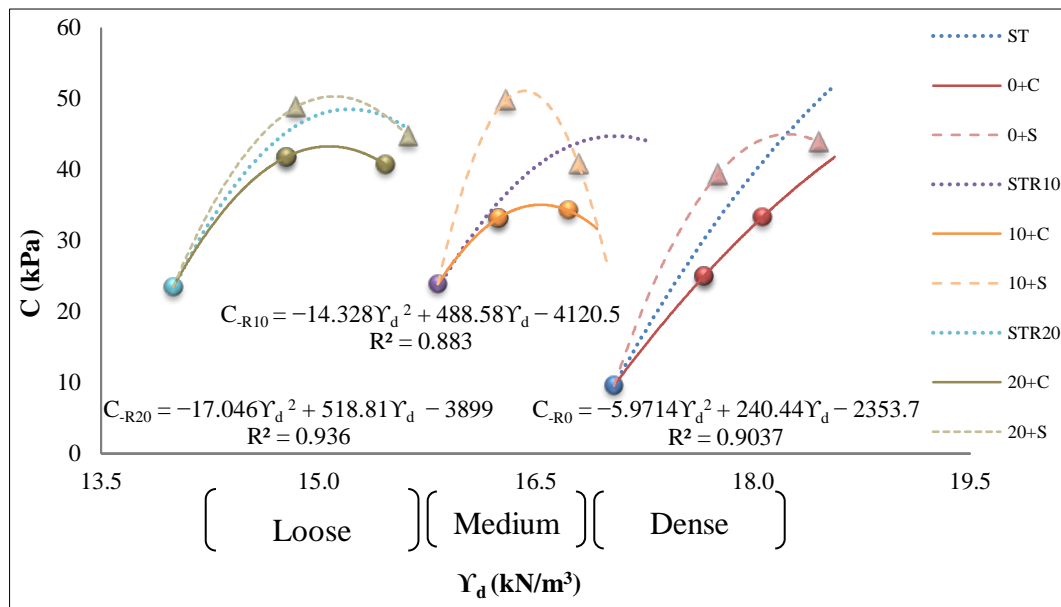


Figure5- 30. The cohesion of pure sand and treated sand composites versus the maximum dry density, where ST, STR10, and STR20 are representative of all the composites of their classes.

Investigation the results separated by the kind of stabilisers reveal the similar tendency, where tend to be equal at the same density. Moreover, the only difference is related to the maximum value of cohesion, suggesting the different efficiency of cement and slag. Considering this difference, we concluded that the trend-line of ST, STR10, and STR20 represented the results of all the composites in each class.

Using the results shown in Figure5- 26, we calculated the cohesion value of the composites in the constant volume state. The cohesion value of the composites in the critical state followed the same trend as the value at the failure point, as shown in Figure5- 31. Comparing the result of Figure5- 31 with the deduced cohesion angle from the Equation 18(i.e., Figure5- 27), indicate the almost similar value. The results shown in Figure5- 31revealed that the cohesion value of the composite at the constant volume state was associated with the availability of the rubber particles.

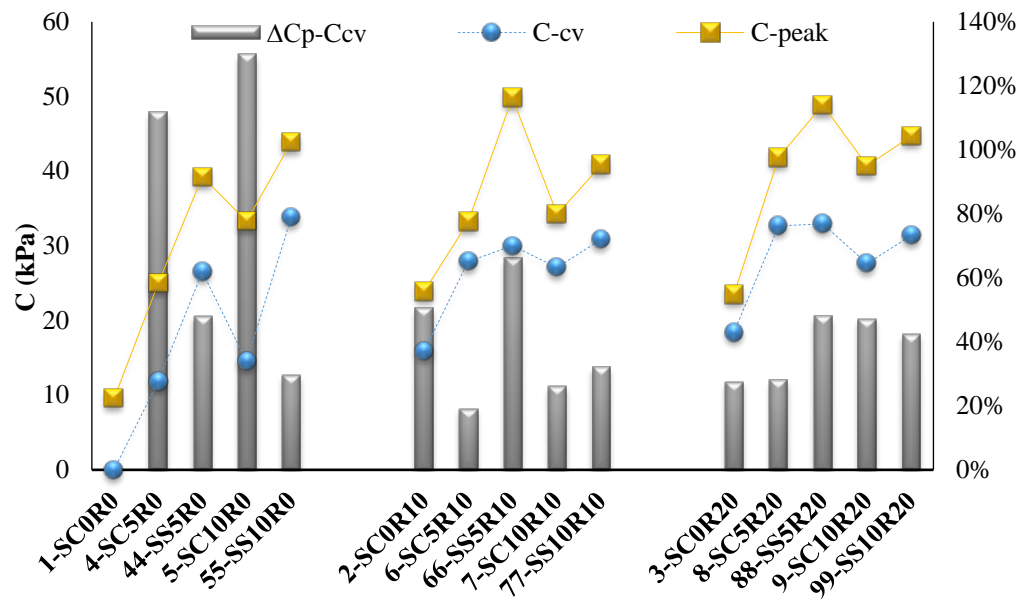


Figure5- 31. Cohesion values of the treated and the untreated composites at the peak and the constant volume state and their difference.

The composites of the STR0 class had the lowest cohesion value. In contrast, the sand mixture containing rubber exhibited similar values, slightly tending to show a greater value with a greater proportion of rubber. However, an analysis of the difference between the cohesion values at two states revealed the effect of the rubber content. Except for the SS5R10 composite, the other composites of the STR10 category showed the minimum reduction of cohesion after a failure. Note that the sand mixtures treated with cement significantly lose their cohesiveness in contrast to the sand–slag-treated composites.

BRIEF SUMMARY...

Table5- 6 summarises the apparent cohesion values of pure sand and the reinforced sand mixtures. The correlation between the cohesion value for the peak shear stress and MDD of the composites is also provided.

Table5- 6. Summary of the obtained equation for the cohesion of three categories of composites: loose, medium and dense. The cohesion of the treated and the untreated sand composites.

Soil structure	Proposed equation for cohesion (Peak shear stress)	Cohesion (Peak)	Cohesion (Residual)
Loose (STR20)	$C = -17.046\gamma_d^2 + 518.81\gamma_d - 3899$ $R^2 = 0.936$		
3-SC0R20		23.48	18.41
8-SC5R20		41.48	32.68
88-SS5R20		48.84	32.96
9-SC10R20		40.70	27.66
99-SS10R20		44.69	31.42
Medium (STR10)	$C = -14.328\gamma_d^2 + 488.58\gamma_d - 4120.5$ $R^2 = 0.883$		
2-SC0R10		23.88	15.87
6-SC5R10		33.2	27.89
66-SS5R10		49.82	29.98
7-SC10R10		34.26	27.14
77-SS10R10		40.83	30.90
Dense	$C = -5.9714\gamma_d^2 + 240.44\gamma_d - 2353.7$ $R^2 = 0.9037$		
1-SC0R0		9.53	0
4-SC5R0		25	11.8
44-SS5R0		39.24	26.54
5-SC10R0		33.31	14.5
55-SS10R0		43.87	33.86

5.6.3 SHEAR STRENGTH IMPROVEMENT INDEX (C_i)

In this section, the shear strength improvement index (C_i) is defined to estimate the shear strength improvement of a treated soil sample compared with that of an untreated soil sample. Here, the index is defined as the ratio of the shear strength of the reinforced sand mixtures to the shear strength of the pure sand at similar applied normal stress values. Integrating ideas from the existing literature on the interface efficiency of treated soils (Infante et al., 2016), we obtained the following equation:

$$C_i = \frac{C_r + \sigma \tan \varphi_r}{C + \sigma \tan \varphi} \quad (5.20)$$

where C_i denotes the shear strength improvement index, C_r represents the cohesion of the reinforced sand, C indicates the apparent cohesion angle of pure sand obtained by the experimental tests, σ refers to the applied normal stress, φ_r stands for the friction angle of the reinforced sand mixtures, and φ denotes the friction angle of the untreated sand. Table 5-7 presents the values of the shear strength improvement index of stabilised sand in two large and small scales. An analysis of the C_i value revealed that the composite's shear strength was reasonably enhanced. The shear strength improvement index of stabilised sand varied from 1.01 to 2.25, depending on the type and proportion of the additives. As expected, the C_i value gradually decreased with an increase in the normal stress, where the maximum improvement of 2.25 was observed for the SS5R10 mixture.

Another way to study on the scale effect on the shear strength of the composites, where analysed by investigation into the difference of shear strength improvement index obtained by small and large scale, present in Figure 5-32.

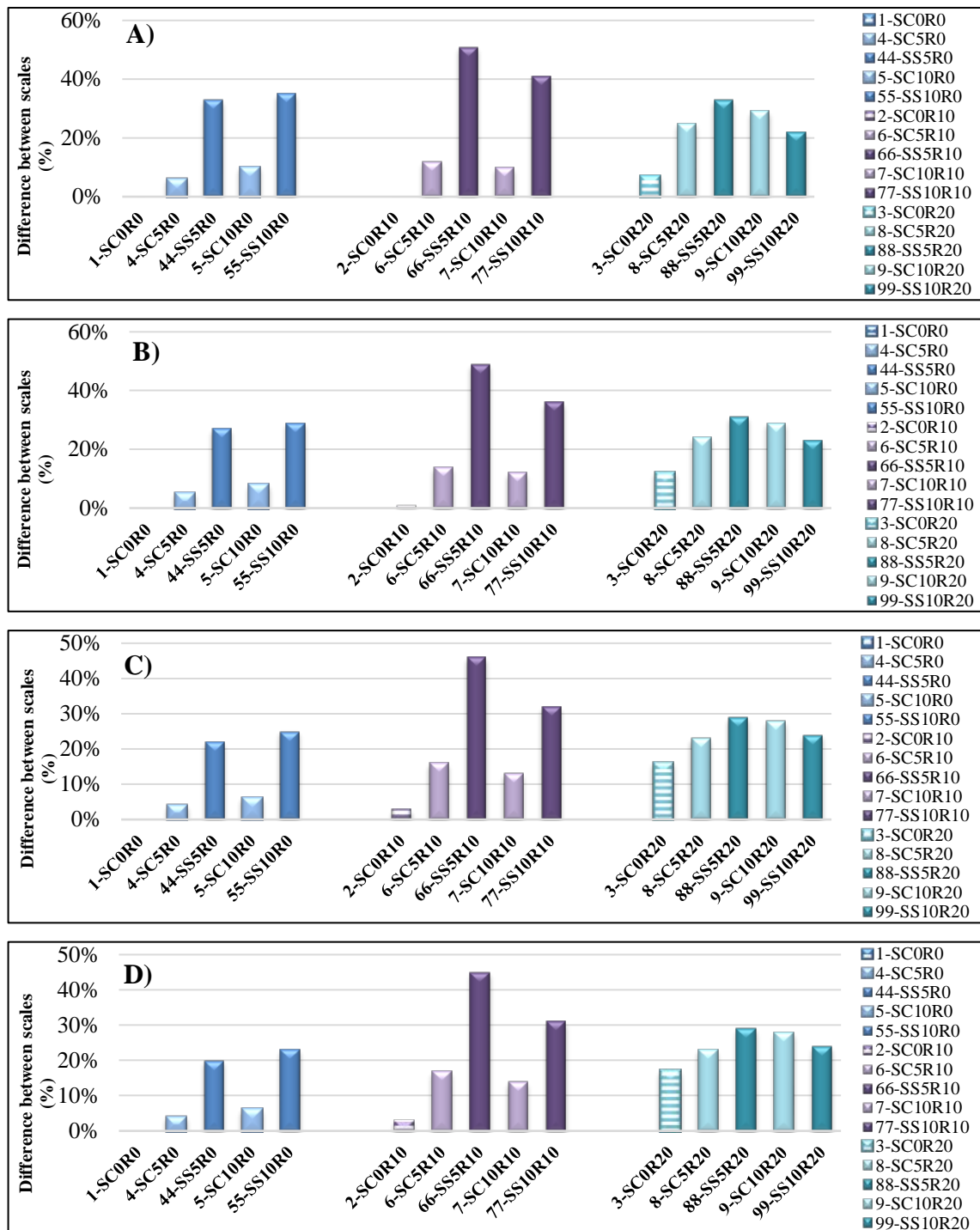


Figure 5-32. The difference of shear strength improvement index in small and large scales obtained by normal stresses; A) 50kPa, B) 100kPa, C) 250kPa, D) 500kPa.

Subsequently, the percentage difference of the C_i values for the two scales was calculated. The scale effect results revealed minor differences between the two scales for the sand sample treated with cement only. In contrast, the composites containing sand and slag exhibited a noticeable scale effect on their shear strength. Note that the results of the sand reinforcement with only 10% rubber were relatively similar in the cases of both large and small boxes.

BRIEF SUMMARY...

To provide a comprehensive and more accurate conclusion, data of all normal stresses are presented in Table 5-7. The results obviously reveal that, the cohesion of soil can be slightly increased by adding a dosage of rubber particles. Moreover, this effect can be remarkably enhanced by using a combination of rubber and stabilisers.

Although, the large direct shear result has also validated the reliability of performing the small direct shear method for this investigation, study on shear strength improvement index suggests that the difference between two scales might be affected by using a different stabilisers. However, this difference is fairly acceptable, which is associated with the material properties of stabiliser, revealing different effect. Thus, the possible reasons behind this assumption will be discussed in the microstructural study section.

Table5- 7. Summary of shear strength improvement index (Ci) for the peak shear stress of reinforced sand composites, obtained from the large and small direct shear tests.

Test type	Large direct shear				Small direct shear				Difference between two scales (%)			
Composite	Normal stress (kPa)				Normal stress (kPa)				Normal stress (kPa)			
	50	100	250	500	50	100	250	500	50	100	250	500
4-SC5R0	1.44	1.32	1.24	1.20	1.36	1.26	1.19	1.16	6%	5%	4%	4%
44-SS5R0	1.90	1.67	1.51	1.46	1.43	1.32	1.24	1.21	33%	27%	22%	20%
5-SC10R0	1.71	1.53	1.41	1.36	1.55	1.42	1.32	1.29	10%	8%	6%	6%
55-SS10R0	2.09	1.83	1.66	1.59	1.54	1.42	1.33	1.30	35%	29%	25%	23%
2-SC0R10	1.33	1.21	1.12	1.09	1.33	1.19	1.09	1.06	0%	1%	3%	3%
6-SC5R10	1.70	1.52	1.39	1.34	1.51	1.33	1.20	1.15	12%	14%	16%	17%
66-SS5R10	2.25	1.95	1.74	1.66	1.49	1.31	1.19	1.14	51%	49%	46%	45%
7-SC10R10	1.73	1.55	1.41	1.37	1.57	1.38	1.25	1.20	10%	12%	13%	14%
77-SS10R10	2.01	1.78	1.61	1.55	1.42	1.30	1.22	1.19	41%	36%	32%	31%
3-SC0R20	1.40	1.29	1.22	1.19	1.31	1.16	1.05	1.01	7%	12%	16%	17%
8-SC5R20	1.87	1.61	1.44	1.37	1.50	1.30	1.16	1.11	25%	24%	23%	23%
88-SS5R20	2.11	1.81	1.59	1.51	1.59	1.38	1.23	1.18	33%	31%	29%	29%
9-SC10R20	1.93	1.69	1.52	1.46	1.49	1.32	1.19	1.15	29%	29%	28%	28%
99-SS10R20	1.99	1.71	1.52	1.45	1.63	1.39	1.23	1.17	22%	23%	24%	24%

CHAPTER6
SHEAR AND COMPRESSIBILITY
BEHAVIOUR OF SAND- RUBBER
COMPOSITES

This chapter presents the following section:

6-1: Introduction	199
Shear behaviour	201
Strain behaviour.....	202
Compressibility Behaviour.....	202
6-2: Material and experimental methodology	204
6-3: Result and Discussion	206
6-3-1: One-dimensional consolidation test	206
6-3-1-1 Compression and recompression indices.....	206
6-3-1-2 One-dimensional elastic modulus	212
6-3-1-3 Classification the compression evolution of composites.....	217
6-3-2: Consolidated-undrained triaxial test.....	222
6-3-3-1 Effect of the ratio of additives on the deviatoric behaviour	223
6-3-3-2 Effect of the confining pressure	228
6-3-3-3 Maximum principle stress ratio	232
6-3-3-4 Analysing the shear strenght characteristic	234
6-3-3-4 Young's modulus	235
6-4: Compression and analysis the results of triaxial tests and direct shear tests	237
6-4-1: Assessing the intrinsic constants for shear strength.....	237
6-4-2: Experimental data of sand composites	237
6-4-3: Regression model	238
6-5: Microstructural analysis of the cemented sand-rubber composite	245
6-5-1: Material characteristics and phases of composite	245
6-5-2: Microstructure of composite	246
6-5-2-1: Cementitious binders.....	247
6-5-2-3: effect of rubber particles on cementitious binders	250
6-5-2-3: Pore structure	252
6-5-2-4: Interfacial Transition Zone (ITZ).....	254

6-5-3: Potential of rubber and slag to create a high-performance composite .	256
6-5-3-1: Characterisation of composites components	256
6-5-3-2: Slag.....	257
6-5-3-3: Effect of slag on cemented sand composite.....	260
6-5-3-4: Effect of rubber on alkali-silica reaction in cemented sand composite	262
To sum up briefly.....	266
6-5-4: A physical model of failure in composite.....	268
6-5-4-1: Mechanism of deformation and binary medium theory	268

6-1: INTRODUCTION

Because the amount of scrap tire is rapidly increasing in all around the world as a result of an increase in the number of vehicles, seeking various solutions have been recognised (Neaz Sheikh et al., 2013, Feraldi et al., 2013). The Australian government reported that about 52.5 million EPU (i.e., equivalent passenger unit) scrap tire were generated in 2007-2008, whereas only about 35% of these wastes have been recycled (Neaz Sheikh et al., 2013, Australian Government 2010). If this alarming trend continues, all the lands in Australia will be filled with scrap tires by 2030 (Australian Government 2010).

Preventing this vital issue requires replacing the common methods such as stockpiling with a new and environment-friendly solution. Utilising the waste tire for civil engineering application such as soil stabilisation, soil reinforcement in road constructions, slope stability, backfilling of retaining wall structures, rubber modified asphalt, and ductile concrete have been recognised as a sustainable way (Neaz Sheikh et al., 2013). Although, concern has been raised regarding the possible risk of using pure rubber to develop an exothermic reaction (Neaz Sheikh et al., 2013, Humphrey, 1996, Gacke et al., 1997). However, the researches performed on the sand-tire mixtures have not reported any exothermic reaction (Neaz Sheikh et al., 2013, Zornberg et al., 2004). Hence, the application of rubber material in civil engineering has been investigated from a variety of viewpoints including flexibility, strength, resilience, friction resistance for more than two decades (Neaz Sheikh et al., 2013). The results suggested that, the geotechnical properties of sand-rubber mixtures can be improved by modifying some effective parameters such as ingredient ratio, considering the rubber particle size ratio to the sand, and adding cementitious materials like cement, slag to increase the bonding connection (Zhang et al., 2016, Kaniraj and Havanagi, 2001, Lee et al., 2007, Lee et al., 2010, Guleria and Dutta, 2011, Lee et al., 2014). For example, the particle size has been recognised as effective parameters on the rubber-

sand mixture in the performed research by Youwai and Bergado, (2003). They reported that the notable effect obtained when the particle size ratio of rubber to sand was limited to less than 6. It can be considered as the ratio of flexible to rigid particles, suggesting the microstructure behaviour affected by the connection behaviour among the particles. Several studies have been performed to investigate the ratio of rubber to sand, using different methods (Neaz Sheikh et al., 2013, Ahmed and Lovell, 1993, Youwai and Bergado, 2003, Zornberg et al., 2004, Rao and Dutta, 2006, Edil and Bosscher, 1994, Foose et al., 1996, Masad et al., 1996, Bosscher et al., 1997, Tatlisoz et al., 1998, Ghazavi and Sakhi, 2005, Lee et al., 2007, Kim and Santamarina, 2008, Lee et al., 2010). With the similar content, a few other related parameters including aspect ratio, and unit weight of the mixture, have also been explored (Neaz Sheikh et al., 2013, Edil and Bosscher, 1994, Foose et al., 1996, Bosscher et al., 1997, Tatlisoz et al., 1998, Edil and Bosscher, 1994, Foose et al., 1996, Bosscher et al., 1997, Zornberg et al., 2004, Ghazavi and Sakhi, 2005, Zornberg et al. 2004, Rao and Dutta 2006).

Moreover, a considerable number of scholars have been investigating the shear strength and compression strength properties of rubber only or sand-rubber mixtures (Zhang et al., 2016, Fattuhi and Clark, 1996, Foose et al., 1996, Wu et al., 1997, Son et al., 2011). These research have reported that a combination of sand, rubber, and stabilisers considering the particle size and types of rubber can significantly affect the strength properties of sand. The researches also have taken into account the effect of confining pressure in triaxial tests (Neaz Sheikh et al., 2013, Ahmed and Lovell, 1993, Masad et al., 1996, Youwai and Bergado, 2003, Zornberg et al. 2004, Rao and Dutta, 2006).

Therefore, based on the aim of this chapter the previous researches have been reviewed into the three main parts.

SHEAR BEHAVIOUR

The first study on the behaviour of sand-rubber chips was conducted by Ahmed, (1993). The triaxial test with several confining pressures studied the effect of soil type, sample preparation, and the size and ratio of tire chips (i.e., 12.5mm to 50mm). The maximum shear strength has been achieved through the combination of 39% of rubber chips with sand. The compaction effort and size of tire had an insignificant effect on the composites behaviour. While, the confining pressure, and gravimetric ratio were found the most effective parameters.

In (1998), Tatlisoz et al. reported that adding 30% by volume of tire chips to the sandy silt help in obtaining the greatest improvement in shear strength properties. The results suggested the similar interlocking among the sandy sit and chips particles with fiber reinforcement, led to an increase in the cohesion of soil.

The rectangular-shaped tire chips with the specified dimension in a various thickness of tire chips were used by Zornberg et al. (2004) and Rao and Dutta, (2006). A similar procedure analysed the shear strength behaviour of sand mixtures in both the studies. The maximum achievements in shear strength obtained by two different percentage of rubber were reported to be 35% and 20% respectively. However, the highest results were observed at the lowest confining pressure.

However, the experimental investigation on the granulated rubber reported the inefficiency of tire crumb to increase the shear strength of soil Masad et al., (1996). The result of performing the triaxial test by confining pressures from 15Kpa to 350Kpa on the composites with an equivalent portion of rubber and sand did not lead to any improvement. A similar trend was observed in 2003 by ouwai and Bergado. The result reported the reduction of shear strength by increasing the dosage of rubber crumbs, which suggested the incapability of rubber crumbs for sand stabilising, the same as sand reinforcement Foose et al.(1996) by random fiber.

STRAIN BEHAVIOUR

Regarding the resilient characteristic of rubber material, it can be expected that treating the sand with the tire rubber could increase the strain capacity of the sand-rubber mixture. Although the shear failure in the sand had occurred within the larger strain due to the rubber application, a few studies have been specifically reported the axial capacity of soil-rubber mixtures. For example, reviewing the earlier researches carried out by Edil and Bosscher (1994) and Foose et al., (1996) revealed that the failure point was not defined explicitly. Moreover, experimenting with the 60mm horizontal displacement did not lead to detect the clear peak strength (Tatlisoz et al., 1998). However, in (1996), Masad et al., had reported that the peak deviator strength of sand increased from 2%-4% to 10%-22% by rubber addition. Once more, the peak strength was not clearly observed as the peak strength of pure sand (Zornberg et al., 2004, Rao and Dutta, 2006). However, the results of Youwai and Bergado (2003) study reported that a well-defined peak strength performed the gravimetric ratio of tire less than 30%. It was also suggested that the axial strain at the peak value mutually increased with the rubber addition.

COMPRESSIBILITY BEHAVIOUR

Generating an accurate estimation of the compressibility characteristics of the sand-rubber composite is very critical and important for designing the geotechnical constructions considering the stability of structures. Consideration has been realised due to the high compressibility capacity of scrap tire, which affected by the design of permanent constructions. However, research has been conducted to study the application of rubber material in transportation area (Zhang et al., 2016, Youwai and Bergado, 2003, Edinçliler et al., 2004, Kim and Santamarina, 2008). Overall, the carried out research presented that the sand's compressibility was lower than the compressibility of rubber. Therefore, the mixture's compressibility can be conducted by the dosage of rubber material.

The compression behaviour of sand-tire mixtures has been studied by performing a series of loading and unloading cycles test in (1993) by Ahmed and Lovell. Based on the results found, the chip's content played a pivotal role showing the compressibility of specimens. Moreover, the compaction efforts, sample preparation and the size of rubber chips were studied. Nevertheless, the effect of compaction efforts on the load-deformation reaction of the sand-chips samples was found insignificant.

Investigation of the soil-rubber mixture under the application of cycles load have also been conducted by Edil and Bosscher, (1994), and Humphrey et al. (1998). Their founding reported that the porosity of composite was increased by tire addition, and it can be significantly related to the initial plastic deformation. Subsequently, with the higher initial porosity, the sample behaved a greater initial compression under the vertical stress. The composite with the lower initial porosity also revealed an unrecoverable strain behaviour under the first applied load, and alternatively, an elastic behaviour under the application of further loads.

Moreover, a comparative study of the smaller chips and larger shreds have revealed a similar result Bosscher et al., (1997). It is worth mentioning that, utilising a combination of soil and scrap tire as a cost-effective seismic isolation have been studied by few scholars (Tsang 2009; Tsang et al., 2012). The results indicated that the successfulness of this method was connected to the geotechnical characteristics of the soil-rubber specimens.

Taking into account that only a few types of researches have studied the compression behaviour of the sand-rubber mixture in detail, in this chapter the compressibility of sand, sand-rubber, and a combination of stabiliser with the sand-rubber have been experimentally investigated. In the next step, the strain capacity and shear behaviour of the composite will be analysed to study the shear strength characteristic of composites.

The typical failure modes – rupture, bulging or shear band – will also be analysed, to approximate the progressive failure of the material. Furthermore, to generate an accurate study, the results of small direct shear, large direct shear are compared with the triaxial test. Eventually, the experimental data of small direct shear, and large direct shear and triaxial are conducted to develop an empirical equation which is capable of predicting the shear intrinsic constants of sand composites.

6-2: MATERIAL AND EXPERIMENTAL METHODOLOGY

Fifteen mixtures including sand, sand rubber, sand stabilisers and sand-rubber-stabilisers composites were separated into three main groups. To prepare the sand-rubber composites, the oven dried sand with the different ratio of well dried rubber was mixed. The gravimetric basis used for the rubber fractions (RF), were performed as 0%, 10%, and 20% (rubber) for the mixtures with and without the cementitious materials. The percentage of cement and slag utilised in the experiment study was 5% and 10%. Thus, the designation of ST, SR and STR represent a group of mixtures containing stabilisers only, rubber only and both stabilisers and rubber respectively. To generate the homogenous composite the materials were mixed by de-aired water in the steel container and cured for 30 minutes in the plastic bags. Eventually, the initial weight of composite was calculated based on the MDD and OMC results and was compacted within the device mold respectively.

The one-dimensional consolidation test was applied to determine the compressibility characteristics of sand composites according to (ASTMD2435, 2011). The sample preparation has been carried out using the data of compaction test for each composite. Compaction was performed in the three layers of equal thickness by tamping each layer inside the consolidation ring to reach the desired density. The initial diameter and initial height of composite were 63.5 mm and 25.34 mm respectively.

The composites were all subjected to cumulative vertical effective stress with the ratio of 2 for loading phase initialising with 25kPa. Completing the last loading step conducted 1600kPa vertical stress, subsequently, reducing the normal stress was started with the ratio of 1/4 for the unloading stage. The duration time for loading and unloading stages were considered 1 and 3 hours respectively. This hours obtained by performing a series of trial tests on the prototype specimens to obtain an estimation for the duration of load maintenance in each stage. The utilised consolidation device was approximately estimated the minimum time for each step after calculating the T50 mean of samples.

Triaxial compression tests were performed on the pure sand, sand-rubber and sand-rubber cement treated composites. Material were mixed manually, making a homogeneous combination. The shear strength and compression characteristics of composites were examined by LoadTrac II triaxial compression test apparatus. The consolidated-undrained triaxial (CU) test method were performed under total saturation at effective confining pressure of 50, 100, 250 and 500 kPa according to (ASTMD4767, 2011). Back pressure of up to 1000KN/m² ensured *B* values of at 0.95. The specimens (with 63 mm diameter and 130 mm height) of sand mixtures were prepared in split mold, marked with a latex membrane, and gently compacted in five layers to reach the essential maximum dry density determined by standard compaction test.

The main properties of all the sand and sand-rubber mixture are summarised in and show the specific gravity for each composite and the sieve analysis of the sand, rubber and sand-rubber particles Table6- 1.

Table6- 1. Material properties. C_u : Coefficient of Uniformity, G_s : Specific gravity, ρ_{min} : minimum density, ρ_{max} : maximum density

Soil	$D_{60}(\text{mm})$	$D_{10}(\text{mm})$	C_u	G_s	ρ_{min}	ρ_{max}
Sand	0.18	0.45	2.5	2.65	1.53	1.82
Rubber	2.0	1.5	1.3	1.01	0.43	0.50
SC0R10	0.3	0.4	0.6	2.17	1.4	1.68
SC0R20	0.3	0.4	0.6	2.00	1.21	1.5

The material/chemical characterisation and mineralogical and elemental investigations on the specimens were performed using energy dispersive X-ray spectroscopy (EDS) and scanning electron microscopy (SEM). The microstructural and morphological analyses of the platinum-coated specimens were carried out using a Zeiss Evo 40XVP scanning electron microscope (SEM). The SiLi X-ray detector Energy-dispersive X-ray (EDS) with an ultrathin window and Oxford Inca software were used to analyse the elemental and chemical conformations of composites.

6-3: RESULT AND DISCUSSION

6-3-1: ONE-DIMENSIONAL CONSOLIDATION TEST

The compression behaviour of composites has been investigating by performing the one-dimensional consolidation test. The results were precisely analysed defining the compression index C_c , swell index C_s , the coefficient of volume compressibility m_v , one-dimensional elastic modulus E'_{oed} , vertical strain ϵ , normalised vertical strain and residual deformation ϵ_r .

6-3-1-1 COMPRESSION AND RECOMPRESSION INDICES

One-dimensional tests have been performed on treated and untreated sand composites to study the compressibility and plastic characteristics. The mixtures were

firstly loaded from 25 kPa to 1600 kPa and eventually unloaded to the first applied load. Figure6- 1 presents the typical results obtained from the consolidation tests conducted on the pure sand, and sand reinforced mixtures. The presentive composites have been selected for investigating the effect of both rubber and stabilisers on compression behaviour of sand. This results also are compared by using cement and slag as two different kinds of stabilisers. From the results can be clearly observed that performing 10% of either cement or slag for sand reinforcement, was reduced the sand's compressibility. The initial void ratio of sand was reduced to 0.42 and 0.4 by using cement and slag respectively, which was suggested that slag is more effective than cement for decreasing the compression behaviour.

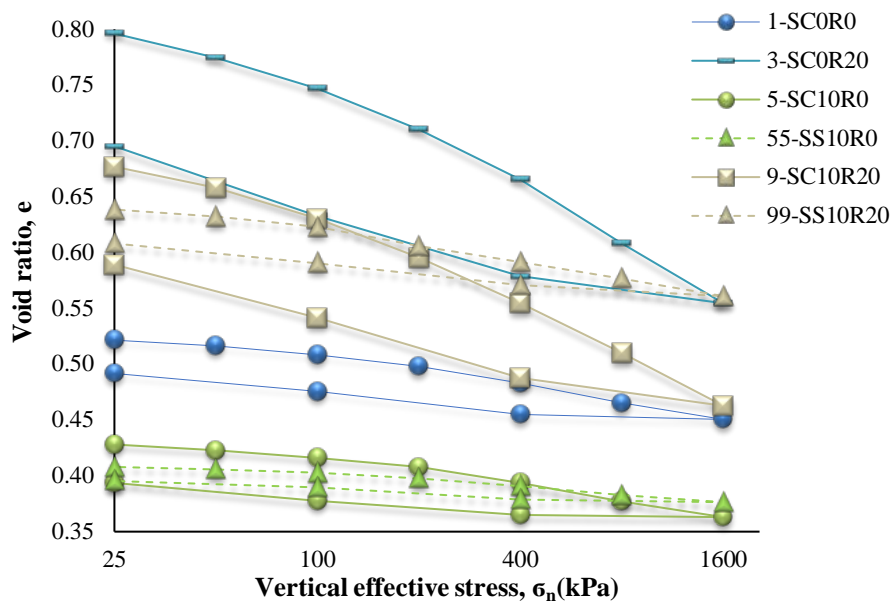


Figure6- 1. Vertical effective stress against void ratio for loading and unloading stages for pure sand and stabilised sand composites.

However, the addition of rubber into the sand composite has significantly affected on the compression behaviour of mixtures. The initial void ratio of sand was increased from 0.55 to about 0.80 by mixing with 20% rubber. It is evident from the result that, the compressibility characteristic of sand is increased by the application of the compressible material. Although this behaviour was just slightly minimised by

addition 10% of stabilisers, the existence of 20% rubber resulted in increasing the compressibility ability of the pure sand. One more time, to modify the compressibility potential of the composite, the addition of slag was found more effective than cement.

It is worth mentioning that, the results also suggested the effectiveness of rubber on the compression behaviour of sand mixtures. Considering the different components of the composites, it can be hypothesised that it can be found a relationship between the compressibility and density of soil. Subsequently, the composites were categorised into three main groups with respect to their maximum dry densities (MDD). The MDD of the composites was strongly related to the proportion of rubber added to generate the composite structure. Subsequently, ST, STR10 and STR20 were considered specimens with a dense, medium and loose structure, respectively. A combination of the maximum rubber ratio and the minimum stabiliser ratio led to the formation of the loosest composite (i.e., SC0R20: 13.998 kN/m³). In contrast, the composite with the maximum density contained the maximum content of stabilisers as the finer material, with 0% rubber inclusion (i.e., 18.453 kN/m³). Therefore, based on the rubber ratio, the material categories were defined as described in Table6- 2. Note that the separation was relatively defined on the basis of the composites investigated in this research.

Table6- 2. Definition of the three categories of composites divided by their maximum dry density.

Soil structure	Category	MDD (kN/m³)
Loose	STR20	13.98–15.62
Material with 20% rubber, and its combination with cement or slag.	SC0R20, SC5R20, SS5R20, SC10R20,	
Medium	STR10	15.82–16.79
Material with 10% rubber, and its combination with cement or slag.	SC0R10, SC5R10, SS5R10, SC10R10,	
Dense	ST	17.04–18.45
Material with 0% rubber, and its combination with cement or slag.	SC0R0, SC5R0, SS5R0, SC10R0,	

In addition, the compression index (C_c) of composite has been defined by calculating the gradient of the composite's curved during the loading phase. Eventually, the compression index was plotting versus maximum dry density of composite. Thus, Figure6- 2 is presented a correlation between C_c and MDD of sand mixtures, verifying the suggested hypothesis. The finding correlation has shown a good agreement (i.e., $R^2=90$) with the experimental results. It is evident from Figure6- 2 and Table6- 1 that the composites with the lower density has obtained, the lower compressibility characteristics. Given these facts, the compression properties of sand can be respectively, increased and reduced by the addition of rubber and stabilisers.

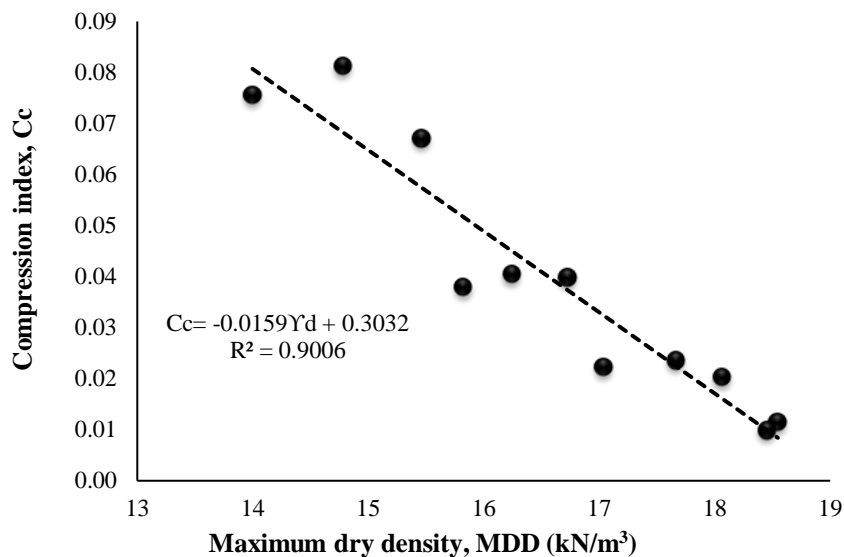


Figure6- 2. Compression index versus maximum dry density of sand mixtures.

Another key thing to deduce from Figure6- 1, is analysing the unloading curves of the composites indicating the swelling potential of specimens. Performing the unloading stage, on the pure sand and treated sand composite suggested the effect of additives on the swelling behaviour of sand. The sand composite containing only 10% stabilisers have obtained the lowest void ratio at the end of unloading phase. Unloading curve of sand tends to become flat as a result of losing its porosity during the loading phase and preventing the swelling of sand. It was happened due to the increment of composite's

uniformity due to escaping the void ratio and increasing the particle connection by the cementitious material. In contrast, the elastic properties of rubber caused to provide the ability for returning to the initial structure in the sand composite. This behaviour is remarkably observed in the unloading curve of composites containing 20% rubber. However, the application of cementitious material lightly minimised the resilient properties of the mixture, especially with the addition of slag. Overall, the application of slag was found more effective than cement to control the compressibility of composites with and without rubber. To create a clear understanding, the swell index C_s of composite has been calculated from the slope the unloading phase.

Figure6- 3 present the swell index results of sand composites with and without additives. It can clearly be seen that increasing the dosage of rubber in sand matrix leads to increase the swell index of the composite, which can verify the resilient properties of rubber to make the compressible composite. However, sand's swelling potential was restricted by adding the cementitious material, notably by slag addition. The effectiveness of slag was repeatedly observed in the mixtures containing the rubber as well. While, utilising a dosage of cement could not minimise the compressibility of rubber particles. It worth mentioning that, the result also suggests the close connection between the swell behaviour and density of mixtures. It can clearly observe from the

Figure6- 3, a denser composite has a lower swelling index, which can be suggested the uniform structure of composite matrix, with the minimum porosity.

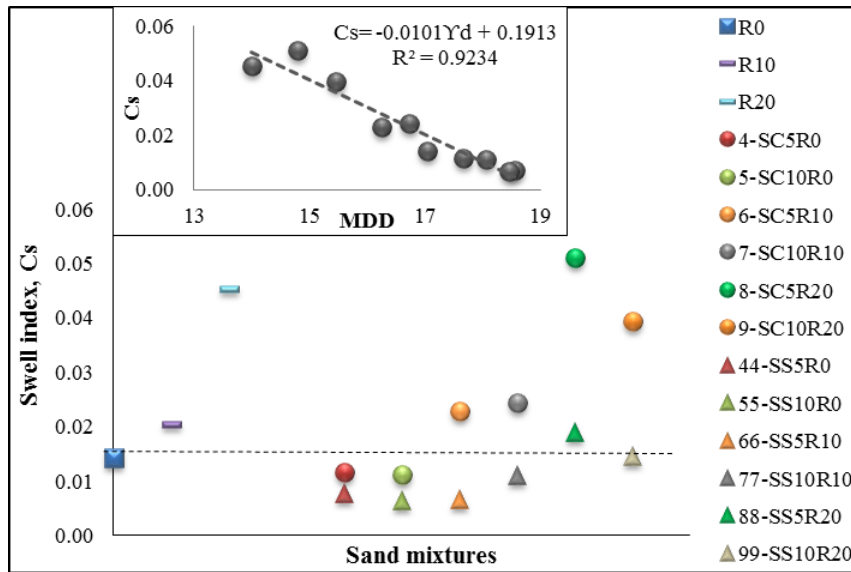


Figure6- 3. Swell index versus the amount of untreated and treated sand composites.

To draw a conclusion of one-dimensional consolidation test, the obtained results of compression index, swell index and initial settlement are presented in Table6- 3. Summary of consolidation tests results performed on the untreated and treated sand composites.. The available pore in the sand composites was undergone the consolidation tests filed by water caused to deform the soil skeleton. Investigating the initial deformation of composites can provide a comprehensive estimation of the composite structures. It will be expected, if the composite with the higher density has shown, the greater primary settlement, associating with the above findings. Subsequently, the composite containing 20% rubber have revealed the highest amount of initial deformation. Another time the effectiveness of slag for limiting the sand deformation has been observed analysing the initial settlement results Table6- 3. Summary of consolidation tests results performed on the untreated and treated sand composites.

Table6- 3. Summary of consolidation tests results performed on the untreated and treated sand composites.

SAMPLE	Cc	Cs	Sc
1-SC0R0	0.022	0.014	0.139
2-SC0R10	0.038	0.021	0.313
3-SC0R20	0.076	0.045	0.791
4-SC5R0	0.023	0.012	0.289
5-SC10R0	0.020	0.011	0.246
6-SC5R10	0.040	0.023	0.531
7-SC10R10	0.040	0.024	0.602
8-SC5R20	0.081	0.051	0.801
9-SC10R20	0.067	0.039	0.962
44-SS5R0	0.011	0.008	0.154
55-SS10R0	0.010	0.006	0.063
66-SS5R10	0.014	0.007	0.109
77-SS10R10	0.017	0.011	0.143
88-SS5R20	0.031	0.019	0.320
99-SS10R20	0.024	0.015	0.334

6-3-1-2 ONE-DIMENSIONAL ELASTIC MODULUS

The compression behaviour of composites can be analysed from a different concept, which is related to investigate the volume change of soil matrix. Measuring the gradient of curve line defining the variation of vertical strain between applied normal stresses is clearly demonstrated the deformation of composites. Consequently, the coefficient of volume compressibility (m_v) is performed to calculate the deformation change of composite during the loading phase:

$$m_v = \frac{\varepsilon_2 - \varepsilon_1}{\sigma_2 - \sigma_1} \quad (6.1)$$

where ε and σ are defined the strain and stress during the consolidation test. Figure6- 4 present the coefficient of volume compressibility of untreated sand and treated sand composite. It can clearly be seen that, the application of cement for reducing the compression behaviour of sand was slightly effective. However, this

effectiveness was not strong enough to reduce the ductile properties of rubber. For example, m_v result of sand-rubber with and without cement addition was not really different. Therefore, the coefficient of volume compressibility was divided into three identical curves, remarkably affecting by the rubber content. It might be suggested that, the composite plastic deformation are related with its density. It should be noted that, the coefficient of recompressibility can also be calculated from the unloading phase of consolidation test, which is not focused in this chapter.

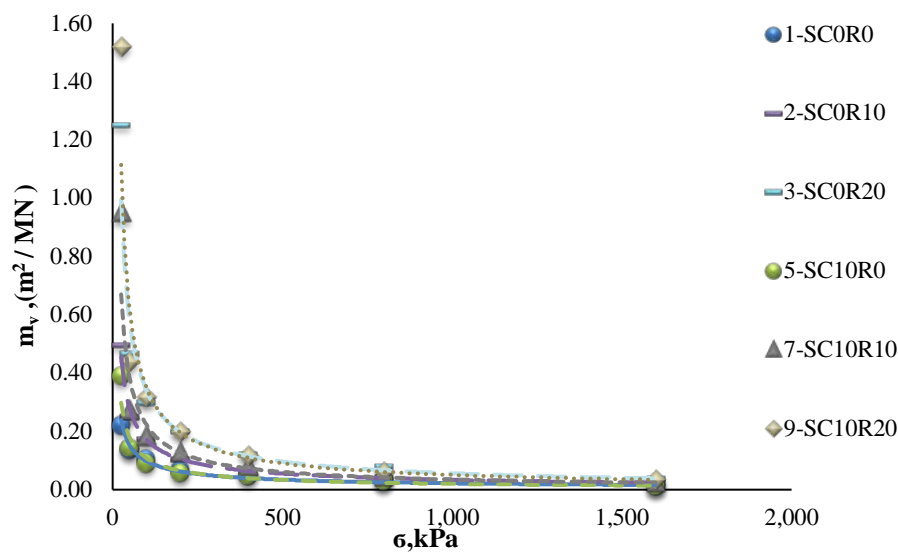


Figure6- 4. Coefficient of volume compressibility of sand composites for loading phase of consolidation test.

Based on the Hooke's law, the importance of a study on the coefficient of volume compressibility can be recognised (Knappett and Craig, 2012).

$$E'_{\text{oed}} = \frac{\Delta\sigma}{\Delta\varepsilon} = \frac{E(1 - \nu)}{(1 + \nu)(1 - 2\nu)} \quad (6.2)$$

where ν and E are define the Young's modulus based on the normal stress and Poisson's ratio respectively.

Thus, the equation can be rewritten as a new form:

$$E'_{\text{oed}} = \frac{1}{m_v} \tag{6.3}$$

Hereinafter, E'_{oed} is defined as the one-dimensional elastic modulus, having the units of stiffness, MPa. Figure6- 5 presents the one-dimensional elastic modulus for pure sand and treated sand. At first glance, composite with the no rubber particles have the greatest value, which is suggested the lowest deformation among the other composite. However, the loosest composite have shown the lowest elastic modulus, containing either 10% or 20% rubber. Consequently, the mixtures with 20% rubber have notably indicate the higher deformation than composites including 10% rubber.

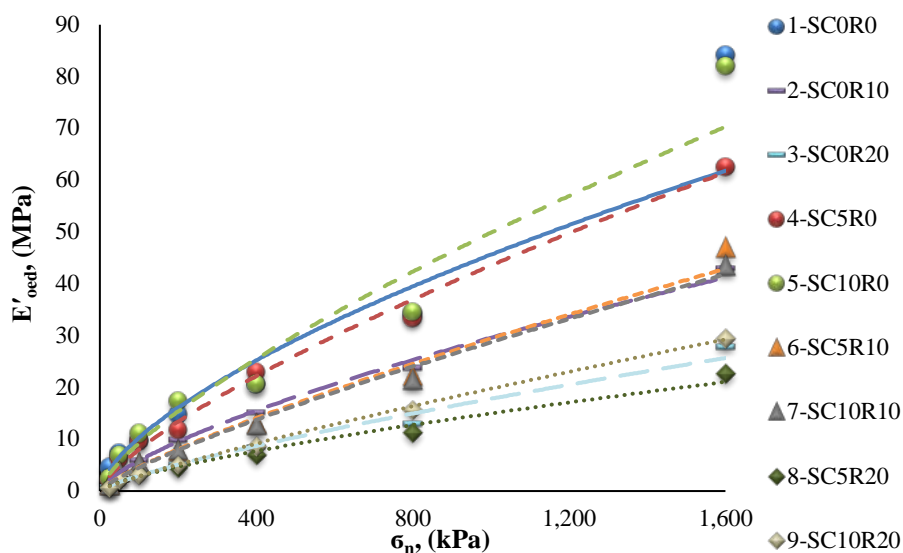


Figure6- 5. One-dimensional elastic modulus of treated and untreated sand composites.

Another way to look at the elastic modulus behaviour of the composite is investigating the effect of applied vertical stress on the mixture's elasticity. It is evident from the Figure6- 5 that, the difference among E'_{oed} of sand mixtures are mutually raised by increasing the normal stress value. It seems that, conducting test with the

higher loads particularly revealed the properties of sand matrixes Table6- 4 presents a summary of the obtained correlations for m_v and E'_{oed} from the one-dimensional tests.

Table6- 4. Summary of the coefficient of volume compressibility and the one-dimensional elastic modulus of the composite obtained from the consolidation tests.

SAMPLE	m_v (m²/MN)	E'_{oed}
1-SC0R0	$m_v = 1.91\sigma^{-0.647}$ $R^2 = 0.97$	$E'_{\text{oed}} = 0.52\sigma^{0.647}$ $R^2 = 0.97$
2-SC0R10	$m_v = 4.38\sigma^{-0.704}$ $R^2 = 0.99$	$E'_{\text{oed}} = 0.23\sigma^{0.704}$ $R^2 = 0.99$
3-SC0R20	$m_v = 12.25\sigma^{-0.78}$ $R^2 = 0.98$	$E'_{\text{oed}} = 0.08\sigma^{0.78}$ $R^2 = 0.98$
4-SC5R0	$m_v = 3.67\sigma^{-0.735}$ $R^2 = 0.97$	$E'_{\text{oed}} = 0.27\sigma^{0.735}$ $R^2 = 0.97$
5-SC10R0	$m_v = 3.14\sigma^{-0.732}$ $R^2 = 0.96$	$E'_{\text{oed}} = 0.32\sigma^{0.732}$ $R^2 = 0.96$
6-SC5R10	$m_v = 8.74\sigma^{-0.803}$ $R^2 = 0.98$	$E'_{\text{oed}} = 0.11\sigma^{0.803}$ $R^2 = 0.98$
7-SC10R10	$m_v = 8.84\sigma^{-0.801}$ $R^2 = 0.97$	$E'_{\text{oed}} = 0.11\sigma^{0.801}$ $R^2 = 0.97$
8-SC5R20	$m_v = 9.94\sigma^{-0.724}$ $R^2 = 0.97$	$E'_{\text{oed}} = 0.10\sigma^{0.724}$ $R^2 = 0.97$
9-SC10R20	$m_v = 16.54\sigma^{-0.838}$ $R^2 = 0.97$	$E'_{\text{oed}} = 0.06\sigma^{0.838}$ $R^2 = 0.97$

All things considered, the composite's elastic modulus can be divided into the three main categories, affecting by the rubber fraction. Three rubber fractions were defined based on the %0, %10 and 20% rubber content for both cemented and uncemented composites.

Consequently, a persuasive correlation can be defined as the one-dimensional elastic modulus of composites. All the suggested correlation have shown a great agreement with the experimental results (i.e., R^2 was more than 0.95) Figure6- 6.

Considering the density condition, the presented correlation might also be useful for the composite with the different soil and similar MDD. The result also indicated that, increasing the rubber fraction, caused by increasing the domination of rubber particle to present the elastic behaviour of the composite. The cement efficiency on the elastic behaviour was reduced, obtaining almost the same result with and without cement addition.

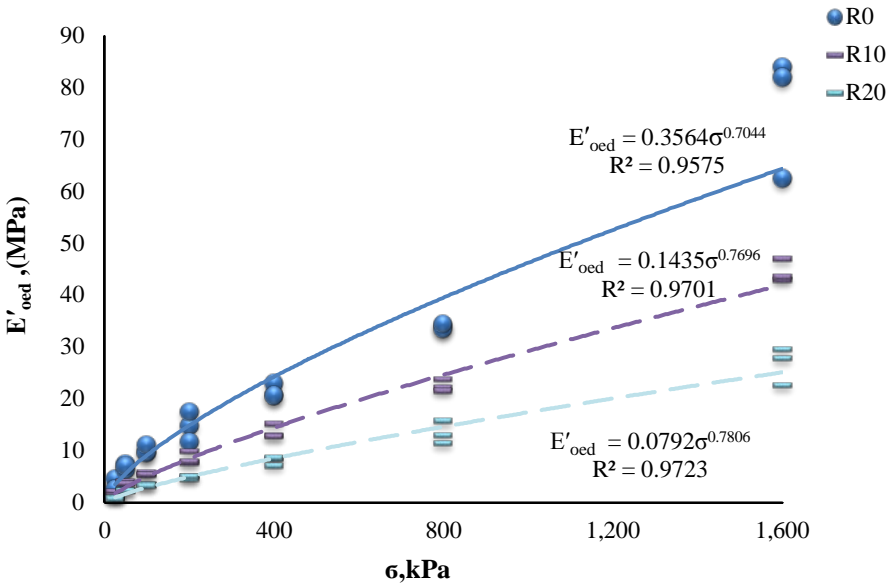


Figure6- 6. One-dimensional elastic modulus correlation ,deduced for sand composites with different RF.

Eventually, the experimental results of composite’s elastic modulus can be compared with the elasticity of granular soils reported by researchesTable6- 5. The comparison revealed that increasing the rubber content in composites can be generated the sand matrix with the structure similar to the medium sand.

Table6- 5. Modulus of elasticity for granular soils(Das, 2013).

Type of soil	E (MPa)
Loose sand	10.35–24.15
Silty sand	10.35–17.25
Medium-dense sand	17.25–27.60
Dense sand	34.5–55.2
Sand and gravel	69.0–172.5

Therefore, the application of rubber in sand reinforcement was remarkably changed the mechanical response of sand matrix. This transform was happened due to the generation a composite with the lower specific gravity, density, and stiffness and simultaneously, the higher capacity for damping and compressibility. Thus, a composite containing both the rigid and flexible elements are capable of controlling the bulking and also tolerate the load.

6-3-1-3 CLASSIFICATION THE COMPRESSION EVOLUTION OF COMPOSITES

Figure6- 7 illustrates the compression curves of sand composites with and without the cement addition. The application of 10% cement on the compressibility of sand composites with RF=0 and RF=20% were investigated. It is evident from the results that, the composite containing 20% rubber have shown a higher vertical strain. The results suggested the consequence of rubber addition where caused to increase in compressibility of sand by introducing the ductility properties. This behaviour did not significantly change event after utilising the 10% cement. Moreover, a closer look at the data indicates that, for a given vertical stress, a vertical strain lightly increased by the addition of 10% cement into the mixtures. The residual strain observation also indicated the similar behaviour, where the cemented sands have reached to the similar vertical strain as its uncemented composites. Analysing the compression behaviour of composites can be suggested the separation of this progression into the three main

states (Zhang et al., 2016). Analysing Figure6- 7 shows that the vertical strain tendency of composites versus the effective vertical stress were linearly behaved passing its identical effective stress. Identifying the points where the vertical strain has shown a curve with a new gradient can be revealed the mechanism of inter-particles in the soil. Consequently, the particle forces can be classified into particle level force, contact level force and the force generated by applied boundary stresses. Investigation the contact level force, where are mostly affected by the available cementitious agents in the mixtures can be persuasively explained the reason for composite behaviour as is shown in Figure6- 7.

The cementation is normally affected by the dosage and kinds of cementitious material, grain size distribution of composites, density and the confining pressure during the cementation hardening (Lee et al., 2010). Subsequently, the granular materials can be affected by cementation caused to increase the particle to particle connection. Therefore, the cemented material might be divided into the three main areas based on the elastic behaviour. The cemented material tends to behave like a composite material in the condition of low stress level. Bonding control as a first stage is defined at the low level of stress, where the strength and stiffness of soil are significantly affected by cementation. The area, where the cemented combination was suffered the load higher than the bonding force caused to generate the second area, which known as bonding degradation. The third region is defined by finishing the bond degradation, where soil structure is controlled with the applied stress, and the bonded soils tend to behave as a particulate material, is stress control region. It should be noted that, based on the kind and dosage of cementitious material, the transition stress from the bonding degradation to stress control would be taken. Thus, the reason of great stiffness of the cemented material, even after the failure might be explained by bonding degradation, where partially happened after applying the additional stress (Lee et al., 2010). The cementation bond can be ruined at the interatrial connection during the unloading stage of consolidation test, may also be happened due to bonding

degradation, which is normally observed by the expansion of cemented mixtures (Lee et al., 2010).

Figure6- 7can reveal that the bonding control in all three composite was completed at the vertical stress of 25kPa. However, the ratio of vertical deformation was remarkably affected by the rubber fraction, increasing by using more dosage of the compressible material. The contact level force, associating with the cementation was reduced by introducing the rubber material resulted in the higher incremental strain rate.

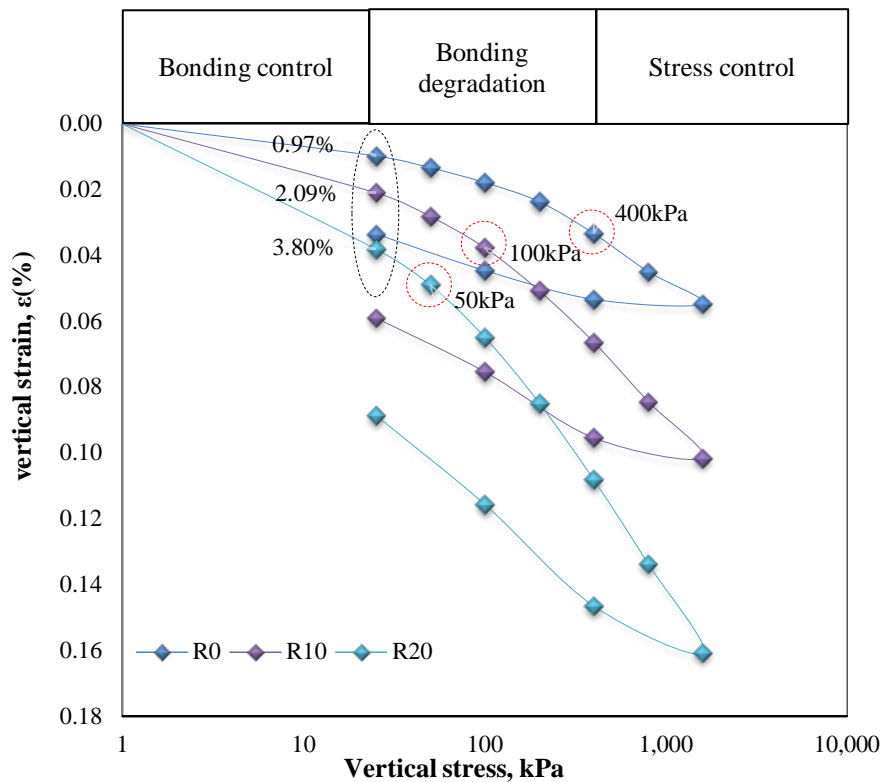


Figure6- 7. Compression curves of the lightly cemented sand composite with the 0%RF, 10% RF and 20% RF.

Moreover, the most significant effect of rubber application was observed by investigating the bonding degradation region of composites. The effectiveness of a

cementitious material to prevent completing the bonding degradation was also reduced by increasing the rubber fraction in sand matrixes. Notably, the stress control was started at the normal stress of 400kPa, was gradually decreased to 100kPa and 50kPa accordingly performing 10% and 20% rubber.

However, inter- particle forces in composite containing 20% rubber were mostly generated by applied boundary stresses for loading phases. It might be concluded that the compression behaviour of the composite with 20% rubber fraction is dominantly influenced by the applied vertical load. Consequently, once the unloading stage was started, the greatest expansion behaviour was observed in composites of this group, eventually showing the highest residual strain.

In order to an additional investigation into the bonding effect on the composites containing the cementitious material, the normalised vertical strain of mixtures have been analysed. Figure6- 8 presents the variation of normalised strain versus of the applied vertical stress specifically are divided into two bonding control and bonding degradation regions. The normalised strain has been calculated through the individual ratio of a vertical strain of cemented to an uncemented mixture of the categories of sand matrixes. Analysing the results suggest that, the mixtures during the bonding control region tend to have a reducing behaviour. It means that the composite was gradually loosed its contact level force and finally were behaved the same as uncemented specimens. Once more time the result suggested that increasing the rubber content resulted in reducing the efficiency of cementitious material to increase the particle to particle contact forces.

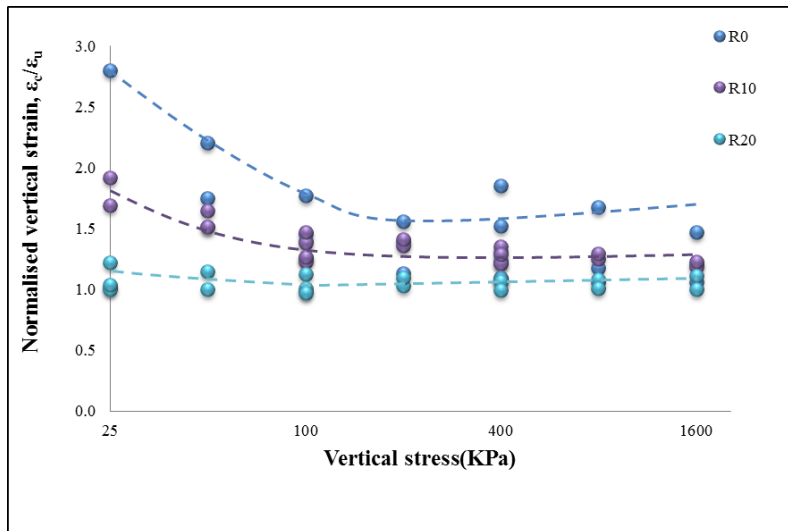


Figure6- 8. The normalised strain of the composites with the 0%RF, 10% RF and 20% RF.

This behaviour notably indicates with the composites containing 20% rubber, were generated the almost similar result with and without cement addition. Therefore, it can be assumed that the only parameter that can be related to the bonding effect on the mixture's particle is the content of the cementitious material.

As a last note, the residual strain of composites was divided based on the rubber participation in mixtures. Figure6- 9 is demonstrated the residual deformation versus the rubber fraction of cemented and uncemented sand mixtures. It can clearly be seen that the residual deformation increases with the increment of rubber fraction. The obtained correlation between residual strains has shown an acceptable agreement with the experimental results (i.e. $R^2=0.93$). Moreover, this suggests that the residual deformation is only connected with the rubber content utilised in the sand matrix, regardless of the dosage of cementitious material.

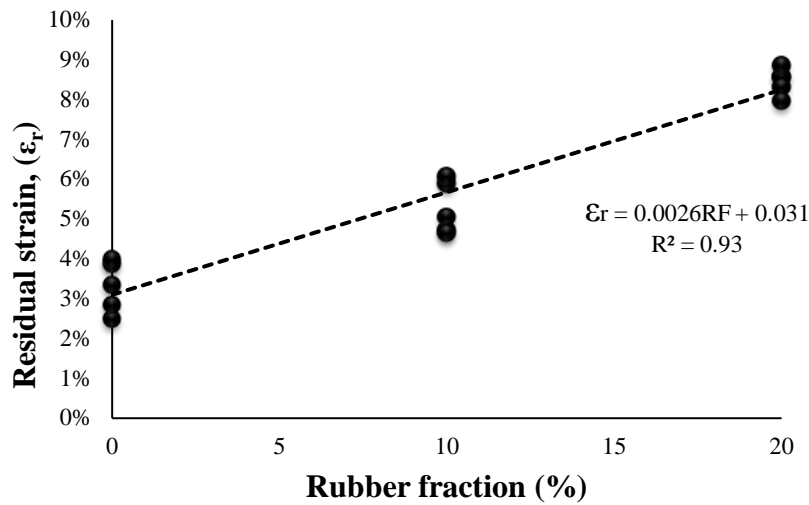


Figure6- 9. The relationship between residual strain and rubber fraction of the cemented and uncemented sand composites.

6-3-2: CONSOLIDATED-UNDRAINED TRIAXIAL TEST

The experimental testing investigation has been conducted to evaluate two critical properties of the sand composite with and without the additives. All the experiments have been performed with no limitation on the vertical movement with the intention of obtaining peak shear strength for the mixtures. The consolidated-undrained triaxial (CU) test method were performed under total saturation at effective confining pressure of 50, 100, 250 and 500 kPa on nine composites including; pure sand and sand-rubber with and without cement.

6-3-3-1 EFFECT OF THE RATIO OF ADDITIVES ON THE DEVIATORIC BEHAVIOUR

The effect of the rubber and cement additives on the deviatoric stress of sand composites conducting a confining pressure of 50kPa is presented by Figure6- 10. It is obvious that the shear strength characteristic of the sand matrix has remarkably changed by the dosage of additives. It is evident that the peak value of deviator stress has been increased with the increase in the dosage of only cement in the specimens.

However, the axial strain corresponding with deviator stress at the failure point remains almost constant with the increase in the cement content. Moreover, the results suggest an increment in the rigidity of sand due to the addition of cement into the sand matrix. The result also suggest that, the deviatoric stress of sand increases with increasing the rubber ratio in the specimens. The addition of the rubber particles in sand mixtures caused to increase the shear resistance of specimens. The failure points of specimens have been enhanced by increasing the rubber content. The stress-strain curves of sand behaved as similar as a ductile composite. It can be suggested that the increase of inter-particle interaction of the sand to rubber in the sand-rubber composites (Neaz Sheikh et al., 2013, Kim and Santamarina, 2008).

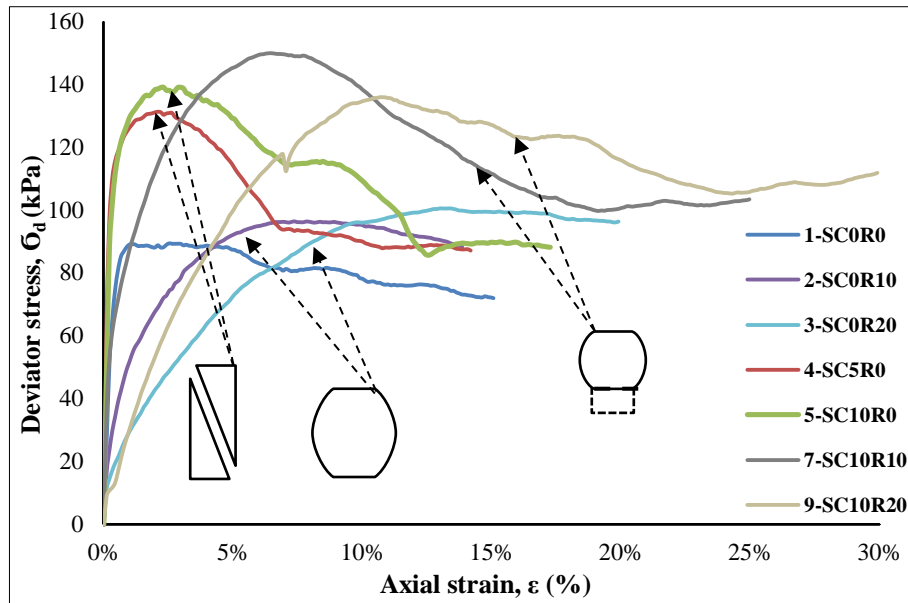


Figure6- 10. Effect of the rubber and cement on the deviatoric stress results of sand composites at the confining pressure 50kPa.

However, the shear strength behaviour of sand-rubber has been altered by adding the cement in the mixtures. The deviator stress has been improved with the addition of a dosage of cement in the sand-rubber mixtures (

). However, the ductility behaviour and strain resistance of composites have been reduced as a result of using the cementitious material in the composite. Reducing the ductility capacity of sand-rubber mixtures has obviously observed by transforming the stress-strain curves from the ductile to brittle with the addition of cement.

To explain the deviatoric stress behaviour of composite another way, the observed failure patterns of sand mixtures present in Figure6- 11. To begin with, sand specimens containing only cement have failed with the localised shear band. This failure mode suggests the brittle behaviour of composites caused to progress the softening behaviour of mixtures after peak strength Figure6- 11(a). The second failure pattern assigned to the sand-rubber mixtures with zero dosage of cement, which is indicated the localised bulging failure mode Figure6- 11(b). Finally, the combination of rubber and cement

for sand treatment reveals the failure mode with a combination of crushing at the lower part and localised bulging Figure6- 11(c). This kind of failure suggests the strong hardening due to the application of the mixture of both rubber and cement, where remarkably observed at the higher confining pressure.

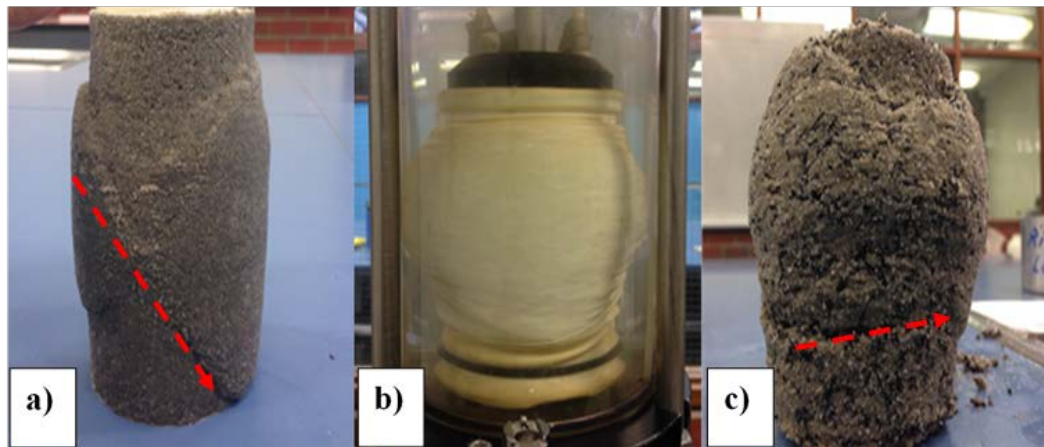


Figure6- 11. Failure patterns of sand composites; (a) shear banding, (b) and(c) bulging failure.

Analysing the different types of failure modes have suggested that the band formation and failure mode mostly connected with the parameters such as confining pressure, density of sample, physical shape and size of particle, and the porosity of soil skeleton (Chabannes et al., 2017, Ma et al., 2016, Kumruzzaman and Yin, 2012). Referring to the maximum dry density of composite (i.e. it was defined with the standard compaction test) the observed kinds of failure is reasonable Figure6- 11. For that reason a composite with the lower density normally shows a bulging failure. Increasing the composite density, caused to transform the failure mode to crushing kind, shows a typical failure type of brittle mixtures. However, in all types of composites the failure occurs at the lower half of specimens. Due to the fact that, the micro-cracks are started in the weaker part of samples. Owing to the higher density and lower porosity, more uniform structure and more similarity in particle shapes of cemented sand composite failure patterns is a shear banding Figure6- 11(a). However, due to inherent of rubber particles, increasing in density and reducing the composite

uniformity caused to change the failure mode to bulging failure Figure6- 11(b). Eventually, a composite with the combination of cementitious and ductile constitutes may be simultaneously revealed the bulging and shear banding failure Figure6- 11(c). In this case, because of the edge effect generated by alumina cement, the bulging may occur in the weaker part of composite Figure6- 11(c).

The effect of rubber and cement on the shear strength behaviour of sand are separately investigated for peak deviatoric stress and the associating axial strain at the variation of confining pressures. Figure6- 12 presents the effect of rubber content on the peak deviatoric stress of the cemented and uncemented sand composites at confining pressures of 50kPa, 250kPa and 500kPa. At first glance, the composite with 10% of cement has revealed the greatest peak deviator stress at each confining pressure.

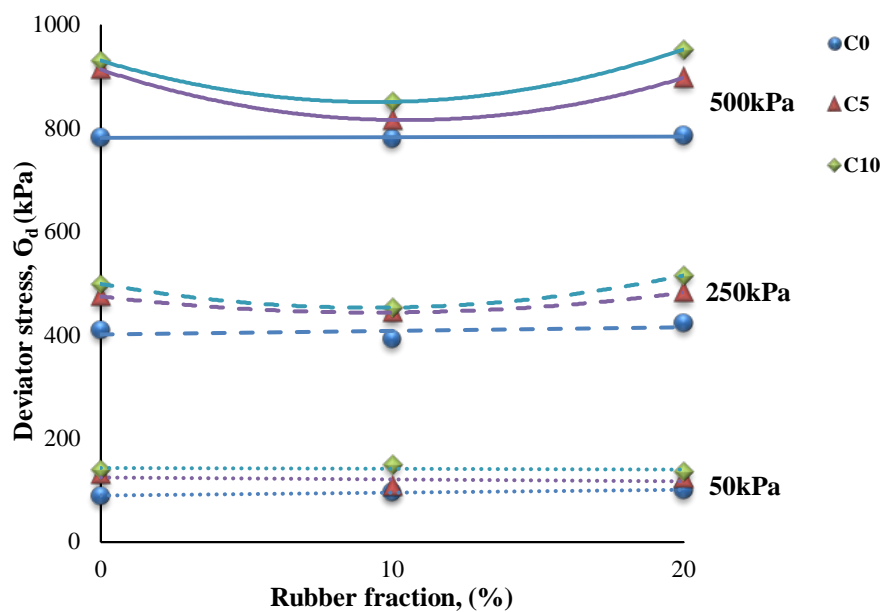


Figure6- 12. Effect of the rubber and cement addition on the peak deviator stress of sand mixtures.

It is evident that the shear strength capacity of composites is mutually increased with the increase in the dosage of cement in the specimens. Moreover, at all confining

pressures, the peak deviator stress was improved by increasing the rubber content. Although the peak deviator stress of sand was slightly reduced with using 10% rubber, this behaviour has been modified by the addition of a dosage of cement to the mixtures. It is worth mentioning that, performing the triaxial test with a higher confining pressure caused to reduce the effectiveness of the dosage of rubber on the peak deviatoric stress in sand-rubber mixtures.

Figure6- 13 presents the effect of the rubber content on the axial strain of sand composites with and without cement addition corresponding with the peak deviator stress at 50kPa and 500kPa confining pressures. At all confining pressures, the axial strain corresponding with the peak deviatoric stress was increased by the increasing dosage of rubber in sand mixtures. Moreover, it can clearly be seen that the axial strain behaviour is affected by the confining pressure. The axial strain corresponding to peak shear stress demonstrates a liner trend at confining pressure 50kPa. However, this behaviour has been altered to a polynomial curve by performing the test with the higher amount of confining pressures.

It seems that, estimating the optimum dosage of additives is required for generating the composite with the optimum shear resistance capacity. The result also suggests that the effectiveness of cement is minimised by increasing the rubber content. In other words, the compressive shear strain capacity of the composite is dominantly related with the rubber content. Consequently, the axial strain increment is associated with the ductility characteristics of the composite. The ductility behaviour of composites needs to be critically analysed for utilising composites for seismic isolation application (Neaz Sheikh et al., 2013, Tsang et al., 2009 and 2012).

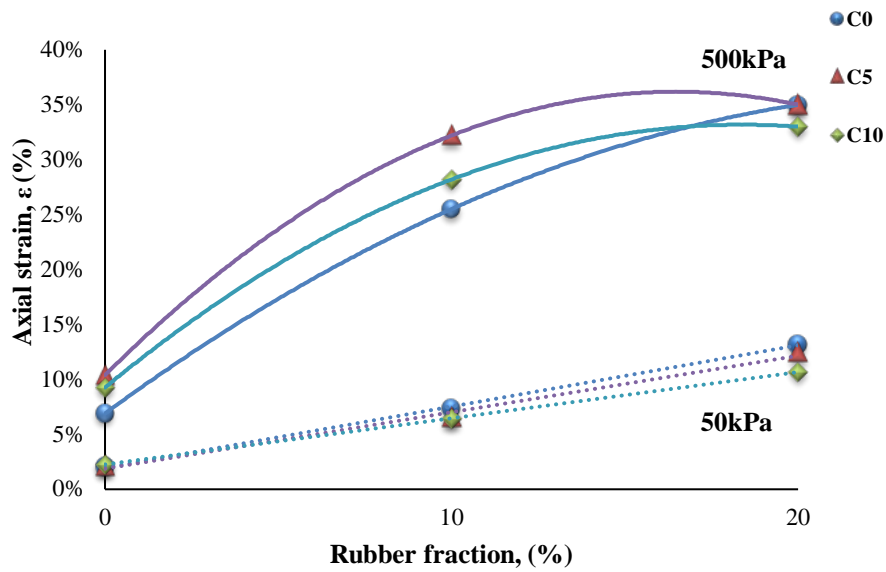


Figure6- 13. Effect of rubber content on the cemented and uncemented sand mixtures strain failure.

6-3-3-2 EFFECT OF THE CONFINING PRESSURE

Figure6- 14, presents the shear strength behaviour of cemented sand composites containing 10% and 20% rubber. The effect of confining pressure studied by investigating deviator stress versus axial strain of the lightly cemented sand-rubber mixtures at confining pressures 50kPa, 250kPa and 500kPa. First and foremost, it can obviously be seen that the confining pressure serves a pivotal role in the behaviour of the lightly cemented sand-rubber composite. The peak deviatoric stress, axial strain at the failure point and stiffness are increased with the increase in confining pressure.

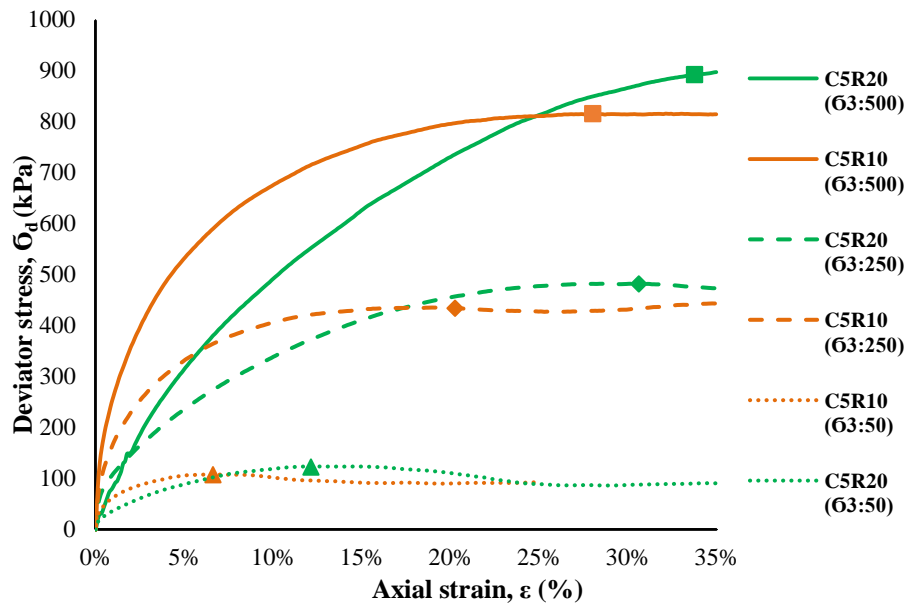


Figure6- 14. Effect of confining pressure on the deviator stress of cemented sand with 10% and 20% rubber.

Secondly, utilising more dosage of rubber has enhanced the above-mentioned characteristic of composites. One more time, the effect of confining pressure on the mixtures behaviour has been revealed by bolding the key role of rubber ratio in strength properties of composites.

The effect of confining pressure on the peak deviator stress of sand composites precisely presents in Figure6- 15. It can be observed that the peak deviator stress of cemented sand-rubber mixtures is greater than of pure sand and sand-rubber composites. Therefore, the maximum and minimum increment of sand peak deviator stress were obtained by using a combination of 10% cement with 20% rubber, and only 10% rubber respectively.

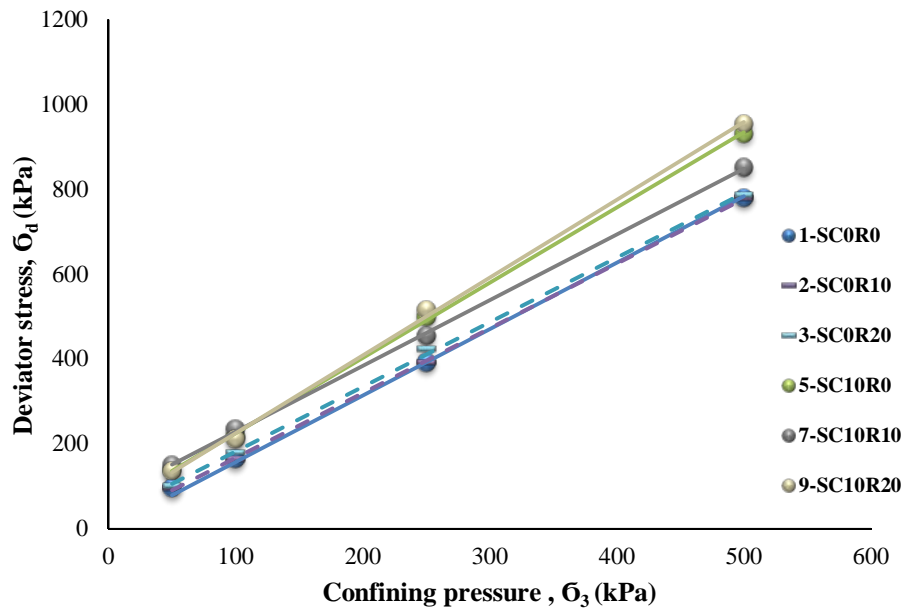


Figure6- 15. Peak deviator stress versus confining pressure of sand composites.

It is worth mentioning that the peak deviator stress is linearly increased by progressing the confining pressure. Moreover, the gradient of the peak deviator-confining pressure curves of cemented sand-rubber is sharper than of sand mixtures with no cement content.

However, analysing the axial strain of sand composite at the failure point versus confining pressure clearly demonstrates three different behaviours corresponding the rubber content of mixtures. It is evident from Figure6- 16 that the axial behaviour of composites not only is influenced by the confining pressure but also significantly related to the dosage of rubber in the mixtures. It was earlier mentioned that the ductility behaviour of the composite is mostly related to the dosage of rubber particles in the mixture. Therefore, the sand composites with no rubber participation have only shown a minor increment in axial strain failure due to increase the confining pressure. However, the application of 10% and 20% rubber show two different behaviours affecting by confining pressure and cementitious material. In all confining pressures, the uncemented sand containing 20% rubber was failed 10% later than the uncemented

sand including 10% rubber. However, this linear difference was transformed into a nonlinear behaviour through the cement addition. From Figure6- 16 can clearly be seen that confining pressure of 250kPa plays a boundary role in the plastic behaviour of cemented sand-rubber composites. It seems that with the greater confining pressure a 10% of rubber can also be capable as a cemented sand with 20% rubber fraction for increasing the strain capacity of cemented sand mixtures. It is worth mentioning that, the curves of SC10R10 and SC10R20 may be predicted the same axial strain at the confining pressures greater than 500kPa. However, due to the limited capacity of the triaxial cell, the experimented were subjected to 750kPa confining pressure were unsuccessful.

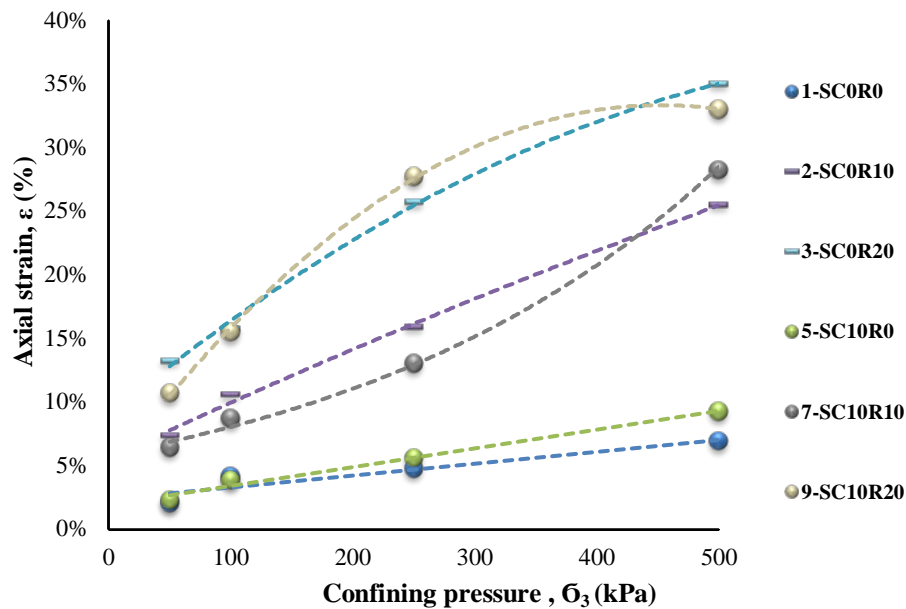


Figure6- 16. Effect of confining pressure on the axial strain at failure of sand composites.

Take everything into account, the shear characteristic of sand composite remarkably improves by using a reasonable dosage of cement and rubber. Because, a new mixture contains various numbers of inter-particle connection with remarkable flexibility and strength capacity.

6-3-3-3 MAXIMUM PRINCIPLE STRESS RATIO

In order to precisely analyse the shear strength characteristic of sand mixtures the stress ratio has been calculated from the maximum principle stresses results. The maximum principle stress (i.e. σ_1) is identically defined at the peak value of deviatoric stress (i.e. σ_d) corresponding with conducted confining pressure (i.e. σ_3). Thus, for the variation of confining pressure the stress ratio can be defined as the ratio of maximum principal stress to the conducted confining pressure (i.e. σ_1/σ_3). The results of maximum principle stress of sand composite versus the variation of confining pressure is presented by Figure6- 17. It can clearly be seen that the stress ratio decreases with the increase in confining pressure. This behaviour observes for all mixture, although depends on the constituent of composite the stress ratio at each confining pressure is different.

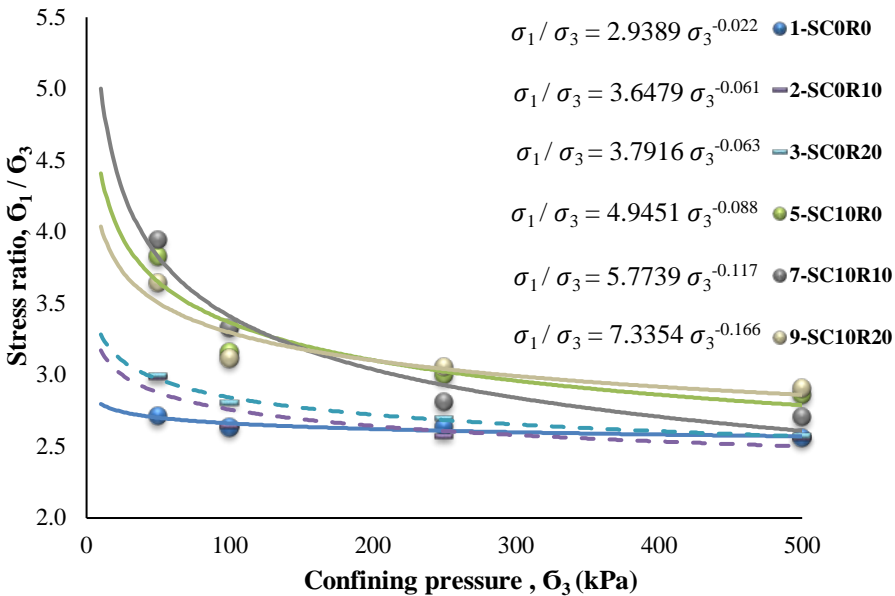


Figure6- 17. Maximum stress ratio results of sand composites at different confining pressures.

Considering the stress ratio behaviour, the result can be presented by a nonlinear correlation proposed in (Neaz Sheikh et al., 2013, Indraratna et al., 1998):

$$\sigma_1/\sigma_3 = a (\sigma_3)^b \quad (6.4)$$

where a is defined the value of maximum principal stress ratio at $\sigma_3=1\text{kPa}$ and b is an empirical index identical for each composites.

Investigating into the sand-rubber mixture shows a slight improvement in the stress ratio of sand due to rubber fraction. It is evident that with the increase in dosage of rubber the stress ratio slightly increases. However, this improvement is just obtained with the lower amount of confining pressure, and with conducting confining pressure greater than 250kPa pure sand has a higher stress ratio than of sand-rubber composites. On the hand, the combination of rubber-cement in sand composite increased the stress ratio of pure sand at all confining pressures. However, analysing the effect of rubber content on the cemented sand composites reveals the opposite behaviour with sand-rubber has been observed by increasing the confining pressure. Moreover, confining pressure at 250kPa known a boundary role again to alter the rubber effect on cemented sand mixtures. As a consequent, the cemented sand mixtures containing 10% rubber and 20% rubber have the greatest maximum principle stress ratio before and after 250kPa confining pressure, respectively. The variation of stress ratio of the composite with the different amount of confining pressure may be suggested the importance of composite's density. It seems that the importance of composite structures and density may be better realised by conducting the higher amount of confining pressures. Because, the composite with the higher packing density has normally, the higher number of inter-particle connections (Neaz Sheikh et al., 2013, Indraratna et al., 1998, Hossain and Yin, 2015). Therefore, taking advantage of the physical characteristics of rubber the density also need to be considered to define the optimum ratio of mixture's constituent for generating a composite with the greater strength capacity even at higher confining pressures.

6-3-3-4 ANALYSING THE SHEAR STRENGTH CHARACTERISTIC

The shear strength behaviour of the mixture has been evaluated based on the Cambridge diagram.

The mean effective pressure is defined as following equations:

$$p = \frac{\sigma_1 + 2 \sigma_3}{3} \quad (6.5)$$

where σ_1 and σ_3 are respectively defined the maximum and minimum principal stresses and p is the mean effective pressure. The deviatoric stress (q) can be defined as the difference of maximum and minimum principle stresses:

$$q = \sigma_1 - \sigma_3 \quad (6.6)$$

Figure6- 18 presents the failure envelopes results of sand composites, plotting the deviatoric stress versus the confining pressures. Shear enveloped of sand and cemented sand suggest a linear trend. However, the composites including the rubber particles demonstrated a non-linear behaviour. It may be occurred due to the presence of rubber particles in the mixtures resulted in the redistribution of the composite structure by applying the confining pressure. Increasing the confining pressure caused to reduce the sand-to-sand particle and increase the rubber-to-rubber particle. It might be attributed to the movement of sand particles into the voids of rubber, leading the non-linear behaviour of the composite. However, the rearrangement of sand particles can be minimised by performing the higher confining pressure and lower dosage of rubber. Similar with this result, the non-linear strength envelope has been reported by Maher and Gray, (1990), Foose et al., (1996), Indraratna et al., (1998) and Neaz Sheikh et al., (2013).

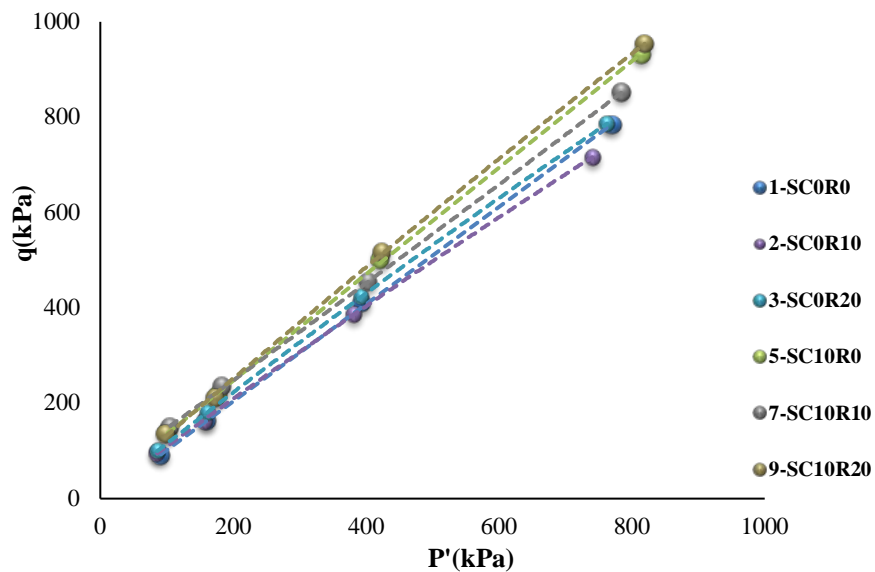


Figure6- 18. Summary of shear failure envelopes result of sand composites.

6-3-3-4 YOUNG’S MODULUS

To analysis the effect of rubber particles on the elastic behaviour of the composite, Young’s modulus (E) of the composite is calculated. The Young’s modulus value also compared with the one-dimensional elastic modulus, to evaluate the effect of the test method and the effect of confining pressure on the elastic behaviour of the composite. Subsequently, Figure6- 19 presents the elastic modulus of sand composites versus the confining pressure deduced from the triaxial test and one-dimensional consolidation test. Since it validates to be complex to the failure type of composites, and with the absence of small strain investing, the only way for evaluating the effect of confining pressure on the elastic behaviour of the composite is a comparable analysis of Young’s modulus.

It can obviously be seen that sand composites with zero rubber content have shown the greatest value. This behaviour may be justified by referring to the failure mode of the mixtures of this group (i.e. RF0) Figure6- 11. It can be acceptable that the composites with a localised shear banding mode have the higher stiffness value. In

terms of the comparison of the elastic modulus results , composites similary behave in both one-dimensional consolidation and triaxial tests. The greatest and lowest values are respectively obtained by the minimum and maximum dosage of rubber inclusion in the mixtures.

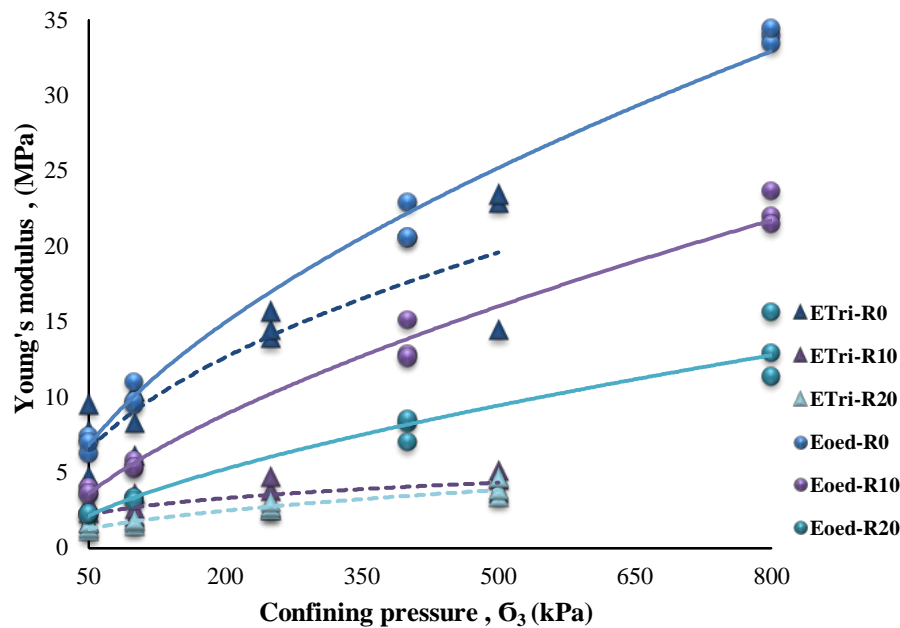


Figure6- 19.Young's modulus results of sand composites obtained from triaxial and consolidation tests.

A case by a case basis study on the results of one- dimensional consolidation test and triaxial test suggest that, although the elastic modulus value is quite similar at the lower confining pressure, this similarity was reduced by increasing the confining pressure. Figure6- 19 may be suggested that investing the elastic behaviour of a composite containing the ductile material through the triaxial test is more appropriate than one-dimensional consolidation test. By performing the cell pressure, the heterogeneous composite may be failed at the section with the higher porosity, which is the weaker part of the soil matrix (BECQUART, 2006, Chabannes et al., 2017). It is evident composites with 10RF and 20RF were also revealed the bulging failue mode, corresponding the of ductile properties of mixtures.

However, composites containing a dosage of rubber show a lower Young's modulus value suggesting the flexible composites Figure6- 11. The observed failure behaviour of the form the Figure6- 19 that, Young's modulus of composites with 10 and 20 rubber fraction are linearly behaved by increasing the confining pressure.

6-4: COMPRESSION AND ANALYSIS THE RESULTS OF TRIAXIAL TESTS AND DIRECT SHEAR TESTS

6-4-1: ASSESSING THE INTRINSIC CONSTANTS FOR SHEAR STRENGTH

In this section, the experimental data of small direct shear, large direct shear and triaxial are conducted to develop an empirical equation which is capable of predicting the shear intrinsic constants of sand composites. For this purpose, a large series of direct shear test data has been carried out on the various types of sand mixtures was assembled. The collected data were then used to propose a regression model based on the availability of input data. Eventually, the proposed model, including the cementitious factor and rubber fraction, was compared with the result of the triaxial test, and also the effect of cement and rubber parameters in the model of sand mixtures was evaluated for the various dosage of cement and rubber.

6-4-2: EXPERIMENTAL DATA OF SAND COMPOSITES

To begin with, a remarkable number of experimental results of the direct shear test on 18 composites were conducted in this research. The laboratory data is comprehensively including the scale effect study (i.e. small box and large box), the effect of rubber fractions (i.e. 0RF, 10RF, and 20RF), the effect of different kind and dosage of cementitious materials (i.e. %5 and 10% of cement, slag and cement-slag),

the effect of low and high normal stress on shear strength behaviour (i.e. 50kPa, 100kPa, 250kPa, 502kPa, 750kPa and 1000kPa).

6-4-3: REGRESSION MODEL

In this research, the intrinsic concept was used as a basic frame of reference for interpreting and evaluating the shear strength properties of the sand-rubber mixture. Moreover, the effect of cementitious material, including cement and slag on shear strength characteristics of composites has been assessed using a broad range of experimental data. In fact, two regression models were established based on the degree of availability of shear strength parameters of the studied sand composites. Based on the following function, the regression model was finally defined for predicting the shear strength value at the failure point and constant volume state:

$$\tau = f(\sigma, C, R, SL) \quad (6.7)$$

Thus, the main effective parameters of this research including normal stress (σ), cement (C), slag (SL) and rubber (R) were defined as a predictors to achieve the empirical equations for estimating the intrinsic constants in this research.

Therefore, the equations for this model can be presented as follows;

Small direct shear:

$$\tau_p = 0.771\sigma + 0.01C - 0.007R + .02SL - 0.001SL^2 \quad R^2 = 0.995 \quad (6.8)$$

$$\tau_{cv} = 0.61\sigma + 0.005C + 0.004R + .013SL - 0.001SL^2 \quad R^2 = 0.989 \quad (6.9)$$

where τ_p and τ_{cv} are defined the shear strength at the peak value and constant volume state in small direct shear test.

It is evident that the R-squared for the regression models shows an excellent agreement with the experimental results. Moreover, the equations (6.8) and (6.9) reveal the importance of normal stress, where it was earlier observed from the laboratory results. The predicted model also suggests that the efficiency of slag can be found greater than of cement. The overall accuracy of the proposed model is eventually compared by the laboratory data of small direct shear tests. It can clearly be seen that the probability graphs lie on a straight line, which reveals the reasonable accuracy of the proposed model for predicting the shear strength behaviour of sand-rubber composites Figure6- 20.

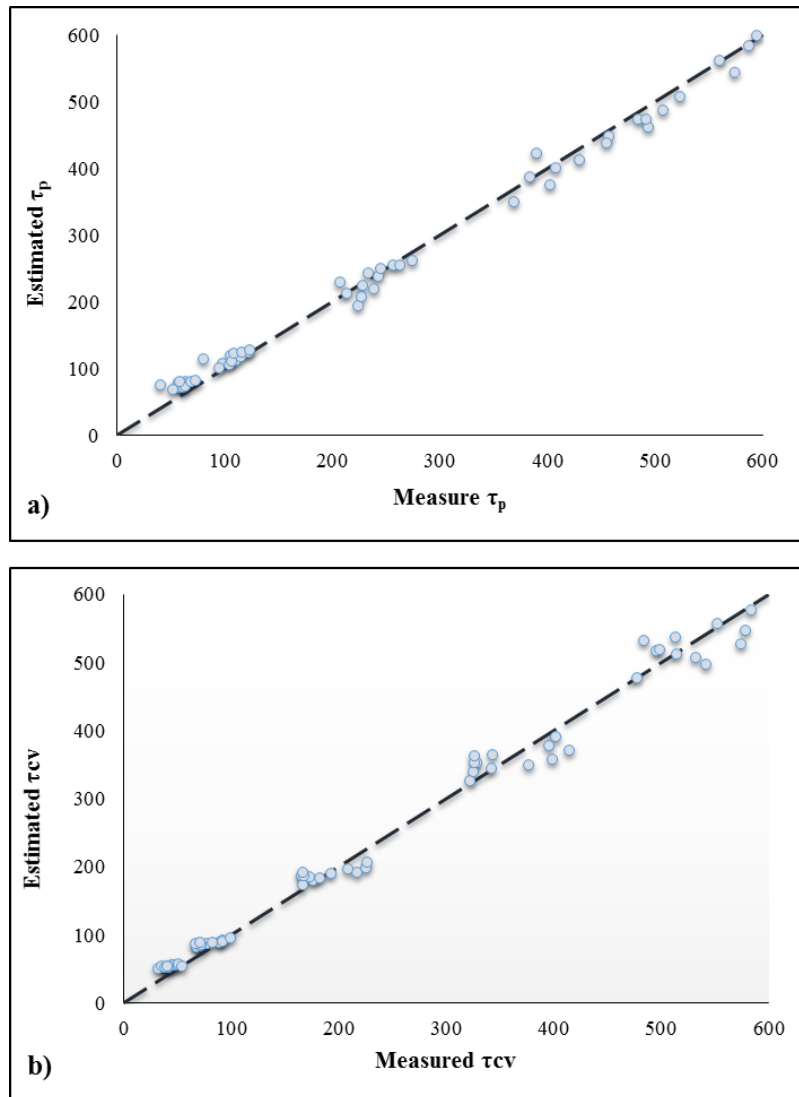


Figure6- 20. Comparison of predicted intrinsic constants and examined data of small direct shear test: a) τ_p , b) τ_{cv}

With the similar method, the following regression model proposed for:

Large direct shear:

$$\tau_p = 0.704\sigma + 0.013C - 0.001R + .056SL - 0.004SL^2 \quad R^2 = 0.992 \quad (6.10)$$

$$\tau_{cv} = 0.636\sigma + 0.011C + 0.005R + .038SL - 0.003SL^2 \quad R^2 = 0.992 \quad (6.11)$$

where, τ_p and τ_{cv} are defined the shear strength at the peak value and constant volume state in large direct shear test.

It is evident that the R-squared for the regression models shows an excellent agreement with the experimental results. The same as the regression model of small direct shear, the equations 32 and 33 suggest the importance of normal stress and a greater effectiveness of slag in compared with cement addition.

However, comparing the equation of proposed models in two scales shows an insignificant difference which might be indicated the scale effect results. However, this comparison suggests that the pivotal role of rubber for increasing the shear capacity of the composite at the residual state can be better recognised with performing the large direct shear test.

The scale effect study also indicates that the application of slag as a cementitious material for improving the shear strength of sand-rubber composites can be found more effective than a cement addition.

Taking everything into account, an overall accuracy of the proposed model is eventually compared by the laboratory data of small direct shear tests. It can clearly be seen that the probability graphs lie on a straight line, which reveals the reasonable accuracy of the proposed model for predicting the shear strength behaviour of sand-rubber composites Figure6- 21.

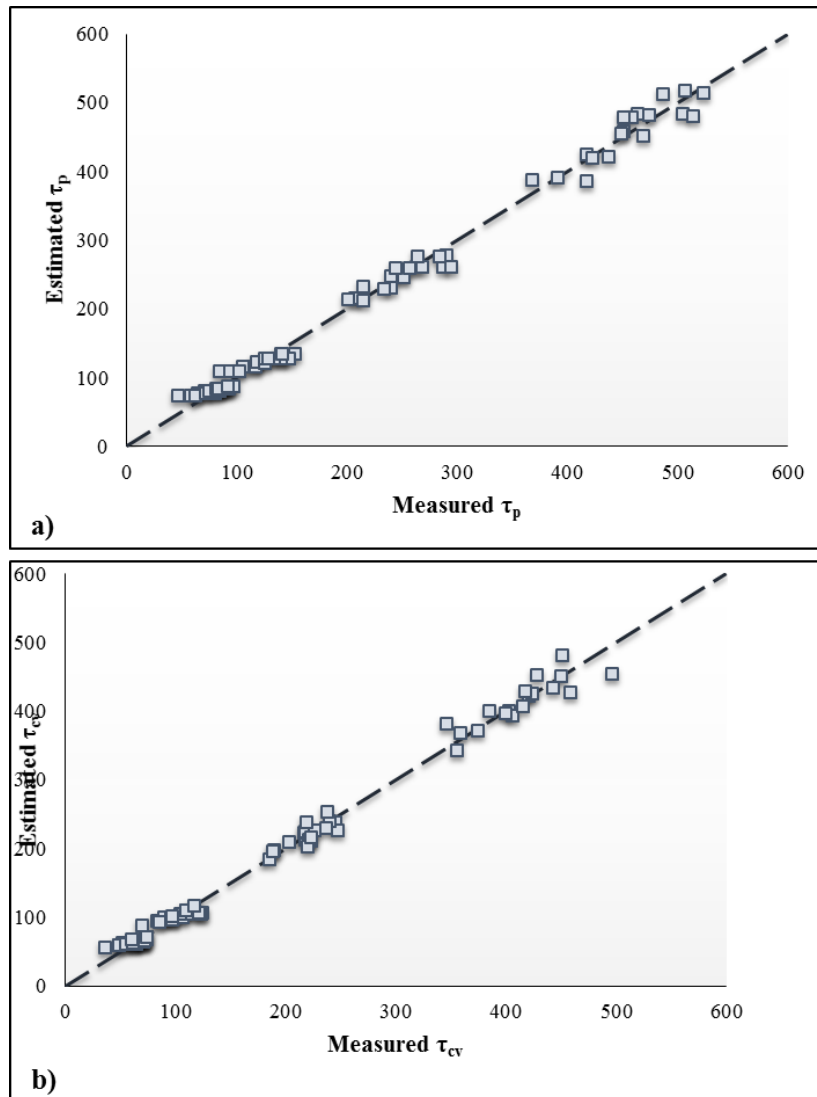


Figure6- 21. Comparison of predicted intrinsic constants and examined data of large direct shear test: a) τ_p , b) τ_{cv}

Considering all of the above, the accuracy of small and large direct shear test data were evaluated by triaxial test results. To keep the proposed form of a regression model of the direct shear test, the data of composites with a dosage of slag were used for the direct shear tests. Moreover, in this way, the ability of the proposed model to predict the intrinsic constant based on the direct shear test is evaluated by triaxial test results.

Therefore, the equations for this model can be presented as follows;

Consolidated-undrained triaxial test:

$$\tau_p = 0.724\sigma + 0.014C - 0.002R + .054SL - 0.003SL^2 \quad R^2 = 0.989 \quad (6.12)$$

$$\tau_{cv} = 0.673\sigma + 0.012C + 0.005R + .034SL - 0.003SL^2 \quad R^2 = 0.988 \quad (6.13)$$

where τ_p and τ_{cv} are defined the shear strength at the peak value and constant volume state in triaxial test. It is evident that, the R-squared for the regression models still shows an excellent agreement with the experimental results. It seems that, the proposed model can be used for predicting the shear strength results of sand composite in triaxial test as well.

Figure6- 22 presented the predicted value of peak shear strength and residual shear strength versus the related examined values obtained by laboratory results. It can clearly be seen that the estimated values of τ_p and τ_{cv} are in good agreement with the measured values. Therefore, probability graphs lie on a straight line, which reveals the sensible accuracy of proposed model for predicting the shear strength characteristics of sand-rubber composites Figure6- 22.

It might be suggested that the intrinsic strength of composite can be constant, although the experimental evaluation of shear strength related to the laboratory condition.

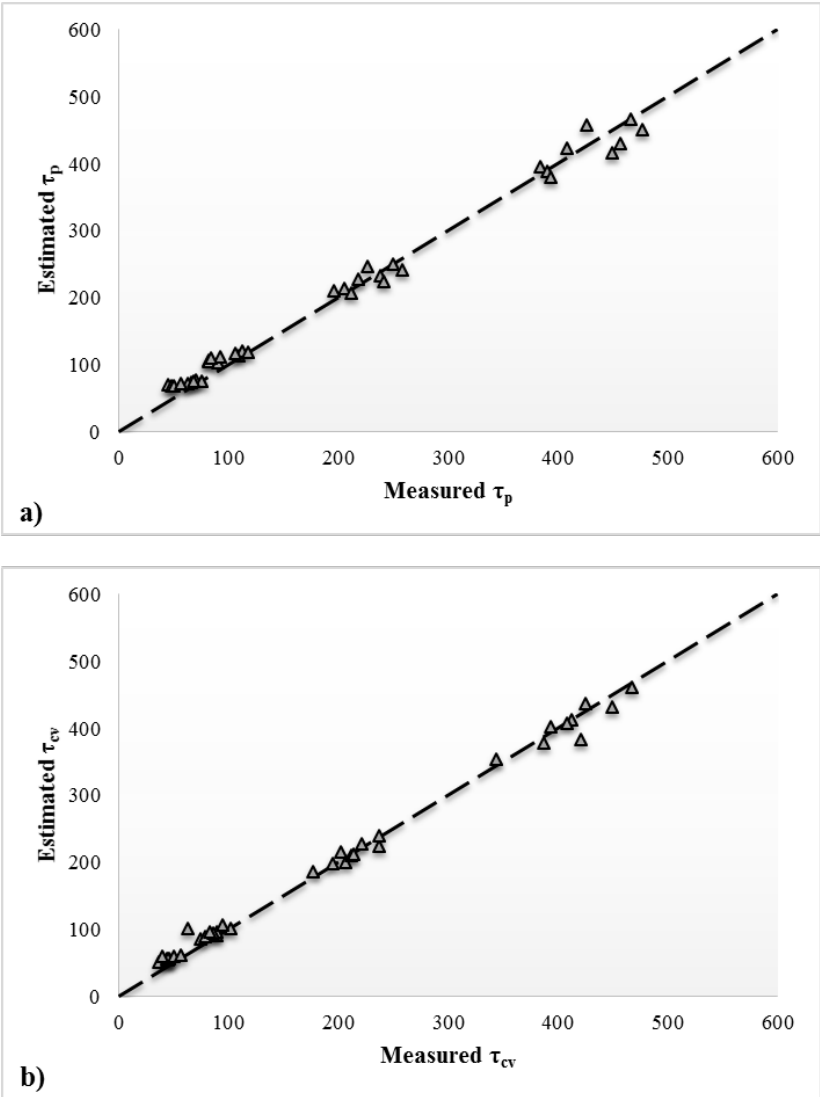


Figure6- 22. Comparison of predicted intrinsic constants and examined data of triaxial test: a) τ_p , b) τ_{cv}

6-5: MICROSTRUCTURAL ANALYSIS OF THE CEMENTED SAND-RUBBER COMPOSITE

The mechanical characteristic of a various number of sand-rubber mixtures has investigated through a comprehensive series of geotechnical tests. Taking the similarities in the components of cemented sand composite and a concrete mixture into account, it might be possible to investigate the microstructural properties of cemented sand composite the same way as a concrete mixture. Moreover, the application of rubber particles as an aggregate in the concrete mixture has been recognised over the few decades (Li et al., 2004, Turatsinze et al., 2005, Bignozzi and Sandrolini, 2006, Gratchev et al., 2006, Ganjian et al., 2009, Najim and Hall, 2010 and 2013, Afshinnia and Poursaee, 2015, Gupta et al., 2016)

Rubberised concrete can be utilised in concrete construction, which needs the strength resistance capacity between 28 MPa and 35 MPa, for instance (Kosmatka et al., 2002, Zheng et al., 2008, Najim and Hall, 2013). In general, replacing the natural aggregates with the rubber particles cause an increase of heterogeneity of cement (Neville, 1995, Najim and Hall, 2013). However, the ductile characteristic of rubber particles may be attributed to the interfacial bonding between cement paste and aggregate (Neville, 1995, Najim and Hall, 2012 and 2013).

Hereinafter, the present study will analyse the microstructural properties of the cemented sand-rubber composite by considering the mentioned possibility.

6-5-1: MATERIAL CHARACTERISTICS AND PHASES OF THE COMPOSITE

Concrete is a composite mixture made of cement, aggregate, water and a dosage of mixtures (Guedes et al., 2013, Hilal, 2016). By definition, hardening of concrete is caused by hydration reaction between the available oxides in the cement and water,

which generates a composite microstructure that evaluates the characteristics of the hardened material (Guedes et al., 2013, Hilal, 2016). Moreover, to generate a composite with higher performance, the additives are mixed with the other components of concrete to introduce the physical action by pozzolanic reaction (Hilal, 2016). Due to the pozzolanic reactions, the available voids are filled by the finer particles. Subsequently, the filler or physical effect happens as a result of alteration in pore structure occurs by the decrease in the grain size. Eventually, the paste microstructure of composite is improved by generating pozzolanic reaction and filler effect (Hilal, 2016). In this way the microstructure of composite turns out to be more uniform and homogeneous, accelerating the geotechnical properties like strength compared to a normal mixture (Hilal, 2016). Moreover, the porosity of cement paste serves a critical role in the strength characteristic of the composite. To create a composite with a high strength ability, the capillary porosity needs to be minimised. This achievement can be obtained by decreasing the gel porosity, leading to alteration in the composite microstructure (Hilal, 2016). It is clear that the microstructure of composite plays a pivotal role in composite's strength characteristic. Hence, the relationship between the microstructure of composite with strength characteristics needs to be investigated.

6-5-2: MICROSTRUCTURE OF COMPOSITE

A cemented sand rubber composite can be considered as mixtures with a heterogeneous microstructure including of some binding medium and aggregate particles. It might be considered to include three phases: a) the hardened cement paste b) the pore structure c) interfacial transition zone (ITZ), which is the weakest phase generating between the aggregate skeleton and cement paste (Guedes et al., 2013, Hilal, 2016 , Gupta et al., 2016). The shear strength characteristic of a cemented sand-rubber mixture can be improved by enhancing the main phases of the composite.

6-5-2-1: CEMENTITIOUS BINDERS

Cemented composite mostly contains silica (SiO_2) or (S), alumina (Al_2O_3) or (A), lime (CaO) or (C), and iron oxide (Fe_2O_3) or (F). The key compounds in the composite are Tri-calcium silicate $3\text{CaO}.\text{SiO}_2$, di-calcium silicate $2\text{CaO}.\text{SiO}_2$, tri-calcium aluminate $3\text{CaO}.\text{Al}_2\text{O}_3$ and tetra-calcium aluminoferrite $4\text{CaO}.\text{Al}_2\text{O}_3.\text{Fe}_2\text{O}_3$ which are labelled as C_3S , C_2S , C_3A and

C_4AF , respectively (Domone and Illston, 2010, Guedes et al., 2013, Hilal, 2016). Consequently, the microstructure of hydrated composite paste is mainly contained the key phases such as (I) calcium silicate hydrate (C-S-H); (II) calcium hydroxide (CH); (III) ettringite; (IV) monosulfate; (V) unhydrated cement particles and (VI) air voids (Monteiro, 2006, Hilal, 2016). For that reason, the hydrous calcium aluminium sulphate ettringite [$\text{C}_a6\text{Al}_2 (\text{SO}_4)_3(\text{OH})_{12} . 26\text{H}_2\text{O}$] is initially formed by reaction between C_3A and C_4AF with gypsum ($\text{CaO} . \text{SO}_3 . 2\text{H}_2\text{O}$). This reaction approximately occurs within the first 24 hours of hydration (Guedes et al., 2013, Hilal, 2016). Subsequently, initial phases of hydration are completed by monosulfate [$3\text{CaO} . (\text{Al}, \text{Fe})_2\text{O}_3 . \text{CaSO}_4 . n\text{H}_2\text{O}$]. However, shear strength behaviour of hardened composite and calcium hydroxide is mainly related to the calcium silicate hydrate (C-S-H) phase. By definition, aggregate and water are the basic components of a cemented sand-rubber mixture. It is a common practice that, a various kind of additives can be added into the mixture to enhance the desirable characteristic of composite (Guedes et al., 2013, Hilal, 2016). Moreover, partial replacement of cement can be alternatively used for adding the supplementary admixtures (Guedes et al., 2013, Hilal, 2016). All things considered, sand and rubber are utilised as the basic component of the proposed composite are. Moreover, various dosages of cement and slag are used as a binder. Investigations using SEM micrographs and EDS elemental analysis yielded more accurate data on cement and sand composition Figure6- 23.

As illustrated in Figure6- 23 (a), calcium (Ca) may be the main component of cement, followed by oxygen (O) and silicon (Si).

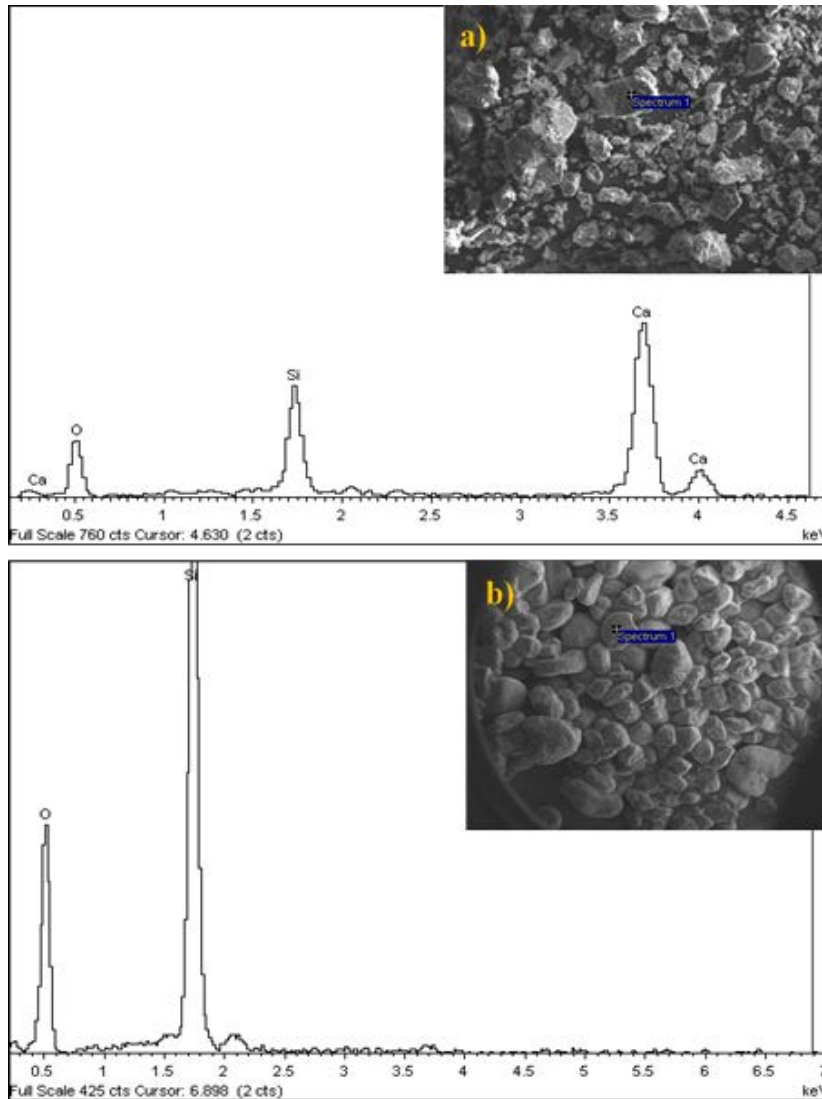


Figure6- 23. EDS line spectrum results for cement (a) and sand (b).

It is clear that the high peak in the line spectrum graph is associated with the high proportion of calcium in cement. It can be assumed that, all the main components of calcium silicate hydrate has been observed. However, the Figure6- 23 (b) suggest that

the silicon can be the only component of sand with the presence of oxygen atoms could suggest the availability of SiO₂, as the basic oxides for creating the pozzolanic reaction. As a consequence, the pozzolanic activity can be established by the interaction between available calcium and silicon atoms of cement and sand (Amiralian et al., 2015).

However, the application of water-reducing admixtures for increasing the strength properties of composite has been suggested by researches (Guedes et al., 2013, Hilal, 2016). The fluidity of system can be remarkably increased by the addition of rubber particles into the composites. It might be the hypothesis that the rubber particles helps to reduce the surface tension of surrounding water after adsorbed on cement particles (Guedes et al., 2013, Hilal, 2016).

The results of the optimum moisture content of studied composite might be justified the above assumption. Therefore, it is evident that the application of rubber into the cemented sand mixture composites mostly leads to reduce in the moisture of composite Table6- 6.

Table6- 6. Results of optimum moisture content of the treated and the untreated sand composites

SAMPLE	OMC (%)
1-SC0R0	13.81%
2-SC0R10	14.77%
3-SC0R20	10.21%
4-SC5R0	12.90%
44-SS5R0	12.66%
5-SC10R0	12.54%
55-SS10R0	11.30%
555-SC5S5R0	11.34%
6-SC5R10	11.66%
66-SS5R10	12.07%
7-SC10R10	11.85%
77-SS10R10	11.10%
777-SC5S5R10	10.45%
8-SC5R20	11.12%
88-SS5R20	14.16%

9-SC10R20	10.96%
99-SS10R20	10.38%
999-SC5S5R20	10.96%

6-5-2-3: EFFECT OF RUBBER PARTICLES ON CEMENTITIOUS BINDERS

To explain the mechanism of action, the role of cement and rubber needs to be explained. As surfactants are adsorbed on cement particles and sand surfaces. The effectiveness of cement addition for improving the strength properties of the composite is schematically illustrated in Figure6- 24. Additional interactions at the solid-liquid-air interfaces also occur during the mechanism.

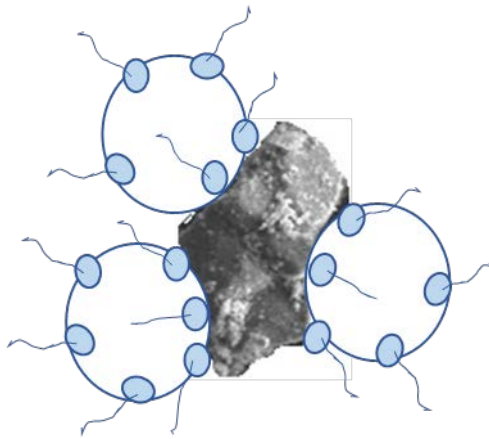


Figure6- 24. Schematic illustration of the interaction among a cement particle surrounded by air bubbles(Du and Folliard, 2005).

Generating the selective adhesion among the solid, liquid and air particles with a precise surfactant is called froth floatation (Du and Folliard, 2005, Guedes et al., 2013, Hilal, 2016).

The inclusion of cement causes an increase in the adhesion of air bubbles to cement particles. Scattering the air bubbles in the composite leads to a decrease in the tendency of particles to float on the surface. Nevertheless, the probability of settlement of finer particles is reduced by increasing the floatation force of the air bubbles.

However, regarding the efficiency of rubber particle for reducing the moisture of composite (Table6- 6), it might be reasonable if the role of rubber particles are considered as the same as superplasticizer admixtures in the cemented composite. By definition, rubber particle does not contain any inion, however, hereinafter the effect of rubber on the microstructural behaviour of cemented-rubber mixtures will be explored with the assistance of the application of superplasticizer admixtures in the cemented composite. The mechanism of composite behaviour by the inclusion of rubber particles is schematically illustrated in Figure6- 25. From the point of view the electrostatic potential, the composite contains a mixture of positive and negative charges.

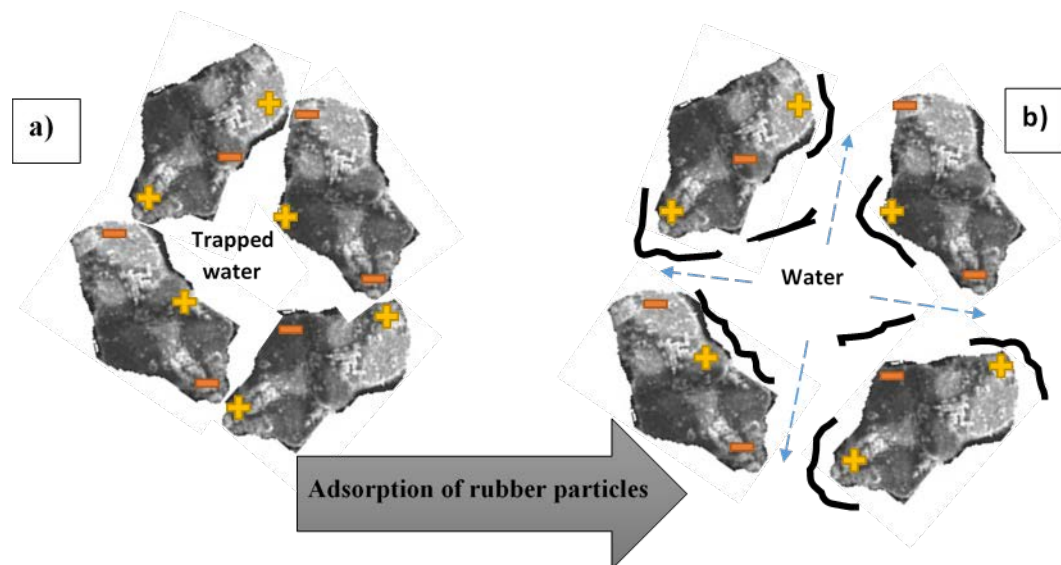


Figure6- 25. Schematic representation of rubber application in the cemented composite; (a) cemented particles, (b) cemented-rubber particles (Du and Folliard, 2005, Hilal, 2016).

As illustrated in Figure6- 24, combining cement particles in a few parts of the composite, resulted in the in the establishment of fluctuation in mixture Figure6- 25(a).

This action can be affected by the addition of rubber particles to the mixtures. The cement particles might be scattered by the addition of rubber particles within a similar manner as the steric effect and electrostatic repulsion (Du and Folliard, 2005, Monteiro, 2006, Hilal, 2016). Consequently, the rubber particles might be adsorbed on the surface of cemented particles. Eventually, the rubber particles might insulate the composites particles, leading to disperse the cemented particles. Once the cement particles are dispersed the fluidity of mixture is increased by releasing the trapped water among the particles Figure6- 25(b). All things considered, this explanation might justify the experimental results of the cemented-rubber mixture such as high strength capacity, flexibility, reduction of the moisture content of composite and a higher compressibility.

6-5-2-3: PORE STRUCTURE

One of the other factors that can be affected by the characteristics of the cemented composite is the pore structure of mixture (Monteiro, 2006, Ramamurthy et al., 2009, Hilal, 2016). Some of the main properties of composite like strength, permeability and pore size distribution are associated with the pore structure of mixture (Monteiro, 2006, Ramamurthy et al., 2009, Hilal, 2016). Figure6- 26 presents typical sizes of the different kinds of voids in a mixture.

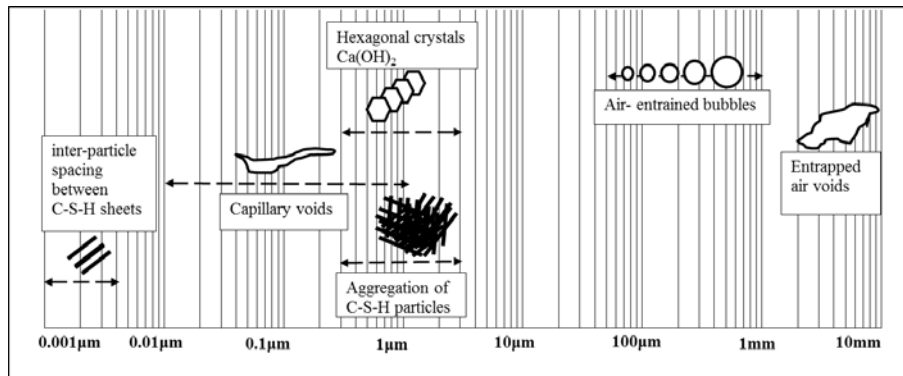


Figure6- 26. The typical dimensional range of possible pores in a composite (Monteiro, 2006).

Although rubber particle has the low density, it can be assumed that the addition of rubber into the cemented composite filling the pores with the higher dimension. Reducing the diameter of the pores might be formed air voids, resulting in generating a more uniform composite with the greater comprehensive strength (Monteiro, 2006, Just and Middendorf, 2009, Ramamurthy et al., 2009, Hilal, 2016).

Furthermore, this action can be enhanced by the using the additional admixtures into the mixture. Considering the ability of slag o reduce the moisture of mixture, it can be expected that the particles of slag are more homogeneous than cement particles. This characteristic can be established a denser mixture by reducing a wider range of air voids in the mixture. SEM image reveals that slag contains various shapes, which can be affected by the microstructure of composite Figure6- 27.

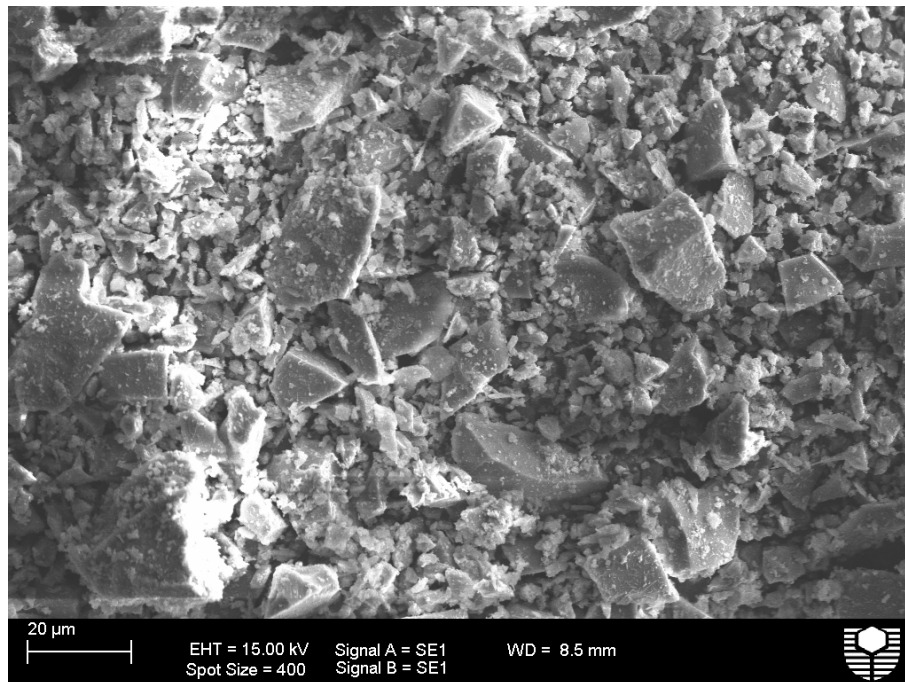


Figure6- 27. Secondary electron image of slag.

Therefore, utilising a variation types of additives can be provided with a more possibility to generate a composite with the higher strength to weight ratio.

6-5-2-4: INTERFACIAL TRANSITION ZONE (ITZ)

It may be reasonable that consider a cemented mixture as a three phases composite containing the hardened cement paste, the aggregate, and the interfacial transition zone (ITZ), generating between them. Due to the higher porosity and poor combination of particles in ITZ phase, it can be the weakest phase of a cemented composite. The ITZ has generally contained a lower density compared to bulk cement paste. Subsequently, due to the lower density and strength capacity, the micro-crakes might be initiated within ITZ of composite that is influenced by external loads. The mechanism of generation the ITZ in a composite can be represented by Figure6- 28 in three stages (Monteiro, 2006, Maire et al., 2007, Mondal et al., 2007, Just and Middendorf, 2009,

Ramamurthy et al., 2009, Hilal, 2016). First of all, the bulk cement paste is established by creating the water films around the aggregate particles. It can be expected that the area with the larger aggregate contains a higher water-cement ratio than other parts of the composite. Secondly, ettringite and calcium hydroxide is generated as results of the dissolution of calcium sulphate and calcium aluminate compounds. For that reason, the bigger crystals are produced in the vicinity of the larger aggregates, leading to transforming to an area with the greater porous framework in a composite matrix. Moreover, the platelike calcium hydroxide crystals tend to be perpendicularly aligned with the aggregate surface.

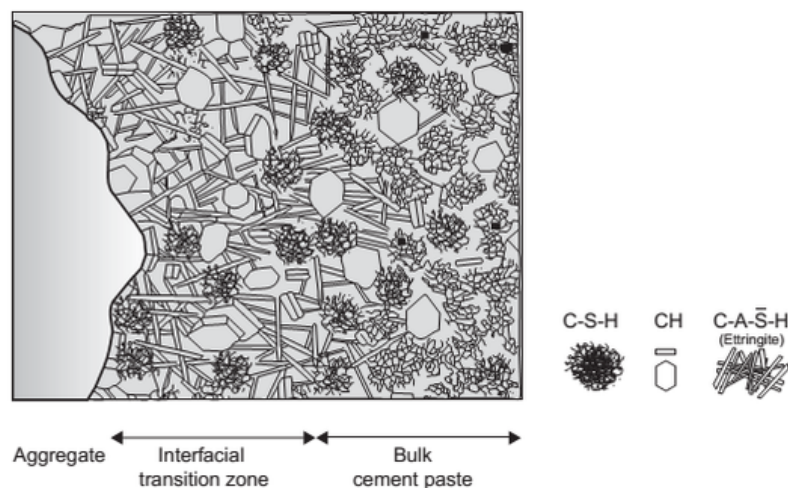


Figure6- 28. Schematic illustration of the interfacial transition zone in a composite (Monteiro, 2006, Hilal, 2016).

Eventually, as a consequence of the development of hydration process, the available porous between the larger ettringite and calcium hydroxide crystal is occupied by forming the weaker C-S-H and smaller crystal of ettringite and calcium hydroxide. This action can enhance the density of mixture and improved the strength capacity of ITZ.

It seems that some of the parameters such particle shape size, mineral composition, surface roughness and moisture content, the porosity of aggregates and the water-cement ratio can be affected on the characteristic of generated bond in ITZ (Monteiro, 2006, Maire et al., 2007, Mondal et al., 2007, Just and Middendorf, 2009, Ramamurthy et al., 2009, Hilal, 2016). Therefore, utilising rubber and slag as the admixtures with different mechanical and material characteristic can be enhanced the strength properties of a cemented composite.

6-5-3: POTENTIAL OF RUBBER AND SLAG TO CREATE A HIGH-PERFORMANCE COMPOSITE

Evaluation of the microstructure of composite can be performed by investigating the type, dimension, physical shape, dosage and distribution of phases at the micro-level (Monteiro, 2006, Maire et al., 2007, Mondal et al., 2007, Just and Middendorf, 2009, Ramamurthy et al., 2009, Hilal, 2016), which can be mainly represented the specific characteristic of each phase. Firstly, calcium silicate hydrate C-S-H gel is mainly produced by hydrated cement paste components. Secondly, observing the gel pores, capillary pores, and voids can be referred to the pore structure. Moreover, finally, the boundaries between the cement paste and the aggregate particle is defined as the characteristic of the interfacial transition zone (ITZ) (Monteiro, 2006, Maire et al., 2007, Mondal et al., 2007, Just and Middendorf, 2009, Ramamurthy et al., 2009, Hilal, 2016).

Therefore, considering these three concepts, improvement of the composite performance can be achieved by the addition of rubber and slag into the mixture.

6-5-3-1: CHARACTERISATION OF COMPOSITES COMPONENTS

Figure6- 29(a), (b) show the SEM images of the geomaterials were used in this research study. It can clearly be seen that sand has a rounded shape which can be

suggested that, particles can be easily moved over each other with a lower friction

Figure6- 29(a).

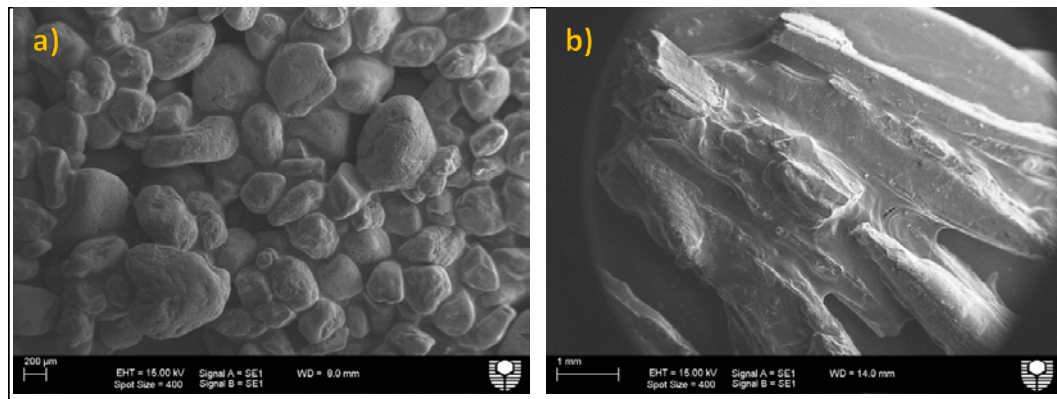


Figure6- 29.Scanning electron micrograph of; (a) sand, (b) rubber.

The SEM image of rubber particles also indicates that rubber can be classified as formless particles Figure6- 29(b). However, rubber shows a structural surface out of irregular hexagonal and rectangular cells with various type of sizes and forms. Containing various shapes including, very angular, angular, sub-angular and might be increased the number of particles that be sucked into each other. In other words, it seems that using the rubber particles might be generated a composite with the similar microstructure to a timber folded plate structures. It can be suggested that a unique shape of rubber, can be improved the composite shear resistance, caused by increasing the inter-particle attachment points inside of the mixture.

6-5-3-2: SLAG

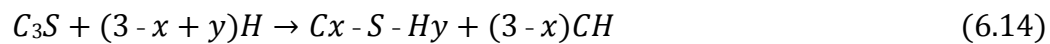
Strengthen the hydrated cement phase can be obtained by adding the supplementary cementitious materials. Slag as a by-product admixture used for increasing the degree of reaction with the water bound by the hydrated paste. Increasing the degree of reaction can be associated with occupying the free space in hydrated cement paste,

leading to a lower paste porosity. This consequence might be justified by an investigation into the particle size of slag Figure6- 27. Moreover, reducing the paste porosity might also be associated with the reduction in capillary porosity. Eventually, it might be expected that a lower capillary porosity in the composite can be associated with the generation of crystal C-S-H gel.

Thus, regarding the phase reaction the following equations are used as the classic method for measurement of the amount of bound water (Kocaba et al., 2012):

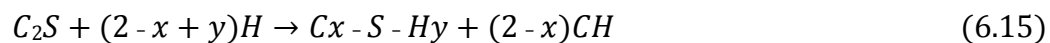
Hydration of tri-calcium silicate:

The compounds of tri-calcium silicate (C_3S) is mainly caused to initial hardness of composite. The composite with the higher ratio of C_3S has the greater early strength.



Hydration of di-calcium silicate:

The compounds of di-calcium silicate (C_2S) is responsible for increasing the strength of composite at the age further than 7 days.



Hydration of tri-calcium aluminate with calcium sulphate:

The compounds of tri-calcium aluminate released a significant amount of heat in first days of hardening. As a result of hydration, the early strength of hardening might be additionally increased by the products of this group.

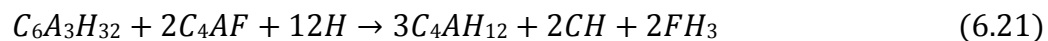
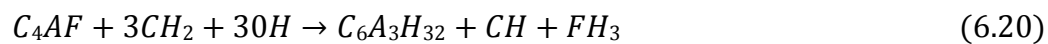


Or



Hydration of tri-calcium aluminoferrite:

The compounds of tri-calcium aluminoferrite are contributed to a slight increment of strength in the composite.



The key ingredients of slag were investigated by microscopy analysis of an area in the specimen. At first glance, the line spectrum behaviour of slag shows (Figure6- 30) the existence of calcium and silicon similar to the cement EDS data Figure6- 23(a). It might be suggested that the dosage of calcium and silicon can be lower than of observed on cement. However, the line spectrum peaks reveal the additional ingredients like aluminium (AL), magnesium (Mg) and oxygen (O), leading to increasing the possibility of hydration reaction.

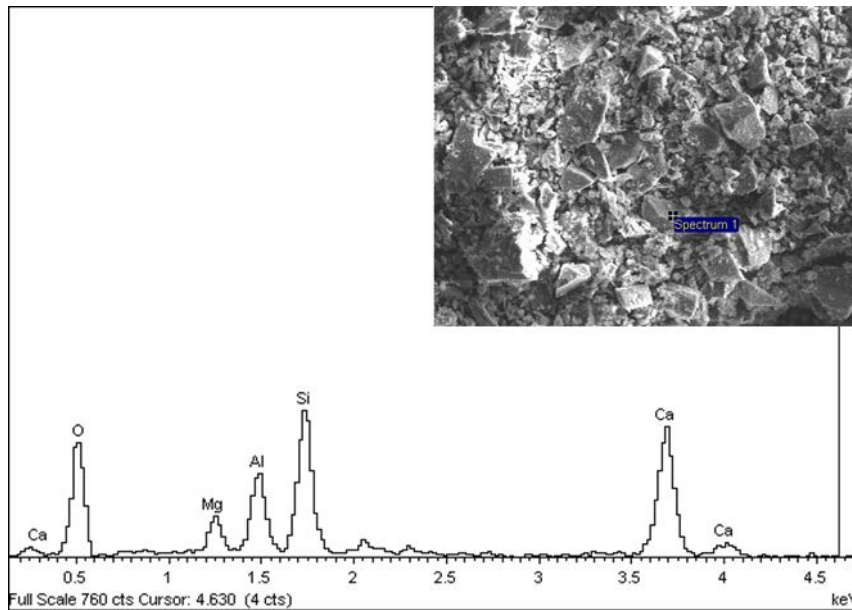


Figure6- 30. EDS line spectrum results for slag.

Moreover, the presence of magnesium and oxygen in the EDS data of slag can be suggested the availability of magnesium oxide (MgO) in a mixture, reducing the expansion in the composite. This possibility might be justified the lower swell index of the slag-sand composite in compared to results of swell index cement-sand mixtures. Further investigations performing SEM micrograph analysis yielded more accurate data and understanding on composite behaviour affected by a dosage of slag.

6-5-3-3: EFFECT OF SLAG ON CEMENTED SAND COMPOSITE

The hydrated cement-sand interface is clearly defined by SEM micrograph of cemented sand mixtures (Figure6- 31). The angular and irregular shapes of sand particles as the main components of the composite are clearly noticeable. The morphology result also indicates that the surface of the composite established a porous C-S-H matrix including calcium hydroxide crystals. However, the amount of C-S-H crystals is scattered at the surface of the composite, where some area has contained

only a poor crystalline fibre. Moreover, capillary pores in the pore structure are observed.

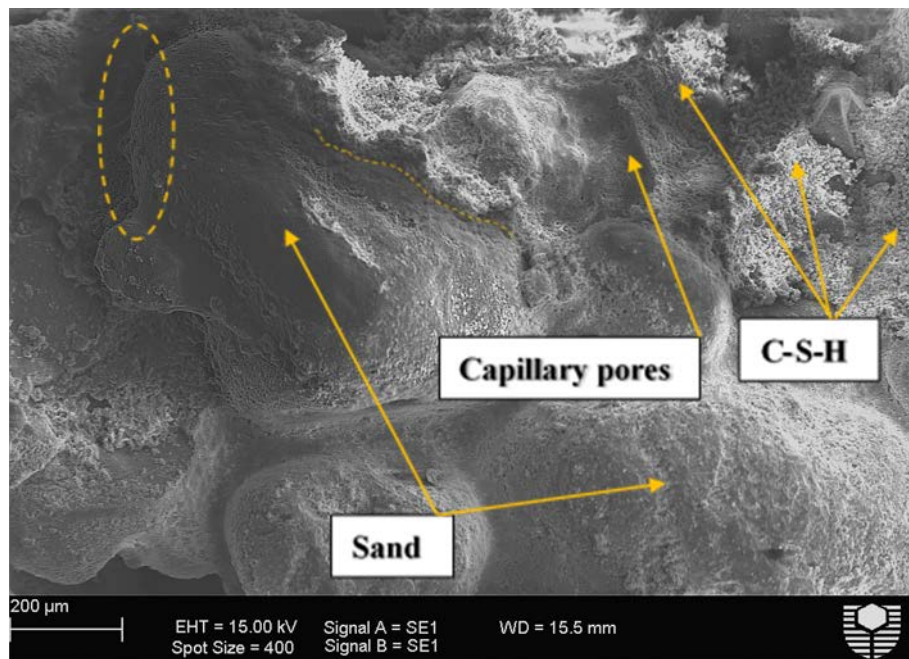


Figure6- 31. SEM micrograph results for cemented sand composite.

SEM micrograph also revealed that the composite contains cracks and gaps on its microstructure Figure6- 31. The micro-crack and gap specially observed in the interface of sand particles and cement matrix. This observation can be reflected a weak boundary connection between cement matrix and sand particles, occurring the micro-cracks in the composite.

The effect of slag addition on the microstructural behaviour of cemented-sand composite has been investigated by SEM micrograph (Figure6- 32).The results show that C-S-H as the key hydration products is typically generated around the sand particles. It seems that the addition of slag into the cemented sand create the well-crystallised C-S-H. This improvement can be achieved by combining aluminium atoms with the cement matrix, resulting to generate the compounds of tri-calcium

aluminoferrite. Although capillary pores in the pore structure are observed, the number of pores and gaps are significantly reduced. It might be suggested the smaller size of slag particles to reduce the porosity of composite. A typical generation of ITZ between bulk cement and aggregates illustrates in Figure6- 32.

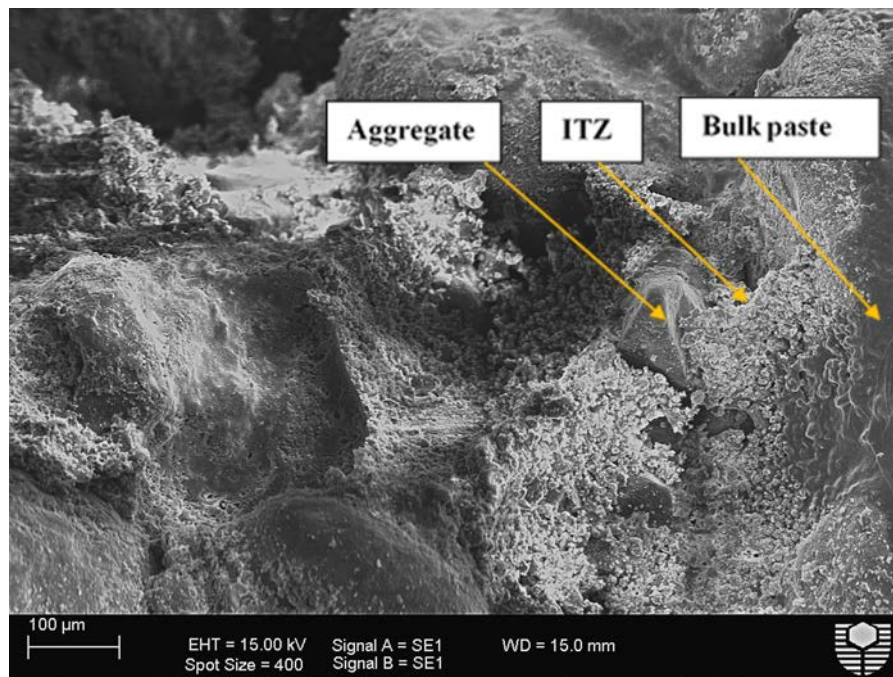


Figure6- 32. SEM micrograph results for effect of slag addition on the cemented sand composite.

6-5-3-4: EFFECT OF RUBBER ON ALKALI-SILICA REACTION IN CEMENTED SAND COMPOSITE

Microscopy analysis of the cemented sand with a dosage of rubber is indicated the effect of the combination of rubber material on the morphology of cemented sand composite. SEM image of the cemented sand containing rubber particles is presented in Figure6- 33. Due to the similarity in the basic components of the composite, the structure of cemented rubber-sand the recognition of rubber particles is possible by distinguishing shapes of rubber from sand. Identification of the rubber particles is made conceivable by their irregular shape and micro-cracks. Analysing the area with

the existence of rubber suggests that the inclusion of rubber can be increased the uniformity of mixture Figure6- 33. C-S-H gel has been established between the sand and rubber as an aggregate phase and the cement past.

Although, cracks in the interface of rubber and sand particles have been observed. It might be occurred due to the generation of a poor ITZ resulting in weak band among the particles.

However, utilising rubber particles in the mixtures (Figure6- 33), caused a reduced amount of surface cracks and gaps in compared to cemented sand composite (Figure6- 31). Reducing and localising surface cracks can be happened due to reducing in the alkali-silica reaction in the composite. Utilising the cement addition in sand matrix caused to generate an alkaline environment.

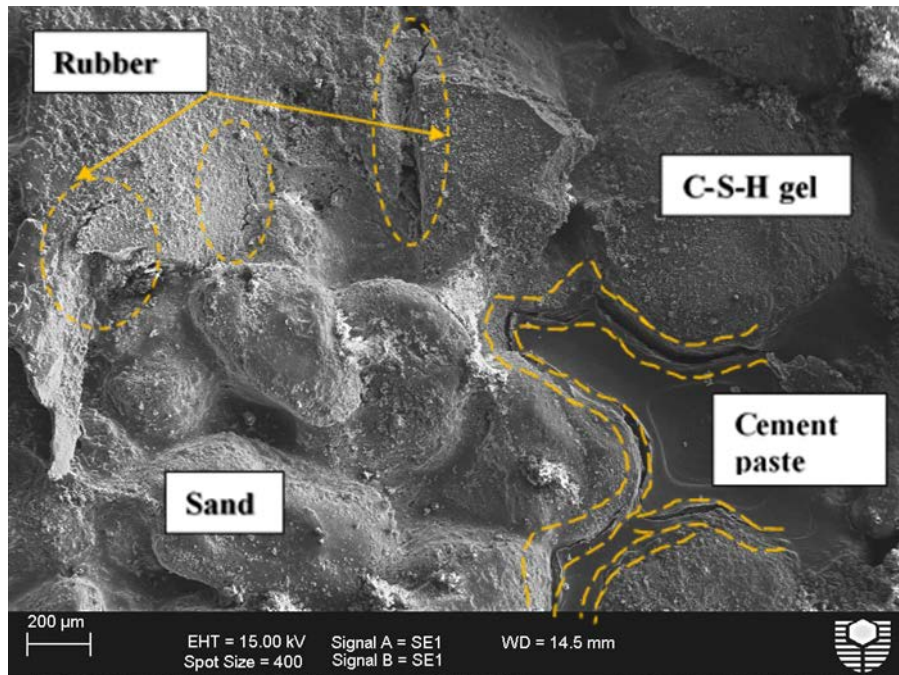


Figure6- 33. SEM micrograph results for cemented sand-rubber composite.

A chemical reaction that mainly occurred as a swelling reaction between a reactive non-crystalline silica of aggregates and hydroxyl ions of cement in a highly alkaline environment is known as an alkali-silica reaction (ASR) (Afshinnia and Poursaee, 2015). It seems that in the presence of rubber particles a smaller amount of moisture is absorbed by ASR gel and subsequently, the amount of ASR distress is reduced. Absorbing an amount of ASR gel by the rubber particle might explain the presence of minor cracks in the area with rubber content. It might be hypothesised that a limited expansion can be achieved by using the rubber particles in the cemented composite. Surface cracking might be localised to a particular place containing the rubber particles.

Figure6- 34 shows the micrograph of cemented sand-rubber mixture with the addition of slag particles. It seems that by adding slag into a cemented mixture, a larger amount of hydrated products might be established. The adhesion among the particles

of hydrated cement phase in a composite is the key parameter for increasing the strength of the composite. Because, composite with a strengthen characteristic can be generated by adding a dosage of slag into the mixture. The adhesion can be explained by the van der Waals forces of attraction depends on the particle characteristics in the composite (Hilal, 2016, Shen, 2006, Domone and Illston, 2010, Najim and Hall, 2012, Domone and Illston, 2010, Just and Middendorf, 2009, Monteiro, 2006). Subsequently, aluminium atoms of slag can be provided a chance for establishing hexagonal calcium aluminate hydrates in addition to products of hydrated cement paste (Hilal, 2016, Shen, 2006, Domone and Illston, 2010, Najim and Hall, 2012, Domone and Illston, 2010, Just and Middendorf, 2009, Monteiro, 2006). In other words, the presence of slag, the alkali binding capacity of hydration products in the cement paste has been increased. Accordingly, the alkali fixation is occurred by developing C-S-H crystals products through the slag particles, refining the pores in cement past of mixtures.

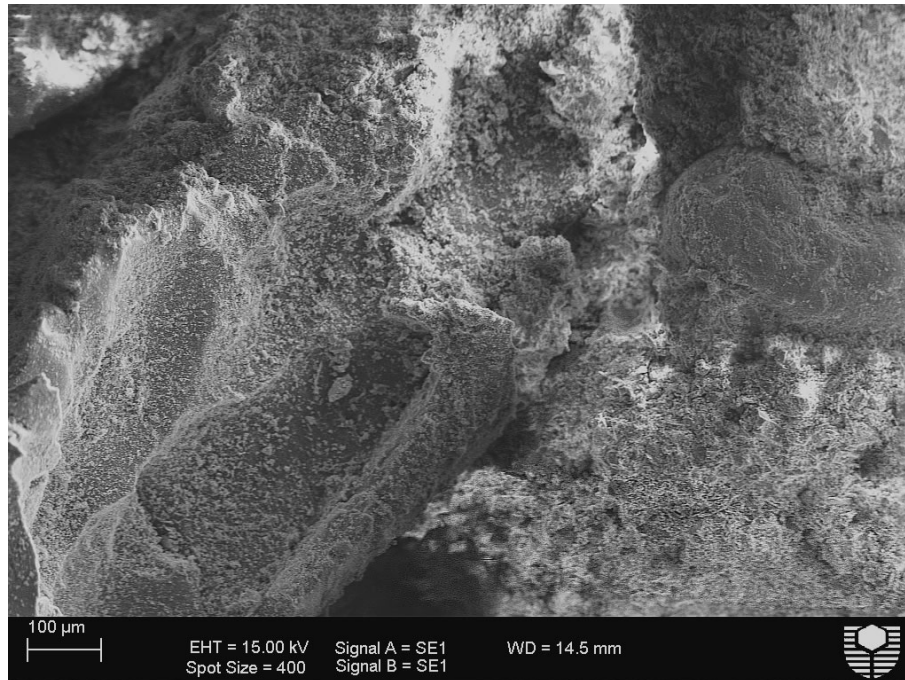


Figure6- 34. SEM micrograph results for effect of slag addition on the cemented sand-rubber composite.

Moreover, surface cracking generated by ASR has been limited by adding slag into cemented-rubber mixtures (Figure6- 34). It seems that the slag might be effective in reducing the hydroxyl ion content of the cement pore solution. Therefore, the total alkalis in the cement paste are reduced because of the alkali dilution effect, leading to reduce the ASR distress in the cemented composite.

TO SUM UP BRIEFLY...

Accordingly, as per the results, the strength behaviour of the composite is significantly related to the micro-fabric of the composite. In other words, the geotechnical properties of the sand composite are likely to be evaluated by the identical micro-fabric structure. Figure6- 35 illustrates the change in the microstructure of composite due to slag addition, leading to an increase in uniformity of sand matrix.

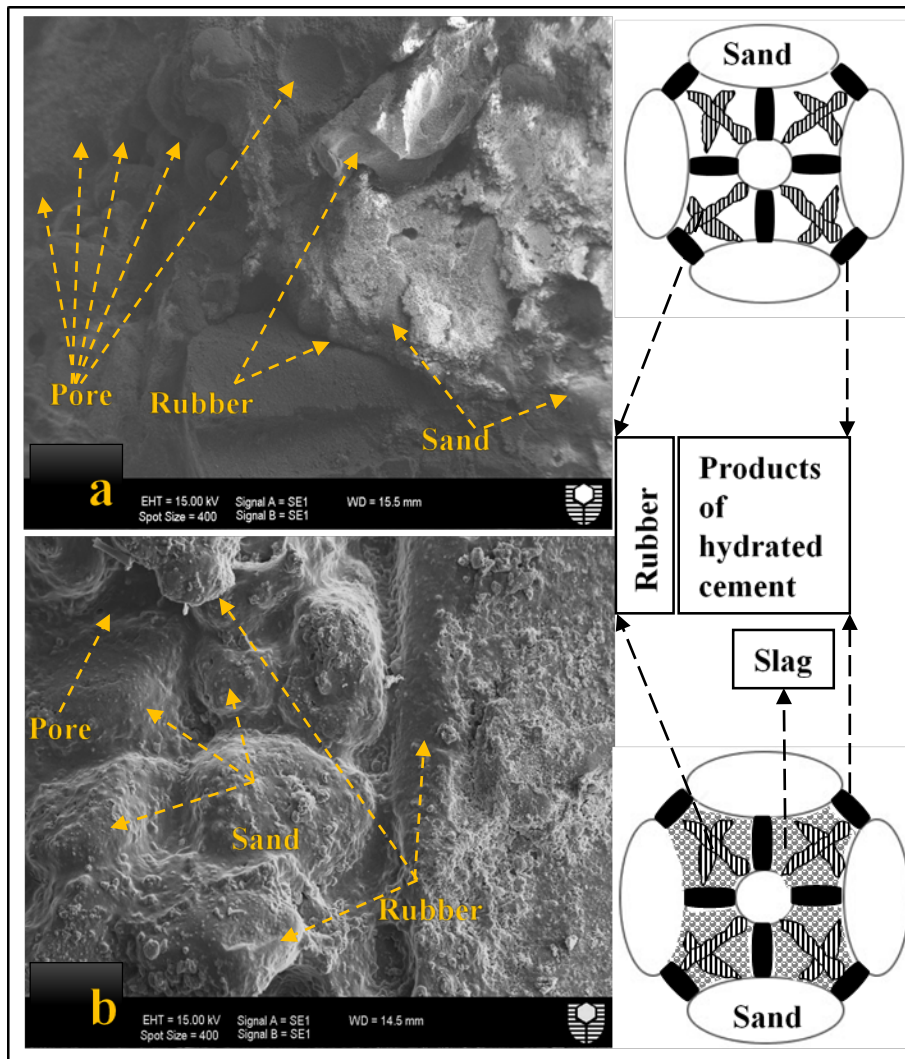


Figure6- 35. Micro-fabric of the cemented sand-rubber composite: a) without slag; b) with slag.

It is evident that the microstructure of composite with a dosage of slag is more homogenous than that of composite without slag addition. The composite structure became uniform as a result of the physical and material contribution of slag particles. Also, by adding slag to cemented composite, the greater amount of cementitious materials can be reacted with the moisture of composite. Therefore, more C-S-H is

generated by the reaction between slag and the greater dosage of calcium and water, leading to a reduction in the porosity of mixture.

Moreover, the micro-fabric illustration of the composite schematically suggested the contact points of mixtures. It can be clearly observed that the rubber particles generate a bridge-like connection between the hydrated cement products and sand particles in both the composite. Furthermore, this behaviour can be extended by adding the slag particles, which reduces the porosity of mixture by generating more particles. Increasing the connection points among the components of the composite leads to increase the uniformity and strength behaviour of the composite.

6-5-4: A PHYSICAL MODEL OF FAILURE IN COMPOSITE

Recently, the homogenisation theory of heterogeneous materials has been extensively conducted for a various type of composite materials (Shen, 2006). In this research, the mechanism of deformation of the sand-rubber composite as a heterogeneous body including two elastic mediums is briefly discussed. Damage and fracture mechanics still considered as two key theories for predicting the cracking in homogenous bodies(Shen, 2006). However, understanding the behaviour of geomaterial is required to predict the cracking behaviour of this material. Because, the structure of geomaterial normally behave in a shear state, and the microelement of mixture keep their friction resistance capacity, the concept of transformation needs to be performed for geomaterial.

6-5-4-1: MECHANISM OF DEFORMATION AND BINARY MEDIUM THEORY

The hybrid mechanical characteristics will be the combination of bonding resistance and friction resistance, which are essentially not triggered simultaneously in the case of a cemented material.

The friction resistance will come into effect only after a definite amount of material deformation has taken place, which is often accompanied with strain softening due to the loss of bonding resistance (Shen, 2006). The loss of bonding resistance finally leads to the addition of friction resistance. The loss-gain mechanism can be calibrated by an alternate combination of three ideal mechanical responses, i.e., elastic deformation, plastic yielding and brittle cracking, which, respectively, correspond to individual mechanical elements, i.e., spring (modulus E), slider (yield strength f) and bonded bar (break strength q), as shown in Figure6- 36(a) (Shen, 2006).

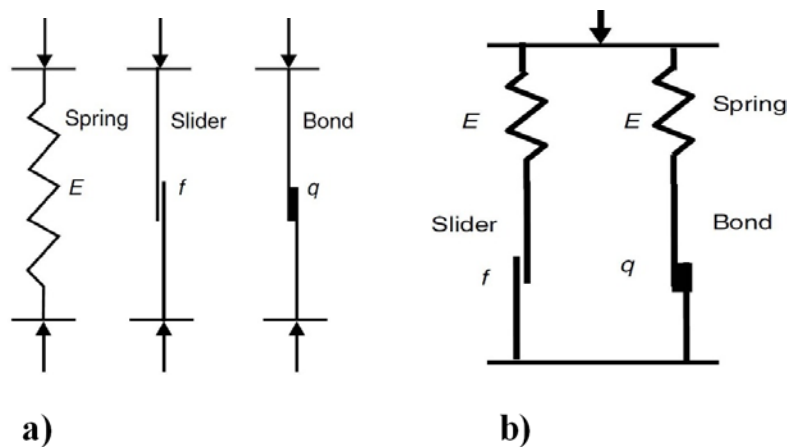


Figure6- 36. Schematic diagram of mechanical response: (a) mechanical elements, (b) binary-medium hybrid unit (Shen, 2006).

One can take advantage of the combination of the elements in modelling the mechanical response of any geomaterial, by imaging a versatile combination of the elements, which will lead to a variety of mechanical modes and match any possible complex behaviour of a geomaterial. Based on these understandings, rubber soil will be calibrated into a mode as shown in Figure6- 36 (b), which consists of a bonding element and a friction element. The former represents a structural resistance, while the latter represents a friction resistance. The two elements can be simulated by an elasto-brittle body and elasto-plastic body, respectively. This will form the basis of the binary-medium hybrid unit for rubber soil modelling framework. As rubber, soil

involves a mixture of two different aggregates, i.e., sand and tire buffing, which essentially differs in physical dimension, mechanical property and mixture orientation. In the shear process, the total stress is concurrently borne by the bonding resistance of the structural element and friction resistance of the friction element, and the progress of failure of rubber soil can be characterised as the break of a bonding element, its conversion into a friction element and the progressive failure of the hybrid unit.

Figure6- 37, presents the scanning electron microscopy results of the cemented sand-rubber composite. It can be seen that the rubber particles are attached to the sand particles by hydrated cement products. The rubber particle can be identified by its specific shapes. Moreover, cracking normally occurred along the interface area between rubber and sand particles. The arrangement of particles in composite has transformed, and the force chains were established to keep composite structure were subjected to a conducted load.

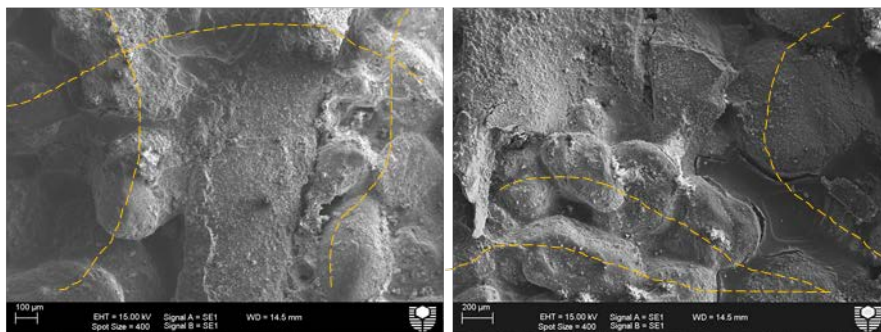


Figure6- 37. SEM micrograph results of the cemented sand-rubber composite.

The presence of rubber particles in composite creates a composite combining soft particles and rigid particles. Therefore, expansion of sand particle chains in the composite can be prevented by rubber particles.

The yellow dashed lines indicate the distributions of force chains in composite (Figure6- 37). The investigation into the force chain behaviour might be suggested the possibility of generation the force network around rubber particles.

Figure6- 38 presents a schematic illustration of deformation mechanism of the cemented sand-rubber composite. The small light grey spherical shapes represent the sand particles, and the big black spots stand for the rubber particles. The presence of cement hydration products in the composite is shown by darker grey rings around the composite particles. The initial phase of the composite depicts that the sand and rubber particles are disorderly organized. The sand particles are initially subjected to normal stress. Subsequently, a series of sand particles were rearranged by applying vertical stress and were stocked together. The direct interconnection between sand particles eventually established the force chains in the composite, resulting in an initial phase of deformation. The red dashed line presented the main force chain generated by sand particles.

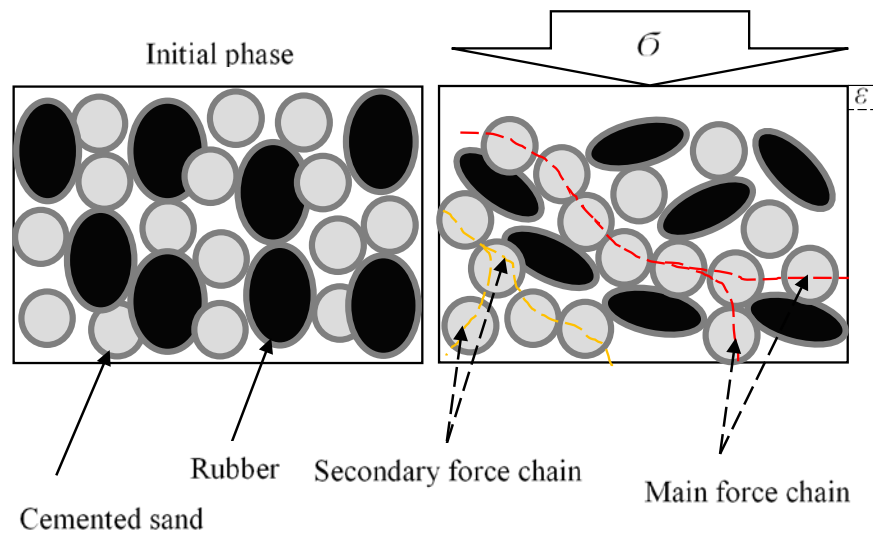


Figure6- 38. Schematic presentation of deformation mechanism of cemented sand-rubber mixture (Zhang et al., 2016)

The occurrence of the next phase of deformation is postponed due to the presence of rubber particles in the composite. The stiff characteristic of rubber particles is contributed to preventing the bulking of force chains at this stage (Lambe and Whitman, 1979 ,Zhang et al., 2016).

It seems that the rubber particles mainly sustain the applied load. The new structure of the mixture is established by changing the rubber shapes and sliding the sand particles. Therefore, a denser structure has been established as a result of particle repositioning and filling the pores of the composite by sand and finer components. Thus, secondary force chain occurs by a greater amount of stress than required for breaking the bonding connection for initial breakage.

CHAPTER7
CONCLUSION AND RECOMMENDATION

7.1 SUMMARY OF CONDUCTED RESEARCH

The carried out research was suggested the benefits of rubber application in geotechnical infrastructure by performing:

- ❖ More than 24 different composites have been studied through a comprehensive series of experimental tests. The composites have been created with a variety percentage of rubber and additives such as cement, slag, and fly ash.
- ❖ Study on the soil compactibility which depends on the soil's texture, characteristic of the soil, particle, and type of the soil. More than 25 standard compaction tests have been performed to an investigation into compaction characteristic of composite soil.
- ❖ Study on the soil compressibility as one of the required parameters in soil design considerations. The compressibility of soil composites has been studied under about 30 one-dimensional compression tests.
- ❖ More than 50 triaxial tests have been performed to examine the soil strength parameters. The efficiency of the application of cement, rubber, and cement-rubber under two conditions (CD and CU) has been investigated.
- ❖ The scale effect has been studied and analysed through near to 300 direct shear tests, in two different scales (large and small).
- ❖ The stress and strain are considered as two main parameters which are play critical role to study the soil strength characteristic. Thus, the triaxial and direct shear tests have been divided into two low and high pressure to find the side of the efficiency of rubber, and cement for these two factors.

The following sections presented a summary of obtained results.

7.1.1 AN OVERVIEW OF SOIL REINFORCEMENT AND CONDUCTED METHODOLOGY

Considering the amount of scrap tire is rapidly increasing in all around the world as a result of an increase in the number of vehicles, seeking various solutions have been recognised (Neaz Sheikh et al., 2013, Feraldi et al., 2013). The Australian government reported that about 52.5 million EPU (i.e. equivalent passenger unit) scrap tire were generated in 2007-2008, whereas only about 35% of these wastes have been recycled (Neaz Sheikh et al., 2013, Australian Government 2010). However, regarding the small diameter and the fibre shape of buffing, it is identified as a perfect additive for establishing the composite material with soil. The integrity, strength, ductility and damping ratio of the backfill can be improved by the solidified cement matrix and altered fabric structure (Lee and Lui, 2000, Shahin et al., 2011, Tsoi and Lee, 2011, Anastasiadis et al., 2012). This research study was performed in four experimental, numerical and microstructural sections. Eighteen mixtures including sand, sand rubber, sand stabilisers and sand-rubber-stabilisers composites were separated into three main groups. The soil composites have been organised into nine categories by ascending degree of cementation, i.e., cement addition of 0%, 5% and 10% by weight, slag addition of 0%, 5% and 10% and the addition of rubber buffing of 0%, 10% and 20% by weight.

Four experimental, numerical and microstructural sections were conducted to study the effects of the addition of rubber and/or a stabiliser for sand reinforcement so as to determine an optimum combination of the stabiliser and rubber Tasks 1-2, the observational scale used in the research, i.e. scale effect study for Tasks 2-3 and to verify the obtained data to propose a regression model based on the availability of input data Tasks 4. By performing Tasks 1-4, a numerical simulation was carried out for predicting the shear strength with different confining pressures. Eventually, the

microstructural observation explained deformation mechanism of composites. The obtained results summarised and presented regarding following objectives.

7.1.2 A SUMMARY OF FUNDAMENTAL EXPERIMENT RESULTS

The minimum compactness amount of sand composites were examined by performing standard test methods for minimum and maximum density and unit weight of soils. The results indicated that the maximum density of mixtures was separated into three groups influenced by the rubber content. The maximum value obtained by applying the stabilisers only and, then, the material with the contribution of 10% and 20% rubber have low density, respectively. In contrast, the minimum void ratio value revealed the opposite behaviour.

Furthermore, results were verified by performing the standard compaction tests. The addition of stabilisers to sand increased the MDD and decreased the OMC of the mixtures. In contrast, the addition of rubber to sand reduced the MDD and the OMC of the sand matrix. This tendency was boosted by increasing the proportion of rubber added; this boost was attributed to the lightweight characteristics of rubber. However, further investigations revealed that the application of rubber into the cemented sand mixture composites mostly leads to reduce in the moisture of composite.

The MDD of the composites was strongly related to the proportion of rubber added to generate the composite structure. Subsequently, ST, STR10 and STR20 were considered specimens with a dense, medium and loose structure, respectively.

Moreover, the addition of a stabiliser to the sand–rubber composites changed the floating case of the matrix to a non-floating case, in which a relatively large number of particles affected the soil behaviour. The similar behaviour observed in specific gravity tests results, which was suggested the influence of shape, size, amount and type of additives on sand's density.

Eventually, the results of MDD were separately modelled by simple linear regression (SLR). The accuracy of the SLR model was reasonable, and the MDD was determined using a correlation value of $R^2 = 0.9047$, $R^2 = 0.9805$ and $R^2 = 0.9718$ for the reinforcement of pure sand, sand with 10% rubber and sand with 20% rubber, respectively, with a stabiliser. The maximum dry density results demonstrated that the optimum mixing ratio was related to the shape, size, amount and type of additives. The smallest and biggest minimum void ratio among the sand-stabiliser-rubber composites were associated with SS10R10 and SC5R20, respectively.

7.1.3 A SUMMARY OF SMALL DIRECT SHEAR TEST RESULTS

108 small direct shear test was conducted on 18 sand specimens with varying amounts of cement and slag (cementitious material), rubber, and a mixture of cementitious material and rubber. Small direct shear tests were performed to study the effect of, normal stress (i.e. low and high vertical load classifications), void ratio and rubber content on the shear strength characteristics of sand composites.

The degree of enhancement in shear strength was related to the dosage of rubber in the composites. The treated sand with rubber only had the minimum shear strength, which behaves similarly to the loose sand. The maximum shear strength was achieved by the combination of 5% of both slag and cement on sand mixtures with no participation of rubber.

However, the strain capacity of the composite was classified by their rubber content, which was the higher rubber content generated specimens with, the greater strain resistance. The connections between the minimum void ratio of composites and the elastic modulus parameters were observed. Creating denser composites occurred because of the reduction of the matrix void ratio. Increasing the normal stress also leads to the decreasing of the matrix void ratio due to increasing the inter-particles friction under higher vertical loads

Also, the highest dilation ratio was obtained by applying equally the 5% cement and slag sample. On the contrary, the maximum contraction behaviour was generated by application of 20% rubber only. Therefore, the addition of either 5% or 10% of any of the stabilisers with 20% rubber has the minimum value of dilation angle, which has the most stable behaviour before and after failure.

The maximum improvement in cohesion value of sand was achieved by introducing the soil tension and cementation, by using equally the 5% cement and slag and 20% rubber sand mixture. Moreover, the friction angle of sand was effectively improved in the composites of ST5R20 and ST10R20 group, with an eight-degree improvement, whereas the minimum improvement was assigned to the SC5S5R0 group.

7.1.4 A SUMMARY OF LARGE DIRECT SHEAR TEST RESULTS

A denser composite was obtained by the addition of a stabiliser material and by filling the pores of the sample. Sand stabilisation with a cementitious material led to a significant degree of interlocking which improved the internal friction on the interface of the composite particles. The improvement in the elastic phase of the shear stress behaviour of sand was attributed to the ductile behaviour of rubber. Moreover, a quasi-elastic behaviour was observed in composites containing both rubber and stabilisers. The results also indicated the importance of the amount of normal stress applied concerning the strength behaviour of the composites.

The scale effect triggered a new type of shear strain behaviour of the sand composite. Increasing the grain boundaries in the same slip led to strain hardening for plastic deformation. The addition of a cementitious material increased the number of connections among the grain boundaries and subsequently, improved the strength characteristic of the mixture. The scale effect also observed by analysing the shear resistance characteristics were caused a failure at a larger displacement.

Overall, the composite containing rubber obtained a greater value in the LDS test than in the SDS test. Moreover, the use of cementitious materials only for sand reinforcement yielded the same results as the small box. A comparison of the stabiliser material also revealed that the same percentage of slag was more effective than cement.

A reasonable correlation between the MDD and the internal friction angle of the sand composites was found. The result suggested the existence of the optimum content of the stabiliser required for generating the maximum friction angle. Moreover, the stabilised sand mixtures exhibited a relatively high friction angle in the constant volume state, which was a roughly similar trend to that of the results of the SDS test.

Also, the results suggested a strong relationship between the composite density and its friction angle either at the failure point or in a constant volume area for each series of the sand matrix. All the three categories exhibited a similar trend with the existence of the optimum ratio of the combination of additives. Increasing the ratio of additives in the sand matrix decreased the friction angle.

The scale effect study on the volumetric behaviour of composite suggested that the relatively large scale provided more space for particle movement to demonstrate the characteristics brought about by the additives. Composites with a larger scale exhibited a wider vertical movement. The contraction behaviour of the sand–rubber mixtures was more obvious on the larger scale, which revealed the shape and the ductility of rubber.

Moreover, the results revealed the importance of the mechanical properties of the composite constituents, which were revealed in the large-scale experiment. In particular, the physical shape and the ductility of rubber play an important role in the shear strength and the shear strain behaviour. The composites containing 20% rubber exhibited more strength at a larger displacement; this could be attributed to the generation of more interactions among the composite particles and the shear box.

Furthermore explanation of dilation ratio considering the zero extension lines theory suggested three typical types of dilation ratio behaviour depending on the components of the composites. The addition of rubber to the sand composites significantly reduced the dilation ratio of the composites the composite did not expand at the failure point.

The stress- dilation law was defined by plotting the peak friction angle and the maximum dilation angle against the normal stress for composites. The maximum values of the friction angle and the dilation were increased by increasing the stabiliser content and subsequently, reduced by adding the rubber content to the composites. Overall, increasing the rubber ratio for sand stabilisation caused to generate a composite which was considerably affected by the rubber properties.

Moreover, a composite's friction angle at a constant volume exhibited an almost similar behaviour to the maximum friction angle. Associating the capacity of cementitious material for connecting a greater number of particles, also of the elastic capacity of rubber particles, leads to generate the composite with a greater strength capacity and significant elastic tension for reducing the dilatancy behaviour.

Eventually, by plotting φ_p versus ψ_{max} , the constant volume friction angle was obtained from the best fit line. Increasing the value of φ_p not only led to a higher ψ_{max} value but also increased the difference between the two angles and subsequently, reduced φ_{cv} . Based on the composite structure three equations were proposed to define the stress-dilation law of composites.

The relationship between apparent cohesion and maximum dry density also suggested indicated that the maximum cohesion was obtained at a specific density. Moreover, an analysis of the difference between the cohesion values at failure point and constant volume state has revealed the effect of the rubber content. Note that the sand mixtures treated with cement significantly lose their cohesiveness in contrast to the sand-slag-treated composites.

7.1.5 A SUMMARY OF COMPRESSIBILITY TEST RESULTS

The results suggest that the compressibility characteristic of sand is increased by the application of compressible material and reduced by the addition of stabiliser materials. Considering the different components of the composites, a relationship was defined between the compressibility and density of soil. The compression index was plotting versus maximum dry density of composite. The compression properties of sand were respectively, increased and reduced by the addition of rubber and stabilisers.

Moreover, increasing the dosage of rubber in sand matrix leads to increase the swell index of the composite, which can verify the resilient properties of rubber to make the compressible composite. However, sand's swelling potential was restricted by adding the cementitious material, notably by slag addition. With a similar behaviour, a denser composite has a lower swelling index, which can be suggested the uniform structure of the composite matrix, with the minimum porosity.

The coefficient of volume compressibility shows the three identical curves, remarkably affecting by the rubber content. The composite with the no rubber particles has the greatest value of one-dimensional elastic modulus which is suggested the lowest deformation among the other composite. The mixtures with 20% rubber have notably indicated the higher deformation and lower elastic modulus than composites including 10% rubber.

Moreover, a persuasive correlation can be defined as the one-dimensional elastic modulus of composites. The composite's elastic modulus was divided into the three main categories, affecting by the rubber fraction. Three rubber fractions were defined based on the %0, %10 and 20% rubber content for both cemented and uncemented composites.

Further investigation of the elastic behaviour of composite performed by triaxial tests was shown a similar trend for Young's modulus behaviour of composites. The greatest and lowest values are respectively obtained by the minimum and maximum dosage of rubber inclusion in the mixtures. However, case by case basis study on the results of one-

dimensional consolidation test and the triaxial test shows reducing the similarity of the result by increasing the confining pressure.

The application of rubber in sand reinforcement was remarkably changed the mechanical response of sand matrix due to the generation a composite with the lower specific gravity, density, and stiffness and simultaneously, the higher capacity in damping and compressibility.

The compression evaluation of composites was classified by analysing the vertical strain tendency of composites versus the effective vertical stress. The particle forces can be classified into particle level force, contact level force and the force generated by applied boundary stresses. Subsequently, the contact level force is mostly affected by the cementitious agents. Also, the cemented material might be respectively divided into bonding control area, bonding degradation and stress control region. The bonding control in all three composite was completed at the vertical stress of 25kPa. However, the ratio of vertical deformation was remarkably affected by the rubber fraction, increasing by using more dosage of the compressible material. Moreover, the most significant effect of rubber application was observed by investigating the bonding degradation region of composites. Notably, the stress control was started at the normal stress of 400kPa, was gradually decreased to 100kPa and 50kPa accordingly performing 10% and 20% rubber. Eventually, inter- particle forces in a composite containing 20% rubber were mostly generated by applied boundary stresses for loading phases.

The normalised strain has been suggested that the mixtures in the bonding control region tend to have a reducing behaviour. It means that the composite was gradually loosed its contact level force and finally were behaved the same as uncemented specimens. Also, the residual deformation increases with the increment of rubber fraction.

7.1.6 A SUMMARY OF TRIAXIAL TEST RESULTS

The effect of the rubber and cement additives on the deviatoric stress of sand composites were studied by conducting the triaxial tests. The shear strength characteristic of the sand matrix has been increased by the dosage of additives. The deviatoric stress of sand increases with increasing both cement and rubber ratio in the specimens. Moreover, the failure points of specimens have been enhanced by increasing the rubber content by increasing the inter-particle interaction in the composite.

Three failure patterns were observed in triaxial specimens accompanying with the composite ingredient. Sand specimens containing only cement have failed with the localised shear band caused to progress the softening behaviour of mixtures after peak strength. A localised bulging failure was observed in sand-rubber mixtures. Eventually, a failure mode with a combination of crushing at the lower part and localised bulging was observed in cemented sand-rubber mixtures, suggested a strong hardening in the composite.

Moreover, at all confining pressures, the peak deviator stress was generally improved by increasing the rubber content. Performing the triaxial test with a higher confining pressure caused to reduce the effectiveness of the dosage of rubber on the peak deviatoric stress in sand-rubber mixtures.

The similar behaviour observed for strain resistance of composites. At all confining pressures, the axial strain corresponding with the peak deviatoric stress was increased by the increasing dosage of rubber in sand mixtures. The compressive shear strain capacity of the composite is dominantly related with the rubber content. The peak deviatoric stress, axial strain at the failure point and stiffness are increased with the increase in confining pressure.

Furthermore, maximum principle stresses analysis revealed that the stress ratio decreases with the increase in confining pressure. Depends on the constituent of composite

the stress ratio at each confining pressure is different and affected by cement content. Increasing the confining pressure caused to reduce the sand-to-sand particle and increase the rubber-to-rubber particle.

Eventually, the intrinsic concept was used as a basic frame of reference for interpreting and evaluating the shear strength properties of the sand-rubber mixture. The obtained data was firstly verified the result of direct shear test. The collected data were then used to propose a regression model based on the availability of input data. Two regression models were established based on the degree of availability of shear strength parameters of the studied sand composites. An overall accuracy of the proposed model is eventually compared by the laboratory data of small direct shear tests.

7.1.7 A SUMMARY OF MICROSTRUCTURAL STUDY

Further investigation into the effectiveness of additives on sand composites was conducted by a microstructural study on cemented sand rubber composite. Results suggest that, composites can be considered as a mixtures with a heterogeneous microstructure including of some binding medium and aggregate particles consist of three phases: a) the hardened cement paste b) the pore structure c) interfacial transition zone (ITZ).

The results suggest that the presence of rubber particles in composite serve a similar role as superplasticisers in the high performance concrete cause to reduce the surface tension of surrounding water, after adsorbed on cement particles. The cement particles might be scattered by the addition of rubber particles within a similar manner as the steric effect and electrostatic repulsion.

Moreover, the ability of slag o reduces the moisture of mixture leads to generate a denser mixture by decreasing the porosity and increasing the homogeneity of the composite.

Subsequently, the strength capacity of composite increased by improving the properties of interfacial transition zone (ITZ). Alternating the particle shape size, mineral composition, surface roughness and moisture content, the porosity of aggregates and the water-cement ratio were enhanced the characteristic of generated bond in ITZ.

Another factor that plays a pivotal role in sand reinforcement is the establishment of the chemical components, leads to increasing the shear strength characteristic of the cemented sand-rubber composite. Adding slag to the mixture cause to generate the more compounds of tri-calcium aluminoferrite in the composite by increasing the hydration products.

Moreover, in the presence of rubber particles a smaller amount of moisture is absorbed by ASR gel, and subsequently, the amount of ASR distress is reduced. Subsequently, absorbing an amount of ASR gel by the rubber particle, firstly the micro-cracks in the composite was reduced and secondly was localised in the area with rubber content.

Eventually, the mechanism of deformation of composite simulated by an elasto-brittle body and elasto-plastic body. Cracking normally occurred along the interface area between rubber and sand particles. The sand particles are initially subjected to normal stress. Subsequently, a series of sand particles were rearranged by applying vertical stress and were stocked together. The direct interconnection between sand particles eventually established the force chains in the composite, resulting in an initial phase of deformation. Therefore, a denser structure has been established as a result of particle repositioning and filling the pores of the composite by sand and finer components.

7.2 RECOMMENDATION AND FUTURE STUDY

Based on the research program conducted in this study, the following recommendations are suggested for future study.

7.2.1 RECOMMENDATION

1. This research study recommends that the application of small-strain dynamic properties could provide the accurate data of composites composed of cemented and uncemented sand with rubber buffing.
2. Providing a constitutive model for rubber soil composites to evaluate the mechanical response of rubber soil and predict the response of that the material to external stimuli, mimicking the situations in field applications.
3. Development of a numerical model based on the binary-medium model to predict the progressive breakage of bonding elements, its conversion to friction elements, the generation of shear zone or band, and the failure mode of the materials.
4. This research study recommends that the application of rubber buffing in the cemented mixture can provide the high performance cemented composite. This research also suggests the additional microanalytical examinations on the composite to provide an accurate understanding of the microstructural characteristic on cemented and uncemented sand rubber composites.

7.2.2 FURTHER PERFORMED RESEARCH

The additional researches were conducted to verify the finding of this research study:

1. The comparative experimental study was conducted to study the applicability of the optimum dosage of additives, was defined in this research, on the three different kinds of WA soil.
2. The additional research was performed by the other type of cementitious material, and its effectiveness was compared with the results of slag and cement application were used in this research study.
3. Analysing the curing time as an effective parameters factor on shear strength properties of the composite were also evaluated by performing a series of experimental tests.

REFERENCES:

- ACI COMMITTEE 229. (1999) Controlled Low-Strength Materials. American Concrete Institute.
- A. BERNAL, R. SALGADO, R.H. SWAN & LOVELL, C. W. 1997. Interaction Between Tire Shreds, Rubber-Sand and Geosynthetics .pdf.
- AFSHINNIA, K. & POURSAEE, A. 2015. The influence of waste crumb rubber in reducing the alkali-silica reaction in mortar bars. *Journal of Building Engineering*, 4, 231-236.
- AFZALI-NEJAD, A., LASHKARI, A. & SHOURIJEH, P. T. 2017. Influence of particle shape on the shear strength and dilation of sand-woven geotextile interfaces. *Geotextiles and Geomembranes*, 45, 54-66.
- AHMED, I. & LOVELL, C. 1993. Rubber soils as lightweight geomaterials. Transportation research record.
- AIREY, D. 1993. Triaxial testing of naturally cemented carbonate soil. *Journal of Geotechnical Engineering*, 119, 1379-1398.
- AL-REFEAI, T. O. 1991. Behavior of granular soils reinforced with discrete randomly oriented inclusions. *Geotextiles and Geomembranes*, 10, 319-333.
- AMINI, Y., HAMIDI, A. & ASGHARI, E. 2014. Shear strength-dilation characteristics of cemented sand-gravel mixtures. *International Journal of Geotechnical Engineering*, 8, 406-413.
- AMIRALIAN, S., BUDIHardjo, M. A., CHEGENIZADEH, A. & NIKRAZ, H. 2015. Study of scale effect on strength characteristic of stabilised composite with sewage sludge – Part A: Preliminary study. *Construction and Building Materials*, 80, 339-345.
- ANASTASIADIS, A., SENETAKIS, K. & PITILAKIS, K. 2012. Small-strain shear modulus and damping ratio of sand-rubber and gravel-rubber mixtures. *Geotechnical and Geological Engineering*, 30, 363-382.
- ANBAZHAGAN, P., MANOHAR, D. R. & ROHIT, D. 2016. Influence of size of granulated rubber and tyre chips on the shear strength characteristics of sand-rubber mix. *Geomechanics and Geoengineering*, 1-13.
- ANVARI, S. M., SHOOSH PASHA, I. & KUTANA EI, S. S. 2017. Effect of granulated rubber on shear strength of fine-grained sand. *Journal of Rock Mechanics and Geotechnical Engineering*.
- ASTM D698 2015. ASTM D698-Standard Test Methods for Laboratory Compaction Characteristics of Soil Using Standard Effort Method A (Standard Proctor).
- ASTM D854 2014. Standard Test Methods for Specific Gravity of Soil Solids by Water Pycnometer.
- ASTM D2435 2011. ASTM D2435-Standard Test Methods for One-Dimensional Consolidation Properties of Soils Using Incremental Loading.
- ASTM D3080 2011. ASTM D3080-Standard Test Method for Direct Shear Test of Soils Under Consolidated Drained Conditions. ASTM International.
- ASTM D4253 2016. ASTM D4253-Standard Test Methods for Maximum Index Density and Unit Weight of Soils Using a Vibratory Table. ASTM International.
- ASTM D4254 2016. ASTM D4254-Standard Test Methods for Minimum Index Density and Unit Weight of Soils and Calculation of Relative Density. ASTM International.
- ASTM D4767 2011. Standard Test Method for Consolidated Undrained Triaxial Compression Test for Cohesive Soils.
- ASTM D6913 2017. ASTM D6913-Standard Test Methods for Particle-Size Distribution (Gradation) of Soils Using Sieve Analysis.
- ATTOM, M. F. 2006. The use of shredded waste tires to improve the geotechnical engineering properties of sands. *Environmental Geology*, 49, 497-503.
- AUSTRALIAN TYRE RECYCLERS ASSOCIATION (2006) ATRA Response to Productivity Commission Issues Paper on Waste Generation and Resource Efficiency.
- AUSTRALIAN GOVERNMENT. (2010). "Product stewardship for the end of life tyres." Dept. of Sustainability, Environment, Water, Population and Communities, Canberra, ACT, Australia, (<http://www.environment.gov.au/settlements/waste/tyres/index.html>) (Jun. 10, 2013).

- BAREITHER, C. A., BENSON, C. H. & EDIL, T. B. 2008. Comparison of shear strength of sand backfills measured in small-scale and large-scale direct shear tests. *Canadian Geotechnical Journal*, 45, 1224-1236.
- BECQUART, F. 2006. Caractérisation du comportement mécanique d'un mâchefer dans la perspective d'une méthodologie de dimensionnement adaptée aux structures de chaussées. XXIVèmes rencontres universitaires de Génie Civil.
- BIGNOZZI, M. & SANDROLINI, F. 2006. Tyre rubber waste recycling in self-compacting concrete. *Cement and concrete research*, 36, 735-739.
- BOLTON, M. 1986. The strength and dilatancy of sands. *Geotechnique*, 36, 65-78.
- BOLTON, M. 1987. Discussion: The strength and dilatancy of sands. *Geotechnique*, 37, 219-226.
- BOSSCHER, P. J., EDIL, T. B. & ELDIN, N. N. 1992. Construction and performance of a shredded waste tire test embankment. *Transportation Research Record*.
- BOSSCHER, P. J., EDIL, T. B. & KURAOKA, S. 1997. Design of highway embankments using tire chips. *Journal of Geotechnical and Geoenvironmental Engineering*, 123, 295-304.
- CABALAR, A. F. 2011. Direct Shear Tests on Waste Tires–Sand Mixtures. *Geotechnical and Geological Engineering*, 29, 411-418.
- CERATO, A. & LUTENEGGER, A. 2006. Specimen Size and Scale Effects of Direct Shear Box Tests of Sands. *Geotechnical Testing Journal*, 29, 10.
- CHABANNES, M., BECQUART, F., GARCIA-DIAZ, E., ABRIAK, N.-E. & CLERC, L. 2017. Experimental investigation of the shear behaviour of hemp and rice husk-based concretes using triaxial compression. *Construction and Building Materials*, 143, 621-632.
- CHRIST, M. & PARK, J.-B. 2010. Laboratory determination of strength properties of frozen rubber–sand mixtures. *Cold Regions Science and Technology*, 60, 169-175.
- CONSOLI NILO, C., MONTARDO JÚLIO, P., PRIETTO PEDRO DOMINGOS, M. & PASA GIOVANA, S. 2002. Engineering Behavior of a Sand Reinforced with Plastic Waste. *Journal of Geotechnical and Geoenvironmental Engineering*, 128, 462-472.
- COOP, M. & ATKINSON, J. 1993. The mechanics of cemented carbonate sands. *Geotechnique*, 43, 53-67.
- CRISTELO, N., GLENDINNING, S., FERNANDES, L. & PINTO, A. T. 2012. Effect of calcium content on soil stabilisation with alkaline activation. *Construction and Building Materials*, 29, 167-174.
- CUCCOVILLO, T. & COOP, M. 1998. Yielding and pre-failure deformation of structured sands. Pre-failure deformation behaviour of geomaterials, 105.
- DAS, B. M. 2013. *Advanced soil mechanics*, CRC Press.
- DAVIS, E. H. & POULOS, H. G. 1968. The use of elastic theory for settlement prediction under three-dimensional conditions. *Geotechnique*, 18, 67-91.
- DENG, A. & FENG, J.-R. Granular lightweight fill composed of sand and tire scrap. *Characterization, Modeling, and Performance of Geomaterials: Selected Papers From the 2009 GeoHunan International Conference*, 2009. 78-85.
- DENG, A. & FENG, J. 2011. Shear behavior of sand-tire bead mixtures.
- DENG, A. & XIAO, Y. 2008. Shear behavior of sand-expanded polystyrene beads lightweight fills. *Journal of Central South University of Technology*, 15, 174-179.
- DICKSON, T., DWYER, D. & HUMPHREY, D. 2001a. Prototype Tire-Shred Embankment Construction. *Transportation Research Record: Journal of the Transportation Research Board*, 1755, 160-167.
- DICKSON, T., DWYER, D. & HUMPHREY, D. 2001b. Prototype tire-shred embankment construction. *Transportation Research Record: Journal of the Transportation Research Board*, 160-167.
- DOMONE, P. & ILLSTON, J. 2010. *Construction materials: their nature and behaviour*, CRC Press.

- DOVE, J. E. & JARRETT, J. B. 2002. Behavior of dilative sand interfaces in a geotribology framework. *Journal of geotechnical and geoenvironmental engineering*, 128, 25-37.
- DU, L. & FOLLIARD, K. J. 2005. Mechanisms of air entrainment in concrete. *Cement and concrete research*, 35, 1463-1471.
- DUNCAN, J. M. & CHANG, C.-Y. 1970. Nonlinear analysis of stress and strain in soils. *Journal of Soil Mechanics & Foundations Div.*
- EDIL, T. B. & BOSSCHER, P. J. 1992. DEVELOPMENT OF ENGINEERING CRITERIA FOR SHREDDED WASTE TIRES IN HIGHWAY APPLICATIONS. FINAL REPORT.
- EDIL, T. B. & BOSSCHER, P. J. 1994. Engineering properties of tire chips and soil mixtures. *Geotechnical testing journal*, 17, 453-464.
- EDINÇLILER, A. Using waste tire-soil mixtures for embankment construction. Proceedings of the international workshop on scrap tire derived geomaterials—opportunities and challenges, Yokosuka, Japan, 2007. 319-328.
- EDINÇLILER, A. & AYHAN, V. 2010. Influence of tire fiber inclusions on shear strength of sand. *Geosynthetics International*, 17, 183-192.
- EDINÇLILER, A., BAYKAL, G. & DENGİLİ, K. 2004. Determination of static and dynamic behavior of recycled materials for highways. *Resources, conservation and Recycling*, 42, 223-237.
- EDINÇLILER, A., BAYKAL, G. & SAYGILI, A. 2010. Influence of different processing techniques on the mechanical properties of used tires in embankment construction. *Waste Management*, 30, 1073-1080.
- ELGART, E. S., GUSOVSKY, T. & ROSENBERG, M. D. 1975. Preparation and characterization of an enzymatically active immobilized derivative of myosin. *Biochim Biophys Acta*, 410, 178-92.
- FATTUHI, N. & CLARK, L. 1996. Cement-based materials containing shredded scrap truck tyre rubber. *Construction and building materials*, 10, 229-236.
- FERALDI, R., CASHMAN, S., HUFF, M. & RAAHAUGE, L. 2013. Comparative LCA of treatment options for US scrap tires: material recycling and tire-derived fuel combustion. *The International Journal of Life Cycle Assessment*, 18, 613-625.
- FIORAVANTE, V. 2002. On the shaft friction modelling of non-displacement piles in sand. *Soils and Foundations*, 42, 23-33.
- FOOSE, G. J., BENSON, C. H. & BOSSCHER, P. J. 1996. Sand reinforced with shredded waste tires. *Journal of Geotechnical Engineering*, 122, 760-767.
- FRAGASZY, R., SU, W. & SIDDIQI, F. 1990. Effects of Oversize Particles on the Density of Clean Granular Soils.
- FROST, J., DEJONG, J. & RECALDE, M. 2002. Shear failure behavior of granular-continuum interfaces. *Engineering Fracture Mechanics*, 69, 2029-2048.
- GACKE, S., LEE, M. & BOYD, N. 1997. Field performance and mitigation of shredded tire embankment. *Transportation Research Record: Journal of the Transportation Research Board*, 81-89.
- GANJIAN, E., KHORAMI, M. & MAGHSOUDI, A. A. 2009. Scrap-tyre-rubber replacement for aggregate and filler in concrete. *Construction and Building Materials*, 23, 1828-1836.
- GARGA, V. K. & O'SHAUGHNESSY, V. 2000. Tire-reinforced earthfill. Part 1: Construction of a test fill, performance, and retaining wall design. *Canadian Geotechnical Journal*, 37, 75-96.
- GHAZAVI, M. 2004. Shear strength characteristics of sand-mixed with granular rubber. *Geotechnical & Geological Engineering*, 22, 401-416.
- GHAZAVI, M. & SAKHI, M. A. 2005. Influence of optimized tire shreds on shear strength 382.pdf>.
- GRATCHEV, I. B., SASSA, K., OSIPOV, V. I. & SOKOLOV, V. N. 2006. The liquefaction of clayey soils under cyclic loading. *Engineering Geology*, 86, 70-84.

- GRAY, D. & MAHER, M. Admixture stabilization of sand with discrete randomly distributed fibers. Proceedings of XII International Conference on Soil Mechanics and Foundation Engineering, Rio de Janeiro, Brazil, 1989. 1363-1366.
- GRAY, D. H. & AL-REFEAI, T. 1986. Behavior of fabric-versus fiber-reinforced sand. *Journal of Geotechnical Engineering*, 112, 804-820.
- GUEDES, M., EVANGELISTA, L., DE BRITO, J. & FERRO, A. C. 2013. Microstructural Characterization of Concrete Prepared with Recycled Aggregates. *Microscopy and Microanalysis*, 19, 1222-1230.
- GULERIA, S. & DUTTA, R. 2011. Unconfined compressive strength of fly ash–lime–gypsum composite mixed with treated tire chips. *Journal of Materials in Civil Engineering*, 23, 1255-1263.
- GUPTA, T., CHAUDHARY, S. & SHARMA, R. K. 2016. Mechanical and durability properties of waste rubber fiber concrete with and without silica fume. *Journal of Cleaner Production*, 112, 702-711.
- HATAF, N. & RAHIMI, M. M. 2006. Experimental investigation of bearing capacity of sand reinforced with randomly distributed tire shreds. *Construction and Building Materials*, 20, 910-916.
- HAZARIKA, H. & YASUHARA, K. 2007. Scrap Tire Derived Geomaterials-Opportunities and Challenges: Proceedings of the International Workshop IW-TDGM 2007 (Yokosuka, Japan, 23-24 March 2007), CRC Press.
- HIDALGO SIGNES, C., MARTÍNEZ FERNÁNDEZ, P., MEDEL PERALLÓN, E. & INSA FRANCO, R. 2015. Characterisation of an unbound granular mixture with waste tyre rubber for subballast layers. *Materials and Structures*, 48, 3847-3861.
- HILAL, A. A. 2016. Microstructure of Concrete. In: YILMAZ, S. & OZMEN, H. B. (eds.) *High Performance Concrete Technology and Applications*. Rijeka: InTech.
- HILL, R. 1963. Elastic properties of reinforced solids: some theoretical principles. *Journal of the Mechanics and Physics of Solids*, 11, 357-372.
- HOARE, D. Laboratory study of granular soils reinforced with randomly oriented discrete fibers. Proceedings of the International Conference on Soil Reinforcement, 1979. 47-52.
- HORPIBULSUK, S., SUDDEEPPONG, A., CHINKULKIJNIWAT, A. & LIU, M. D. 2012. Strength and compressibility of lightweight cemented clays. *Applied Clay Science*, 69, 11-21.
- HOSSAIN, M. A. & YIN, J.-H. 2015. Dilatancy and Strength of an Unsaturated Soil-Cement Interface in Direct Shear Tests. *International Journal of Geomechanics*, 15, 04014081.
- HUGGINS, E. & RAVICHANDRAN, N. 2011. Numerical study on the dynamic behavior of retaining walls backfilled with shredded tires. *Geo-Risk 2011: Risk Assessment and Management*.
- HUMPHREY, D. Tire derived aggregate as lightweight fill for embankments and retaining walls. Proceedings of the International Workshop on Scrap Tire Derived Geomaterials–Opportunities and Challenges, IW-TDGM, 2007. 59-81.
- HUMPHREY, D. & BLUMENTHAL, M. 2010. The Use of Tire-Derived Aggregate in Road Construction Applications. *Green Streets and Highways 2010*.
- HUMPHREY, D. N. 1996. Investigation of exothermic reaction in tire shred fill located on SR 100 in Ilwaco, Washington, DN Humphrey.
- HUMPHREY, D. N., WHETTEN, N., WEAVER, J., RECKER, K. & COSGROVE, T. A. Tire shreds as lightweight fill for embankments and retaining walls. *Recycled Materials in Geotechnical Applications*, 1998. ASCE, 51-65.
- INDRARATNA, B., IONESCU, D. & CHRISTIE, H. 1998. Shear behavior of railway ballast based on large-scale triaxial tests. *Journal of geotechnical and geoenvironmental Engineering*, 124, 439-449.
- INFANTE, D. J. U., MARTINEZ, G. M. A., ARRUA, P. A. & EBERHARDT, M. 2016. Shear Strength Behavior of Different Geosynthetic Reinforced Soil Structure from Direct Shear Test. *International Journal of Geosynthetics and Ground Engineering*, 2, 17.

- JEWELL, R. 1980. Some effects of reinforcement on the mechanical behaviour of soils. University of Cambridge.
- JUST, A. & MIDDENDORF, B. 2009. Microstructure of high-strength foam concrete. *Materials characterization*, 60, 741-748.
- KANIRAJ, S. R. & HAVANAGI, V. G. 2001. Behavior of cement-stabilized fiber-reinforced fly ash-soil mixtures. *Journal of geotechnical and geoenvironmental engineering*, 127, 574-584.
- KIM, H.-K. & SANTAMARINA, J. 2008. Sand-rubber mixtures (large rubber chips). *Canadian Geotechnical Journal*, 45, 1457-1466.
- KNAPPETT, J. A. & CRAIG, R. F. 2012. *Craig's soil mechanics*, Spon Press.
- KOCABA, V., GALLUCCI, E. & SCRIVENER, K. L. 2012. Methods for determination of degree of reaction of slag in blended cement pastes. *Cement and Concrete Research*, 42, 511-525.
- KOERNER, R. M. 2012. *Designing with geosynthetics*, Xlibris Corporation.
- KOSMATKA, S., KERKHOFF, B. & PANARESE, W. 2002. *Design and Control of Concrete Mixtures*, Portland Cement Association. 2002 (rev. 2008). 372p. ISBN 0-89312-217-3, information on: <http://www.scribd.com/doc/38044723/Design-and-Control-of-Concrete-Mixtures-PCA>.
- KUMRUZZAMAN, M. & YIN, J. 2012. Stress-Strain Behaviour of Completely Decomposed Granite in Both Triaxial and Plane Strain Conditions. *Jordan Journal of Civil Engineering*, 6, 83-108.
- LADE, P., LIGGIO, C. & YAMAMURO, J. 1998. Effects of Non-Plastic Fines on Minimum and Maximum Void Ratios of Sand.
- LAMBE, T. W. & WHITMAN, R. V. 1979. *Soil Mechanics*, SI Version, J. Wiley and Sons, New York.
- LEE, C., SHIN, H. & LEE, J. S. 2014. Behavior of sand-rubber particle mixtures: experimental observations and numerical simulations. *International Journal for Numerical and Analytical Methods in Geomechanics*, 38, 1651-1663.
- LEE, C., TRUONG, Q. H. & LEE, J.-S. 2010. Cementation and bond degradation of rubber-sand mixtures. *Canadian Geotechnical Journal*, 47, 763-774.
- LEE, J.-S., DODDS, J. & SANTAMARINA, J. C. 2007. Behavior of Rigid-Soft Particle Mixtures. *Journal of Materials in Civil Engineering*, 19, 179-184.
- LEE, J., SALGADO, R., BERNAL, A. & LOVELL, C. 1999. Shredded tires and rubber-sand as lightweight backfill. *Journal of geotechnical and geoenvironmental engineering*, 125, 132-141.
- LEE, K. & LUI, L. Permanent and massive utilization of scrap rubber tires as lightweight geomaterials. *Proceedings of the ISWA international symposium on waste management in Asian cities*, Hong Kong, 2000. 367-372.
- LEROUEIL, S. & VAUGHAN, P. 2009. The general and congruent effects of structure in natural soils and weak rocks. *Selected papers on geotechnical engineering by PR Vaughan*. Thomas Telford Publishing.
- LI, G., STUBBLEFIELD, M. A., GARRICK, G., EGGERS, J., ABADIE, C. & HUANG, B. 2004. Development of waste tire modified concrete. *Cement and Concrete Research*, 34, 2283-2289.
- LINGS, M. & DIETZ, M. 2005. The peak strength of sand-steel interfaces and the role of dilation. *Soils and Foundations*, 45, 1-14.
- MA, G., ZHOU, W., CHANG, X.-L., NG, T.-T. & YANG, L.-F. 2016. Formation of shear bands in crushable and irregularly shaped granular materials and the associated microstructural evolution. *Powder Technology*, 301, 118-130.
- MAHER, M. H. & GRAY, D. H. 1990. Static response of sands reinforced with randomly distributed fibers. *Journal of Geotechnical Engineering*, 116, 1661-1677.
- MAIRE, E., COLOMBO, P., ADRIEN, J., BABOUT, L. & BIASETTO, L. 2007. Characterization of the morphology of cellular ceramics by 3D image processing of X-ray tomography. *Journal of the European Ceramic Society*, 27, 1973-1981.

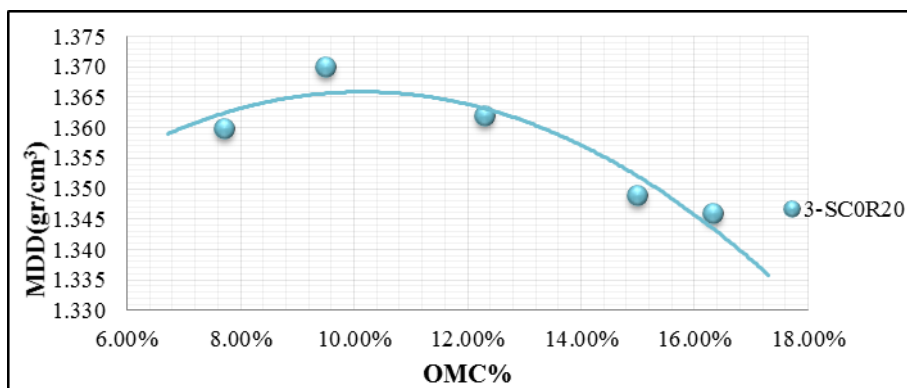
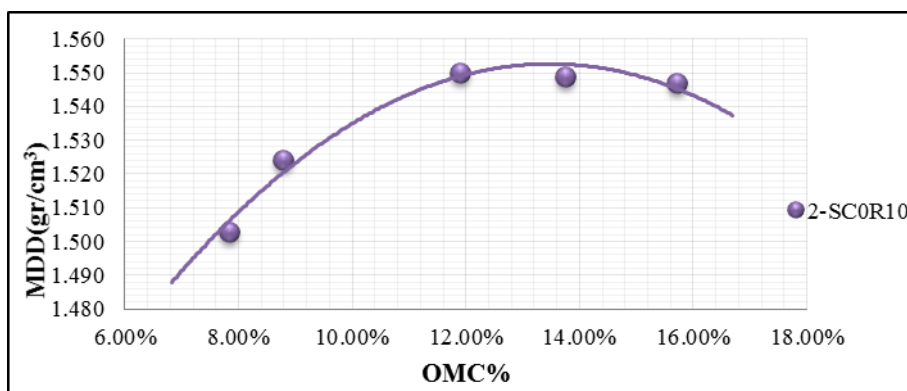
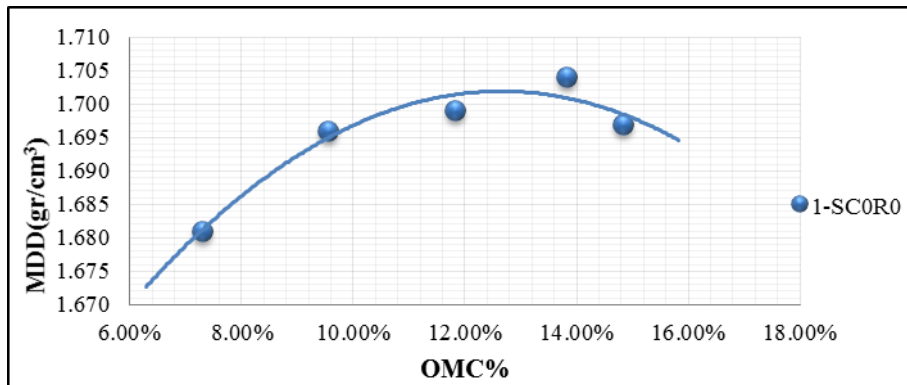
- MASAD, E., TAHA, R., HO, C. & PAPAGIANNAKIS, T. 1996. Engineering properties of tire/soil mixtures as a lightweight fill material.
- MASHIRI, M. S., VINOD, J. S., SHEIKH, M. N. & TSANG, H.-H. 2015. Shear strength and dilatancy behaviour of sand–tyre chip mixtures. *Soils and Foundations*, 55, 517-528.
- MCGOWN, A., ANDRAWES, K. Z. & AL-HASANI, M. M. 1978. Effect of inclusion properties on the behaviour of sand. *Géotechnique*, 28, 327-346.
- MONDAL, P., SHAH, S. P. & MARKS, L. 2007. A reliable technique to determine the local mechanical properties at the nanoscale for cementitious materials. *Cement and Concrete Research*, 37, 1440-1444.
- MONTEIRO, P. 2006. *Concrete: microstructure, properties, and materials*, McGraw-Hill Publishing.
- MOO-YOUNG, H., SELLASIE, K., ZEROKA, D. & SABNIS, G. 2003. Physical and Chemical Properties of Recycled Tire Shreds for Use in Construction. *Journal of Environmental Engineering*, 129, 921-929.
- NAJIM, K. & HALL, M. 2010. A review of the fresh/hardened properties and applications for plain-(PRC) and self-compacting rubberised concrete (SCRC). *Construction and building materials*, 24, 2043-2051.
- NAJIM, K. B. & HALL, M. R. 2012. Mechanical and dynamic properties of self-compacting crumb rubber modified concrete. *Construction and building materials*, 27, 521-530.
- NAJIM, K. B. & HALL, M. R. 2013. Crumb rubber aggregate coatings/pre-treatments and their effects on interfacial bonding, air entrapment and fracture toughness in self-compacting rubberised concrete (SCRC). *Materials and Structures*, 46, 2029-2043.
- NEAZ SHEIKH, M., MASHIRI, M. S., VINOD, J. S. & TSANG, H.-H. 2013. Shear and Compressibility Behavior of Sand–Tire Crumb Mixtures. *Journal of Materials in Civil Engineering*, 25, 1366-1374.
- NEVILLE, A. 1995. Chloride attack of reinforced concrete: an overview. *Materials and Structures*, 28, 63.
- NGO, A. T. & VALDES, J. R. 2007. Creep of Sand–Rubber Mixtures. *Journal of materials in civil engineering*, 19, 1101-1105.
- ÖZKUL, Z. H. & BAYKAL, G. 2007. Shear behavior of compacted rubber fiber-clay composite in drained and undrained loading. *Journal of geotechnical and Geoenvironmental engineering*, 133, 767-781.
- PARK, S.-S. 2009. Effect of fiber reinforcement and distribution on unconfined compressive strength of fiber-reinforced cemented sand. *Geotextiles and Geomembranes*, 27, 162-166.
- PEDLEY, M. J. 1990. *The performance of soil reinforcement in bending and shear*. University of Oxford.
- POULOS, S. J. 1981. The steady state of deformation. *Journal of Geotechnical and Geoenvironmental Engineering*, 107.
- RAMAMURTHY, K., NAMBIAR, E. K. & RANJANI, G. I. S. 2009. A classification of studies on properties of foam concrete. *Cement and Concrete Composites*, 31, 388-396.
- RAO, G. V. & DUTTA, R. 2006a. Compressibility and strength behaviour of sand–tyre chip mixtures. *Geotechnical and Geological Engineering*, 24, 711-724.
- RAO, G. V. & DUTTA, R. K. 2006b. Compressibility and Strength Behaviour of Sand–tyre Chip Mixtures. *Geotechnical & Geological Engineering*, 24, 711-724.
- ROSCOE, K. H. 1970. The influence of strains in soil mechanics. *Geotechnique*, 20, 129-170.
- ROWE, P. 1969. The relation between the shear strength of sands in triaxial compression, plane strain and direct. *Geotechnique*, 19, 75-86.
- ROWE, P. & BARDEN, L. 1964. Importance of free ends in triaxial testing. *Journal of Soil Mechanics & Foundations Div*, 90.
- SCHOFIELD, A. & WROTH, P. 1968. *Critical state soil mechanics*, McGraw-Hill London.

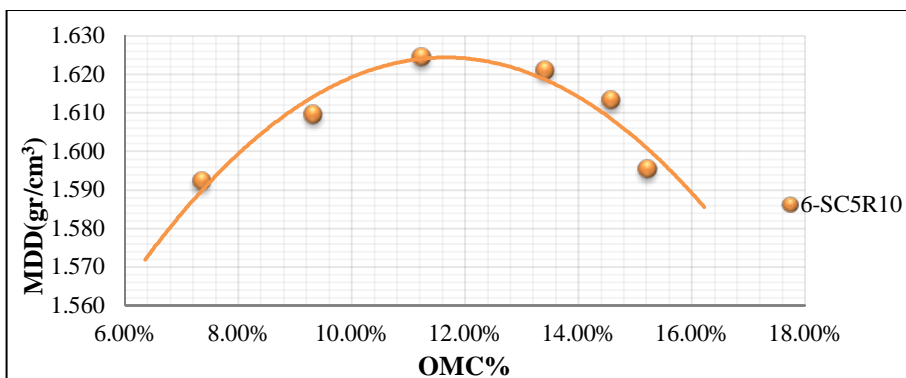
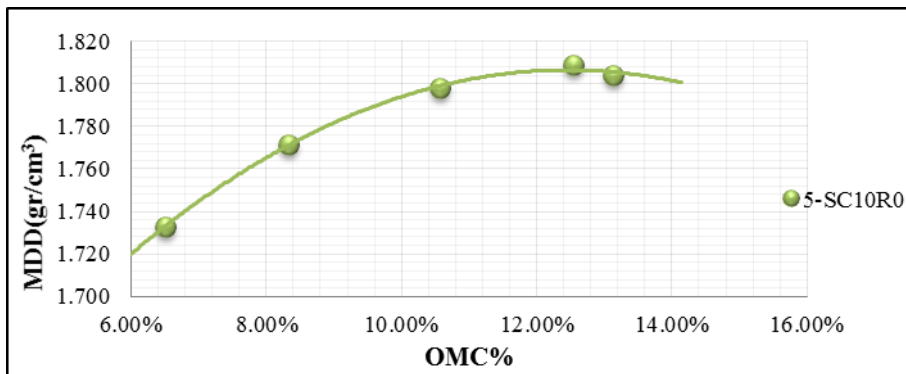
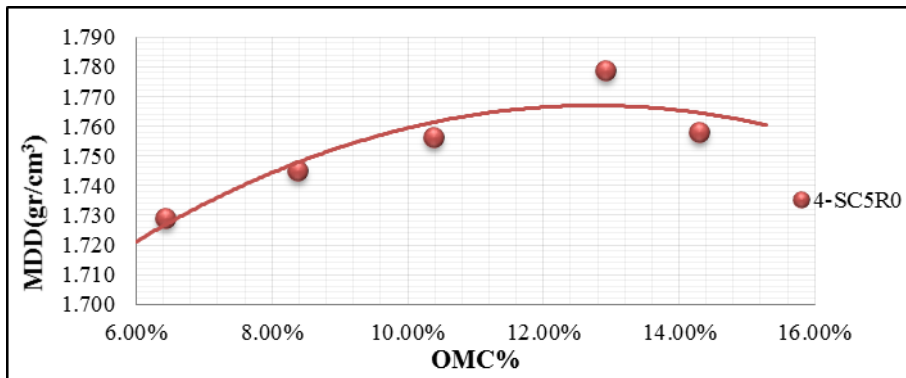
- SHAHIN, M., MARDESIC, T. & NIKRAZ, H. 2011. Geotechnical characteristics of bauxite residue sand mixed with crumbed rubber from recycled car tires. *Journal of GeoEngineering*, 6, 63-72.
- SHALABY, A. & AHMED KHAN, R. 2002. Temperature monitoring and compressibility measurement of a tire shred embankment: Winnipeg, Manitoba, Canada. *Transportation Research Record: Journal of the Transportation Research Board*, 67-75.
- SHEN, Z.-J. 2006. Progress in binary medium modeling of geological materials. *Modern Trends in Geomechanics*. Springer.
- SIMONI, A. & HOULSBY, G. T. 2006. The Direct Shear Strength and Dilatancy of Sand-gravel Mixtures. *Geotechnical and Geological Engineering*, 24, 523-549.
- SON, K. S., HAJIRASOULIHA, I. & PILAKOUTAS, K. 2011. Strength and deformability of waste tyre rubber-filled reinforced concrete columns. *Construction and building materials*, 25, 218-226.
- TABUCANON, J. T., AIREY, D. W. & POULOS, H. G. 1995. Pile skin friction in sands from constant normal stiffness tests.
- TANCHAISAWAT, T., VOOTTIPRUEX, P., BERGADO, D. & HAYASHI, S. 2008. Performance of full scale test embankment with reinforced lightweight geomaterials on soft ground. *Lowland Technology International*, 10, 84-92.
- TANDON, V., VELAZCO, D. A., NAZARIAN, S. & PICORNELL, M. 2007. Performance Monitoring of Embankments Containing Tire Chips Case Study.pdf.
- TATLISOZ, N., EDIL, T. B. & BENSON, C. H. 1998. Interaction between reinforcing geosynthetics and soil-tire chip mixtures. *Journal of Geotechnical and Geoenvironmental Engineering*, 124, 1109-1119.
- TAVENAS, F. & ROCHELLE, P. L. 1972. Accuracy of relative density measurements. *Geotechnique*, 22, 549-562.
- TAYLOR, D. 1948. *Fundamentals of soil mechanics*, Chapman And Hall, Limited.; New York.
- TSANG, H.-H., LAM, J. Y., YAGHMAEI-SABEGH, S. & LO, S. 2009. Protecting underground tunnel by rubber-soil mixtures. *TCLEE 2009: Lifeline Earthquake Engineering in a Multihazard Environment*.
- TSANG, H.-H., LO, S. H., XU, X. & NEAZ SHEIKH, M. 2012. Seismic isolation for low-to-medium-rise buildings using granulated rubber-soil mixtures: numerical study. *Earthquake Engineering & Structural Dynamics*, 41, 2009-2024.
- TSOI, W. & LEE, K. 2011. Mechanical properties of cemented scrap rubber tyre chips. *Géotechnique*, 61, 133-141.
- TURATSINZE, A., BONNET, S. & GRANJU, J.-L. 2005. Mechanical characterisation of cement-based mortar incorporating rubber aggregates from recycled worn tyres. *Building and environment*, 40, 221-226.
- TWEEDIE, J., HUMPHREY, D. & SANDFORD, T. 1998. Tire shreds as lightweight retaining wall backfill: active conditions. *Journal of geotechnical and geoenvironmental engineering*, 124, 1061-1070.
- VALDES, J. R. & EVANS, T. M. 2008. Sand-rubber mixtures: Experiments and numerical simulations. *Canadian Geotechnical Journal*, 45, 588-595.
- VALLEJO, L. E. & MAWBY, R. 2000. Porosity influence on the shear strength of granular material-clay mixtures. *Engineering Geology*, 58, 125-136.
- VARDANEGA, P. & BOLTON, M. 2013. Stiffness of clays and silts: Normalizing shear modulus and shear strain. *Journal of Geotechnical and Geoenvironmental Engineering*, 139, 1575-1589.
- VEISKARAMI, M., JAHANANDISH, M. & GHAHRAMANI, A. 2011. Prediction of the bearing capacity and load-displacement behavior of shallow foundations by the stress-level-based ZEL method. *Scientia Iranica*, 18, 16-27.

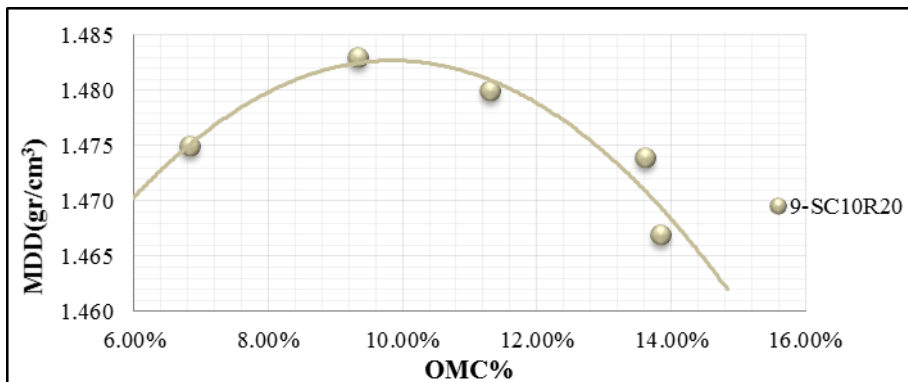
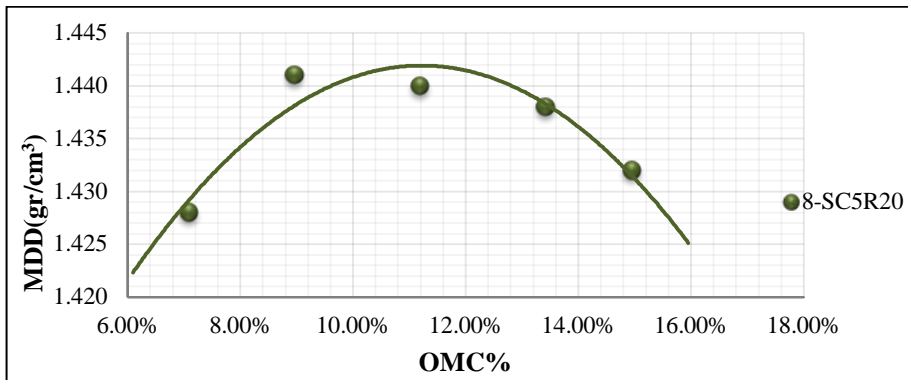
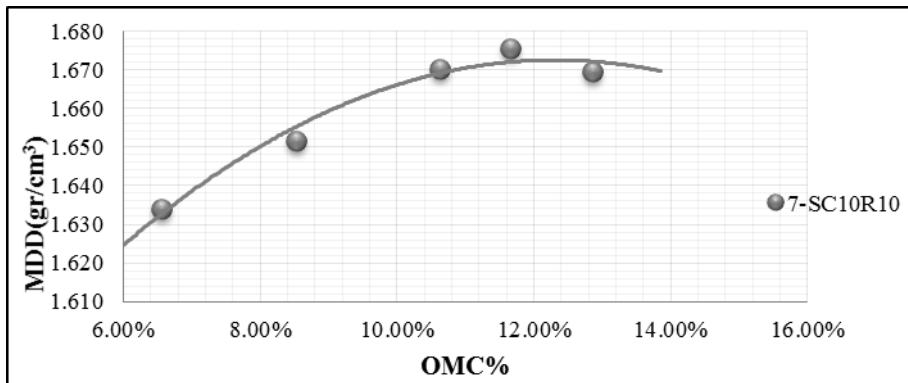
- WANG, Y.-M., CHEN, Y.-K. & LIU, W. 2008. Large-scale direct shear testing of geocell reinforced soil. *Journal of Central South University of Technology*, 15, 895-900.
- WEBSTER, S. L. & SANTONI, R. L. 1997. Contingency airfield and road construction using geosynthetic fiber stabilization of sands. ARMY ENGINEER WATERWAYS EXPERIMENT STATION VICKSBURG MS GEOTECHNICAL LAB.
- WU, W. Y., BENDA, C. C. & CAULEY, R. F. 1997. Triaxial determination of shear strength of tire chips. *Journal of Geotechnical and Geoenvironmental Engineering*, 123, 479-482.
- XIAO, M., LEDEZMA, M. & HARTMAN, C. 2015. Shear Resistance of Tire-Derived Aggregate Using Large-Scale Direct Shear Tests. *Journal of Materials in Civil Engineering*, 27, 04014110.
- YADAV, J. & TIWARI, S. 2017. A study on the potential utilization of crumb rubber in cement treated soft clay. *Journal of Building Engineering*, 9, 177-191.
- YANG, S., LOHNES, R. & KJARTANSON, B. 2002. Mechanical Properties of Shredded Tires.
- YOKOI, H. 1968. Relationship between soil cohesion and shear strength. *Soil Science and Plant Nutrition*, 14, 89-93.
- YOON, S. & ABU-FARSAKH, M. 2009. Laboratory investigation on the strength characteristics of cement-sand as base material. *KSCE Journal of Civil Engineering*, 13, 15.
- YOON, S., PREZZI, M., SIDDIKI, N. Z. & KIM, B. 2006. Construction of a test embankment using a sand-tire shred mixture as fill material. *Waste Management*, 26, 1033-1044.
- YOON, Y.-W. Engineering characteristics of tire treads for soil reinforcement. *International Workshop on Scrap Tires Derived Geomaterials, Yokosuka, Japan, 2007*. 80-101.
- YOUWAI, S. & BERGADO, D. T. 2003. Strength and deformation characteristics of shredded rubber tire sand mixtures. *Canadian Geotechnical Journal*, 40, 254-264.
- ZAITSEV, Y. & WITTMANN, F. 1981. Simulation of crack propagation and failure of concrete. *Materials and Structures*, 14, 357-365.
- ZHANG, T., CAI, G., LIU, S. & DUAN, W. 2016. Laboratory observation of engineering properties and deformation mechanisms of cemented rubber-sand mixtures. *Construction and Building Materials*, 120, 514-523.
- ZHENG, L., HUO, X. S. & YUAN, Y. 2008. Experimental investigation on dynamic properties of rubberized concrete. *Construction and building materials*, 22, 939-947.
- ZORNBERG, J., COSTA, Y. & VOLLENWEIDER, B. 2004a. Performance of Prototype Embankment Built with Tire Shreds and Nongranular Soil. *Transportation Research Record: Journal of the Transportation Research Board*, 1874, 70-77.
- ZORNBERG, J. G., CABRAL, A. R. & VIRATJANDR, C. 2004b. Behaviour of tire shred – sand mixtures. *Canadian Geotechnical Journal*, 41, 227-241.

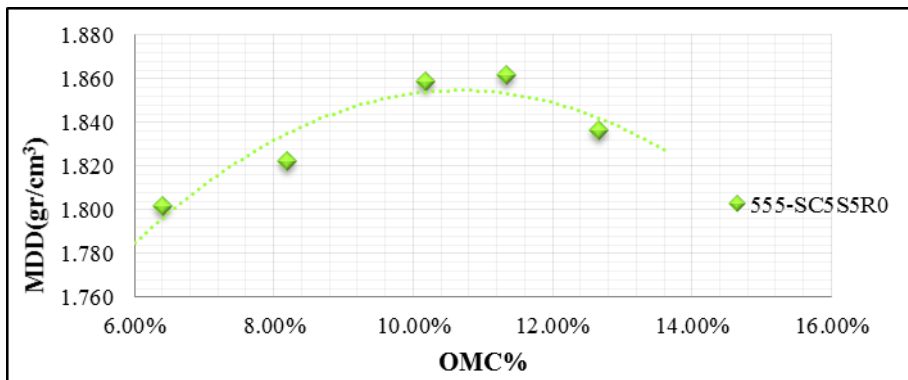
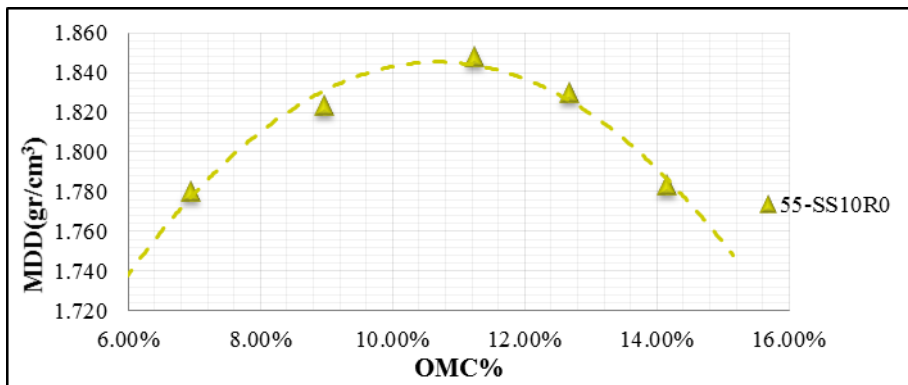
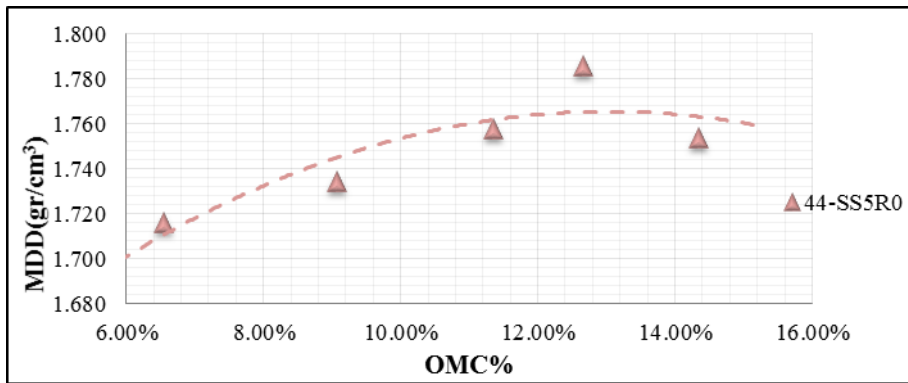
APPENDIX

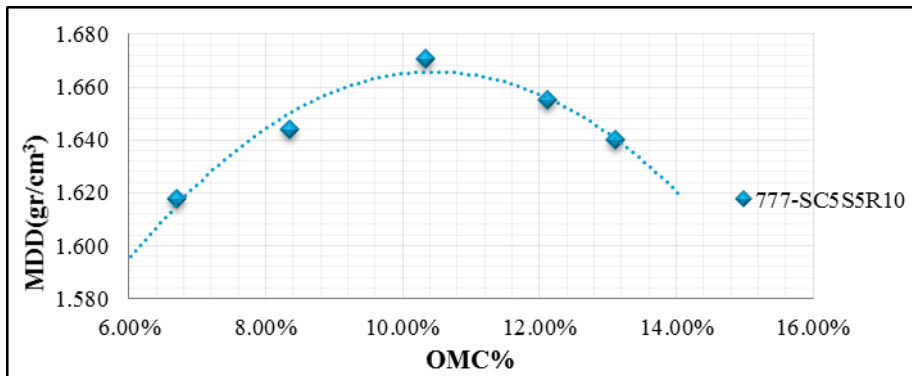
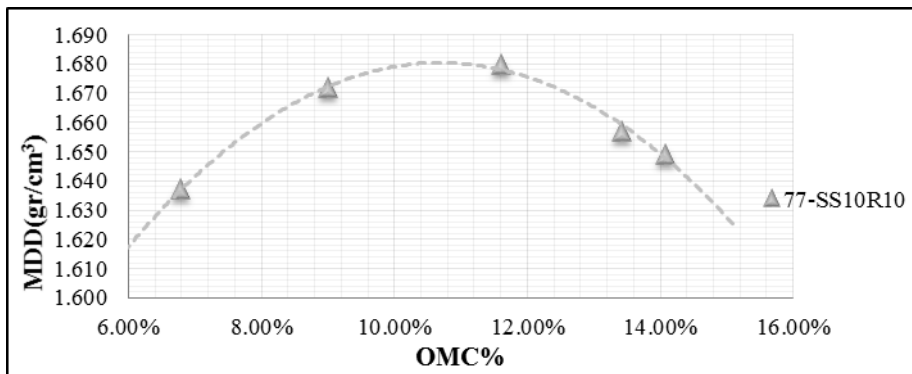
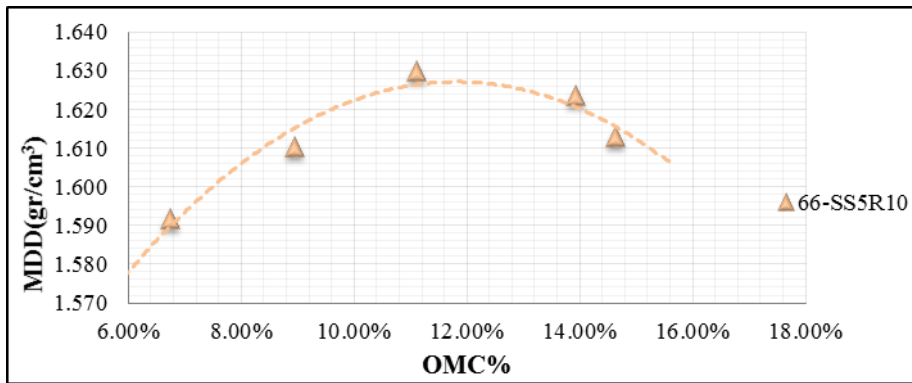
COMPACTION TEST RESULTS

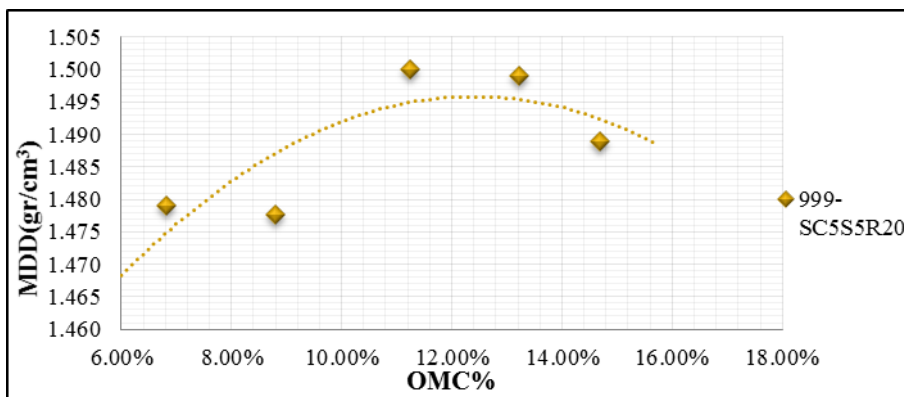
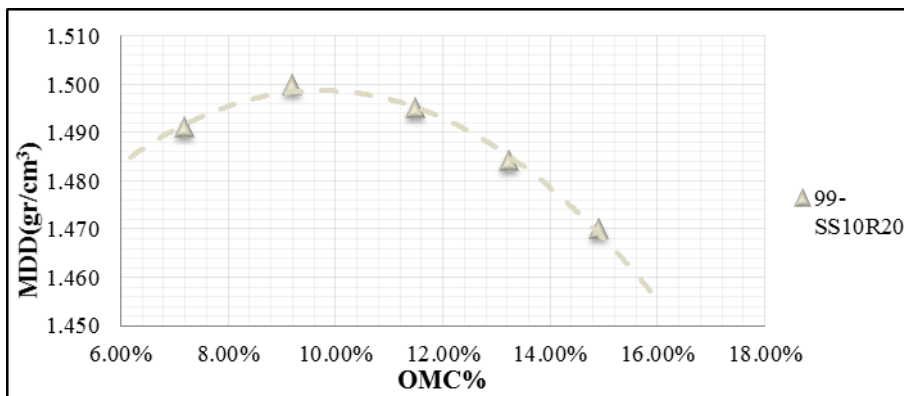
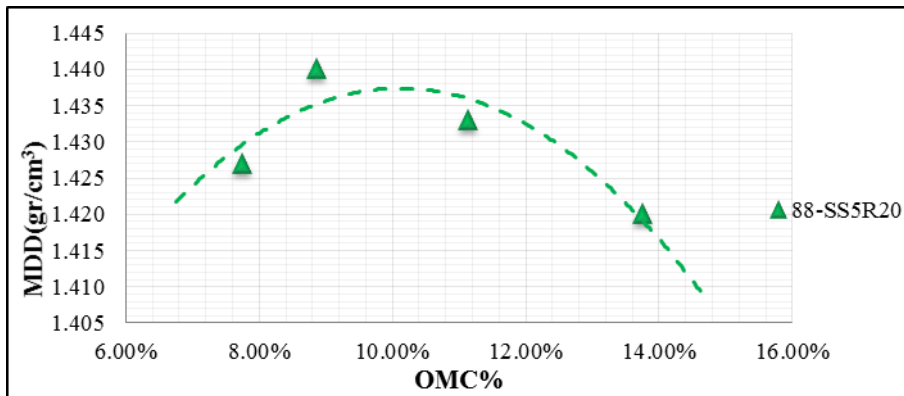




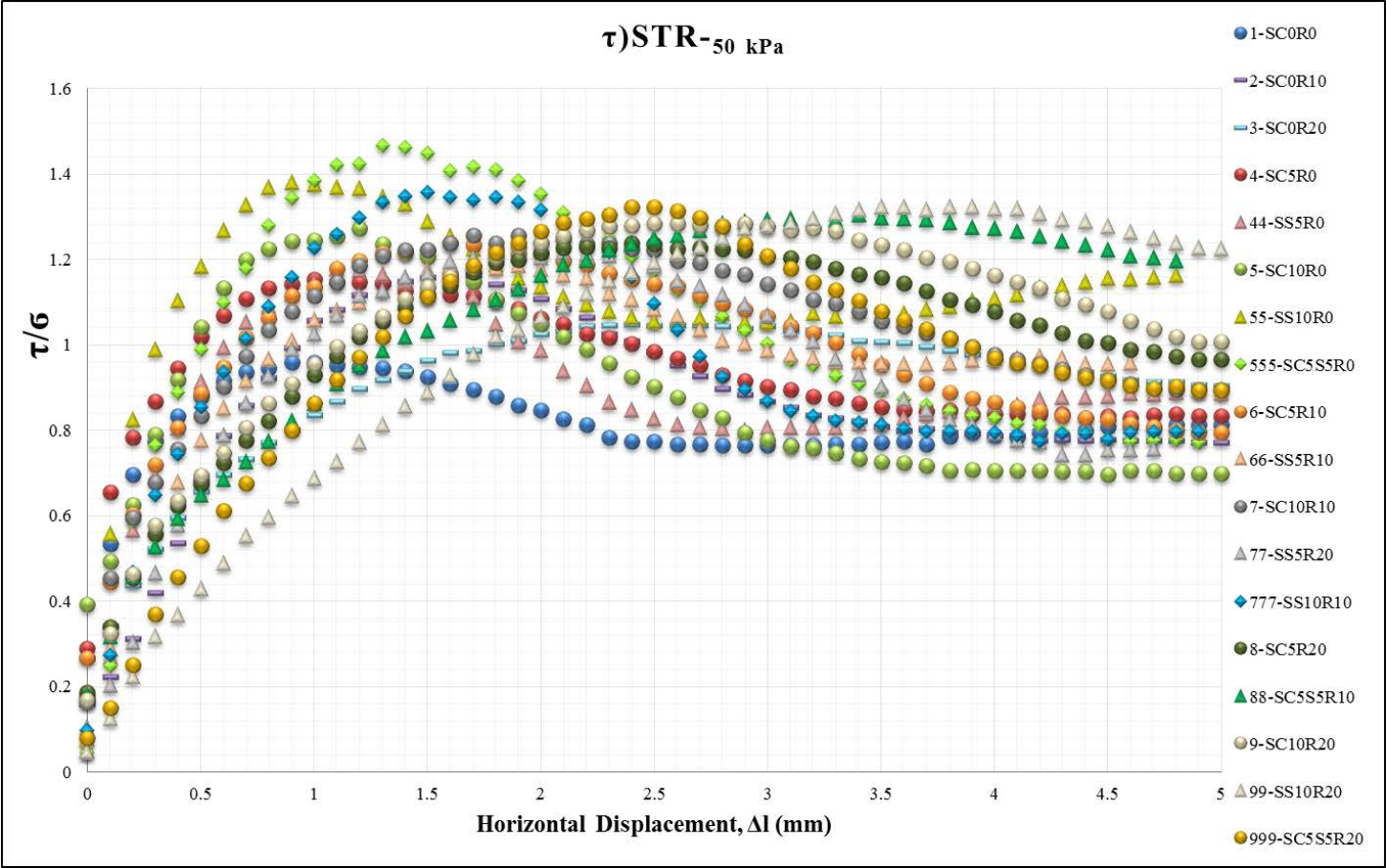


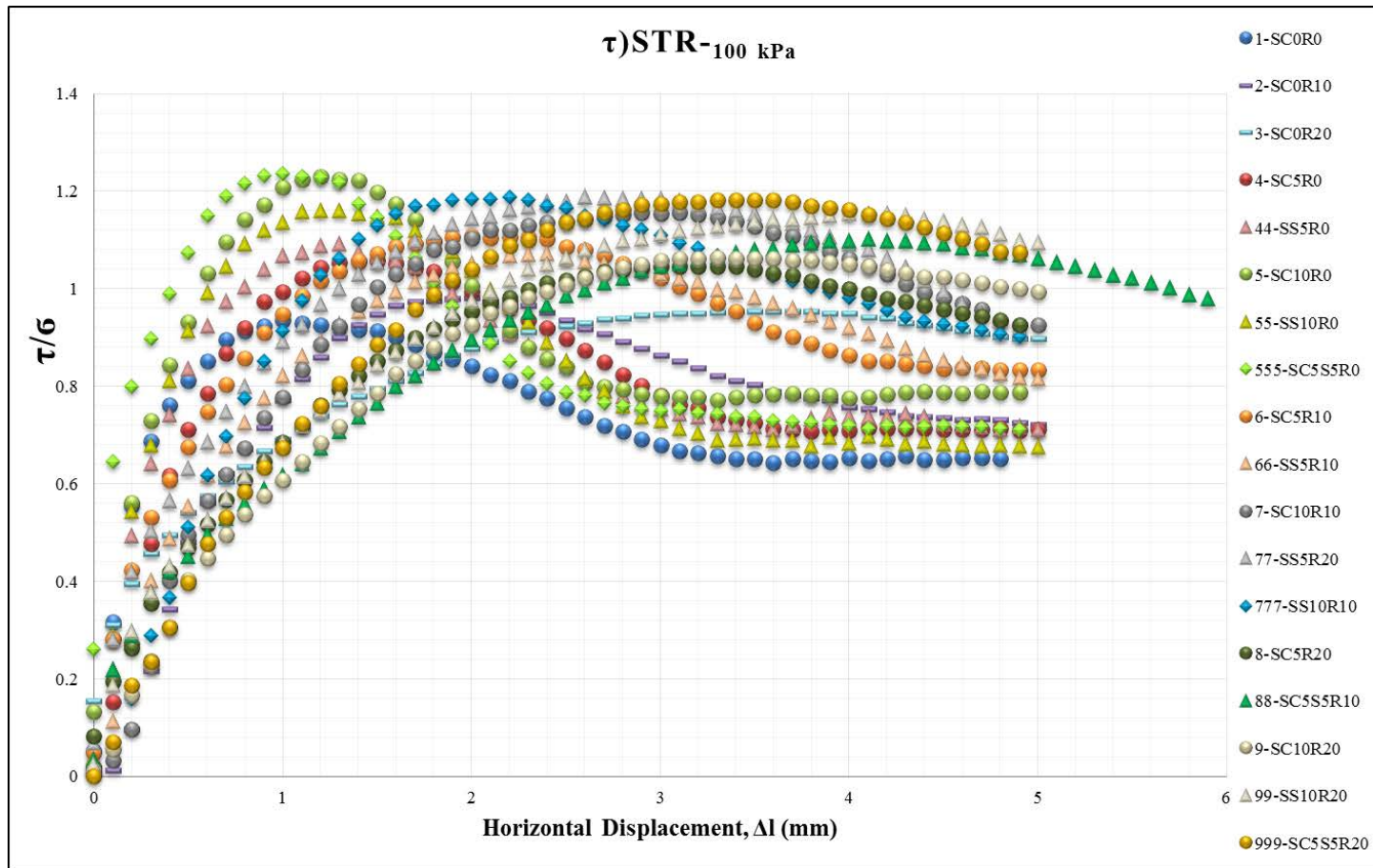


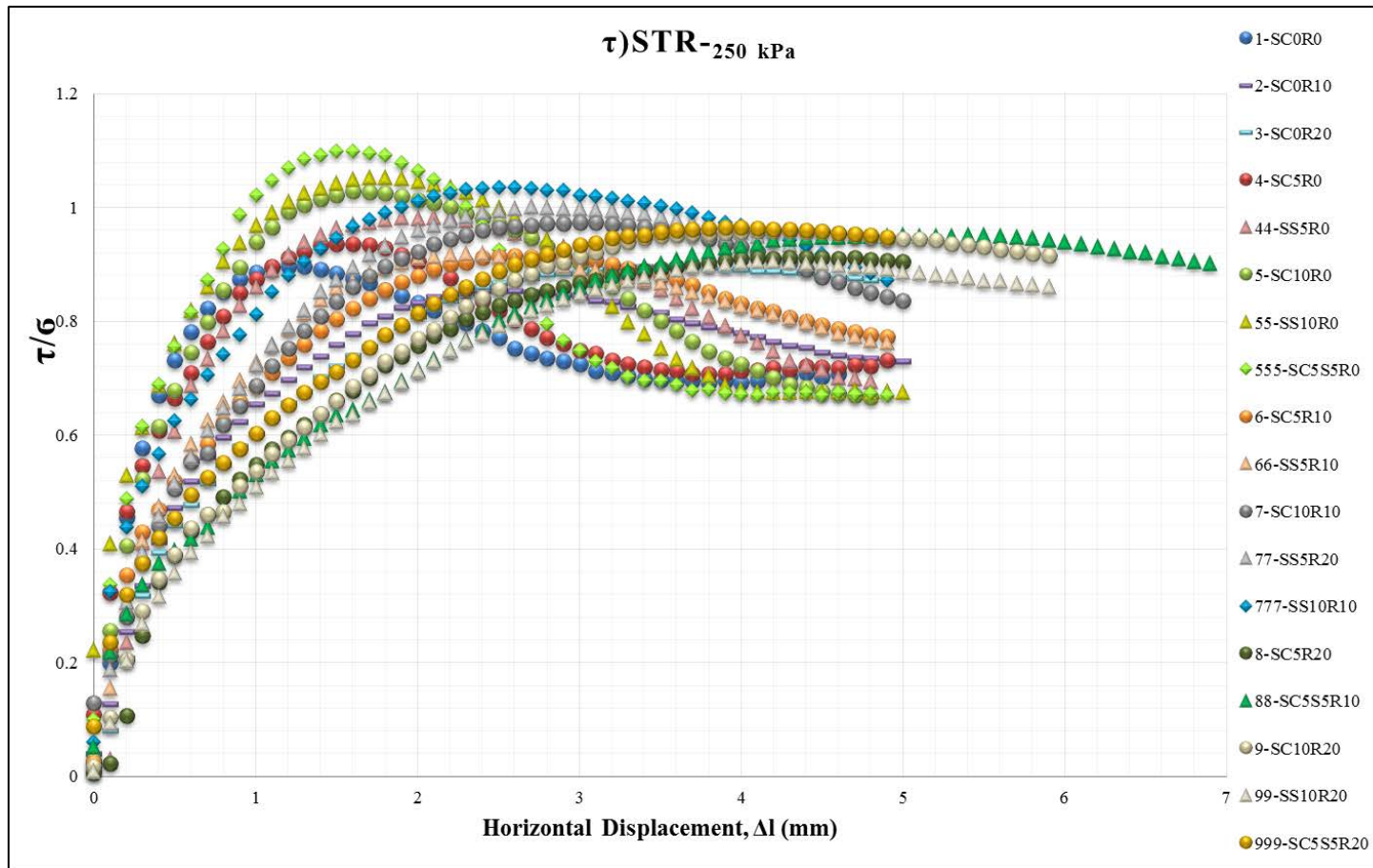


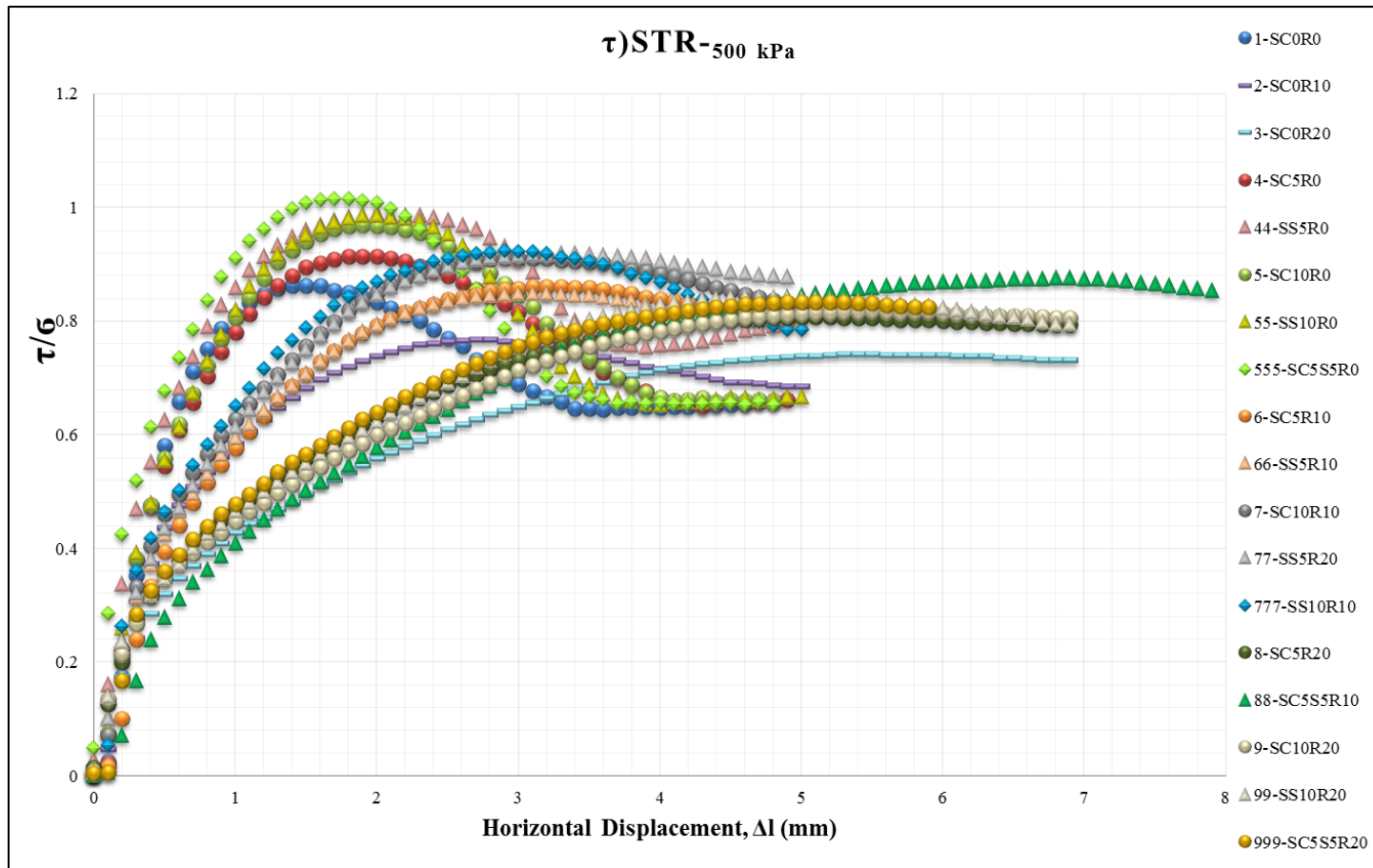


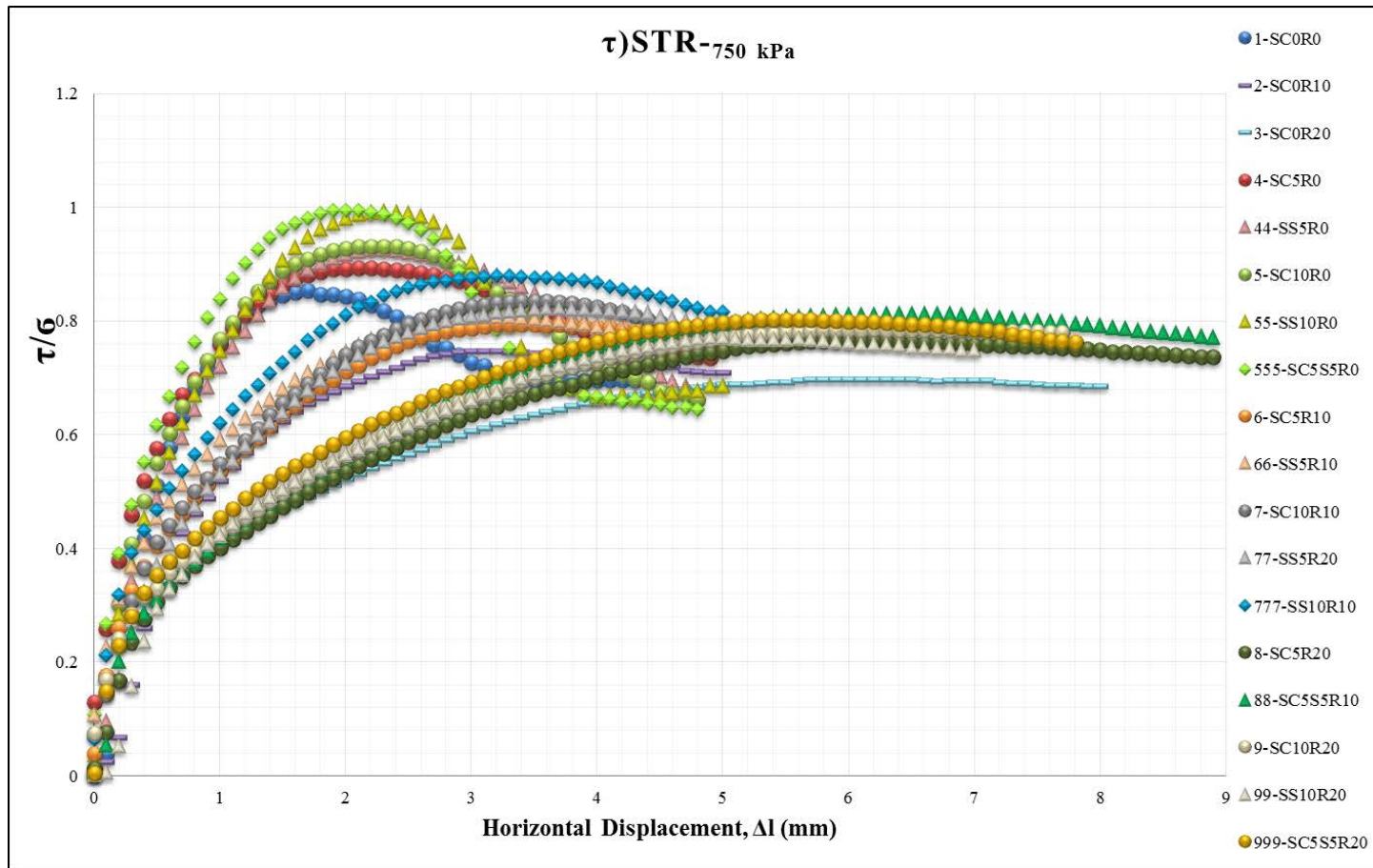
SMALL DIRECT SHEAR RESULTS

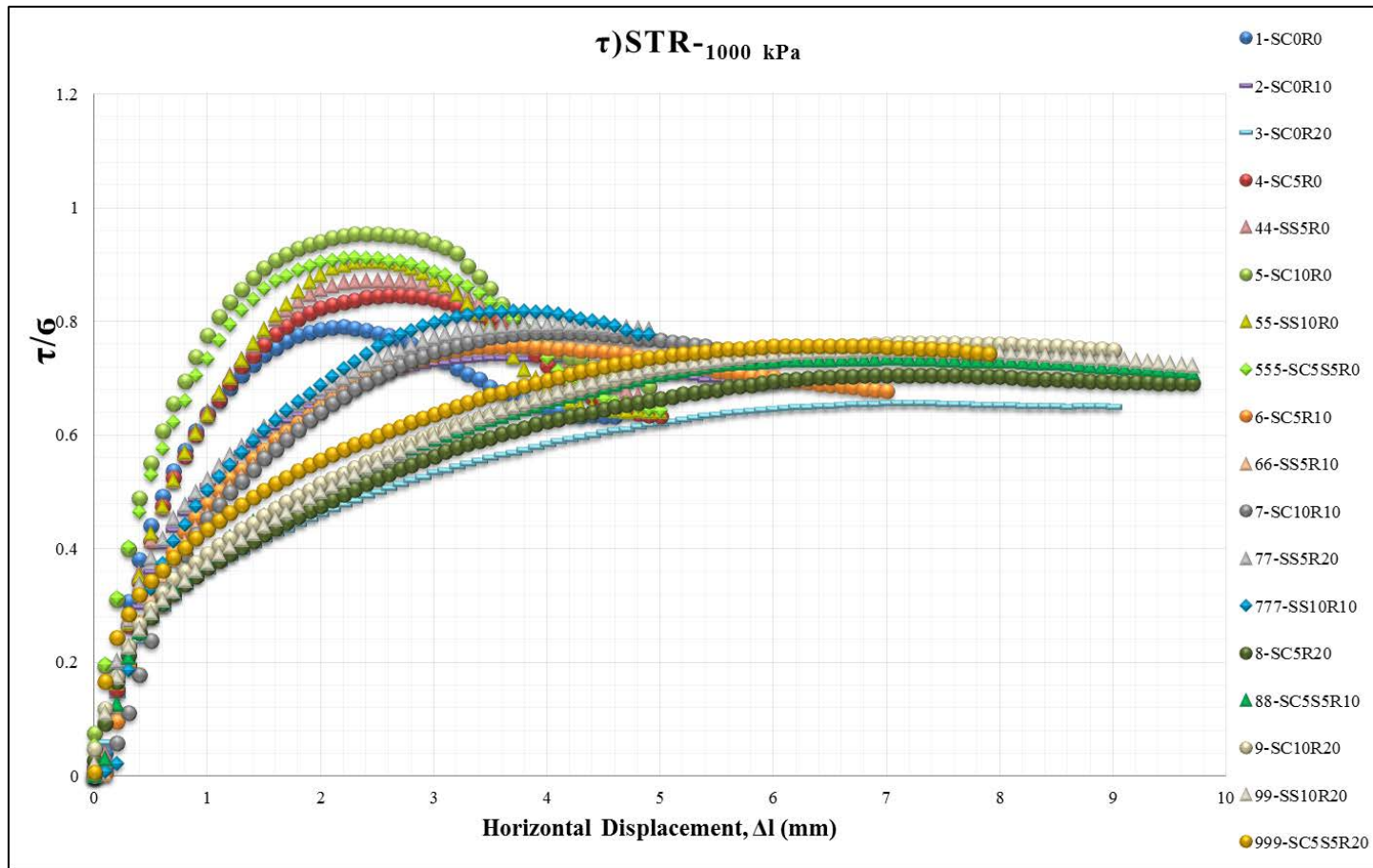




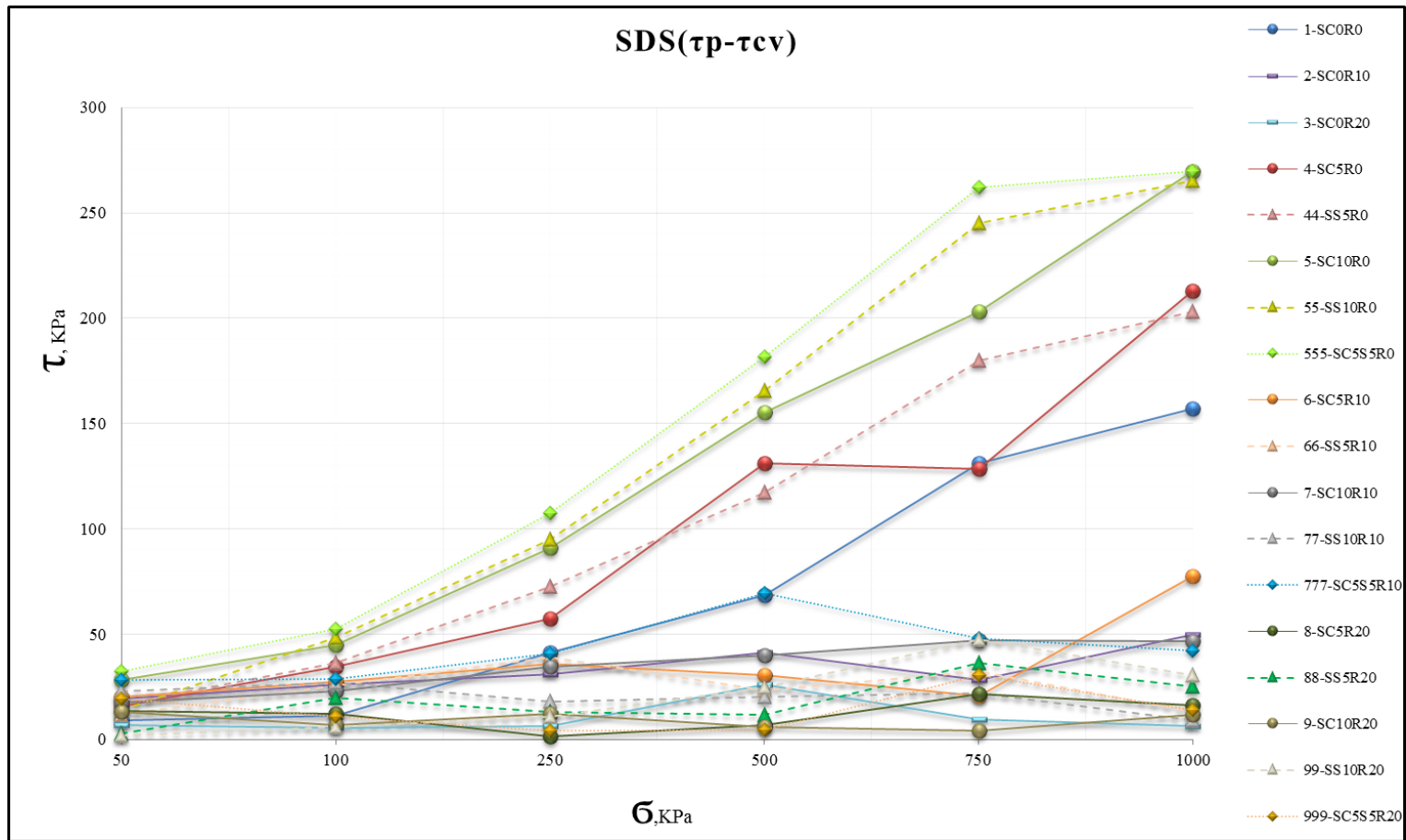




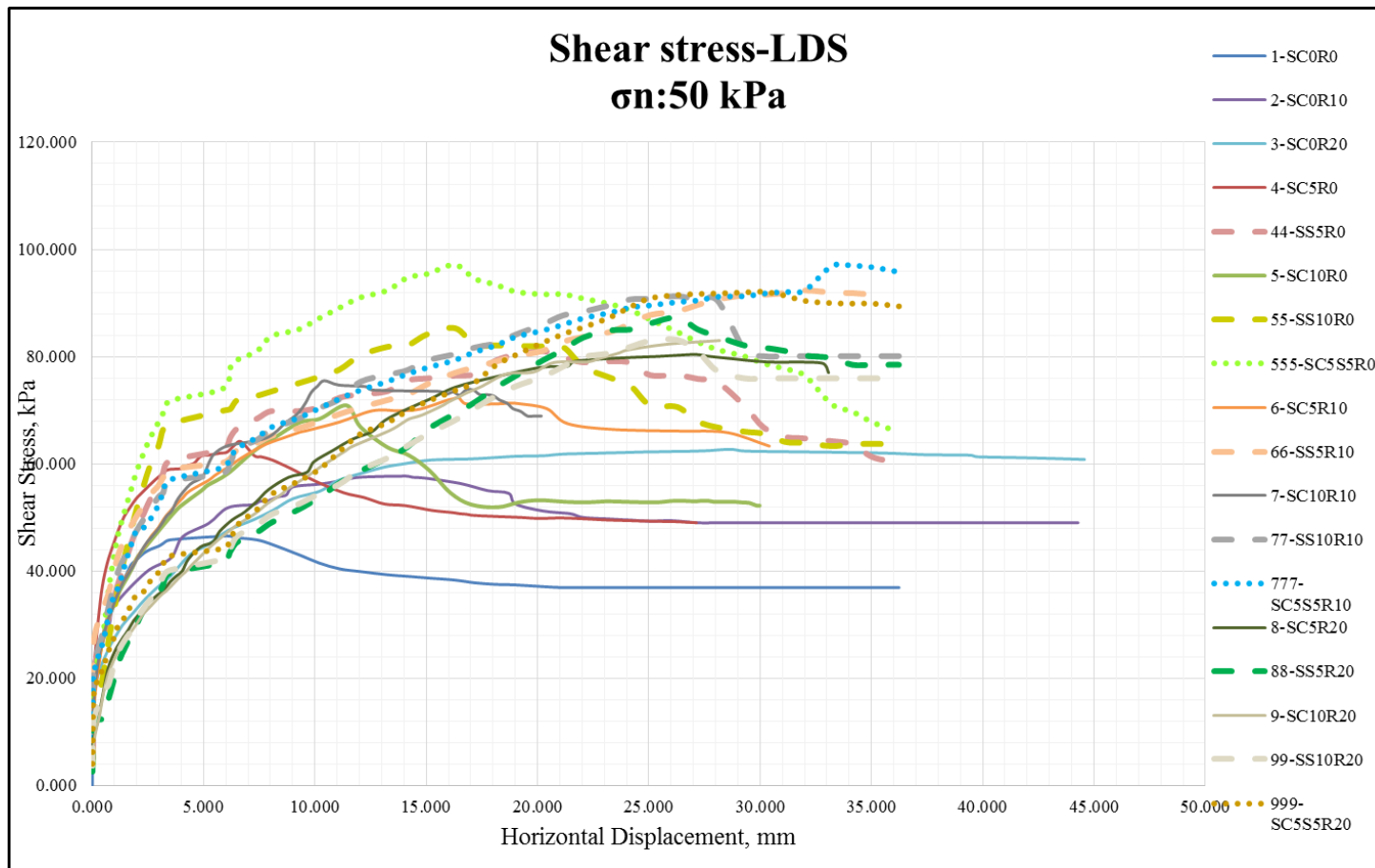


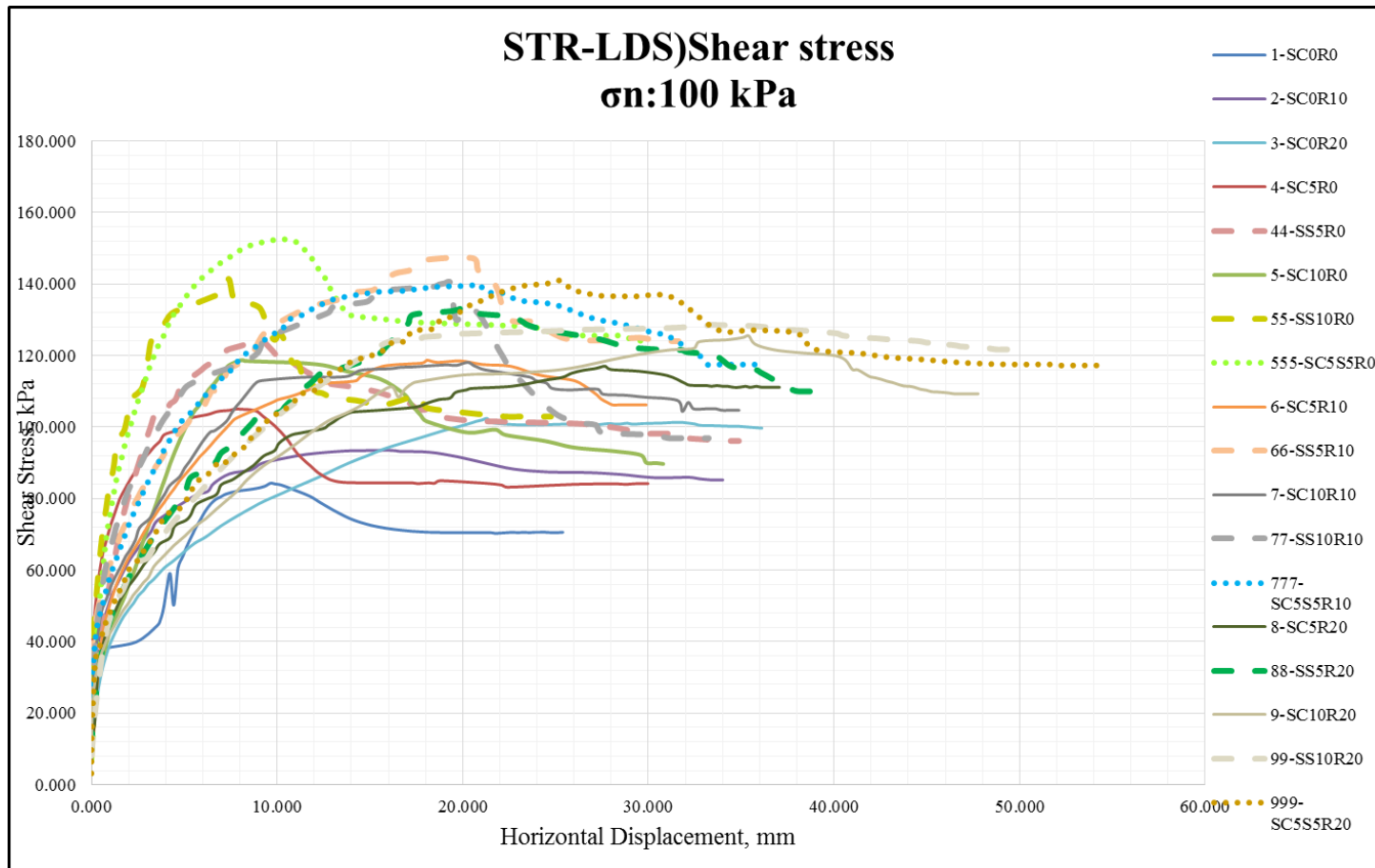


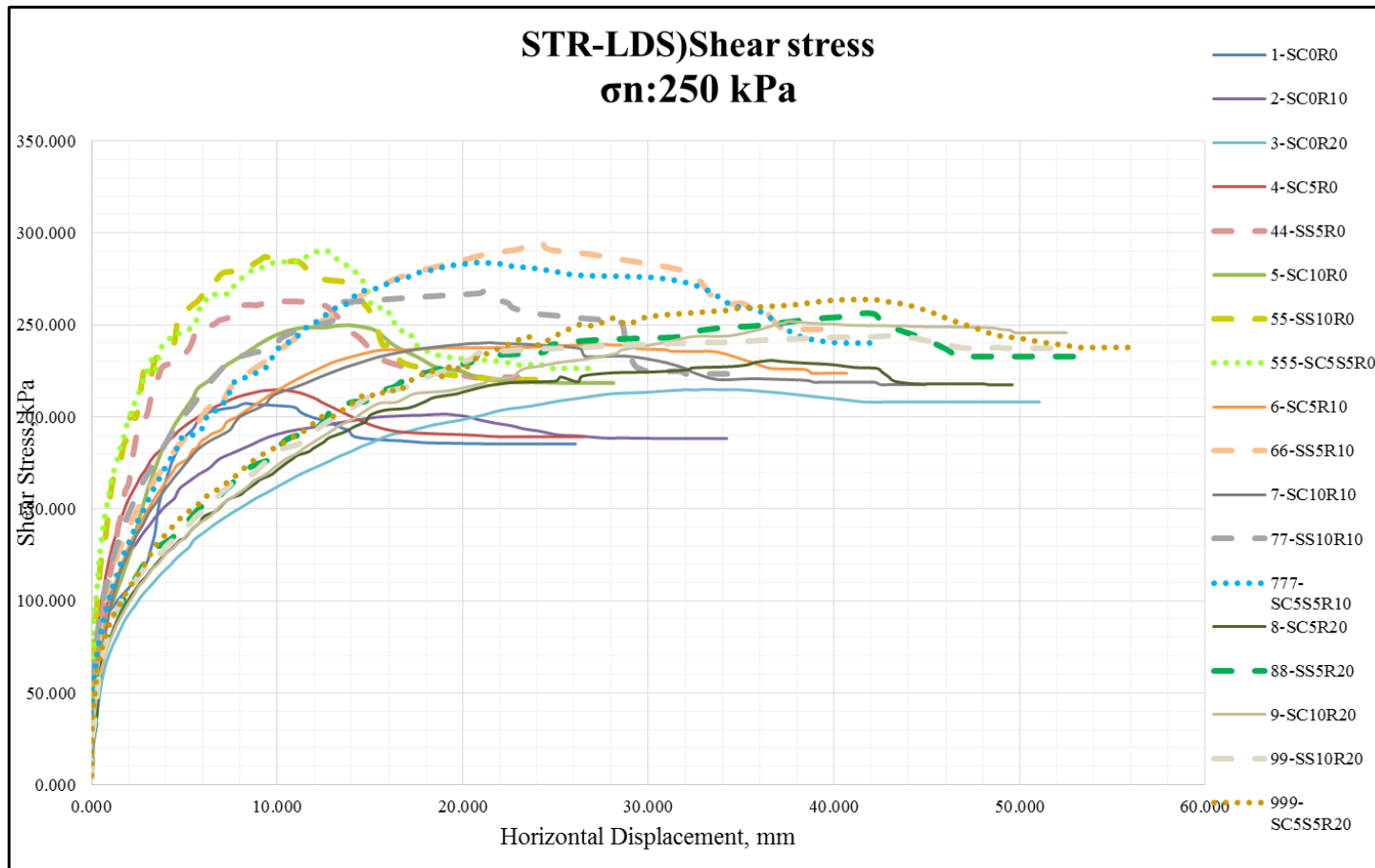


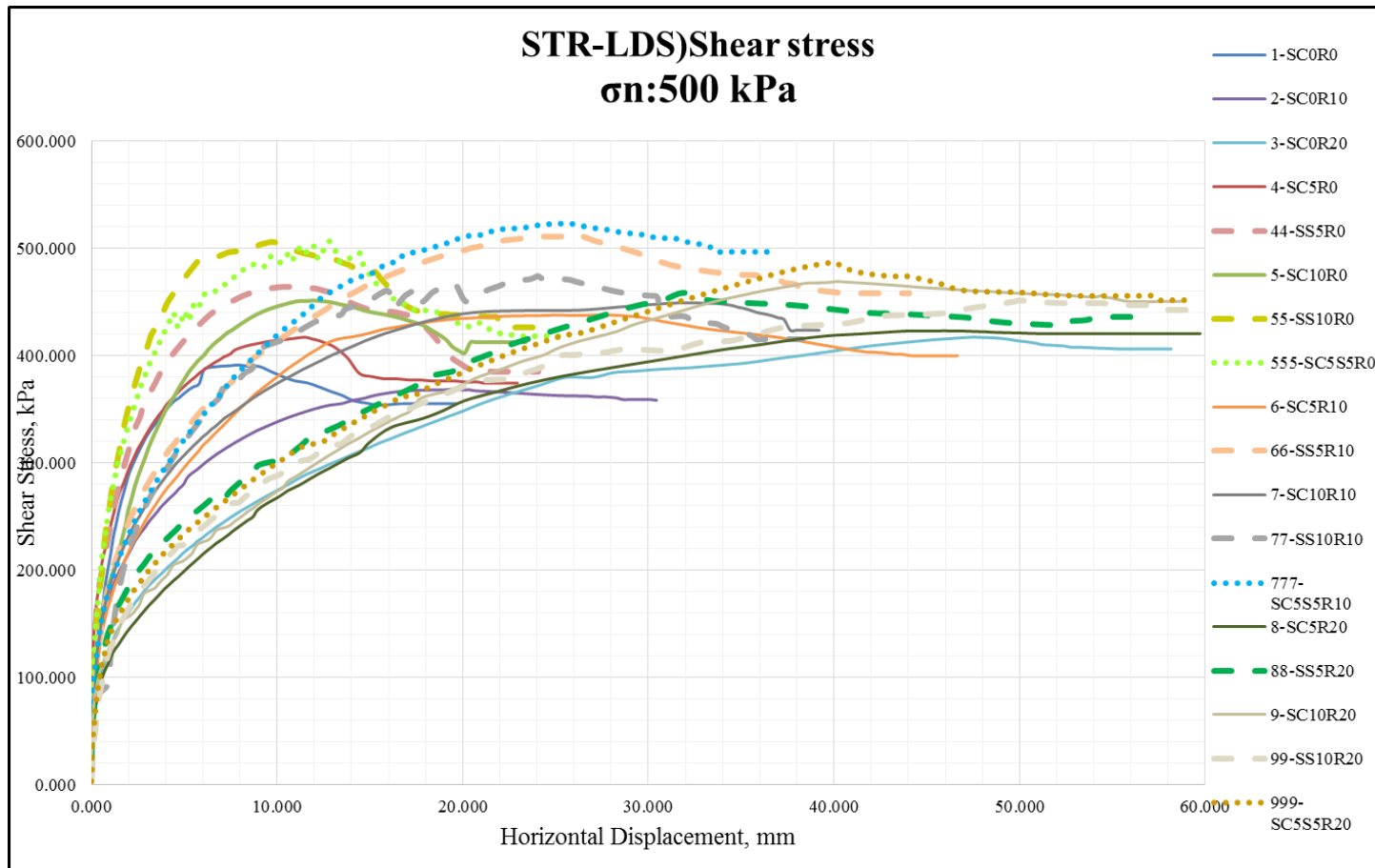


LARGE DIRECT SHEAR RESULTS

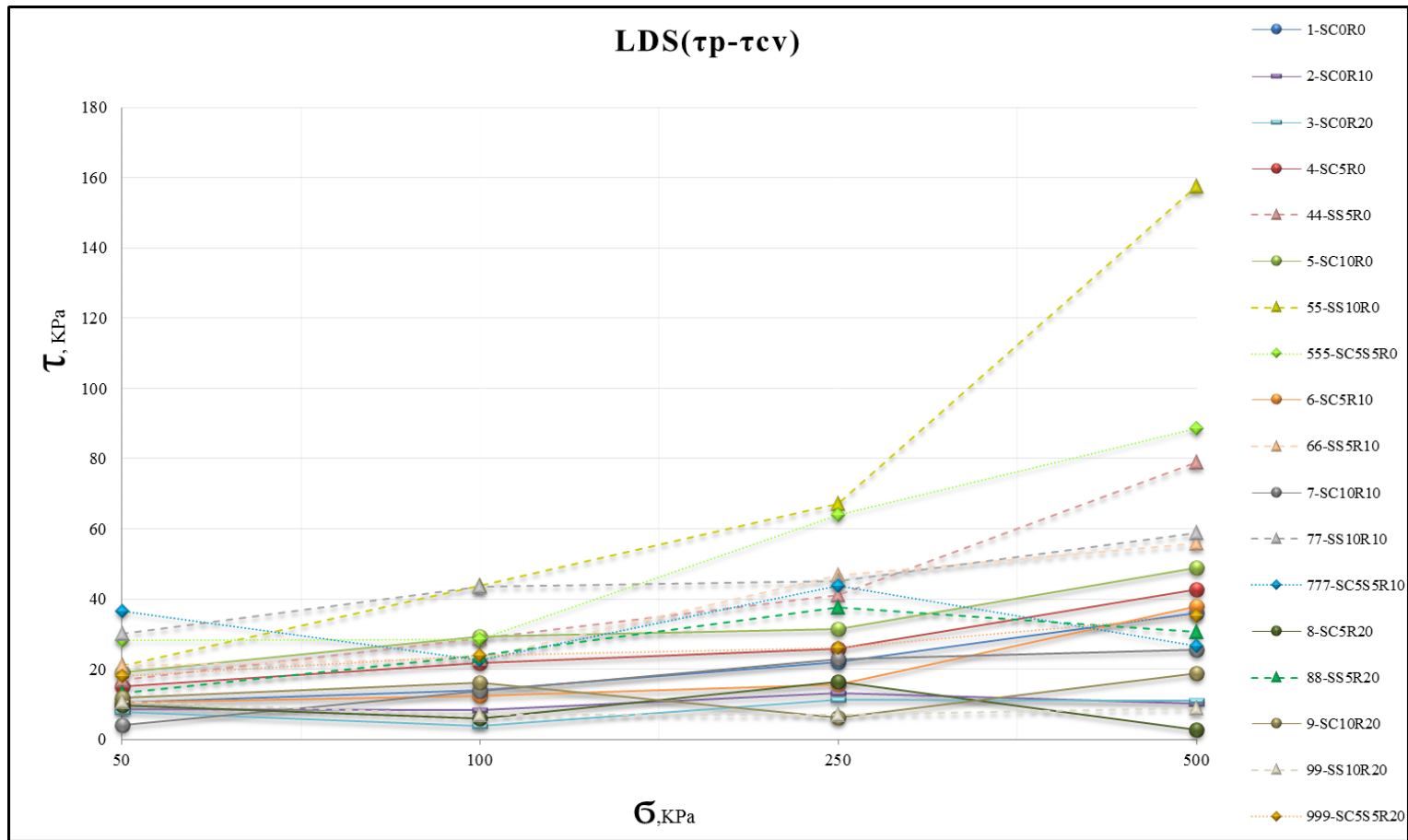




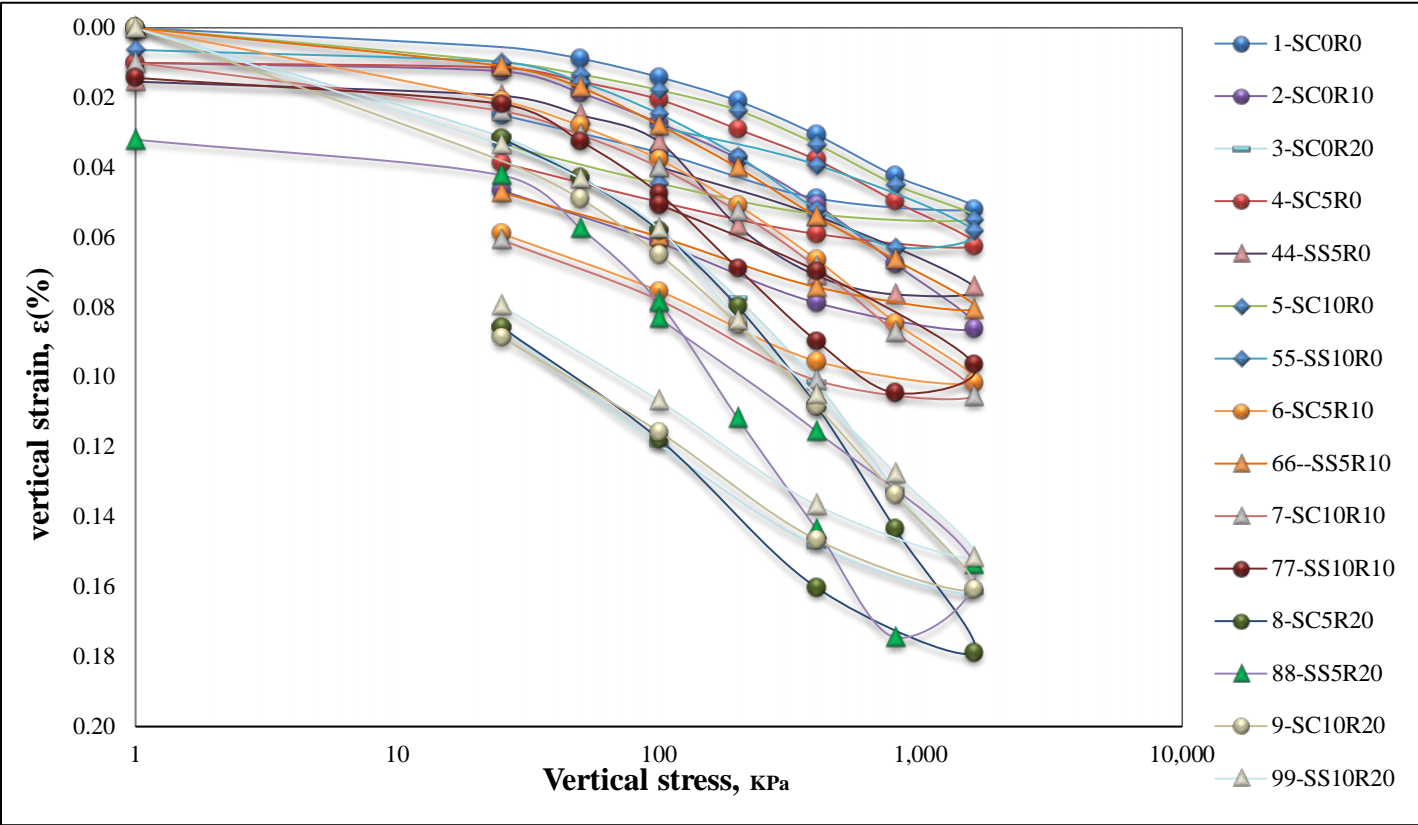








ONE-DIMENSIONAL CONSOLIDATION TEST RESULTS



TRIAXIAL TEST RESULTS

